Experimental and Clinical Results to Support Digital Workflows in Implant Dentistry

PhD Thesis

DR. HENRIETTE LERNER, DDS

SUPERVISOR: PROF. KATALIN NAGY, DDS, PhD, DS
UNIVERSITY OF SZEGED, FACULTY OF DENTISTRY, DEPARTMENT OF ORAL SURGERY

University of Szeged, Hungary

2021

TABLE OF CONTENTS

LIST OF PUBLICATIONS PROVIDING THE BASIS OF THIS THESIS

1. Mangano, F.G., Admakin, O., Bonacina, M. *et al.* Trueness of 12 intraoral scanners in the full-arch implant impression: a comparative *in vitro* study. *BMC Oral Health* 2020. **20:**63 https://doi.org/10.1186/s12903-020-01254-9

IF: 2.13

2. Imburgia M, Kois J, Marino E, Lerner H, Mangano FG. Continuous Scan Strategy (CSS): A Novel Technique to Improve the Accuracy of Intraoral Digital Impressions. Eur J Prosthodont Restor Dent., 2020. 31;28(3):128-141. doi: 10.1922/EJPRD_2105Imburgia14.

IF: 0.81

3. Lerner H, Mouhyi J, Admakin O, Mangano F. Artificial intelligence in fixed Implant Prosthodontics: a retrospective study of 106 implant-supported monolithic zirconia crowns inserted in the posterior jaws of 90 patients. BMC Oral Health, 2020. 19;20(1):80. doi: 10.1186/s12903-020-1062-4.

IF:2.13

4. Lerner H, Hauschild U, Sader R, Ghanaati S. Complete-arch fixed reconstruction by means of guided surgery and immediate loading: a retrospective clinical study on 12 patients with 1 year of follow-up. BMC Oral Health, 2020. 16;20(1):15. doi: 10.1186/s12903-019-0941-z.

 IF: 2.13

Summed impact factor: 6.954

ABBREVIATIONS

AI - Artificial Intelligence

AR - Augmented Reality

CAD - Computer Aided Design

CAM - Computer Aided Manufacturing

CMA - Custom Measuring Aid

CMM – Coordinate Measuring Machine

DICOM - Digital Imaging and Communications in Medicine

FA - Full Arch

IOS - Intraoral Scanner

ISQ - Implant Stability Quotient; implant stability as measured by the Osstell device

RFA- Resonance Frequency Analysis

IT – Insertion Torque

ML – Machine Learning

MZC- Monolithic Zirconia Crown

PEEK- Polyether-Ether-Ketone

PMMA - Polymethyl Methacrylate

PP - Partial Prosthesis

SB - Scan Body

SC - Single Crown

STL - Standard Tessellation Language

VR- Virtual Reality

I. INTRODUCTION

Technology has made the world a new place and created a new discipline in dentistry. Today, we are practicing a new kind of dentistry, where all the patient information is digital. This ranges from patient registration information to diagnostic and treatment planning data that is acquired from 3-Dimensional imaging (stored as DICOM and STL files) to digital photography and facial scanning, caries detection, temporomandibular joint analysis and digital dental occlusal analysis. This digital revolution also includes the treatment of patients with Computer-aided Design/Computer-aided Manufacturing systems, to the processing of data used to manufacture indirect restorations by milling and 3D printing systems, to computer-supported implant dentistry and computer-assisted surgeries, to the designing and manufacturing of implants, to the applications of lasers in dentistry, and lastly, to the new trends in computer-assisted dental education (1).

This thesis aimed to define a group of evidence-based recommendations for predictably proceeding through the digital workflow of guided surgery, based on four scientific studies (1-4) These studies were undertaken to improve the workflow of digital implant dentistry, by offering definitive evidence that supports the use of certain tools and methods. In particular, the studies concentrated on answering questions related to intraoral scanners, guided implant surgery techniques, and the possibility of implementing artificial intelligence (AI) in digital implant dentistry.

I.1. The trueness of intraoral scanners in the full-arch implant impression

Intraoral, desktop and facial scanners, and cone-beam computed tomography (CBCT) allow practitioners to acquire three-dimensional (3D) patient information, that when imported into and combined with computer-assisted-design (CAD) software, enhances patient virtualization that can be used to make a definitive diagnosis and plan in advance any needed treatment. Further, powerful milling machines and 3D printers allow for the physical production of many differing types of devices that can be used in various clinical disciplines (such as in restorative dentistry, prosthodontics, surgery and orthodontics) (5,6).

Since guided surgery potentially offers higher precision results than does "free-handed" surgery, the trueness, accuracy, and precision of all the gathered digital information is of primary importance in obtaining a precise result in the final esthetics, restorative stability, and patient function. Guided surgery virtual planning is concerned not only with implant locations, bone volume, soft tissue levels, and biotype quality but also with the final restorative prosthetic components. When the digital

surgical plan is complete, the manufacturing of surgical guides and prosthetic parts follows, which ultimately makes it possible to accurately transfer the virtual planning to the surgical site (7-9).

One of the most important and necessary digital data sets to be acquired as the basis for all of the follow-on steps is making the digital impression with an intraoral scanner (IOS). Intraoral scanners have changed the world of implant prosthodontics, as their predictability (trueness, accuracy, precision) has been validated in at least one IOS scanning study, involving single units and short span impressions (9). However, the literature has not yet validated the use of intraoral scanners (IOSs) for full-arch (FA) implant impressions. Hence, the aim of the first *in vitro* study presented in the thesis was to assess and compare the trueness of 12 different intraoral scanners when making full-arch implant impressions (10-13).

IOSs emit a structured light grid (or less commonly, a laser beam) with known characteristics, to capture optical impressions in a sequence of images of a patient's dental arches. When the light grid impacts the surface of the dental arch, the grid undergoes deformation that is captured by powerful cameras, which send the signal to powerful reconstruction software (15,16), which then reconstructs the arch surfaces in 3-dimensions (3D). The reconstruction software produces a point cloud by combining all the images captured from different angles resultant from the scanner's relative movements around the dental arches. This point cloud is triangulated to generate a mesh reconstruction of the scanned surfaces, that is displayed as a virtual model of the patient's dental arches.

The advantages of IOSs are many. IOS optical impressions capture virtual models of the patient's dental arches without conventional impression trays and materials, which eliminates the discomfort caused by conventional tray impressions, and is extremely helpful in patients who possess a strong gag reflex. There is no need to pour a plaster cast, which saves both time and space, and the virtual models (saved as standard tessellation language .STL files), can be immediately sent to the laboratory without being disinfected or incurring any shipping expense. Optical impressions also improve dental laboratory communication, as they are more efficient to work with than are stone models. Most importantly, IOSs simplify clinically capturing the impression, particularly when there are multiple implants to impress and the patient presents with deep anatomic undercuts that can lock in a tray filled with set polyether or addition silicone. Finally, IOSs represent a powerful marketing tool with the patient, while opening the gateway to the world of computer-aided design and manufacturing (CAD/CAM) (14).

Intraoral scanners (IOSs) are changing the world of implant prosthodontics (18), but to ensure high precision predictable clinical results, validation of the component technologies is necessary. As

such, several recent studies have been researching the trueness, precision, and accuracy of different IOS systems.

In metrics, accuracy is defined as "the close agreement between a measured quantity value and a true quantity value of a measurand" (a quantity intended to be measured) (JCGM 200:2012; ISO 5725–1). However, concerning IOSs, accuracy is somewhat influenced by an individual IOS's combined trueness and precision. Trueness is the most important factor, being defined as "the close agreement between the arithmetic mean of a large number of test results, and the true or accepted reference value". Trueness then expresses how much the average of a series of measurements approaches reality. An individual measurement is truer, the closer it is to the actual measured value of the object.

I.2. Improving the Accuracy of Intraoral Digital Impressions

In implant prosthodontics, IOSs allow for the direct capture of the dental arches, including the position of any implants by using scan bodies (SBs), which are the digital version of analog impression transfer copings. The SBs are mathematically coupled to an implant library within the CAD software, affording the dental technician the ability to replace SB surface mesh with a bonding base, upon which can be modeled a screw-in superstructure or a customized abutment, either of which could support a future prosthetic restoration.

Although there are statistically significant differences in the accuracies of various commercially available IOSs, a few scientific studies (19,20) and reviews of the literature (21-23) have confirmed the intrinsic difficulty that scanners encounter when optically impressing multiple implants, particularly in completely edentulous patients. Importantly, the inaccuracy of models generated by direct intraoral scanning does not depend solely on the scanner itself, and/or the technology involved in the image acquisition. Other factors influence the scanner's inherent capabilities, including the lighting conditions (24), the operator's experience and scanning methodology (25), the position, inclination, and depth of any present implants, and the SB's design and material composition (26).

Several studies and reviews have reported a persistent accuracy problem with intraoral scanning when long-span prosthetic restorations must be fabricated (fixed partial prostheses supported by multiple implants, and full arches [FAs]). Screw-retained superstructures, (fixed prostheses screwed directly onto multiple implants) require the highest accuracy because the acceptable tolerances are minimal, and the fit must be passive.

Although recent IOS technological improvements have been made, IOSs still face challenges when scanning multiple implant fixtures, because the IOS must "attach" the individually acquired frames to each other during the scanning process. Regardless of the acquisition technology, this intrinsic error increases with the extent of the region to be scanned. In fully edentulous patients that lack definitive reference points, accuracy is more difficult to achieve as the IOS reads the distances between different SBs, which sit at different heights above the soft tissues. Reducing the distances (or the "jump") between implant SBs may improve the accuracy of the scan, thereby reducing the intrinsic scan error. This approach was used in one retrospective study, where the authors reduced the distances between the different SBs and provided artificial landmarks, hoping to reduce IOS inaccuracies so that long-span screw-retained superstructures could be fabricated to fit passively onto the supporting implants (27).

I.3. Artificial Intelligence (AI) in Fixed Implant Prosthodontics

The third study of this thesis presents a protocol for the use of artificial intelligence (AI) to fabricate implant-supported monolithic zirconia crowns (MZCs) cemented onto customized hybrid abutments.

Artificial intelligence (AI) technology is a branch of computer science concerned with building smart software or machines that are capable of performing tasks that typically require human intelligence. Machine learning (ML) is commonly defined as "the ability of a system to interpret external data, learn from that data, and use what was learned to achieve objectives and goals through flexible adaptation". Machine learning (ML) is a subset and foundation of AI, where computer systems perform specific tasks that approximate human cognition, without using explicit instructions. The machine solely relies on patterns and mathematical models involving computer algorithms that allow computer programs to improve their performance automatically through experience. Simply explained, machine learning feeds the computer data, and then uses statistical techniques to help the computer "learn" how to get progressively better at a specific task (28).

Several augmented reality (AR) and virtual reality (VR) technologies are already present in dentistry. In orthodontics, IOS software is used to pre-plan tooth movement strategies with aligners. In digital implant planning, AI technology allows for tooth segmentation, automatic structure isolation and segmentation, procedural annotation, and image data conversion into .STL files (29).

In modern digital implant protocols, the dentist must capture an intraoral scan of the implant scan body as accurately as possible, and then the technician must carefully replace the mesh captured

by scan with companion implant library files, to model the future restoration. Therefore, the implant library files stored within the CAD software must accurately reflect the implant size and shape without displaying significant spatial errors. However, despite the technician managing the above procedures well, it still may not be sufficient to ensure precise restorative outcomes. In fact, during the extraoral cementation of customized zirconia abutments onto their bonded bases, tolerances between the different components may cause cementation errors. Even when these errors are only off by a few degrees, they can generate positional problems during the delivery of the customized abutment and the seating of the provisional restoration, because the components will not be located in the mouth in their exact CAD-planned positions. During the delivery of the provisional restoration, small adjustments can be made to the interproximal contacts or the occlusion in the polymethylmethacrylate (PMMA) to compensate for this type of spatial error. But these types of adjustments are not acceptable for monolithic ceramic zirconia (MZC) restorations. The definitive monolithic zirconia restorations cannot be retouched in the mouth, so they must not demonstrate positional errors during their delivery.

To overcome this problem, experienced dental technicians will position the already-assembled individual abutments into implant analogs contained within a 3-Dimensional (3D) printed model, and then scan the abutments using a desktop scanner. This method obtains the relative positions and the anatomy of the abutments, which includes the margin line. However, this extra step forces the technician to print a cast on which to model the definitive zirconia restorations, made of solely surface reconstruction mesh, that by definition, is only a geometric approximation of the actual scanned abutments. These additional steps can be avoided with the help of artificial intelligence (AI). AI is a wide-ranging branch of computer science concerned with building smart software or machines, capable of performing tasks that typically require human intelligence. AI, therefore, represents a valuable addition to fixed Implant Prosthodontics.

I.4. Complete-Arch Fixed Reconstruction Using Guided Surgery and Immediate Loading

The last study described in this thesis covered all the steps within the digital workflow. It was a retrospective study comprised of outcome data from 12 full arch implant rehabilitations, performed with immediate implant placement into fresh extraction sockets, and immediate loading.

In 2002, the concept of guided implant planning linked to immediate functional loading was first introduced in Leuven, Belgium (30). These first immediate loaded treatments were limited to edentulous jaws, and required full-thickness flaps because the surgical templates were bone-

supported. Since that time, planning procedures have been optimized, opening the way for increasingly precise surgical templates that can be fabricated for both dental arches of partially and completely edentulous patients, employing both mucosal and dental support.

In immediate implant placement and immediate loading of cases fabricated without a pink tissue component, high success rates have been reported by standardizing and respecting certain planning parameters that account for the differing implant and abutment design features. By performing specific immediate loading protocols, a pleasing aesthetic result can be predictably achieved, even when implants are placed into fresh extraction sockets (32). Therefore, today, the immediate functional loading of implant-supported full-arch fixed prostheses represents a predictable solution for the rehabilitation of edentulous patients.

The use of a flapless approach is an important benefit of present-day guided surgery. It reduces the invasiveness and the duration of surgical treatment, which simplifies the procedure for the clinician while reducing discomfort and morbidity for patients (31). However, the survivability of flapless guided surgery cases where implants are placed in post-extraction sockets, that are immediately loaded with complete-arch fixed reconstructions absent of artificial gingiva, have not yet been thoroughly evaluated. As such, this present retrospective clinical study aimed to document the survival and success of this specific type of immediately complete-arch fixed reconstructions.

It is important to note that, the immediate placement of implants in post-extraction sockets and their immediate functionalization with a complete-arch provisional, represents a serious challenge for clinicians to accomplish. Surgically, clinicians must be able to mentally visualize the future prosthetic rehabilitation, and consequently, the ideal positions and axes of the implant insertions. This can be particularly complex in an edentulous arch, which is a large surgical field. Additionally, it can be difficult to obtain adequate primary implant stability when placing implants in post-extraction sockets. These mental and clinical challenges may combine to result in non-optimal implant placements.

Although non-optimal implant positioning may not violate important anatomical structures (such as the inferior alveolar nerve or the maxillary sinus), it can have serious aesthetic consequences, which may displease the patient (33). The literature is clear that the aesthetic outcome and the long-term stability of implant-supported restorations do not solely depend on the volume of supportive bone and mucosal tissues available, but also the implant insertion axis.

Modern digital technologies, and those used with guided implant surgery, offer solutions to these problems. Conceived in the mid-1990s, guided implant surgery has rapidly grown in popularity to become widely used all over the world. And, the introduction of Cone-Beam Computed Tomography

(CBCT), has allowed for the simple acquisition of 3-dimensional (3D) jaw bone volumes, while subjecting patients to considerably less radiation compared to conventional Computerized Tomography (CT) (33). The patient's bony anatomy, captured with CBCT, may be imported into specific implant surgical planning software as Digital Imaging and Communication in Medicine files (DICOMs), to be then combined with a wax-up of the ideal prosthetic restoration. Within such a planning software, the surgeon can design optimal implant insertions, based upon the available residual bony anatomy and the ideal prosthetic restoration. Then, from this defined optimal plan, a surgical guide is produced using additive digital printing techniques (like SLA printing) that, during implantation, guides precise fixture placement (34).

However, within the literature, most clinical studies of full arch implant restorations studied "Toronto Bridges", also known as "All-on-Four" and/or "All-on-Six" hybrid fixed prostheses. These restorations contain a connecting bar between the implants, that is covered by artificial gingival tissue fabricated from either porcelain or resin. There is no doubt that even with this type of hybrid prosthesis, guided implant surgery provides more precise implant placement concerning the location of the screw holes, and affords the clinician the ability to pre-fabricate a milled provisional for same- or next-day delivery. Despite that these implant-supported dentures are easy to manage, they do not offer ideal aesthetics because of the presence of the artificial gingiva. Moreover, with these types of hybrid prostheses, effective daily oral hygiene can be much more difficult for the patient to manage.

Conversely, an immediately loaded prosthesis inserted after immediate placement of implants into fresh extraction sockets without a pink gingival component is greatly appreciated by patients. This type of final restoration is highly esthetic, reduces surgical invasiveness, lessens the number of surgical and prosthetic treatment sessions, and markedly reduces overall treatment times.

II. OBJECTIVES AND HYPOTHESES

In performing the studies that comprise this thesis, we sought to accomplish the following objectives:

1. To date, the scientific literature in fixed implant prosthodontics has validated the use of IOSs for capturing optical impressions when designing and manufacturing short span restorations, such as single crowns (SCs) and partial prostheses (PPs) (35-37). However, several studies and reviews of the literature (38 -40) have reported that with long-span and full-arch restorations (FAs), IOSs do not yet demonstrate sufficient accuracy. The purpose of the *in vitro* study regarding IOSs[1] was to assess and compare the overall trueness of 12 different commercially available IOSs with full arch rehabilitations, using two different investigation methods (mesh-to-mesh and nurbs-to-nurbs superimposition): by calculating the exact linear distances between different SBs during a progressing scan, and by calculating the cross-distances between different SBs that sit in different positions within the arch. It was hypothesized that in full-arch rehabilitations, the accuracy of intraoral scans using the "mesh-to-mesh method" is not enough for long-span restorations. For this reason, it was decided to study the accuracy of intraoral scans after replacing each of the SBs in the mesh with its' corresponding library file, and then by superimposing two different nurbs files (one SB's position obtained with a reference scanner, and each IOS's SB scan). We hypothesized that this approach would improve the accuracy of IOS scans in full-arch cases.

2. As stated earlier, several *in vitro* and *in vivo* studies have demonstrated that IOSs represent an accurate and reliable solution when taking optical impressions of partially edentulous patients to fabricate short-span restorations (single crowns [SCs] and partial prostheses [PPs] (35-37). However, other studies (41,42) and reviews (43-45) have reported a persistent accuracy problem with intraoral scanning when long-span prosthetic restorations are being fabricated (fixed partial prostheses supported by multiple implants, and with full arch restorations [FAs]).

The second study covered in this thesis[2] focused on this latter accuracy problem, by presenting the clinical results obtained using a novel scanning technique, known as the "Continuous Scan Strategy" (CSS). This scanning method eliminates the "jump" between different SBs, by connecting the scan bodies with thermoplastic resin, so as to possibly reduce intrinsic scan errors. The hypothesis was that in fully edentulous patients, due to a lack of anatomic reference points, it is more difficult

---

[1] Mangano, F.G., Admakin, O., Bonacina, M. *et al.* Trueness of 12 intraoral scanners in the full-arch implant impression: a comparative in vitro study. *BMC Oral Health* **20,** 263 (2020). https://doi.org/10.1186/s12903-020-01254-9.

[2] Imburgia M, Kois J, Marino E, Lerner H, Mangano FG. Continuous Scan Strategy (CSS): A Novel Technique to Improve the Accuracy of Intraoral Digital Impressions. Eur J Prosthodont Restor Dent. 2020 Aug 31;28(3):128-141. doi: 10.1922/EJPRD_2105Imburgia14.

to obtain accuracy when an IOS reads the distance between different SBs, that sit at different heights away from the soft tissues. Therefore, reducing the distances and the "jump" between SBs could theoretically help to improve scan accuracy.

3. In modern digital protocols, the dentist must accurately capture the Scan Bodies with an IOS scan. Then, the technician must carefully replace the IOS scan mesh, using implant library files on which to model the future restoration. Importantly then, the implant libraries incorporated within the CAD software must not contain spatial errors. During the extraoral cementation of the customized zirconia abutments onto their bonding base, tolerances between the components may cause cementation errors, which then generate customized abutment positional problems that impact the delivery of the provisional restoration. These errors unfortunately cannot be corrected in the final phase of monolithic zirconia.

The purpose of the third study of the thesis[3] was to present a protocol to demonstrate the advantages of using AI within a full digital workflow when fabricating implant-supported, monolithic zirconia crowns (MZCs) to be cemented onto customized hybrid abutments. It was hypothesized that an entirely digital workflow involving AI could be efficiently used for restorations involving single implants and customized hybrid abutments with monolithic zirconia crowns.

4. Guided implant surgery is considered safe and minimally invasive when performed as a flapless procedure. However, flapless guided surgery with implants placed into post-extraction sockets, which are then immediately loaded with complete-arch fixed provisionals without artificial gingiva, has not yet been thoroughly evaluated. As such, questions remain as to whether these types of immediate loaded complete-arch fixed reconstructions can offer both successful implant treatment and esthetic outcomes. Therefore, the fourth study of the thesis aimed to present the outcomes of guided flapless implant placement surgeries, where the implants were immediately functionally loaded with complete-arch fixed prostheses absent of artificial gingiva. This study sought to verify the use of a fully digital workflow for FA restorations. The hypothesis was that the short-term results would not be inferior to those achievable with more conventional approaches, either esthetically or functionally.

---

[3] Lerner H, Mouhyi J, Admakin O, Mangano F. Artificial intelligence in fixed implant prosthodontics: a retrospective study of 106 implant-supported monolithic zirconia crowns inserted in the posterior jaws of 90 patients. BMC Oral Health. 2020 Mar 19;20(1):80. doi: 10.1186/s12903-020-1062-4.

III. DEMONSTRATION OF THE ACCOMPLISHED RESEARCH WORK

III.1.   Trueness of 12 Intraoral Scanners with Full-arch Implant Impression Scanning - A Comparative *in vitro* Study

III.1.1. Background

Evaluating trueness requires a known reference. Concerning dental models, this acquisition can be made with a coordinated measuring machine (CMM), or with an industrial optical or desktop scanner with certified accuracy (within +/- ≤ 5 μm) (9,12,14). Specifically, the IOS acquisitions must be compared with those obtained with one of these reference machines to be mathematically validated.

Precision is "the close agreement between measured quantity values obtained by replicating measurements of the same object under specified conditions". Precision, therefore, refers to the close agreement of the deviations between similar test results. Evaluating precision does not require a reference, because it is sufficient to compare the measurement deviations made with the same IOS (9,12,14)

Recently, a few authors have introduced intraoral indexes (47,48) or geometric shapes with known dimensions (known as custom measuring aids) (49,50) to evaluate optical impression distortions *in vivo*. But most IOSs trueness studies have been performed on plaster models *in vitro* (9,11,38).

Most *in vitro* studies have employed the mesh-mesh method, by directly superimposing the virtual model mesh derived from different IOSs, onto a reference mesh obtained with a certified industrial or desktop scanner (20, 21, 24). Although this approach is intuitive and fast and does provide reliable information about the overall trueness of a scan, it has some limitations. Firstly, the mesh-mesh method relies on surface reconstruction mesh, that is, a geometric approximation of a scanned model, on which it is impossible to perform reliable distance calculations between different scan bodies (SBs) that digitally transfer an implant's position. Additionally, the mesh-mesh approach does not truly replicate what occurs during the early stages of prosthetic CAD modeling. Investigating the accuracy of an intraoral scan after replacing each of the SBs in the mesh with their corresponding library file and then superimposing the two nurbs files, which positions the SBs in the space obtained with the reference scanner and with the IOSs, may obtain more reliable information on the overall scan trueness. This is because one can calculate the exact distances between SBs using 3D calculation software that automatically identifies the SB centroids. This approach requires substantial work and potentially hundreds of superimpositions. However, it is most suited to identify both the overall and

local trueness of an IOS, by accounting for the distances between SBs that cannot be properly calculated on a mesh.

III 1.2. Methods

The present *in vitro* study assessed and compared the trueness of 12 different IOSs when making full arch (FA) implant impressions, which were as follows: ITERO ELEMENTS 5D (Align Technologies, San José, CA, USA); PRIMESCAN and OMNICAM (Dentsply Sirona, York, PA, USA); CS 3700 and CS 3600 (Carestream Dental, Atlanta, GA, USA); TRIOS3 (3-Shape, Copenhagen, Denmark) ; i500M (Medit, Seoul, South Korea); EMERALD S and EMERALD (Planmeca, Helsinki, Finland); VIRTUO VIVO and DWIO (Dentalwings, Montreal, Canada); and RUNEYES QUICKSCAN (Runeyes Medical Instruments, Ningbo, Zhejiang, China).

A type IV gypsum model of an edentulous maxilla with 6 implant analogs placed in positions #11, #21, #14, #24, #16, and #26 had high-precision non-reflective polyether-ether-ketone (PEEK) SBs (Megagen, Daegu, South Korea) screwed on to the analogs, and then the model was scanned (Figure 1). The SBs in the different positions were labeled as S1 (#26), S2 (#24), S3 (#21), S4 (#11), S5 (#14) and S6 (#16). The model had pink gingiva around the implant analogs to clinically simulate an implant-supported fixed FA prosthesis.

Figure 1. The model used in the study with the analogs screwed on.

The gypsum model was initially scanned with a powerful desktop scanner (Freedom UHD, Dof Inc., Seoul, South Korea), to acquire the reference virtual model. This desktop scanner had a white light-emitting diode and two 5.0-megapixel cameras, that acquired the images with patented stable

scan stage technology, that allowed the cameras and lights to move and rotate above and around the stationary model. This scanner captures a detailed model in less than 1 minute, generating virtual models in .STL file format that can be immediately used by any CAD software.

The desktop scanner captured 3 virtual models that were saved in a dedicated folder, labeled with the scanner's name. Then, the quality of each model's mesh was evaluated and reverse-engineered with software (Studio, Geomagics, Morrisville, NC, USA). In the same software, the virtual models were cut and trimmed to isolate the SBs and eliminate the pink gingiva. Once uniformly trimmed, each mesh was superimposed to validate the superimposition method, and to choose the reference model (RM) that was to be used in the study (as previously described (29)). The RM was saved in a specific folder, ready for use.

Once the preparation of the desktop RM was complete, a single operator with over 10 years' experience using intraoral scanners began capturing scans with each IOS being studied. All scans were taken in the same two-month period (January - February 2020) using the latest acquisition software available for each IOS. The operator captured 10 scans for each IOS that included the entire area of the pink gingiva and the 6 different SBs. To minimize the potential effects of operator fatigue, the sequence of scan capture with the different IOSs was randomized, with the scans being spaced out from each other with a rest period of 5 minutes. In all acquisitions, the operator began in the posterior sectors (right or left) and proceeded along the arch using a zig-zag technique. As reported in previous studies (9, 51), this technique provides a slow and constant advancement of the scan along the arch, beginning in the buccal area, then moving occlusally and palatally, and returning to the buccal area. Each arch was scribed above the pink gingiva and the implant SBs. Ten virtual models were captured for each IOS, totaling 120 .STL files. These files were saved in dedicated folders, labeled with the IOS name, and progressively numbered from 1 to 10.

Three different evaluations were performed using the RM acquired with the desktop scanner, and the models derived from the different IOSs. These were: a) a mesh-mesh evaluation to assess the overall general trueness of the intraoral scanning models, b) a nurbs-nurbs evaluation also to assess the overall general trueness of the intraoral scanning models, and c) an evaluation of the linear and cross distances between the different SBs to analyze the local trueness of the intraoral scanned models. The latter being an ancillary measurement from the standpoint of the hypothesis, this thesis focuses only on a) and b). The interested reader may find the distance measurement results in the original article in the Appendix.

The overall general trueness evaluation with the mesh-mesh and nurbs-nurbs methods was performed using reverse engineering software (Studio, Geomagics, Morrisville, NC, USA), by the

same experienced operator (FGM) who captured all the scans. The linear and cross distance between SBs evaluation used the.STL files generated during the nurbs-nurbs evaluation and was performed by another operator with many years of experience using 3D calculation software (Magics, Materialise, Leuven, Belgium).

III.1.3. Results

III.1.3.1. Mesh-Mesh Evaluation

The 10 mesh files generated by the 12 IOSs were imported into the reverse engineering software, where each mesh was cut and trimmed to a uniform size, by using a pre-formed template that removed the pink gingival area. Then, each mesh was superimposed onto the desktop scanner RM mesh, to evaluate the mean distance differences between the models. The signed mean distances between the two superimposed models (in μm) were calculated using a "3D deviation" function, that generated a colorimetric map. The color scale ranged from $+ 100$ μm to $- 100$ μm, and the best deviation results ranged between $+ 30$ μm and $- 30$ μm. Figure 2 shows a colorimetric map with the best results for each IOS.
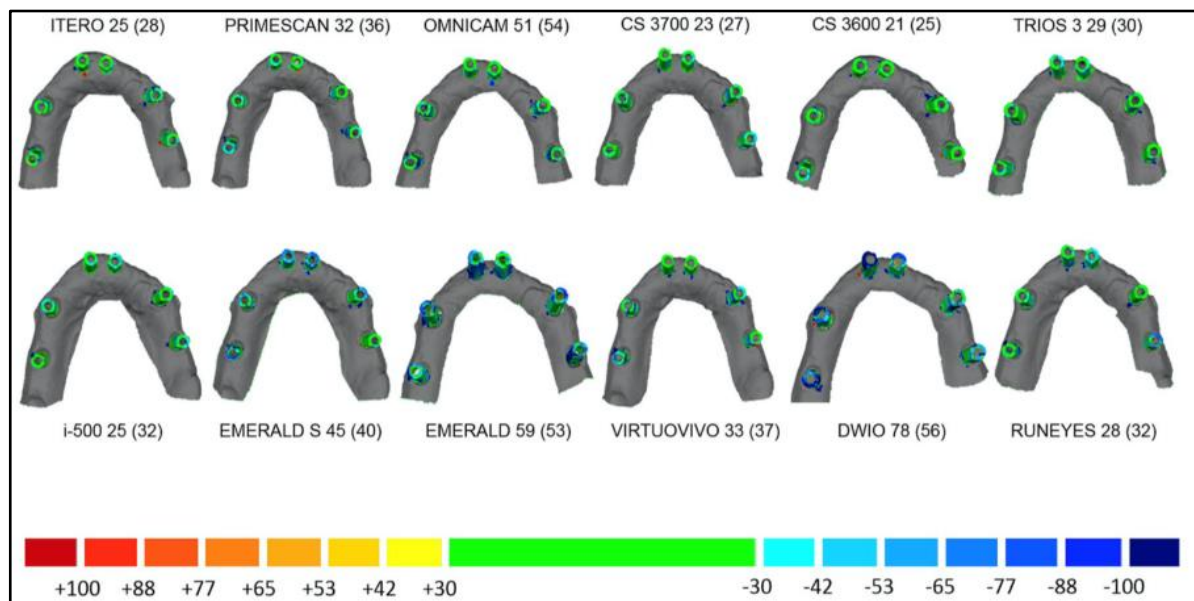
Figure 2. The best single results for each IOS using the mesh-mesh method. The color scale indicates the range of difference between the RM and each IOS in μm. Yellow to red indicates outward deviation, cyan to deep blue indicates inward deviation. Green indicates minimal displacement (< 30 μm) in any direction.

III.1.3.2. Nurbs-Nurbs Evaluation

This evaluation was performed after cutting and trimming the original .STL files as previously described. Then, in the RM and each of the IOSs virtual models, the 6 SB's meshes were replaced

with the corresponding SB library file that was downloaded from an implant manufacturer's official library (Megagen, Daegu, South Korea). Next, a new .STL file was saved for each virtual model that included only the 6 SB's nurbs files, that represented the implant positions sitting free in space. These nurbs files were then used for model superimpositions. Colorimetric maps were generated like before. Figure 3 shows a colorimetric map with the best results for each IOS.
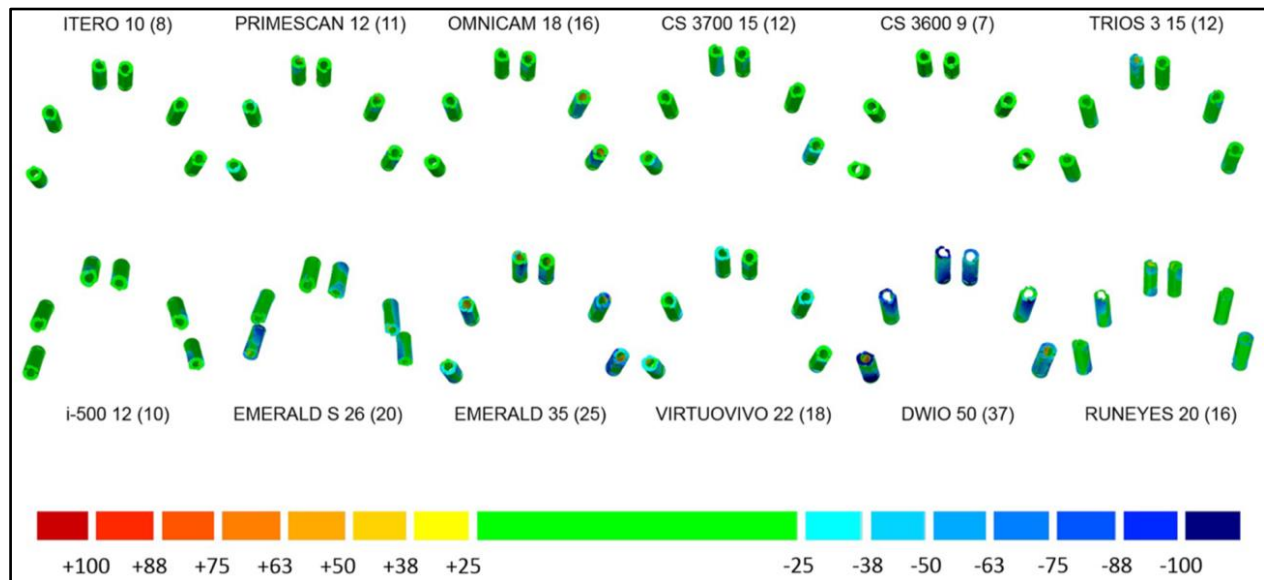

Figure 3. The best single results for each IOS using the nurbs-nurbs method. The conventions are the same as in Figure 2.

The descriptive statistics for the deviations are provided in Table 1 below for both the mesh-mesh and nurbs-nurbs approaches. Figure 4 shows the estimated mean errors (in µm, with 95% CIs) for both approaches.

Table 1. Descriptive statistics for the mesh-mesh and nurbs-nurbs evaluations.

Scanner	Mesh/Mesh		Nurbs/Nurbs	
	Median (Q_1–Q_3)	Mean (95% CI)	Median (Q_1–Q_3)	Mean (95% CI)
CS 3600®	35.5 (31.5–46.0)	36.5 [29.8; 44.6]	23.5 (21.5–34.0)	24.4 [18.0; 33.1]
CS 3700®	29.5 (27.2–34.5)	30.4 [26.7; 34.5]	22.0 (19.8–24.8)	21.9 [19.3; 25.0]
DWIO®	90.5 (84.2–110.8)	98.4 [84.4; 114.8]	65.0 (51.0–82.2)	69.9 [55.0; 88.9]
EMERALD®	76.0 (67.5–81.0)	76.1 [68.1; 85.1]	54.5 (40.8–60.5)	51.9 [43.5; 61.8]
EMERALD S®	51.0 (46.5–54.8)	52.9 [46.8; 59.7]	37.0 (31.2–40.8)	36.8 [31.1; 43.6]
ITERO ELEMENTS 5D®	32.0 (30.2–33.8)	31.4 [29.2; 33.8]	15.0 (14.2–16.8)	16.1 [12.9; 20.1]
MEDIT I-500®	31.5 (29.0–33.8)	32.2 [28.4; 36.6]	20.5 (17.5–25.8)	20.8 [16.9; 25.5]
OMNICAM®	80.5 (72.2–90.8)	79.6 [66.9; 94.6]	56.0 (33.2–62.5)	47.0 [33.7; 65.7]
PRIMESCAN®	39.5 (35.5–41.8)	38.4 [35.8; 41.2]	19.0 (17.0–23.8)	19.3 [16.3; 22.9]
RUNEYES®	41.5 (33.5–56.0)	44.4 [34.9; 56.5]	32.5 (26.0–43.0)	33.9 [26.4; 43.6]
TRIOS 3®	36.0 (35.2–38.5)	36.4 [33.9; 39.1]	20.5 (19.0–23.0)	20.2 [18.1; 22.7]
VIRTUO VIVO®	38.0 (35.2–42.2)	43.8 [33.6; 57.1]	28.0 (26.2–33.2)	32.0 [24.4; 42.0]

Figure 4. Estimated mean errors (in μm, with 95% CIs) for the mesh-mesh and nurbs-nurbs evaluations.

The calculated nurbs-nurbs errors were systematically lower than the mesh-mesh errors. Statistically significant differences were found between the different IOSs (see Table 4 in the original publication in the Appendix, not shown here for reasons of space).

III.1.3.3. Conclusions

Within the limitations of this study, it appears that the nurbs-to-nurbs approach is superior to the mesh-to-mesh approach.

III.2 Continuous Scan Strategy (CSS)-A Novel Technique to Improve the Accuracy of Intraoral Digital Impressions

III. 2.1. Background

Several *in vitro* (52,53,54) and *in vivo* (55, 56,57) studies have demonstrated that IOSs accurately and reliably capture impressions of partially edentulous patients for the fabrication of short-span restorations (single crowns [SCs] and partial prostheses [PPs]). However, other studies (58,59) and reviews (60,61,62) have reported accuracy problems when scanning long-span prosthetic restorations

(fixed partial prostheses supported by multiple implants, and full arches [FAs]). Screw-retained superstructures, (i.e. fixed prostheses screwed directly onto multiple implants) require the highest accuracy because the need for an absolutely passive fit allows for only minimal acceptable tolerances (63).

Although recent technological improvements have been impressive, IOSs still have challenges when scanning multiple fixtures (63). These difficulties result from the mechanism by which an IOS acquires the images; by "attaching" frames to each other during the acquisition procedure. Regardless of the acquisition technology, this intrinsic error increases with the extension of the scan (14,60,61,62). In fully edentulous patients who lack reference points, accuracy is more difficult to achieve when the IOS reads the distance between different SBs, which often stand at different heights above the soft tissues (64). Other potential sources of inaccuracy include the light conditions (65), the operator's IOS experience level (66), the implant position, depth and angulation (64) and the SBs themselves (67).

It has been suggested that reducing the distances (or the "jump") between SBs could improve the accuracy of the scan, thereby reducing the intrinsic scan error. Tallarico et al. (68) introduced a method for totally edentulous patients, based on 3D-printing a duplicate of the patient's pre-existing removable complete prosthesis. This replica, ground out in the SB area and inserted into the mouth, allows for the capture of a sufficiently accurate impression to manufacture FA fixed restorations (Toronto bridges), while also simplifying registering the Vertical Dimension of Occlusion. Mangano et al. (69) developed and applied this strategy to the manufacture of bar-retained overdentures, with the bar being milled in polyether-ether-ketone (PEEK). More recently, a hybrid digital/analog approach was proposed, which used custom measuring aids (CMAs) (49,50) and solid indexes (51) to connect the SBs to improve the accuracy of FA digital impressions. The rationale behind these 2 differing approaches was to reduce the distances between different SBs, while providing artificial landmarks that reduced acquisition inaccuracies, so that long-span, passively fitting, screw-retained superstructures could be fabricated.

To potentially reduce these technology-based errors, we developed a novel scanning technique named "Continuous Scan Strategy" (CSS) was developed, in which the scan bodies are connected with thermoplastic resin to eliminate the "jumps" between different SBs. It was hypothesized that by reducing these "jumps", the accuracy of intraoral scanning for FA restorations would be improved. The method was verified in a series of clinical cases. The retrospective study chosen for this thesis summarizes our clinical experience with CSS.

III. 2.2. Methods

Patients enrolled in this retrospective clinical study were selected from the customized dental records of two private dental centers in Palermo and Milan, Italy. Patients who had been treated with multiple (≥4) implants (Nobel Active Internal Connection®) via a full digital workflow with the Continuous Scan Strategy for restoration with fixed, implant-supported prostheses (PPs and FAs), over 4 years (2014–2017). Demographic data are found in the original publication. The approach that was followed in each case is described below.

A one-piece titanium SB (Scan Abutment, New Ancorvis, Bargellino, Italy) was screwed onto each implant, with the notched surface or the oblique section of the head oriented towards the buccal. After confirming the SBs were screwed to place correctly, thermoplastic resin was heated and molded intraorally to connect the different SBs on their palatal/lingual aspect. To increase the stability and avoid detachment of the thermoplastic resin, flowable composite resin was added in small quantities laterally to both the SBs and the thermoplastic resin. When polymerized, this solidified the entire assembly. Neither the thermoplastic material nor the composite interfered with the notched surface (marker surface) of the SBs, whose heads were left completely free and visible. Once the stability and rigidity of the assembled elements were verified, the IOS scanning was performed (Trios3, 3 Shape, Copenhagen, Denmark) using the "zigzag" technique, beginning with the most distal SB (palatal/lingual aspect), then passing over it while moving towards the buccal aspect, and progressively advancing to the next SB, guided by the thermoplastic resin. Particular attention was paid to capture all the details of each SB.

Once the scan was completed and the mesh quality verified, standard tessellation files (.STL) were sent to the dental technician for modeling the final structure in CAD software. Care was taken during the CAD modeling to perform the best possible superimposition (best-fit) of the SB library files onto their corresponding mesh. The superimposition was deemed ideal when an overall mean deviation of ≤ 20 μm was attained, such that the technician could proceed.

In the CAD software, appropriate titanium bases were selected, and the final prosthetic superstructure was designed. Then, with a 5-axis milling machine (DWX-52, Roland, California, USA) a replica of the same superstructure was milled in a rigid and radiopaque material (polyurethane for the PPs; metal for the FAs). This replica verified intraorally that the final prosthesis fit was passive (the Sheffield test), by being screwed into place on the corresponding titanium bases. The marginal adaptation was verified both clinically and radiographically with a series of intraoral x-rays. Once the passive adaptation was deemed optimal, the technician could proceed with manufacturing the final zirconia prosthesis, beginning with the CAD product itself. If the replica did not optimally fit,

or the best fit values detected in the early stages of the CAD were considered unreliable (≥ 30 μm), the polyurethane replica was separated into several parts that were screwed to place individually, to ensure each part was passively adapted. Then the parts were connected with low-contraction resin. The connected assembly was re-scanned with a desktop scanner, and the CAD product was modified according to the connected replica. After the passive fit and optimal adaptation of the solid second CAD replica had been confirmed, it was deemed ready for use for the manufacturing of the final prosthesis.

The final monolithic zirconia prosthesis (Katana ML, Kuraray, Norithake, Japan) was milled with the same 5-axis milling machine (DWX-52), sintered, and where necessary, colored on the buccal surfaces. Particular attention was paid to milling the titanium luting base engagements, to provide close correspondence and ideal positioning between parts. The position of the luting base was determined exclusively by the milled housing inside the zirconia structure. The milling parameters of the interface were kept tight to minimize any play that would lead to inaccuracies, and consequently, a structure misfit.

At this point, the dental technician cemented the luting bases inside the monolithic structure that were selected during the CAD modeling. This cementation was performed extraorally, using anaerobic cement (Variolink Hybrid Abutment, Ivoclar, Vivadent, Schaan, Lichtenstein) without the aid of a 3D printed model. After this, the final monolithic zirconia prosthesis was delivered to the clinician for patient insertion.

In all cases, the rehabilitations were performed following the CSS protocol, starting from a direct IOS optical impression, to fabricate monolithic full zirconia prostheses that were screwed directly onto the implants. The most important steps of the procedure are demonstrated in Figures 5 to 8 (below). Non-parallel implant orientations were limited due to precise computer-guided implant planning and positioning. However, if anatomic limitations compromised the implant axis to not coincide with the prosthetic axis, a digital correction of the angled screw hole was made, using connection screws with Cardan engagement.
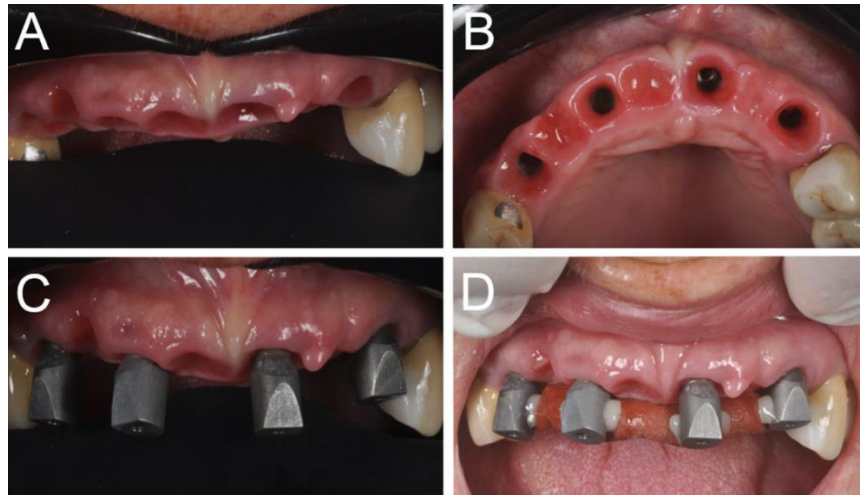
Figure 5. A partially edentulous patient with four implants in the anterior maxilla ready for intraoral scanning. (A) Frontal view showing the mucosal collars after removing the healing abutments. (B) Occlusal view with the mucosal collars visible. (C) The SBs screwed onto four implants. (D) Thermoplastic material and composite resin connecting the SBs avoiding their marker surfaces and heads.
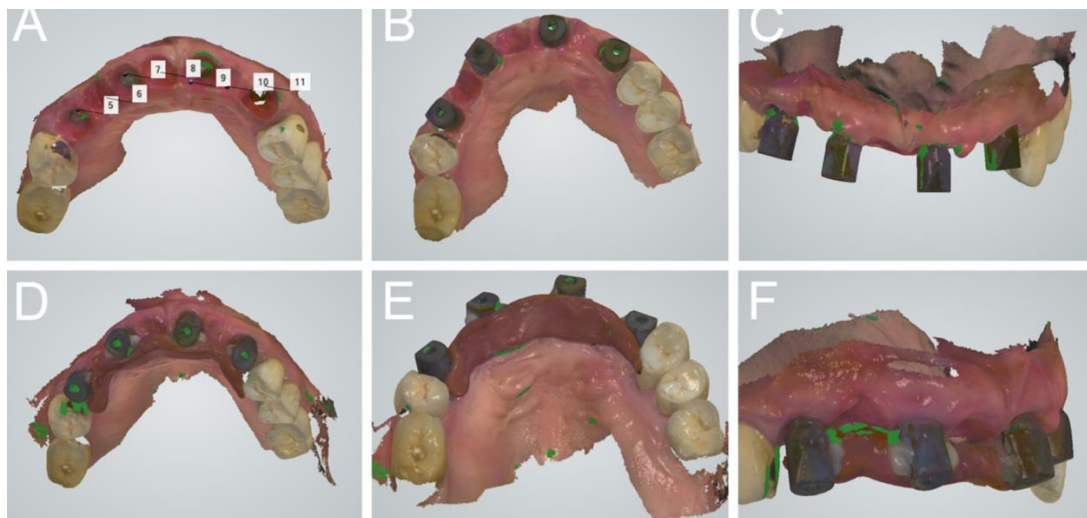
Figure 6. Intraoral scan screenshots made of the same partially edentulous patient (in Figure 6) with four implants in the anterior maxilla. (A) Occlusal view with the mucosal collars removed. (B) Occlusal view with the SBs screwed onto four implants. (C) Frontal view of the SBs. (D) Occlusal view with the thermoplastic material and composite resin lingually connecting the SBs, to avoid interfering with the SB marker surfaces and heads. (E) Palatal view of the SBs linked together with thermoplastic material and resin. (F) Lateral view of the connected assembly.

Figure 7. A replica of the final CAD project milled in polyurethane hard resin and screwed intraorally to verify passive fit and proper marginal adaptation. Intraoral radiographs verified the adaptation. (A) Radiographic image of the replica on the right side implants. (B) The milled replica screwed intraorally. (C) Radiographic image of the replica on the left side implants.

Figure 8. The final screw-retained fixed PP is ready for patient delivery, seen from the (A) right view, (B) the frontal view, and (C) the left view.

III. 2.3. Results

In the studied period, 40 eligible patients were restored with 45 long-span implant-supported restorations (10 fixed PPs supported by ≥ 4 implants, and 35 FAs supported by 6 to 8 implants), fabricated with a complete digital workflow that began with the CSS technique.

The primary outcome of this study was the superstructures' passive fit and marginal closure quality recorded at 2 time points: Time 0 (T0) when the CAD-designed superstructure was tested with a milled polyurethane or metallic replica and Time 1 (T1) when final monolithic zirconia restoration was delivered. The marginal closure and adaptation were determined by careful clinical and manual inspection by a prosthodontist using magnifying lenses (Zeiss 4.5%, Oberkochen, Germany). This was confirmed with intraoral radiographs that captured each implant platform.

At T0, 40 out of 45 replicas demonstrated ideal marginal adaptation and passive fit. At T1, all final monolithic zirconia restorations demonstrated passive fit and excellent marginal adaptation, except for one that exhibited minimal friction and fractured minutes after being screwed to place. The fracture was probably caused by mandibular flexion as it occurred when the patient yawned.

The secondary outcomes of the study were the survival of the implants and the success of the prostheses. These outcomes were assessed 2 years after delivery of the final prostheses (time 2 = T2)

and were recorded during the scheduled recall visits for professional hygiene. Implant survival indicated that all the implants were regularly in function, under masticatory load; implants that were lost for any reason (fracture of the fixture, loss of osseointegration, or removal of the implant due to mechanical overload or infection) were classified as failures. Finally, prosthetic success indicated that the final monolithic zirconia prosthesis was regularly in function during the entire period 2-year follow-up (from delivery to final inspection) without the occurrence of any major mechanical (such as macroscopic fractures of the framework), minor mechanical (related to the pre-established components sold by the implant manufacturer, e.g., screw loosening) or minor technical (related to superstructure problems, such as chipping) complications.

At T2, the implant success rate was high (100%), with all implants in function. As for the prosthetic outcomes, at T2, one prosthesis was found to be chipped in the distal extension beyond the upper right first molar, which was resolved by polishing the surface of the fractured connector. In another case, the prosthesis was found to be fractured. At the end of the study, 42 of the 45 final zirconia prostheses (93.3%) were considered successful because they functioned without any complications over the two-year observation period. The incidence of prosthetic complications was 6.7%. Of these complications, two (fractures of the zirconia framework) were major, and one (chipping) was minor. All these complications were technical.

III. 2.4. Conclusions

At present, the scientific literature does not consider direct intraoral scanning a sufficiently reliable method to capture impressions for the fabrication of long-span implant-supported prosthetic restorations, particularly in the case of full arches. The findings of this study illustrate that the continuous scanning approach makes it possible to work with a low intrinsic scan error rate even in FA cases.

It is important to note that in all of the cases, a discrepancy > 30 μm between the IOS mesh and the multiple SB libraries, was detected during the early stages of CAD production when the technician was attempting to determine the "best-fit" of the SBs. This indicated that important errors were introduced between mesh congruence and the SB library files. The absence of perfect congruence between these two SB files in the early CAD stages can potentially lead to positional errors that will impact the fit accuracy of the final restoration. This is a critical issue that needs to be addressed.

There are also a few limitations to be mentioned. This study was retrospective, with a short follow-up period and with most of the prosthetic restorations delivered in the maxilla, which offers more

stable landmarks for IOS capture (such as the hard palate) than the mandible. Moreover, the design of this study was essentially clinical, in that the protocol did not include proper mathematical quantification of the scanning errors and did not include comparative control subjects treated non-digitally with conventional impression procedures. Finally, only one IOS (Trios3) was used. Further long-term follow-up and prospective studies are needed to confirm these positive results.

Despite these limitations, the results are convincing in that CSS is a viable option for capturing accurate intraoral digital impressions for the fabrication of precise long-span implant-supported restorations.

III. 3. Artificial Intelligence in Fixed Implant Prosthodontics- A Retrospective Study of 106 Implant-supported Monolithic Zirconia Crowns Inserted in the Posterior Jaws of 90 Patients

III. 3.1. Background

In modern digital protocols, the dentist must capture an accurate intraoral scan of the implant scan body (70), and the technician when modeling, must carefully replace the scanned mesh with the implant library files (8). Furthermore, the implant libraries within the CAD software must not contain spatial errors. However, working precisely during these fabrication stages may not be sufficient because during the extraoral cementation of customized zirconia abutments onto their bonding base, tolerances between the components may cause cementation errors (9,71). These errors, even if only a few degrees, during patient delivery can generate positional problems between the customized abutments and the provisional restoration, because the components in the mouth will not be in the exact CAD-planned positions (69). Small adjustments to the provisional can be made to the interproximal contacts or the occlusion in the polymethylmethacrylate (PMMA), to compensate for these spatial errors. But these types of adjustments are not acceptable for the monolithic zirconia restorations (69,72). The definitive monolithic zirconia cannot be retouched in the mouth, (72, 73) so they must be free of positional errors when delivered.

To overcome this problem, experienced dental technicians will position the already-assembled individual abutments into the implant analogs of a 3-dimensional (3D) printed model, and then scan them with a desktop scanner. This method obtains the abutment relative positions, their anatomy, and the margin line (74). This approach requires an extra step that forces the technician to print a cast (with related costs and problems) and to model the definitive zirconia restorations on a mesh that, by definition, is a surface reconstruction and geometric approximation of the actual scanned objects (14,71).

This additional step can be avoided by using artificial intelligence (AI). AI is a wide-ranging branch of computer science concerned with building smart software or machines, capable of performing tasks that typically require human intelligence (76). AI is commonly defined as "the ability of a system to interpret external data, learn from that data, and use what was learned to achieve objectives and goals through flexible adaptation" (76). Machine learning (ML) is a subset and the foundation of AI, where computer systems perform specific tasks that approximate human cognition, without using explicit instructions, by solely relying on patterns and mathematical models involving computer algorithms. In this way, computer programs improve their performance automatically through experience. Simply explained, in machine learning, a computer is fed data, and then the computer uses statistical techniques to help the computer "learn" how to get progressively better at a specific task (28). AI, therefore, represents a valuable addition to fixed Implant Prosthodontics. CAD software can be "instructed" to save an individual abutment's stereolithographic (.STL) file after it had been ideally modeled by a technician, which can then be automatically retrieved when needed (9). At the end of the provisionalization, when the temporary restoration is removed, the dentist can capture a new intraoral impression of the hybrid abutment in the correct position, regardless of whether the abutment margins are visible or subgingival. The mesh captured with this post-provisionalization intraoral impression is then imported into the CAD software. The captured temporary individual abutment is then automatically recognized and removed and replaced with the STL file of the final zirconia abutment that was previously modeled by the dental technician (71).

III. 3.2. Methods

90 patients were included in this retrospective study, whose missing teeth were restored with 106 implant-supported Monolithic Zirconia Crowns (MZCs) on 106 individual customized abutments. The study method consisted of 8 steps, as follows:

1. An intraoral scan of the implant position was obtained with Scan Bodies in place. The IOS-scanned image was carefully verified to confirm the quality of the IOS impression. The clinician then removed and replaced the scan body with a healing abutment, and the IOS optical impression .STL files were sent to the dental laboratory (This is shown in Figure 9).
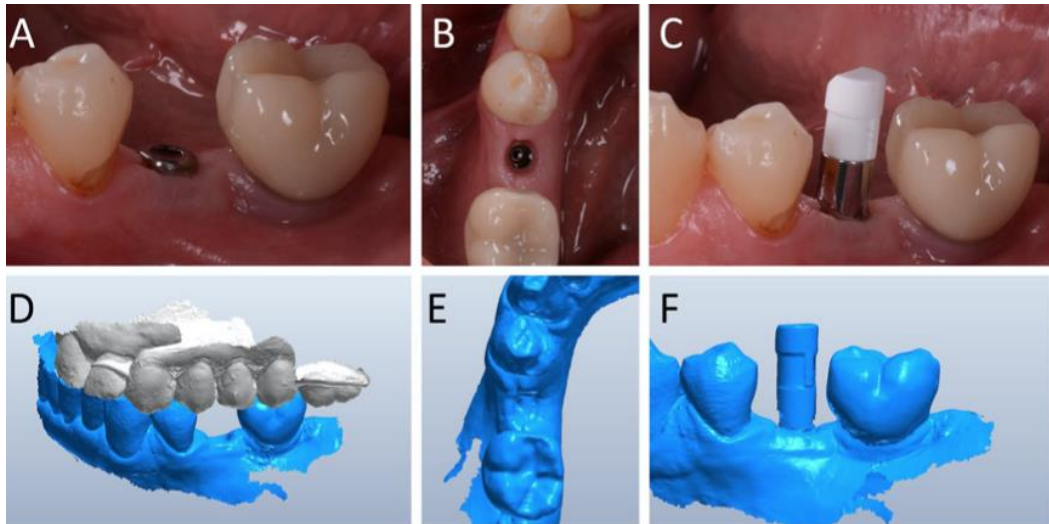
Figure 9. The initial intraoral scan of a mandibular 2nd premolar. (A) The healing abutment in position. (B) The healing abutment is removed for the scan. (C) The scan body is placed in position. (D) Intraoral scan of the master model without the scan body, opposing the antagonist arch. (E) The optical impression of the mucosal collar. (F) The optical impression of the implant scan body in position.

2. Designing the individual/customized abutment and provisional crown using computer-aided design (CAD) software. The technician imported the scan body .STL files into the CAD software, and then by using the software's algorithm, replaced the IOS-captured scan body mesh with the corresponding implant library file, by superimposing key points of the scan body's surfaces. Next, the technician modeled the individual abutment's occlusal clearance and peri-implant tissue components, and the provisional crown to be cemented over it. The .STL files for the abutment and crown were saved in a specific folder created within the CAD software, which contained all the modeled individual abutments of all treated study subjects, where they waited ready for production. (Figure 10).
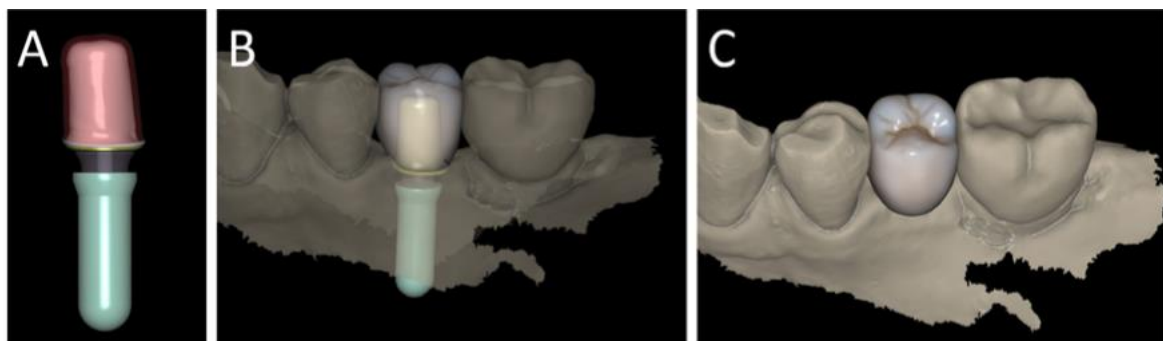

Figure 10. CAD of the individual abutment and the provisional crown. (A) The individual abutment is modeled in CAD and saved in a dedicated folder. (B) The designed individual abutment and the provisional crown in place within the CAD software. (C) A photorealistic rendering of the provisional crown in place within the posterior quadrant.

3.   Generating and milling the individual hybrid zirconia abutment and cementing it onto a titanium bonding base. Then milling the provisional polymethyl-methacrylate (PMMA) crown. The CAD-designed abutment and provisional crown were both milled from their model .STL files, after which the dental technician sent the dentist the hybrid abutment with the provisional crown for clinical insertion.

4.   The clinical insertion of the hybrid abutment and the provisional PMMA crown. The provisional crown verified the adaptation of the implant under load and helped mature the mucosal tissues over the next 1- 2 months. Then the patient was recalled for the final restorative scanning (Figure 11).
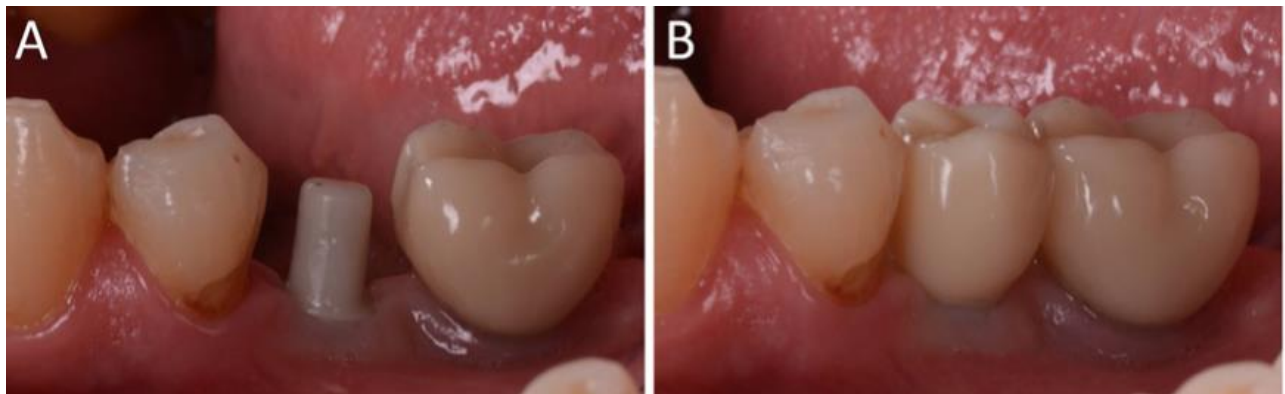
Figure 11. Delivery of the individual hybrid abutment and the provisional crown. (A) The individual hybrid abutment in place on the implant. (B) The provisional polymethyl-methacrylate (PMMA) crown after being cemented onto the abutment.

5. The intraoral scan of the hybrid abutment. With the tissues conditioned and matured by the provisional restoration, the provisional crown was removed, the abutment was carefully cleaned of any residual cement particles, and a 4th scan of the zirconia abutment in position was captured. The provisional crown was re-cemented, and the .STL file mesh derived from the fourth IOS scan was sent to the laboratory (Figure 12).
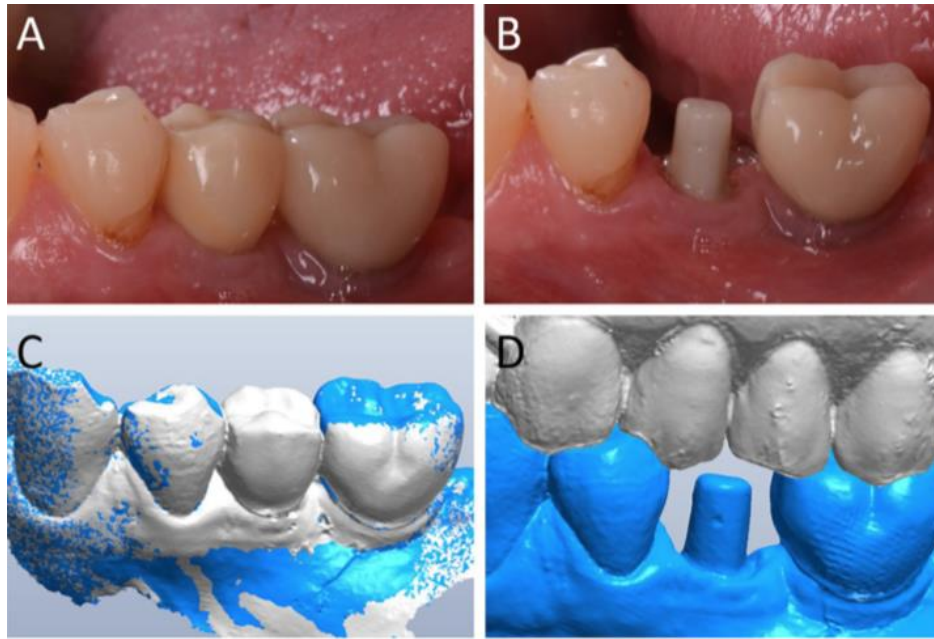
Figure 12. Following the provisionalization period, another digital impression is made with the provisional crown (to capture the occlusal relationship), and without the provisional crown, (to capture the intraoral position of the zirconia abutment and the soft tissue architecture). (A) The PMMA crown in position after 2 months. (B) The individual hybrid abutment after 2 months in place. (C) the master model with the functionalized provisional in position, provides the dental technician with the anatomy of the provisional and its occlusal limits. (D) Without the provisional, the abutment is captured with an intraoral digital impression to generate a master model.

6. The Computer-aided Design of the final crown with an automated margin line designed and determined with artificial intelligence (AI). The following procedures were performed using algorithms within the software that were intrinsic to the AI. The software then replaced only the highlighted portion of mesh captured intraorally, with the corresponding .STL file of the original modeled abutment. The dental technician could test the quality of the overlap in micrometers by generating a colorimetric map. The original modeled abutment file was now integrated with the mesh of the master model, in the correct spatial position. Using the intrinsic AI, although subgingival, the software automatically traced the margin line of the implant abutment (Figure 13), for the technician to design the final crown contours.
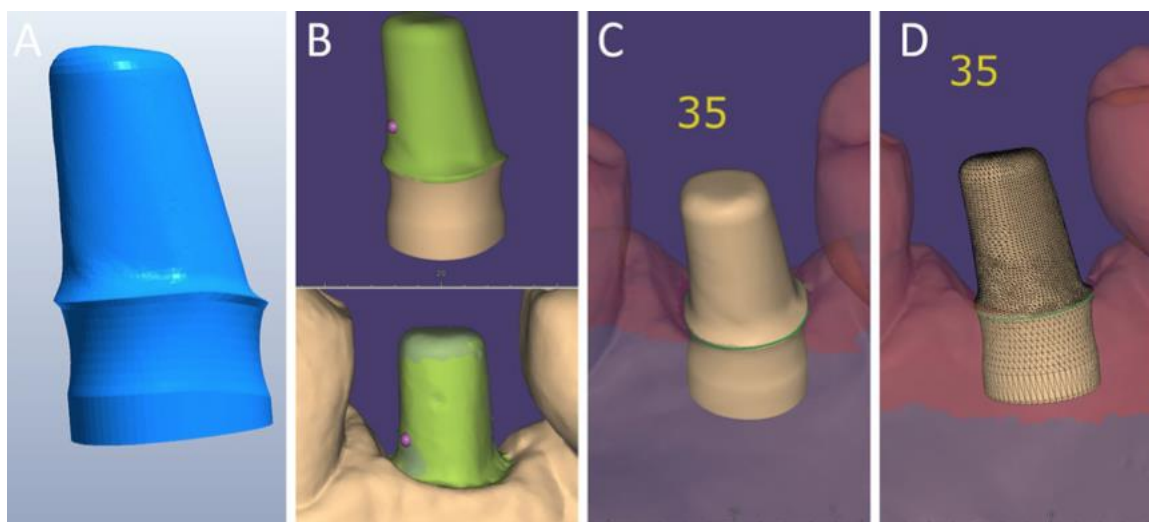
Figure 13. Artificial Intelligence (AI) applications in fixed Implant Prosthodontics. (A) The original.STL file of the CAD designed individual abutment (previously saved in a dedicated folder), was recalled by the system. (B) The original CAD-designed abutment is superimposed on the mesh captured intraorally. (C) AI automatic margin line detection. (D) The original CAD model mesh detail with its subgingival margin clearly represented and visible.

7. The milling, sintering and characterization of the final Milled Zirconia Crown (MZC) (Figure 14)
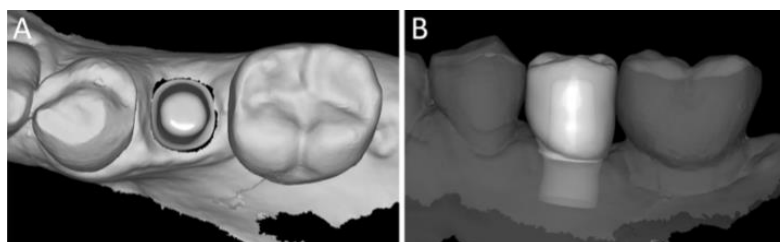
Figure 14. The final CAD scenario. (A) The occlusal view of the individual abutment in position. The technician can now model the final zirconia crown over it using a library file. (B) The facial view of the CAD-designed final crown.

8. The clinical delivery of the final Milled Zirconia Crown (MZC) (Figure 16).
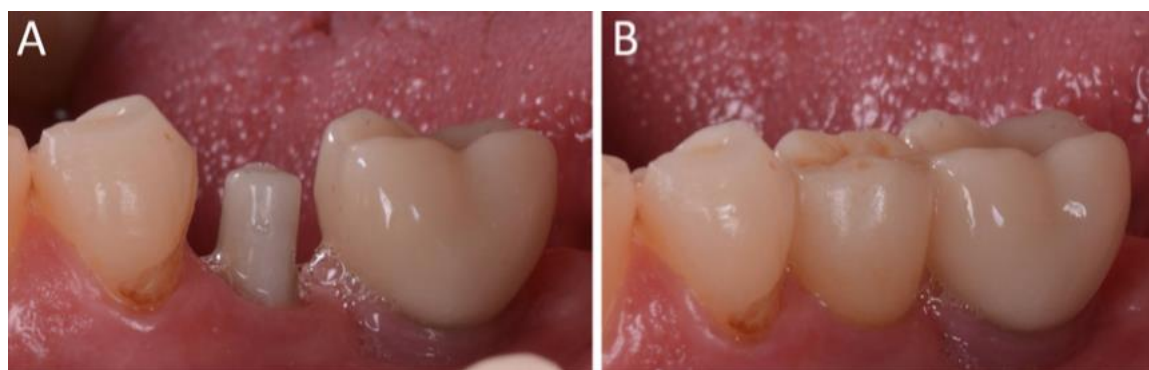
Figure 15. Delivery of the final zirconia crown. (A) The facial view of the individual hybrid abutment in place, ready to receive the MZC crown. (B) The final zirconia crown in place illustrating its' naturally appearing aesthetics.

III. 3.3. Results

The outcomes were quantitative (mathematical) and qualitative (clinical).

The quantitative outcomes were determined by superimposing each original CAD-designed abutment over each abutment's intraorally-scanned mesh of its corresponding digitally produced zirconia abutment. A digital colorimetric map generated by the software highlighted spatial deviations between the two different abutment files of each abutment (n=106), with a 30 μm deviation threshold (Figure 16). Any deviation ≤ 30 μm was represented in green. Deviations > 30 μm were represented along the orange-red spectrum, with red indicating there were major increased dimensional deviations away from 30 μm, and any deviations < 30 μm were represented in blue, with dark blue indicating major decreased dimensional deviations well-below 30 μm. This colorimetric mapping of all abutments revealed a mean deviation of 44 (± 6.3) μm, with a median value of 45 μm and a range of 28 to 64 μm. The 95% confidence interval was 42.9 to 45.1 (Figure 16).
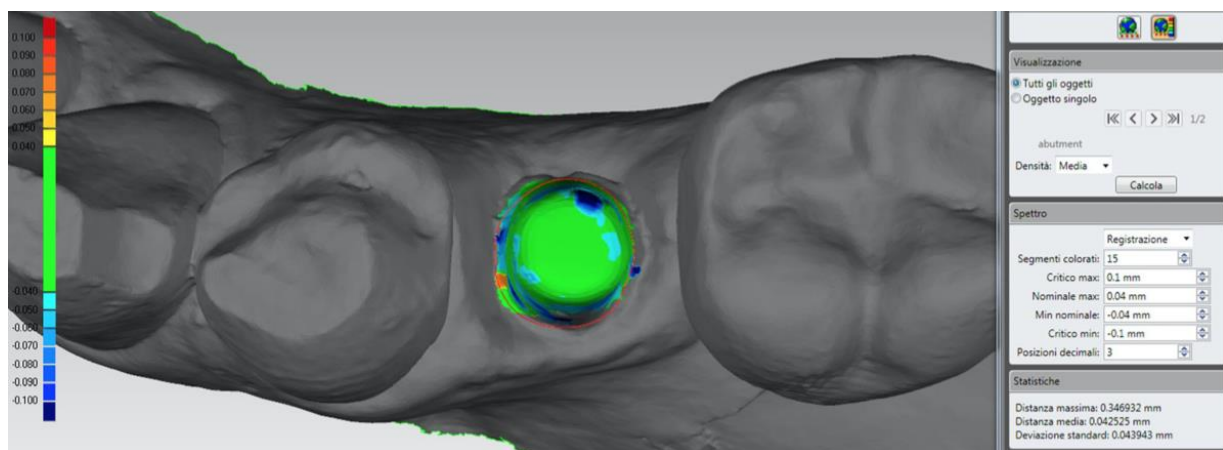
Figure 16. An example of the superimposition of the original CAD-designed abutment over the mesh of the actual zirconia abutment.

As for the qualitative outcomes, these were primary and secondary. The primary outcome was a subjective clinical scoring of 4 characteristics by two experienced clinicians (a prosthodontist and a periodontist). This was a five-level grading and the grades were as follows: 5 - completely satisfactory quality; 4 -satisfactory quality; 3 - acceptable quality; 2 - less than acceptable quality; 1-non-acceptable quality. Means and standard deviations were calculated from the two raters' ratings, and an overall mean was also calculated.

Table 2. Results of the clinical scoring.

	Prosthodontist Mean score (±SD)	Periodontist Mean score (±SD)	Overall Mean score (±SD)
Quality of the marginal adaptation/ closure	4.41 (0.7)	4.41 (0.7)	4.41 (0.7)
Quality of interproximal contact points	4.49 (0.7)	4.43 (0.6)	4.46 (0.6)
Quality of occlusal contacts	3.84 (0.8)	3.94 (0.9)	3.89 (0.8)
Chromatic and aesthetic integration	4.25 (0.7)	4.04 (0.6)	4.15 (0.7)
Overall mean score (±SD)	4.25 (0.8)	4.20 (0.7)	4.23 (0.7)

The secondary clinical outcome measures were the survival and success of the 106 MZCs, as defined by the Cutler and Ederer life-table analysis[4] (Tables 3 and 4).

Table 3. Cumulative survival rates of the 106 implant-supported MZCs, where survival was defined as an MZC still in function at the end of multiple time intervals between 0 months to 36 months.

Time interval (months)	Implant-supported crowns at the start of the interval	Drop-outs during the interval	Implant-supported crowns at risk	Failures during the interval	Survival rate within the period (%)	Cumulative survival rate (%)
0–6	106	2	104	1	99.03%	99.03%
6–12	94	1	93	0	100%	99.03%
12–18	84	0	84	0	100%	99.03%
18–24	75	1	74	0	100%	99.03%
24–30	69	0	69	0	100%	99.03%
30–36	40	0	40	0	100%	99.03%

Table 4. Cumulative success rates of the 106 implant-supported MZCs, where a "success" was an MZC that was absent of any biologic and/or prosthetic complications at the end of multiple time intervals between 0 months to 36 months.

Time interval (months)	Implant-supported crowns at the start of the interval	Drop-outs during the interval	Implant-supported crowns at risk	Failures during the interval	Survival rate within the period (%)	Cumulative survival rate (%)
0–6	106	2	104	5	95.2%	95.2%
6–12	94	1	93	1	98.9%	94.1%
12–18	84	0	84	0	100%	94.1%
18–24	75	1	74	1	98.6%	92.7%
24–30	69	0	69	1	98.5%	91.3%
30–36	40	0	40	0	100%	91.3%

---

[4] Cutler SJ, Ederer F. Maximum utilization of the life table method in analyzing survival. J Chronic Dis. 1958;8(6):699-712. doi: 10.1016/0021-9681(58)90126-7. PMID: 13598782

III. 3.4. Conclusions

In this retrospective clinical study, a complete digital protocol using AI was utilized to optimize restoring single locking-taper implants with 106 MZCs cemented onto customized hybrid abutments. Both the qualitative and quantitative results were favorable, indicating the potential that a fully digital worflow involving AI has in this indication. The MZCs demonstrated high-quality marginal adaptation, interproximal and occlusal contacts, and esthetic integration. Importantly, during the period of study observation and the follow-up (0-36 months), few biologic (1.9%) and few prosthetic (5.7%) complications affected the implant-supported MZCs. Accordingly, high survival and success rates were found (>90%). Additional studies with longer follow-up periods using different prosthetic restorations (such as implant-supported fixed partial prostheses) are necessary to provide further support for this AI-enhanced restorative fabrication protocol.

III.4. Complete-Arch Fixed Reconstruction Using Guided Surgery and Immediate Loading - A 1-year of Follow-up Retrospective Clinical Analysis of 12 Patients[5]

III. 4.1. Background

Within the literature, most clinical studies of full-arch implant restorations are "Toronto Bridges", also known as "All-on-Four" and/or "All-on-Six" dentures. These hybrid fixed prostheses contain a connecting bar between the implants that is covered by artificial gingiva fabricated from either porcelain or resin, depending on the restorative treatment chosen (78-80). There is no doubt that even with these hybrid prostheses, guided implant surgery offers a more precise implant placement concerning the location of the screw holes, and provides for the pre-fabrication of a milled provisional for same (or next) day delivery (78-80, 81-83, 88). However, although these implant-supported dentures are easier to clinically manage, they cannot reproduce ideal aesthetics because of the presence of artificial gingiva (84,85). Moreover, effective daily oral hygiene maintenance can be much more difficult for the patient to manage with these hybrid prostheses (86, 87). Conversely, immediate fixed prostheses without a pink component, that are immediately loaded following placing implants into fresh extraction sockets, are highly appreciated by patients. These fixed restorations are highly esthetic, while they reduce surgical invasiveness and lessen surgical and prosthetic treatment sessions, which markedly reduces overall treatment times.

---

[5] Some figures in this chapter are reprinted from Lerner H. Digital Occlusion in the Workflow of Implant Restorations. In Kerstein, R.B. (2019). Handbook of Research on Clinical Applications of Computerized Occlusal Analysis in Dental Medicine (pp. 945 - 995). Hershey, PA: IGI Global. with the permission of the publisher.

The study described herein is one of only a few endeavors involving complete-arch fixed reconstructions without artificial gingiva, performed with guided, flapless implant placement into post-extraction sockets, with immediate functional loading (89). This study illustrates all the advantages of utilizing a complete digital workflow when restoring naturally appearing, highly aesthetic full-arch implant-supported restorations.

III.4.2. Methods

A retrospective patient record evaluation was conducted involving 12 patient charts held at a private dental clinic in Baden-Baden, Germany (Henriette Lerner Dental Clinic). Over a 3-year long period (from January 2014 - December 2017), the 12 patients were treated with guided implant surgery employing an established digital workflow that has been previously studied (27), and has become known as "scan, plan, make, done".

III.4.2.1. Scan - Digital Data Acquisition

A complete clinical, photographic, and radiographic dataset was acquired for each patient (Figure 17 A-E), accompanied by 2-Dimensional (panoramic) radiographs (Figure 17 F), periodontal probing, and 3-Dimensional CBCT scans of both arches. Conventional impressions were obtained from each patient, with stone casts poured to study each case's specifics (Figure 17 G, H). Digital smile-design software of each patient's photographic data was used to evaluate the length and width of each patient's teeth.
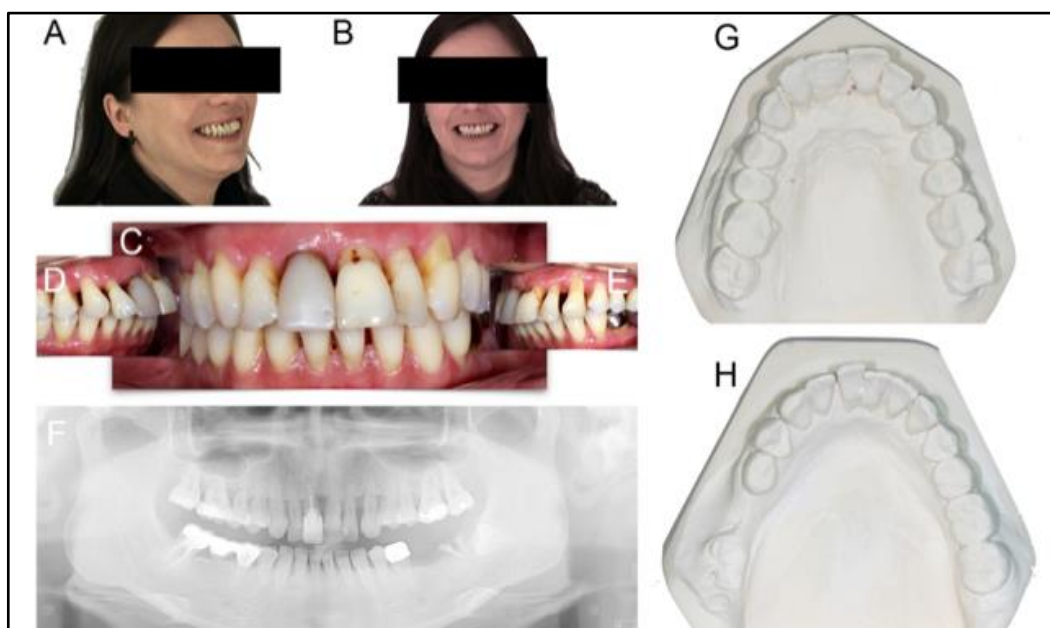
Figure 17. The diagnostic data set of the pre-operative clinical presentation of an example study patient. (A-E) clinical photographs (F) panoramic radiographic image, and (G, H) diagnostic casts.

A diagnostic wax-up that would idealize the problematic morphology of the patient's teeth was prepared on the stone casts to simulate the proposed treatment outcome. Then a desktop scanner (Deluxe, Open Technologies srl, Brescia, Italy) optically impressed the idealized wax-up, to obtain .STL files that were to be uploaded into guided surgery planning software (Figure 18 D).
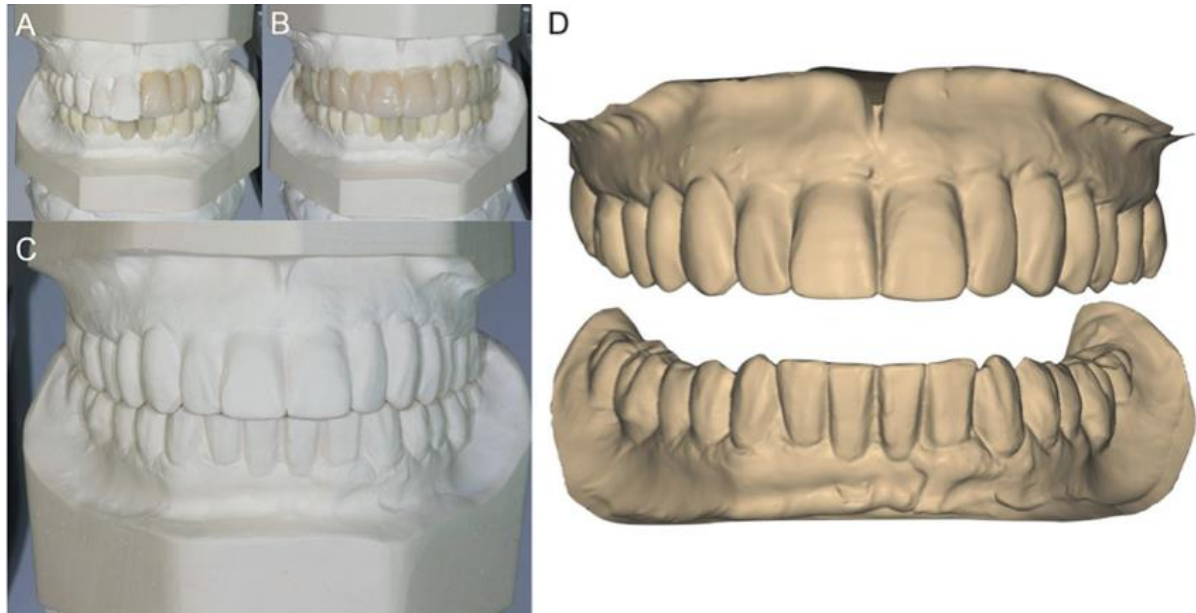
Figure 18. The diagnostic wax-up of the improved dental morphology (A-C), and the .STL files of the wax-up to be uploaded into guided implant surgery planning software (D).

III.4.2.2. Plan - Planning All the Virtual Preoperative Data

In the guided implant surgery software (RealGuide, 3Diemme, Como, Italy), the diagnostic wax-up .STL files, with the ideal teeth morphology, were imported and superimposed on the bony anatomy obtained from CBCT imaging. Then, the surgeon and the dental technician, guided by the prosthetic wax-up, developed a prosthetically-driven surgical plan that placed each implant into the correct position and depth, with an optimal axis of inclination (Figure 19 A-D).
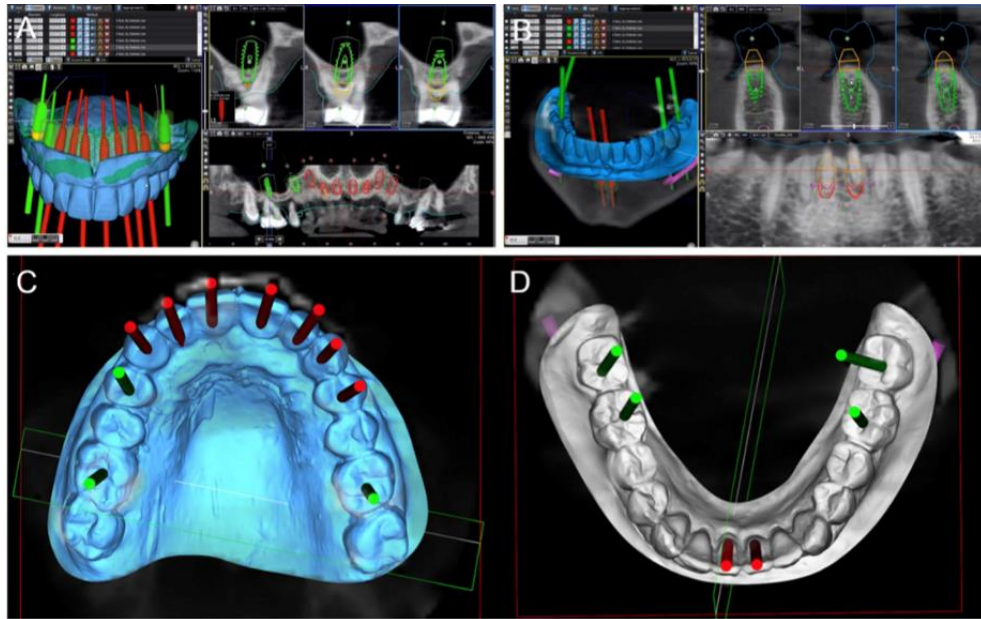
Figure 19. The prosthetically-driven 3D implant planning in the RealGuide software.

To definitively engage the residual bone with the implant fixtures, implant lengths were chosen that often exceeded the apex depth of the fresh extraction sockets by at least 3 to 4 mm. For an optimal prosthetic outcome, the implants were positioned in each socket's palatal aspect, 2 to 3 mm palatal to the residual buccal bone wall, and similarly inclined to the extracted tooth's long axis. This was performed in all positions to be implanted. After planning, 3D models of the digitally- planned software outcome were printed using a desktop printer, with implant analogs inserted into the models (Figure 20 A, B). From these 3D models, surgical guides were fabricated (Figure 20 C, D).
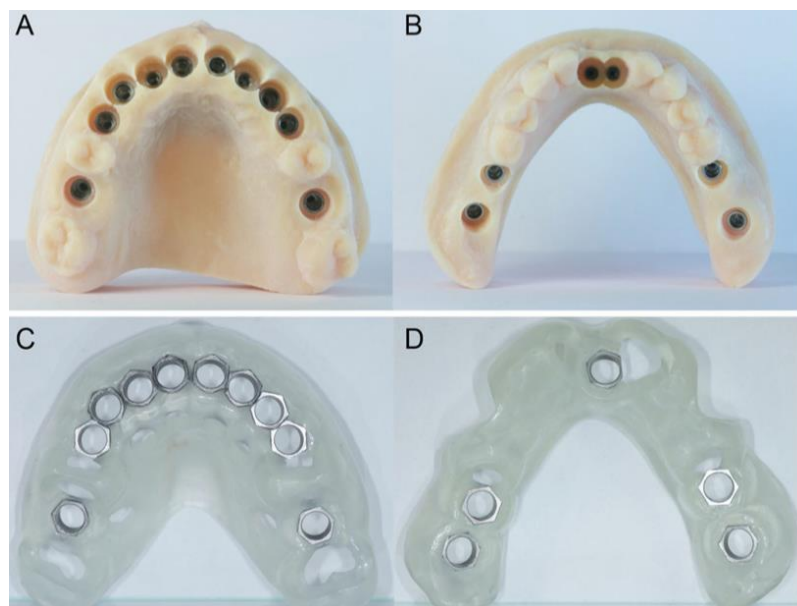
Figure 20. 3D-printed models of the digitally- planned software outcome (A, B), and surgical guides fabricated from those models (C, D).

These models not only included the correct position of the planned implants but also anatomically presented the mucosa and the residual teeth, which were not removed during the planning. Within the guided surgery software, these remaining teeth would facilitate superimposing the digital casts onto the CBCT images. And during the actual implant placement surgery, these teeth will stabilize the surgical guides, whereby any remaining hopeless teeth will be removed after the surgical phase is completed.

III.4.2.3. Make - Manufacturing

Based on the virtual planning, surgical guides were printed, and metal guide sleeves were manually inserted (Figure 21 C and D). In the mandibular guide, the sleeves of the central incisors touched each other, requiring two different guides to be 3D printed, each with only 1 central incisor guide sleeve installed.

The last step before the implant surgery was to prepare a full-arch, functional provisional restoration. A burn-out framework was designed and milled that was based upon both the designed final prosthetic result and the virtually planned implant positions (Figures 22 A and B). This metal infrastructure supported a provisional full-arch prosthesis comprised of manually stratified and highly aesthetic composite resin (Nexco, Ivoclar Vivadent, Schaan, Liechtestein) (Figure 22C). This prosthesis was to be seated on temporary abutments immediately after the implants were surgically placed.
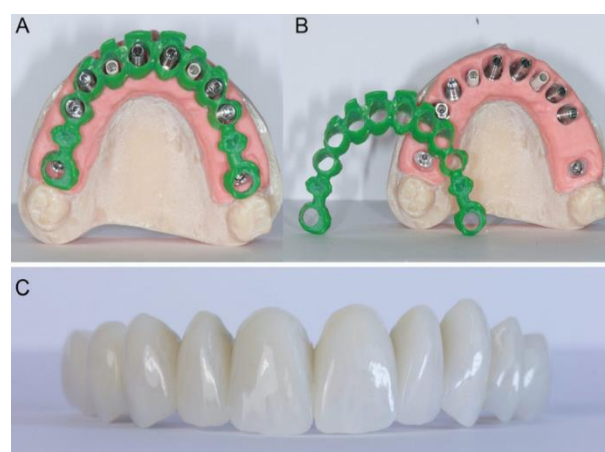
Figure 21. Preparation of the provisional fixed full-arch for immediate loading. (A, B) the burn-out framework and (C) the aesthetic temporary prosthesis.

III.4.2.4. Done - Surgical treatment

The flapless surgery commenced with the atraumatic extraction of most of the hopeless teeth, except for those that stabilized the surgical guide (to be extracted afterward). During the extractions, care was taken not to damage the alveolus, and particularly the delicate maxillary buccal bone wall (Figure 22 A and B). Next, the surgical guide's position and fit were carefully checked (Figure 23C), after which the guided surgery began with the preparation of all the implant sites, using drills of differing incremental diameters, and ending with the placement of all the planned implants through the surgical guide (Figure 22 D and E).

Following the implant placements, the surgeon verified the implant positions and the soft tissue status, and where needed, simultaneous minor/major grafting procedures were performed. Any required grafting forced the clinician to raise a full-thickness flap, but this was limited to areas that required bone augmentation. Cases not requiring augmentation were done entirely flaplessly.
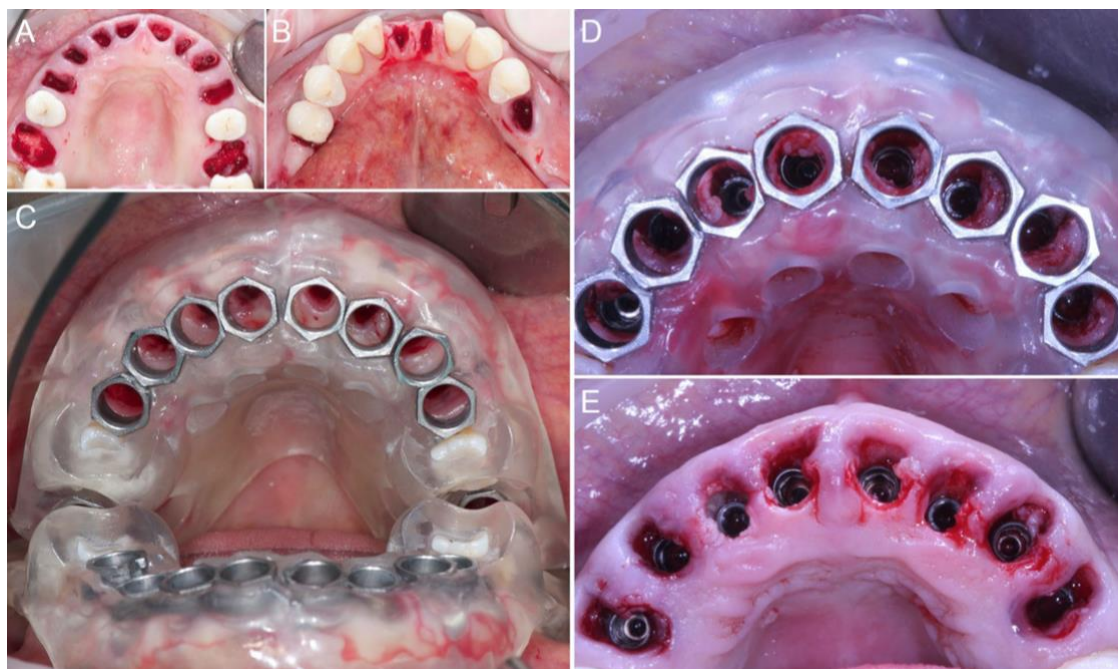
Figure 22. Extraction of the compromised teeth and stages of the guided implant surgery. (A, B) minimally invasive extractions; (C) the surgical guide fit check; (D, E) implants in place through the metal guide sleeves with (D) and without the guide overlaying the implant sites (E).

With the implants precisely placed and the remaining hopeless teeth that stabilized the surgical guide extracted, the full-arch fixed metal-reinforced resin provisional restoration was carefully adapted and relined on the temporary abutments. It was trimmed and accurately polished, and then cemented temporarily and panoramically radiographed (Figure 23A and B).
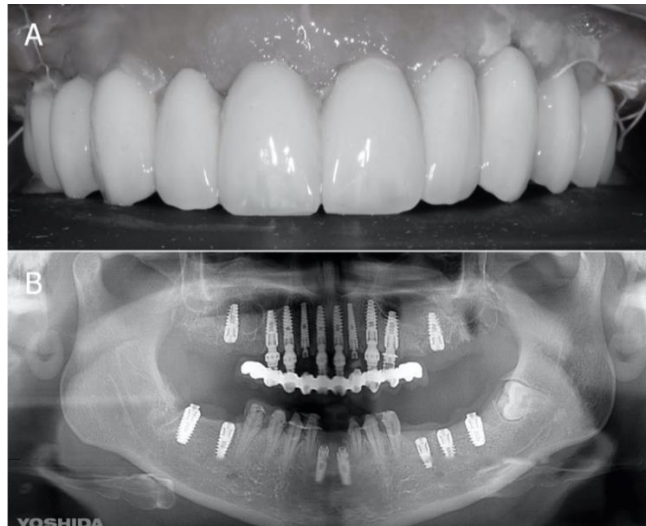
Figure 23. (A) The metal reinforced provisional restoration in situ, and (B) the panoramic control radiograph of the placed implants.

III.4.2.5. The Final Restorations

Six months after the surgery, when the provisionalization period had ended, two different impressions were made: a generic alginate impression of the provisional prostheses in position and a precision open tray polyether impression capturing the multi-unit intermediary abutments that supported the provisional, making sure to avoid damaging the peri-implant structures.

In the dental laboratory, plaster casts were poured into both sets of impressions, with the resultant casts scanned with the same desktop scanner used before provisionalization. These models were then overlapped in CAD software to perform aesthetic modifications and guide the modeling of the final restorations. Any modification was manually performed on the 3D-printed models, such that the corrected final shapes were scanned once again.

At this point, the dental technician could proceed to CAD-design (Exocad, Darmstadt, Germany), the final individual customized abutments (which were cemented extraorally onto titanium bases that mated precisely with the coronal surface of the implants), and the final full-arch prosthesis. To optimize the aesthetic outcome, both the customized abutments and the final restorations were milled in full-ceramic zirconia by a milling machine (M1 WET Heavy Metal, Zirkonzhan, Bolzano, Italy). The single anterior crowns were physiologically shaped to be self-cleansable for a better biological response, while also promoting excellent oral hygiene techniques (dental floss could easily pass through). Posteriorly, fixed partial prostheses were installed to improve the functional response.

At the delivery of the final restorations, the customized abutments, with their already-cemented Titanium bases in place, were screwed into each implant in their correct positions with their margins

ideally positioned subgingivally. Then, following the original surgical and prosthetic plan, all milled zirconia restorations were placed. Before cementation, the marginal adaptation was checked clinically with magnification (Zeiss 4.5x, Zeiss, Oberkochen, Germany), and the occlusion was carefully evaluated with articulating paper (Bausch Articulating Paper, Bausch Inc., Nashua, NH, USA), and the T-Scan 10 computerized occlusal analysis technology (Tekscan, Inc. S. Boston, MA, USA). Clinical pictures and a post-insertion panoramic radiograph were obtained from the patient, along with a final digital analysis of the occlusion (Figure 24 A-D).

Figure 24. Documentation of the final restorations that included a digital occlusion analysis. (A, B) clinical photographs; (C) the post-treatment panoramic radiograph; (D) A mid-delivery mandibular digital occlusion analysis showing 4 supportive implants were under force overload warnings. Further T-Scan guided occlusal adjustments will be required at this delivery appointment, to improve the force profile on the 4 overloaded implants.

III.4.3. Results

In this 12-patient retrospective record analysis, 12 patients received 110 implants (65 of these were post-extraction). For the demographic data, see the original publication in the Appendix. 6 months later, at the end of the provisionalization period, 72 fixed zirconia-ceramic prosthetic restorations (53 single crowns, 17 bridges, and 2 fixed full arches) were delivered. The 1-year implant survival rate turned out to be 98.2%, with 108 out of 110 total implants surviving. The surviving implants also demonstrated good soft tissue stability.

The outcome measures were as follows: implant stability at placement (ISQ, Table 5), implant survival and complications, prosthetic success, marginal bone remodeling, soft tissue stability, and patient satisfaction (Table 6).

Patient data were rigorously collected during the study and entered into a spreadsheet for statistical analysis (Excel 2003; Microsoft, Redmond, WA, USA). Descriptive statistics were used to describe the distribution of patients, implants, and restorations.

Implant survival was calculated at both the implant level and the patient level, with the patient as the statistical unit. The patient was classified as a case of failure if one or more implants failed. Only 1 patient of the 12 experienced implant failure, resulting in a 1-year patient-level survival rate of 91.7%

Similarly, the prosthetic success was calculated at both the restoration level and the patient level, again with the patient as the statistical unit. The presence of at least one biologic or prosthetic complication determined if the patient was categorized as a prosthetic failure. 8/12 prostheses (66%) did not undergo any failure or complication during the entire follow-up period. At the 1-year follow-up control, the soft tissue was stable in all patients and the esthetic results were satisfactory.

	IT at placement < 35 Ncm (%)	IT at placement ≥ 35 Ncm (%)	ISQ at placement < 55 (%)	ISQ at placement 55<x<85 (%)
Overall	25/110	85/110	28/110	82/110
Maxilla	20/75	55/75	21/75	54/75
Mandible	5/35	30/35	7/35	28/35

Table 5. Implant Stability at Placement. The mean implant stability at placement, as measured by insertion torque (IT) and resonance frequency analysis (ISQ).

Question	Very satisfied	Satisfied	Neither satisfied nor dissatisfied	Dissatisfied	Very dissatisfied
Overall, how satisfied are you with the treatment received?	10/12 (83.3%)	2/12 (16.7%)	0/12 (0%)	0/12 (0%)	0/12 (0%)
Are you satisfied with the function of your implant-supported restorations?	12/12 (100%)	0/12 (0%)	0/12 0%	0/12 (0%)	0/12 (0%)
Are you satisfied with the esthetics of your implant-supported restorations?	11/12 (91.7%)	1/12 (8.3%)	0/12 (0%)	0/12 (0%)	0/12 (0%)
Are you satisfied with the cleanability of your implant-supported restorations?	9/12 (75%)	3/12 (25%)	0/12 (0%)	0/12 (0%)	0/12 (0%)

Table 6. Patient satisfaction was determined by each patient answering 4 questions. Overall, the majority of the patients were satisfied with the treatment received, with no patients reporting unsatisfactory treatment outcomes.

III. 4.4. Conclusions

Full-arch rehabilitation in a digital workflow with immediate loading turned out to be a successful, predictable treatment in the short term. The analyzed cases showed that when this approach is applied, a single session is enough for tooth extraction, implantation, and the insertion of a provisional prosthesis. The provisional restoration guided the soft tissue healing and allowed for planning an optimal aesthetic result for the final dental rehabilitation. Furthermore, this approach allowed for a reduction of discomfort and facilitated the patients' return to both their social and professional lives. The results suggest that high survival rates and excellent aesthetic results are expectable with the presented workflow, even in the long term.

Further studies with larger patient sample sizes that include control subjects, and longer follow-up periods of observation will aid in drawing more specific conclusions about the long-term results of the presented technique.

IV. DISCUSSION

IV.1. The Trueness of 12 Intraoral Scanners Used in Full-arch Implant Impressions - A Comparative *in vitro* Study

The trueness of the intraoral scanners is a subject that has been extensively studied in the digital dental literature, while the IOS use is rapidly expanding within the dental profession because their use offers significant advantages to the clinician (14). Because IOS captures optical impressions of teeth and implants with only a light beam, IOS optical impressions are more comfortable for the patient to undergo (13) and they are easier for the clinician to perform (11-14). Therefore, IOS optical impressions are rapidly supplanting conventional impressions (with trays and impression materials), with the latter likely to disappear in the next few years (25).

Several studies and literature reviews have demonstrated that IOS can reliably capture impressions of single and multiple abutments in dentate patients (90). However, only a few studies have assessed the use of IOS in Oral Implantology (91), and little evidence exists regarding IOS capabilities to impress long-span restorations (92-94) and fully edentulous patients (93). Additionally, little is known about the quality of the different IOSs that are currently commercially available. Only a few studies have compared the trueness and precision of different IOSs (19), and most of these analyzed the reproduction of fully dentate models (20,21). Whereas the scientific evidence on the performance of different IOSs in Oral Implantology is rather weak (47,48).

The currently available literature on IOS use with dentate patients has clearly shown that scanning single teeth and/or quadrants/sextants of an arch, is more accurate than when complete arches are scanned (47). Complete arch scanning has accuracy issues, likely due to an accumulation of registration errors involved with the patching together of 3-Dimensional surfaces. Consequently, when optical data is directly acquired with an IOS, the fabrication of complete fixed full arches remains challenging.

Furthermore, all the aforementioned studies that compared different IOS use in Oral Implantology were performed on first-generation devices (19). Since the time of those initial comparative studies, significant technological advances have been made, such that IOS manufacturers have launched a series of new, extremely powerful devices, to improve the accuracy of full-arch dentate and fully edentulous intraoral scanning.

Most existing studies investigating the trueness of optical impressions used a mesh-mesh approach, Mangano et al. superimposed IOS models onto a Reference Model (RM), using best-fit algorithms to align both meshes, to assess the minimum error (36, 38). Consequently, the error was

distributed homogeneously throughout the entire mesh (36, 38, 20). This method of assessing the overall IOS trueness has been deemed valid because it is rapidly accomplished, and is not affected by other variables (i.e. tolerances in the fabrication of the scan bodies) (38).

However, in implant-supported restorations, it is also important to assess the error between fixation points, as even a single error localized in one point can result in a clinical misfit of the prosthetic structure. Therefore, some studies have attempted to assess distance or angulation errors between fixation points (22, 23). But to make reliable linear measurements, it is necessary to work on library files (or nurbs files), on which specific landmarks (such as their centroids) can be precisely and automatically identified by the analysis software. Importantly, working with nurbs files more closely simulates and replicates the early stages of prosthetic CAD design (51).

Our present *in vitro* study, therefore, used three different methods to investigate the trueness of 12 IOSs in the FA implant impression: a mesh/mesh method and a nurbs/nurbs method to evaluate overall trueness, and the computation of linear and cross distances between the SBs to evaluate local trueness. In our study, statistically significant differences were found between the different IOSs, as previously reported (38,39). In particular, the mesh/mesh and nurbs/nurbs analysis have allowed identifying three groups of scanners, characterized by different levels of trueness. The first group, comprising the IOSs with the highest accuracy, consisted of ITERO ELEMENTS 5D, PRIMESCAN, CS 3700, CS 3600, TRIOS3, and i-500. These scanners have an average intrinsic error < 40 μm with the mesh/mesh method and < 25 μm with the nurbs/nurbs method and represent a theoretically compatible solution for taking impressions for FA restorations. The second group of scanners presented positive results, although probably still not compatible with the capture of a FA impression. These were EMERALD S, EMERALD, OMNICAM, VIRTUO VIVO, and RUNEYES, which presented an average intrinsic error between 40 and 80 μm with the mesh/mesh method and between 25 and 50 μm with the nurbs/ nurbs method. DWIO remained distanced from all the others, with an intrinsic error > 80 μm in the mesh/mesh analysis and > 50 μm in the nurbs/nurbs analysis, certainly incompatible with the FA impression. The data of the overall trueness were confirmed by the analysis of the local distances between the SBs, i.e. the linear and cross distances, which again highlighted the existence of three groups of IOSs in this study, characterized by different performances. Linear error analysis along the scan revealed higher reliability for ITERO ELEMEN TS 5D, PRIMESCAN, CS 3700, CS 3600, TRIOS3, and i-500, which showed lower errors than other IOSs. For the particular scanning strategy used in this study, it was not possible to evaluate in detail, for each scanner, the percentage growth of the error as the scan proceeded; however, it was evident that greater variability was present in the paths S2-S3 and S4-S5, corresponding to the area of greatest curvature of the physical model. This finding must be confirmed by further studies, but it would seem to indicate

difficulty for IOSs in accurately detecting stretches of curvature. The evaluation of cross measurements naturally resulted in larger errors, in direct proportion to the actual distance between the SBs. Here, too, the evaluation showed significant differences between the different IOSs.

The main advantage of this study is in having compared 12 IOSs, and done so using different techniques, to understand the intrinsic trueness of the scanners at a global and local level by measuring the distances between the different SBs. On one hand, the evaluation with the mesh/mesh method has the advantage of directly highlighting the quality of the scan. In this study, with the mesh/mesh analysis, the best absolute performance was obtained by CS 3700 (mean error 30.4 μm; 95% CI 26.7–34.5 μm) followed by ITERO ELEMENTS 5D (mean error 31.4 μm; 95% CI 29.2–33.8 μm) and i 500 (mean error 32.2 μm; 95% CI 28.4–36.6 μm). These IOSs were the best in the representation of the SBs and the tissues around them, although in an *in vitro* study, the soft tissues are a resin copy of the real human gums. On the other hand, the nurbs/nurbs evaluation allows replicating what happens clinically, when within the CAD software the meshes of the SBs are replaced with the corresponding library file, generating a hybrid virtual model on which the modeling takes place. This approach specifically assesses the sole trueness of the position of the implants after the mesh/nurbs replacement in CAD, without any interference from the soft tissues; it is also a prerequisite for the correct implementation of the analysis of the distances between the SBs, carried out as an evaluation of the distances between the centroids at their bases. In the analysis of the overall trueness with the nurbs/nurbs method, the best results were obtained by ITERO ELEMENTS 5D (mean error 16.1 μm; 95% CI 12.9–20.1 μm), followed by PRIMESCA N (19.3 μm; 95% CI 16.3–22.9 μm) and TRIOS 3 (mean error 20.2 μm; 95% CI 18.1–22.7 μm). These results reflect a very low error in the position of the SBs with these IOSs, which could certainly be considered compatible, in all cases, with the realization of a FA restoration via a fully digital workflow. The evaluation of the distances between the single SBs confirmed these positive results, particularly concerning the linear distances along the arch. As expected, the local errors tended to grow in the cross distances, particularly between the most distal SBs, but this error is certainly contained compared to what was described only a few years ago in similar studies (25, 33).

However, the intrinsic trueness data of the different IOSs presented in this study must be taken with caution. The IOS is not the only factor involved in determining the final accuracy of an optical impression. Studies have determined that the operator (95) the patient (96), the implant position, depth and angulation (64), the light conditions (65) and the SBs (66,67) are also key. The operator is essential because different scanning strategies and different levels of experience performing intraoral scanning can determine different results (95). In the present study, all models were captured by the same operator with many years of experience with intraoral scanning. However, the choice of scan

strategy may have favored some IOSs over others. To date, unfortunately, little is known about the effects of different scanning strategies, as the scientific literature on this topic is scarce (14), and the manufacturers have not fully clarified the technique-sensitive nature of scanning. Further, implants can be inserted in different positions, inclinations, and depths, and these factors can positively (or negatively) influence the final trueness of a scan (95). Concerning these implant-specific aspects, the literature is also scarce (97), which suggests that more in-depth investigation regarding the effects these variables impart on scan accuracy is needed.

In the present study, the SBs were mostly parallel to each other, because of the guided surgical procedure. This simulated an ideal condition that is not always found in clinical practice, where the SBs have the fundamental role of transferring the implant positions (98,99). Light conditions are another factor of great importance in intraoral scanning (65). In the present *in vitro* study, all scans were captured in the same environment, under controlled light conditions. However, these conditions are very different from those in the oral cavity, which must certainly be investigated in more detail as to how much differing intraoral light conditions can affect scan quality (65).

Finally, the presented study had some limitations. First, it was an *in vitro* study. Although scrupulously conducted, it was not possible to determine the trueness of the IOSs *in vivo*, as an *in vitro* study cannot exactly reproduce the characteristics present in a patient's oral cavity (light conditions, humidity, saliva, available scanner access space). The scanning of plaster models is certainly easier than an intraoral scan, where there are space limitations. Furthermore, the patient's tissues are radically different from a plaster model and demonstrate different optical behavior when illuminated. This must always be kept in mind, especially in an edentulous patient to be rehabilitated with a full-arch restoration. Another limitation already described, was the choice of scanning technique, which could have favored some scanners over others. The use of a desktop scanner for the capture of the reference model could also be considered a limitation. Although this machine is certified to an accuracy of 5 μm, and this approach has been used in previous studies (9), a CMM or an articulated arm could be considered more reliable tools for capturing reference measurements. To potentially improve the measurement accuracies, only the base of the centroids (not the centroids at the top of the SBs) were used for the evaluation of the linear and cross distances. Finally, the present study could have collected additional interesting data relating to the linear error increase that occurs during scan progression. This would have been possible had the scan strategy foreseen a measurement error evolving in a specific sector of the physical model (for example in the right posterior sector only). It has been previously reported (43,45), and then recently confirmed *in vitro* by Renne and colleagues using a dentate model (99), the scan progression tends to be accompanied by an increased

percentage linear error. Unfortunately, in the presented study, making a similar evaluation was not possible, as the operator was free to commence scanning the model indifferently, from either the right or left posterior area. As such, the collected data did not allow for an evaluation of the exact percentage error increase during the scan progression.

In this study, all scans were captured in a specific period (January - February 2020), using at that time, the latest available acquisition software version for each of the IOS machines. However, newly released acquisition software is known to significantly improve the accuracy of an IOS, making the presented study results valid solely for that period, and the specific acquisition software version. Further studies performed with the same IOSs, that employ the latest acquisition software are needed, to better understand the trueness of the currently available different scanners.

IV.2. Continuous Scan Strategy (CSS) - A Novel Technique to Improve the Accuracy of Intraoral Digital Impressions

To date, multiple published reports have proposed that IOS inaccuracy when capturing impressions for the manufacture of long-span restorations (such as FA), is a significant limitation to scanner use in Implant Prosthodontics (58-61). Although there are statistically significant differences in the accuracy of the various commercially available IOSs, various studies (58, 59) and literature reviews (60,61) have confirmed the intrinsic difficulty scanners exhibit when capturing multiple implant impressions, particularly in completely edentulous patients. It is now clear that the inaccuracy of the models generated by direct intraoral scanning does not solely depend on the machine itself used for the acquisition, but also on other factors previously described (65,67).

Concerning IOS intrinsic errors, one of the most significant difficulties for IOS occurs in correctly reading and reproducing the spaces between different SBs (63,64). These spaces are devoid of physical reference points but display "a vertical spatial jump" between two SBs. It is precisely the distance and lack of spatial reference points that create difficulties for the IOS reconstruction software (64). For this reason, some authors have attempted to reduce the space and distance between SBs, by introducing replicas or custom devices that facilitate improved scanner reading (68,69).

Other authors have proposed using custom devices of different shapes that can assess and check the accuracy of intraoral scans (34-36). In one *in vitro* study (68), Iturrate et al. manufactured a custom device of known dimensions, that connected onto an edentulous maxillary model with 4 SBs. This model was then scanned with different IOSs, both with and without the auxiliary device (49). The authors reported that the presence of the auxiliary device proved useful, serving as a scanning

spatial reference rich in anatomical landmarks, that improved the accuracy of the optical impressions, regardless of the type of IOS used (49). A similar strategy was employed by Gomez-Polo et al. (50), who presented a technique that corrected deviations and distortions that occur during direct intraoral scanning of FA prostheses. The strategy employed a reference marked rigid splint, with known geometric features that provided the scanner with reference points, that reduced deviations, and errors produced from the "jump" between different SBs (50). This method was based on sectioning the scanned files, then best-aligning them to generate a more accurate definitive cast, and consequently, a better-fitting final restoration (50).

The presented retrospective clinical study utilized a simpler, more direct, and entirely digital approach, by intraorally connecting implant SBs with composite-reinforced thermoplastic resin. The entire assembly was directly scanned with a Trios3, that several studies have reported as being highly accurate (9,57,63,23). This approach obtained excellent passive fit and marginal adaptation of full-arch implant superstructures at T0 (intraoral try-in of the polyurethane or metal replicas) when only 5/45 replica prostheses demonstrated unsatisfactory clinical precision. In these 5 FA cases, the clinician separated the polyurethane or metal replica into several parts to obtain passive adaptation. These portions were then luted together intraorally with low-contraction resin and re-scanned with a desktop scanner to accordingly modify the CAD design.

It is important to note that one-piece titanium SBs were used in this study. This may represent an advantage because one-piece metal SBs are easier for the manufacturer to fabricate (as manufacturing tolerances with PEEK are more difficult to control), and aid in minimizing the positional errors that potentially affect two-piece SBs (titanium/PEEK), resultant from variable tolerances of a 2-piece assembly (39). It is also important to note that in all the studied cases, during the early stages of CAD design when determining the "best-fit", a > 30 µm distance between the mesh and the multiple SBs libraries was detected. This error highlighted the importance of attaining high congruence between the mesh and the SB library files because an absence of perfect congruence between these two files can induce a positional error. This topic needs to be further explored with future scientific evaluations.

Even if the implant survival rate was 100%, and the prosthetic complication rate was low (6.7%), with an overall 2-year prosthetic success rate of 93.3%, there were some definitive study limitations. First, there was a relatively brief follow-up period after the delivery of the final zirconia restorations (up to 2 years). In addition, a retrospective study is not ideally suited from which to draw definitive conclusions on the reliability of the presented direct intraoral scanning technique. Second, most of the prosthetic restorations were delivered in the maxilla, which has more stable landmarks that aid in

reducing IOS scan inaccuracies (such as the hard palate). The mandible, in comparison, lacks reference points, and the tongue can interfere with scanning. Another limitation was that the study design itself was essentially clinical. The protocol did not allow for proper mathematical quantification of scanning errors, nor for quantitatively verifying the mathematical accuracy of the scans. The only controls were clinical, those being a radiographic assessment of the margin closure, and clinician subjective assessments of the superstructure passive fit. Finally, a highly accurate IOS (Trios 3) was used by an experienced operator, whereby the obtained results should not be generalized as valid for other IOS scanners. Hence, further long-term prospective clinical studies that counter these limitations, are essential to replicate and confirm the positive outcomes observed.

IV.3. Artificial Intelligence in Fixed Implant Prosthodontics - A Retrospective Study of 106 Implant-supported Monolithic Zirconia Crowns (MZC) Inserted in the Posterior Jaws of 90 patients

Less than a decade after breaking the Nazi encryption machine known as Enigma, and helping the Allied Forces win World War II, mathematician Alan Turing changed history a second time by posing a simple question, "can machines think?". In 1950, with the paper entitled *Computing Machinery and Intelligence,* Turing established the fundamental goal and vision of Artificial Intelligence (AI): to replicate or simulate human intelligence in machines (100,101). Several years later, the first famous success of AI occurred when an IBM-manufactured machine named Deep Blue, defeated the reigning chess champion, Garry Kasparov. Although their first encounters were won by Kasparov, the continuous improvements allowed the machine to achieve victory in successive games. The victory, as declared by Kasparov, was only possible because "the machine had reached such a high level of creativity, that went beyond the knowledge of the player". The foundation of AI is Machine Learning (ML), a branch of computer science that builds algorithms to solve problems, guided by statistics and data (76, 77, 100,101).

In the medical field, AI uses algorithms and software applications to approximate human cognition that approaches levels of human expertise, when analyzing complex data. This has changed the role of computer-assisted diagnosis from being a "second-opinion" tool to a more collaborative one (102). The development of AI applications is already remarkable, particularly in radiology and 3-Dimensional imaging, both of which aids human clinicians during both diagnosis and treatment planning. Recently, AI has been integrated into image processing software and CAD, showing promising results (103)

In the field of implant prosthodontics, for example, the new digital workflows use intraoral scanners to capture implant position via the scan body, which is a digital version of the antiquated implant transfer coping (69,70,71). Today, the accuracy of intraoral scanners is high (9, 14) replacing the classic impression made with trays and materials, while offering benefits to both the patient and the entire prosthetic workflow. Making an optical impression is easier and faster for the operator that involves less discomfort for the patient while generating reproducible results (71, 35). Communication with the laboratory is facilitated, and costs and time can be reduced. However, the introduction of digital technologies necessitates adopting new protocols, which is not always easy for the dentist and the dental technician, especially when they are practicing "natively analog" procedures.

In the presented retrospective clinical study, which further developed a previously published method (71), a clinical protocol was detailed that simply and predictably solves these adoption problems with lower overall costs. This protocol is based on a second intraoral scan, made at the end of the provisional period after the mucosal tissues have been suitably conditioned by the provisional restoration. The patient is recalled, the provisional is removed, and an optical impression of the individual hybrid abutments *in situ* is captured, regardless of the marginal preparation, which is generally placed subgingivally. This new mesh is then loaded into the CAD program, where it is automatically recognized by the AI software, and replaced with the originally modeled abutment file that was stored in a special folder. The technician can, therefore, model the final crown directly onto the originally modeled abutment file (and not on the mesh, which by definition is a geometrical approximation of the scanned object). The abutment file is transported within the software to the correct spatial position that matches the actual position of the hybrid abutment in the mouth. Then, the AI software automatically recognizes and traces the margin line. The technician can thus, model the final restoration on an abutment with clear margins despite being clinically subgingival, and perform the restorative modeling on a library file (not on a mesh). This guarantees maximum clinical precision that eliminates several risk factors (Scan Body scanning errors; intrinsic library file errors; and cementation errors), thereby simplifying the modeling procedures.

In the presented study of 90 patients, AI reliable aided the restoration of 106 single locking-taper implants with MZCs cemented onto customized hybrid abutments, fabricated with a fully digital workflow. This protocol demonstrated high mathematical quality and reliability of the hybrid abutment fabrication, demonstrating a mean deviation of 44 ± 6.3 μm, between the original CAD-designed abutment file, and the zirconia abutment mesh captured intraorally at the end of provisionalization. At final MZC delivery, the marginal adaptation, the quality of the interproximal

and occlusal contacts, and the aesthetic integration were deemed excellent, with high satisfaction scores. Moreover, the incidence of failures and complications was low, with 3-year cumulative survival and success rates of 99.0 and 91.3%, respectively.

This clinical protocol with AI can simplify procedures, eliminate steps, and help expand the use of individual hybrid abutments in posterior sites when replacing premolars and molars with implants. This could become important from a mechanical perspective, possibly in reducing prosthetic complications. Presently in the literature, the direct cementation of fixed superstructures (crowns, bridges) glued to titanium bases has not been documented as being predictably successful, often leading to mechanical complications (104). Titanium glued bases are prefabricated with standard heights and thickness, that may not withstand the occlusal forces transmitted by large dimension monolithic structures, over the medium and long term (104).

In addition, with the present AI protocol - as previously reported (9) - , it is possible to mathematically evaluate and precisely quantify the degree of error that occurs during individual zirconia abutment milling and sintering fabrication. Reverse engineering software can calculate the distance differences between the original CAD-designed zirconia abutment surface, and the intraorally captured zirconia abutment mesh. This relevant information helps identify production-induced spatial errors. However, it must be noted that digital impressions themselves, entail a certain degree of error (6), which could, in part, jeopardize the abutment product's quality control.

The present protocol requires that the hybrid abutments, once milled, sintered, and assembled, are not modified further in the laboratory. Otherwise, the AI software may encounter difficulty when coupling the modeled abutment file with the mesh captured in the mouth. In addition, the AI application presented here is "narrow AI", as the product of the applied algorithms managed a singular or limited task. This can be considered a further limitation of the present study because the only task performed automatically by the software, was the recovery of the CAD file originally modeled by the dental technician, and the replacement of the mesh captured within the mouth. The automatic identification of the margins is considered to be a "narrow" application. It would be completely different if the software were able to automatically model the individual abutments, based on specific skills or knowledge acquired through Deep Learning, which would be an example of "strong" AI". However, to date, this is not yet possible. Finally, further studies with an adequate design (randomized clinical trials and/or prospective studies) are certainly necessary to confirm the results of the presented research. These types of studies would potentially validate this clinical protocol, as well as define AI applications with other implant component systems, and alternative

planning software entities. With different implant systems and their specific connections, the results may vary, necessitating adequate future investigation.

IV. 4. Complete-arch Fixed Reconstruction with Guided Surgery and Immediate Loading- A 1-year Follow-up Retrospective Clinical Study on 12 patients

Although guided surgery has become increasingly popular and widespread, there are only a few studies in the literature that present results obtained with guided, flapless implant placement into fresh extraction sockets, followed by immediate functional loading of complete fixed-arch reconstructions absent of artificial gingiva (86,87,89). In one such recent clinical and radiographic study, Ciabattoni et al. (86) successfully installed 285 implants in 32 patients with a double-guided template technique, with 197 implants inserted in fresh extraction sockets (137 in maxillae and 60 in mandibles), and 88 implants into healed sites (58 in maxillae and 30 in mandibles). All the implants were immediately loaded with fixed, full-arch restorations that were followed for 3 years (86). The outcome variables were implant survival, prosthesis survival, and marginal bone level changes (86). The authors reported, a high implant survival rate (97.5%), with only 7 fixtures that failed (3 in maxillary fresh extraction sockets; 2 in mandibular fresh extraction sockets; 2 in maxillary healed sites) (86). All fixed full arches maintained stability and good functionality during the entire follow-up period, with minimal marginal bone loss of 1.32 ± 0.41 mm (86). The authors concluded that flapless, guided implant surgery using a double-guided template technique, was a predictable treatment procedure, capable of providing predictable outcomes while decreasing treatment times and patient discomfort (86).

The results of the presented 12 subject retrospective study confirm the evidence emerging from prior authors (86,87,89). The 12 patients received 110 implants placed with flapless guided surgery (65 were placed into fresh post-extraction sockets), that were immediately loaded with fixed full-arch metal-reinforced provisionals. 6 months later, 72 fixed prosthetic reconstructed complete arches were delivered. The initial implant stability detected at placement was successful, as only 2 implants in one patient failed, and were removed. The 1-year implant survival rate = 98.2% (108/110 surviving implants). Also, only a few biologic and prosthetic complications were reported, with 8/12 prostheses not sustaining any failure or complication during the 1-year follow-up period, when in all cases demonstrated excellent soft-tissue stability, and patients were satisfied with the treatment they had received.

The advantages of the presented guided surgical and prosthetic protocol can be summarized as follows.

First, flapless implant placement reduces intra-and postoperative patient discomfort and morbidity and shortens overall surgical durations, which different systematic reviews (88) and clinical studies have previously reported (105-107). In a controlled study, Arisan et al. demonstrated that flapless guided surgery can significantly shorten the surgical time, as compared to conventional open-flap surgery (106). Since the duration of the surgical intervention influences morbidity for the patient, computer-assisted flapless implant placement can reduce the incidence of surgery-related complications, such as bacteremia and infection (107). And Fortin at al. demonstrated that optimized implant placements with guided surgery, may successfully avoid some bone augmentation procedures (107).

Second, the main advantage of guided surgery is the capability for the clinician to ideally plan each implant's requisite position, inclination, and depth, while avoiding dangerous anatomical structures (inferior alveolar nerve and maxillary sinus), and accounting for the emergence profile of the overlying prosthesis. With this so-called "prosthetically-guided" placement, the implants are planned to optimally support the future prosthesis, which reduces the need for prosthetic compromises. When planning fixture locations within planning software, a digital scan of the prosthetic superstructure is imported into the software. This allows the clinician to optimally design the position of each implant's depth, and mesiodistal and bucco-lingual inclinations, in relation to the ideal orientation of the future prosthetic rehabilitation. The fixtures are optimally planned to support a prosthesis that functions biologically and aesthetically while accounting for the bony anatomy and the future prosthetic boundaries.

In the present study, care was taken to place the implants in the best position, depth, and inclination. And to maximize implant stability, the fixtures engaged the residual bone by exceeding the apex of fresh extraction sockets, by at least 3-4 mm. The implants were purposefully placed 2 to 3 mm palatal to the residual buccal boney wall, to avoid aesthetic problems. However, because the planning was prosthetically-guided, the implant axis was aligned (as much as was possible) within the center of the teeth. The final planning result was, therefore, a compromise between the amount of available residual bone, and the ideal prosthetic emergence profile. This compromise is not a trivial matter, particularly when a fixed full-arch restoration without artificial gingiva is being planned, because, with guided implant surgery, the high implant placement accuracy can provide an ideal supportive platform for the final prosthetic restoration. Also soon after the surgery, a pre-fabricated full-arch provisional can be installed and occlusally loaded, which guides soft tissue healing, controls

recession, and takes advantage of the extraction socket healing potential. Importantly, these prefabricated provisional restorations provide an optimal aesthetic result and improve patient satisfaction, comfort, and treatment acceptance, because there is no removable denture involved.

Various studies (108,109) and literature reviews (81-83) have demonstrated that accurately transferring the implant position from the planning software to the actual surgery, has yet to be definitively solved. Therefore, because implant location deviations depend on several factors that cannot be completely controlled (108,110), clinicians should carefully select their guided surgery candidates, especially in the early stages of the clinician's technique learning curve. In the future, with continuous technological advancements in digital dentistry together with improvements in scanners (110,111), and with the planning softwares' capability to manufacture more precise surgical guides (12), the inaccuracies presently inherent with guided implant placement may be resolved.

Finally, the present study had certain limitations, including the small number of patients enrolled and the short 1-year follow-up time. Also, a retrospective analysis is not the most suitable study design for obtaining indisputable scientific evidence (112, 113). Moreover, the performed protocol utilized a mixed, digital/analog workflow, which could be considered a limitation, because today, using intraoral scanners is well-established (44), which could have potentially reduced the number of steps and procedures of the described method. Therefore, new prospective studies should be conducted with a randomized controlled design, to draw more specific conclusions on the validity and effectiveness of the presented technique.

V. CONCLUSIONS

Through the studies covered in this thesis, we have demonstrated the following and we consider these to be the novel scientific findings related to the work that has been accomplished:

1. It has been demonstrated that the accuracy of intraoral scanning for full-arch restorations can be improved by using the nurbs-to-nurbs method, instead of the mesh-to-mesh method.

2. It has been demonstrated that the quality of intraoral scanning for full-arch restorations can be improved by applying the continuous scan strategy, by eliminating the scanning jumps that normally stem from level differences in the scanned area.

3. It has been demonstrated that an entirely digital workflow involving AI can be efficiently used in for restorations involving single implants and customized hybrid abutments with monolithic zirconia crowns and that the short-term clinical outcomes associated with the said approach are favorable.

4. It has been demonstrated that full-arch fixed implant reconstruction employing guided surgery placing implants into fresh extraction sockets followed by immediate loading is a safe, reliable and successful approach in the short term. The short-term outcomes achieved with this approach are not inferior to those achievable with more conventional approaches, either esthetically or functionally.

These conclusions are to be interpreted and understood within the limitations of the underlying research described in this thesis.

VI. ACKNOWLEDGEMENTS

Throughout the writing of this dissertation, I have received a great deal of support and assistance.

I wish to warmly thank You, my supervisor, Professor Katalin Nagy, former dean of the Faculty of Dentistry, and Head of the Department of Oral Surgery at the University of Szeged, for your patient trust, support and for all the opportunities you have given to me. You provided me with the tools that I needed to choose the right direction and complete my dissertation.

I thank You, Dr. Gábor Braunitzer, for your excellent advice. Your insightful feedback pushed me to sharpen my thinking and brought my work to a higher level.

I am deeply thankful to You, Professor Francesco Mangano for your continuous support and help in my research activities.

I am also grateful to Dr. Robert Kerstein for his assistance with the English editing of this thesis.

REFERENCES

1. Mangano Guest Editor F. Digital Dentistry: The Revolution has Begun. Open Dent J. 2018 Jan 31;12:59-60. doi: 10.2174/1874210601812010059. PMID: 29492170; PMCID: PMC5814950.

2. Ramasamy M, Giri, Raja R, Subramonian, Karthik, Narendrakumar R. Implant surgical guides: From the past to the present. J Pharm Bioallied Sci. 2013 Jun;5(Suppl 1):S98-S102. doi: 10.4103/0975-7406.113306. PMID: 23946587; PMCID: PMC3722716.

3. Pyo SW, Lim YJ, Koo KT, Lee J. Methods Used to Assess the 3D Accuracy of Dental Implant Positions in Computer-Guided Implant Placement: A Review. J Clin Med. 2019 Jan 7;8(1):54. doi: 10.3390/jcm8010054. PMID: 30621034; PMCID: PMC6352035.

4. Happe A, Fehmer V, Herklotz I, Nickenig HJ, Sailer I. Possibilities and limitations of computer-assisted implant planning and guided surgery in the anterior region. Int J Comput Dent. 2018;21(2):147-162. PMID: 29967906.

5. Ganz S. D. Computer-aided design/computer-aided manufacturing applications using CT and cone beam CT scanning technology. Dental clinics of North America, 2008;52(4), 777–vii. https://doi.org/10.1016/j.cden.2008.07.001

6. Mangano C, Luongo F, Migliario M, Mortellaro C, Mangano FG. Combining Intraoral Scans, Cone Beam Computed Tomography and Face Scans: The Virtual Patient. J Craniofac Surg. 2018 Nov;29(8):2241-2246. doi: 10.1097/SCS.0000000000004485. PMID: 29698362.

7. Hussam Mutwalli, Michael Braian, Deyar Mahmood, Christel Larsson, "Trueness and Precision of Three-Dimensional Digitizing Intraoral Devices", International Journal of Dentistry, vol. 2018, Article ID 5189761, 10 pages, 2018.https://doi.org/10.1155/2018/5189761

8. Nedelcu R, Olsson P, Nyström I, Rydén J, Thor A. Accuracy and precision of 3 intraoral scanners and accuracy of conventional impressions: A novel in vivo analysis method. J Dent. 2018 Feb;69:110-118. doi: 10.1016/j.jdent.2017.12.006. Epub 2017 Dec 12. PMID: 29246490.

9. Mangano FG, Hauschild U, Veronesi G, Imburgia M, Mangano C, Admakin O. Trueness and precision of 5 intraoral scanners in the impressions of single and multiple implants: a comparative in vitro study. BMC Oral Health. 2019 Jun 6;19(1):101. doi: 10.1186/s12903-019-0792-7. PMID: 31170969; PMCID: PMC6555024.

10. Joda T, Ferrari M, Gallucci GO, Wittneben JG, Brägger U. Digital technology in fixed Implant Prosthodontics. Periodontol 2000. 2017 Feb;73(1):178-192. doi: 10.1111/prd.12164. PMID: 28000274.

11. Mangano FG, Veronesi G, Hauschild U, Mijiritsky E, Mangano C. Trueness and Precision of Four Intraoral Scanners in Oral Implantology: A Comparative in Vitro Study. PLoS One. 2016 Sep 29;11(9):e0163107. doi: 10.1371/journal.pone.0163107. PMID: 27684723; PMCID: PMC5042463.

12. Joda T, Zarone F, Ferrari M. The complete Digital Workflow in fixed prosthodontics: a systematic review. BMC Oral Health. 2017 Sep 19;17(1):124. doi: 10.1186/s12903-017-0415-0. PMID: 28927393; PMCID: PMC5606018.

13. Joda T, Ferrari M, Bragger U, Zitzmann NU. Patient Reported Outcome Measures (PROMs) of posterior single-implant crowns using Digital Workflows: A randomized controlled trial with a three-year follow-up. Clin Oral Implants Res. 2018 Sep;29(9):954-961. doi: 10.1111/clr.13360. Epub 2018 Aug 24. PMID: 30144159.

14. Mangano F, Gandolfi A, Luongo G, Logozzo S. Intraoral scanners in Dentistry: a review of the current literature. BMC Oral Health. 2017 Dec 12;17(1):149. doi: 10.1186/s12903-017-0442-x. PMID: 29233132; PMCID: PMC5727697.

15. Kihara, H., Hatakeyama, W., Komine, F., Takafuji, K., Takahashi, T., Yokota, J., Oriso, K., & Kondo, H. (2020). Accuracy and practicality of intraoral scanner in Dentistry: A literature review. Journal of prosthodontic research, 64(2), 109–113. https://doi.org/10.1016/j.jpor.2019.07.010

16. Ferrini, F., Sannino, G., Chiola, C., Capparé, P., Gastaldi, G., & Gherlone, E. F. (2019). Influence of Intra-Oral Scanner (I.O.S.) on The Marginal Accuracy of CAD/CAM Single Crowns. International journal of environmental research and public health, 16(4), 544. https://doi.org/10.3390/ijerph16040544

17. Papaspyridakos P, Vazouras K, Chen YW, Kotina E, Natto Z, Kang K, Chochlidakis K. Digital vs conventional implant impressions: a systematic review and meta-analysis. J Prosthodont. 2020. https://doi.org/10.1111/jopr.13211 Online ahead of print.

18. Mangano, F. G., Admakin, O., Bonacina, M., Lerner, H., Rutkunas, V., & Mangano, C. (2020). Trueness of 12 intraoral scanners in the full-arch implant impression: A comparative in vitro study. BMC Oral Health, 20(1). https://doi.org/10.1186/s12903-020-01254-9

19. Gómez-Polo M, Ballesteros J, Perales-Padilla P, Perales-Pulido P, Gómez-Polo C, Ortega R. Guided implant scanning: A procedure for improving the accuracy of implant-supported complete-arch fixed dental prostheses. J Prosthet Dent. 2020 Aug;124(2):135-139. doi: 10.1016/j.prosdent.2019.09.022. Epub 2019 Nov 21. PMID: 31761274.

20. Mangano FG, Veronesi G, Hauschild U, Mijiritsky E, Mangano C. Trueness and Precision of Four Intraoral Scanners in Oral Implantology: A Comparative in Vitro Study. PLoS One. 2016 Sep 29;11(9):e0163107. doi: 10.1371/journal.pone.0163107. PMID: 27684723; PMCID: PMC5042463.

21. Bilmenoglu C, Cilingir A, Geckili O, Bilhan H, Bilgin T. In vitro comparison of trueness of 10 intraoral scanners for implant-supported complete-arch fixed dental prostheses. J Prosthet Dent. 2020 Dec;124(6):755-760. doi: 10.1016/j.prosdent.2019.11.017. Epub 2020 Jan 25. PMID: 31987587.

22. van der Meer WJ, Andriessen FS, Wismeijer D, Ren Y. Application of intra-oral dental scanners in the Digital Workflow of implantology. PLoS One. 2012;7(8):e43312. doi: 10.1371/journal.pone.0043312. Epub 2012 Aug 22. PMID: 22937030; PMCID: PMC3425565.

23. Roig E, Garza LC, Álvarez-Maldonado N, Maia P, Costa S, Roig M, Espona J. In vitro comparison of the accuracy of four intraoral scanners and three conventional impression methods for two neighboring implants. PLoS One. 2020 Feb 27;15(2):e0228266. doi: 10.1371/journal.pone.0228266. PMID: 32106275; PMCID: PMC7046187.

24. Imburgia M, Logozzo S, Hauschild U, Veronesi G, Mangano C, Mangano FG. Accuracy of four intraoral scanners in oral implantology: a comparative in vitro study. BMC Oral Health. 2017 Jun 2;17(1):92. doi: 10.1186/s12903-017-0383-4. PMID: 28577366; PMCID: PMC5455075.

25. Ender A, Attin T, Mehl A. In vivo precision of conventional and digital methods of obtaining complete-arch dental impressions. J Prosthet Dent. 2016 Mar;115(3):313-20. doi: 10.1016/j.prosdent.2015.09.011. Epub 2015 Nov 6. PMID: 26548890.

26. Chochlidakis K, Papaspyridakos P, Tsigarida A, Romeo D, Chen YW, Natto Z, Ercoli C. Digital Versus Conventional Full-Arch Implant Impressions: A Prospective Study on 16 Edentulous Maxillae. J Prosthodont. 2020 Apr;29(4):281-286. doi: 10.1111/jopr.13162. Epub 2020 Mar 24. PMID: 32166793.

27. Imburgia M, Kois J, Marino E, Lerner H, Mangano FG. Continuous Scan Strategy (CSS): A Novel Technique to Improve the Accuracy of Intraoral Digital Impressions. Eur J Prosthodont Restor Dent. 2020 Aug 31;28(3):128-141. doi: 10.1922/EJPRD_2105Imburgia14. PMID: 32750237.

28. Lerner H, Mouhyi J, Admakin O, Mangano F. Artificial intelligence in fixed Implant Prosthodontics: a retrospective study of 106 implant-supported monolithic zirconia crowns inserted in the posterior jaws of 90 patients. BMC Oral Health. 2020 Mar 19;20(1):80. doi: 10.1186/s12903-020-1062-4. PMID:

29. Chander NG. Augmented reality in prosthodontics. J Indian Prosthodont Soc. 2019 Oct-Dec;19(4):281-282. doi: 10.4103/jips.jips_324_19. Epub 2019 Oct 10. PMID: 31649435; PMCID: PMC6803791.

30. Meloni SM, De Riu G, Pisano M, Lolli FM, Deledda A, Campus G, Tullio A. Implant Restoration of Edentulous Jaws with 3D Software Planning, Guided Surgery, Immediate Loading, and CAD-CAM Full Arch Frameworks. Int J Dent. 2013;2013:683423. doi: 10.1155/2013/683423. Epub 2013 Jul 29. PMID: 23983690; PMCID: PMC3745845.

31. Noelken R, Moergel M, Kunkel M, Wagner W. Immediate and flapless implant insertion and provisionalization using autogenous bone grafts in the esthetic zone: 5-year results. Clin Oral Implants Res. 2018 Mar;29(3):320-327. doi: 10.1111/clr.13119. PMID: 29537706.

32. Schuh P, Wachtel H. Implant-Supported Immediately Loaded Fixed Full-Arch Dentures: Evaluation of Implant Survival Rates in a Case Cohort of up to 7 Years. Clin Implant Dent Relat Res. 2017 Feb;19(1):4-19. doi: 10.1111/cid.12421. Epub 2016 May 15. PMID: 27196731.

33. Lerner H, Hauschild U, Sader R, Ghanaati S. Complete-arch fixed reconstruction by means of guided surgery and immediate loading: a retrospective clinical study on 12 patients with 1 year of follow-up. BMC Oral Health. 2020 Jan 16;20(1):15. doi: 10.1186/s12903-019-0941-z. PMID: 31948414; PMCID:

34. Franchina A, Stefanelli LV, Maltese F, Mandelaris GA, Vantaggiato A, Pagliarulo M, Pranno N, Brauner E, Angelis F, Carlo SD. Validation of an Intra-Oral Scan Method Versus Cone Beam Computed Tomography Superimposition to Assess the Accuracy between Planned and Achieved Dental Implants: A Randomized In Vitro Study. Int J Environ Res Public Health. 2020 Dec 14;17(24):9358. doi: 10.3390/ijerph17249358. PMID: 33542168; PMCID: PMC7765074.

35. Mangano F, Veronesi G. Digital versus Analog Procedures for the Prosthetic Restoration of Single Implants: A Randomized Controlled Trial with 1 Year of Follow-Up. Biomed Res Int. 2018 Jul 18;2018:5325032. doi: 10.1155/2018/5325032. PMID: 30112398; PMCID: PMC6077568.

36. Mangano F, Veronesi G. Digital versus Analog Procedures for the Prosthetic Restoration of Single Implants: A Randomized Controlled Trial with 1 Year of Follow-Up. Biomed Res Int. 2018 Jul 18;2018:5325032. doi: 10.1155/2018/5325032. PMID: 30112398; PMCID: PMC6077568.

37. de Oliveira NRC, Pigozzo MN, Sesma N, Laganá DC. Clinical efficiency and patient preference of digital and conventional workflow for single implant crowns using immediate and regular digital impression: A meta-analysis. Clin Oral Implants Res. 2020 Aug;31(8):669-686. doi: 10.1111/clr.13604. Epub 2020 May 28. PMID: 32329094.

38. Di Fiore A, Meneghello R, Graiff L, Savio G, Vigolo P, Monaco C, Stellini E. Full arch digital scanning systems performances for implant-supported fixed dental prostheses: a comparative study of 8 intraoral scanners. J Prosthodont Res. 2019 Oct;63(4):396-403. doi: 10.1016/j.jpor.2019.04.002. Epub 2019 May 7. PMID: 31072730.

39. Wulfman C, Naveau A, Rignon-Bret C. Digital scanning for complete-arch implant-supported restorations: A systematic review. J Prosthet Dent. 2020 Aug;124(2):161-167. doi: 10.1016/j.prosdent.2019.06.014. Epub 2019 Nov 19. PMID: 31757443.

40. Ahlholm P, Sipilä K, Vallittu P, Jakonen M, Kotiranta U. Digital Versus Conventional Impressions in Fixed Prosthodontics: A Review. J Prosthodont. 2018 Jan;27(1):35-41. doi: 10.1111/jopr.12527. Epub 2016 Aug 2. PMID: 27483210.

41. Hack G, Liberman L, Vach K, Tchorz JP, Kohal RJ, Patzelt SBM. Computerized optical impression making of edentulous jaws - An in vivo feasibility study. J Prosthodont Res. 2020 Oct;64(4):444-453. doi: 10.1016/j.jpor.2019.12.003. Epub 2020 Feb 13. PMID: 32061572.

42. Keul C, Güth JF. Accuracy of full-arch digital impressions: an in vitro and in vivo comparison. Clin Oral Investig. 2020 Feb;24(2):735-745. doi: 10.1007/s00784-019-02965-2. Epub 2019 May 27. PMID: 31134345.

43. Wulfman C, Naveau A, Rignon-Bret C. Digital scanning for complete-arch implant-supported restorations: A systematic review. J Prosthet Dent. 2020 Aug;124(2):161-167. doi: 10.1016/j.prosdent.2019.06.014. Epub 2019 Nov 19. PMID: 31757443.

44. Goracci C, Franchi L, Vichi A, Ferrari M. Accuracy, reliability, and efficiency of intraoral scanners for full-arch impressions: a systematic review of the clinical evidence. Eur J Orthod. 2016 Aug;38(4):422-8. doi: 10.1093/ejo/cjv077. Epub 2015 Oct 20. PMID: 26487391.

45. Ahlholm P, Sipilä K, Vallittu P, Jakonen M, Kotiranta U. Digital Versus Conventional Impressions in Fixed Prosthodontics: A Review. J Prosthodont. 2018 Jan;27(1):35-41. doi: 10.1111/jopr.12527. Epub 2016 Aug 2. PMID: 27483210.

46. Benic GI, Sailer I, Zeltner M, Gütermann JN, Özcan M, Mühlemann S.
Randomized controlled clinical trial of digital and conventional workflows for the fabrication of zirconia-ceramic fixed partial dentures. Part III: marginal and internal fit. J Prosthet Dent. 2019;121(3):426–31.

47. Schmidt A, Billig JW, Schlenz MA, Wöstmann B. A new 3D-method to assess the inter implant dimensions in patients - A pilot study. J Clin Exp Dent. 2020 Feb 1;12(2):e187-e192. doi: 10.4317/jced.56557. PMID: 32071701; PMCID: PMC7018487.

48. Mandelli F, Zaetta A, Cucchi A, Mangano FG. Solid index impression protocol: a hybrid workflow for high accuracy and passive fit of full-arch implant-supported restorations. Int J Comput Dent. 2020;23(2):161-181. PMID: 32555769.

49. Iturrate M, Lizundia E, Amezua X, Solaberrieta E. A new method to measure the accuracy of intraoral scanners along the complete dental arch: A pilot study. J Adv Prosthodont. 2019 Dec;11(6):331-340. doi: 10.4047/jap.2019.11.6.331. Epub 2019 Dec 18. PMID: 31897272; PMCID: PMC6933048.

50. Gómez-Polo M, Ballesteros J, Perales-Padilla P, Perales-Pulido P, Gómez-Polo C, Ortega R. Guided implant scanning: A procedure for improving the accuracy of implant-supported complete-arch fixed dental prostheses. J Prosthet Dent. 2020 Aug;124(2):135-139. doi: 10.1016/j.prosdent.2019.09.022. Epub 2019 Nov 21. PMID: 31761274.

51. Mangano F, Lerner H, Margiani B, Solop I, Latuta N, Admakin O. Congruence between Meshes and Library Files of Implant Scanbodies: An In Vitro Study Comparing Five Intraoral Scanners. J Clin Med. 2020 Jul 9;9(7):2174. doi: 10.3390/jcm9072174. PMID: 32660070; PMCID: PMC7408706.

52. Kim RJ, Benic GI, Park JM. Trueness of digital intraoral impression in reproducing multiple implant position. PLoS One. 2019 Nov 19;14(11):e0222070. doi: 10.1371/journal.pone.0222070. PMID: 31743331; PMCID: PMC6863547.

53. Sami T, Goldstein G, Vafiadis D, Absher T. An in vitro 3D evaluation of the accuracy of 4 intraoral optical scanners on a 6-implant model. J Prosthet Dent. 2020 Dec;124(6):748-754. doi: 10.1016/j.prosdent.2019.10.013. Epub 2020 Feb 7. PMID: 32037293.

54. Medina-Sotomayor P, Pascual-Moscardó A, Camps I. Accuracy of four digital scanners according to scanning strategy in complete-arch impressions. PLoS One. 2018 Sep 13;13(9):e0202916. doi: 10.1371/journal.pone.0202916. Erratum in: PLoS One. 2018 Dec 20;13(12):e0209883. PMID: 30212498; PMCID: PMC6136706.

55. Zarone F, Di Mauro MI, Ausiello P, Ruggiero G, Sorrentino R. Current status on lithium disilicate and zirconia: a narrative review. BMC Oral Health. 2019 Jul 4;19(1):134. doi: 10.1186/s12903-019-0838-x. PMID: 31272441; PMCID: PMC6610968.

56. Joda T, Bragger U, Zitzmann NU. CAD/CAM implant crowns in a Digital Workflow: Five-year follow-up of a prospective clinical trial. Clin Implant Dent Relat Res. 2019 Feb;21(1):169-174. doi: 10.1111/cid.12681. Epub 2018 Oct 26. PMID: 30362650.

57. Giachetti L, Sarti C, Cinelli F, Russo DS. Accuracy of Digital Impressions in Fixed Prosthodontics: A Systematic Review of Clinical Studies. Int J Prosthodont. 2020 Mar/Apr;33(2):192-201. doi: 10.11607/ijp.6468. PMID: 32069344.

58. Hack G, Liberman L, Vach K, Tchorz JP, Kohal RJ, Patzelt SBM. Computerized optical impression making of edentulous jaws - An in vivo feasibility study. J Prosthodont Res. 2020 Oct;64(4):444-453. doi: 10.1016/j.jpor.2019.12.003. Epub 2020 Feb 13. PMID: 32061572.

59. Keul C, Güth JF. Accuracy of full-arch digital impressions: an in vitro and in vivo comparison. Clin Oral Investig. 2020 Feb;24(2):735-745. doi: 10.1007/s00784-019-02965-2. Epub 2019 May 27. PMID: 31134345.

60. Wulfman C, Naveau A, Rignon-Bret C. Digital scanning for complete-arch implant-supported restorations: A systematic review. J Prosthet Dent. 2020 Aug;124(2):161-167. doi: 10.1016/j.prosdent.2019.06.014. Epub 2019 Nov 19. PMID: 31757443.

61. Goracci C, Franchi L, Vichi A, Ferrari M. Accuracy, reliability, and efficiency of intraoral scanners for full-arch impressions: a systematic review of the clinical evidence. Eur J Orthod. 2016 Aug;38(4):422-8. doi: 10.1093/ejo/cjv077. Epub 2015 Oct 20. PMID: 26487391.

62. Ahlholm P, Sipilä K, Vallittu P, Jakonen M, Kotiranta U. Digital Versus Conventional Impressions in Fixed Prosthodontics: A Review. J Prosthodont. 2018 Jan;27(1):35-41. doi: 10.1111/jopr.12527. Epub 2016 Aug 2. PMID: 27483210.

63. Rutkunas V, Larsson C, Vult von Steyern P, Mangano F, Gedrimiene A. Clinical and laboratory passive fit assessment of implant-supported zirconia restorations fabricated using conventional and Digital Workflow. Clin Implant Dent Relat Res. 2020 Apr;22(2):237-245. doi: 10.1111/cid.12885. Epub 2020 Feb 5. PMID: 32026603.

64. Abduo J, Elseyoufi M. Accuracy of Intraoral Scanners: A Systematic Review of Influencing Factors. Eur J Prosthodont Restor Dent. 2018 Aug 30;26(3):101-121. doi: 10.1922/EJPRD_01752Abduo21. PMID: 29989757.

65. Revilla-León M, Jiang P, Sadeghpour M, Piedra-Cascón W, Zandinejad A, Özcan M, Krishnamurthy VR. Intraoral digital scans-Part 1: Influence of ambient scanning light conditions on the accuracy (trueness and precision) of different intraoral scanners. J Prosthet Dent. 2020 Sep;124(3):372-378. doi: 10.1016/j.prosdent.2019.06.003. Epub 2019 Dec 19. PMID: 31864638.

66. Motel C, Kirchner E, Adler W, Wichmann M, Matta RE. Impact of Different Scan Bodies and Scan Strategies on the Accuracy of Digital Implant Impressions Assessed with an Intraoral Scanner: An In Vitro Study. J Prosthodont. 2020 Apr;29(4):309-314. doi: 10.1111/jopr.13131. Epub 2019 Dec 16. PMID: 31802574.

67. Moslemion M, Payaminia L, Jalali H, Alikhasi M. Do Type and Shape of Scan Bodies Affect Accuracy and Time of Digital Implant Impressions? Eur J Prosthodont Restor Dent. 2020 Feb 27;28(1):18-27. doi: 10.1922/EJPRD_1962Moslemion10. PMID: 32036633.

68. Tallarico M, Lumbau AI, Scrascia R, Demelas G, Sanseverino F, Amarena R, Meloni SM. Feasibility of Using a Prosthetic-Based Impression Template to Improve the Trueness and Precision of a Complete Arch Digital Impression on Four and Six Implants: An In Vitro Study. Materials (Basel). 2020 Aug 11;13(16):3543. doi: 10.3390/ma13163543. PMID: 32796635; PMCID: PMC7475836.

69. Mangano F, Mangano C, Margiani B, Admakin O. Combining Intraoral and Face Scans for the Design and Fabrication of Computer-Assisted Design/Computer-Assisted Manufacturing (CAD/CAM) Polyether-Ether-Ketone (PEEK) Implant-Supported Bars for Maxillary Overdentures. Scanning. 2019 Aug 22;2019:4274715. doi: 10.1155/2019/4274715. PMID: 31531155; PMCID: PMC6724437.

70. Albdour EA, Shaheen E, Vranckx M, Mangano FG, Politis C, Jacobs R. A novel in vivo method to evaluate trueness of digital impressions. BMC Oral Health. 2018 Jul 3;18(1):117. doi: 10.1186/s12903-018-0580-9. PMID: 29970056; PMCID: PMC6029350.

71. Mangano F, Margiani B, Admakin O. A Novel Full-Digital Protocol (SCAN-PLAN-MAKE-DONE) for the Design and Fabrication of Implant-Supported Monolithic Translucent Zirconia Crowns Cemented on Customized Hybrid Abutments: A Retrospective Clinical Study on 25 Patients. Int J Environ Res Public Health. 2019 Jan 24;16(3):317. doi: 10.3390/ijerph16030317. PMID: 30678357; PMCID: PMC6388107.

72. Schepke U, Gresnigt MMM, Browne WR, Abdolahzadeh S, Nijkamp J, Cune MS. Phase transformation and fracture load of stock and CAD/CAM-customized zirconia abutments after 1 year of clinical function. Clin Oral Implants Res. 2019 Jun;30(6):559-569. doi: 10.1111/clr.13442. Epub 2019 May 3. PMID: 31009128.

73. Moris ICM, Chen YC, Faria ACL, Ribeiro RF, Fok AS, Rodrigues RCS. Fracture loads and failure modes of customized and non-customized zirconia abutments. Dent Mater. 2018 Aug;34(8):e197-e204. doi: 10.1016/j.dental.2018.04.005. Epub 2018 May 5. PMID: 29739624.

74. Oberoi G, Nitsch S, Edelmayer M, Janjić K, Müller AS, Agis H. 3D Printing-Encompassing the Facets of Dentistry. Front Bioeng Biotechnol. 2018 Nov 22;6:172. doi: 10.3389/fbioe.2018.00172. PMID: 30525032; PMCID: PMC6262086.

75. Park ME, Shin SY. Three-dimensional comparative study on the accuracy and reproducibility of dental casts fabricated by 3D printers. J Prosthet Dent. 2018 May;119(5):861.e1-861.e7. doi: 10.1016/j.prosdent.2017.08.020. Epub 2018 Feb 21. PMID: 29475753.

76. Park WJ, Park JB. History and application of artificial neural networks in Dentistry. Eur J Dent. 2018 Oct-Dec;12(4):594-601. doi: 10.4103/ejd.ejd_325_18. PMID: 30369809; PMCID: PMC6178664.

77. Joda T, Waltimo T, Probst-Hensch N, Pauli-Magnus C, Zitzmann NU. Health Data in Dentistry: An Attempt to Master the Digital Challenge. Public Health Genomics. 2019;22(1-2):1-7. doi: 10.1159/000501643. Epub 2019 Aug 7. PMID: 31390644.

78. Daas M, Assaf A, Dada K, Makzoumé J. Computer-Guided Implant Surgery in Fresh Extraction Sockets and Immediate Loading of a Full Arch Restoration: A 2-Year Follow-Up Study of 14 Consecutively Treated Patients. Int J Dent. 2015;2015:824127. doi: 10.1155/2015/824127. Epub 2015 May 12. PMID: 26064119; PMCID: PMC4443938.

79. Browaeys H, Dierens M, Ruyffelaert C, Matthijs C, De Bruyn H, Vandeweghe S. Ongoing Crestal Bone Loss around Implants Subjected to Computer-Guided Flapless Surgery and Immediate Loading Using the All-on-4 Concept. Clin Implant Dent Relat Res. 2015 Oct;17(5):831-43. doi: 10.1111/cid.12197. Epub 2014 Jan 8. PMID: 24397413.

80. Allum SR. Immediately loaded full-arch provisional implant restorations using CAD/CAM and guided placement: maxillary and mandibular case reports. Br Dent J. 2008 Apr 12;204(7):377-81. doi: 10.1038/sj.bdj.2008.252. PMID: 18408683.

81. Vercruyssen M, Laleman I, Jacobs R, Quirynen M. Computer-supported implant planning and guided surgery: a narrative review. Clin Oral Implants Res. 2015 Sep;26 Suppl 11:69-76. doi: 10.1111/clr.12638. PMID: 26385623.

82. D'haese J, Ackhurst J, Wismeijer D, De Bruyn H, Tahmaseb A. Current state of the art of computer-guided implant surgery. Periodontol 2000. 2017 Feb;73(1):121-133. doi: 10.1111/prd.12175. PMID: 28000275.

83. Colombo M, Mangano C, Mijiritsky E, Krebs M, Hauschild U, Fortin T. Clinical applications and effectiveness of guided implant surgery: a critical review based on randomized controlled trials. BMC Oral Health. 2017 Dec 13;17(1):150. doi: 10.1186/s12903-017-0441-y. PMID: 29237427; PMCID: PMC5729259.

84. Montero J, Macedo de Paula C, Albaladejo A. The "Toronto prosthesis", an appealing method for restoring patient candidates for hybrid overdentures: A case report. J Clin Exp Dent. 2012 Dec 1;4(5):e309-12. doi: 10.4317/jced.50877. PMID: 24455041; PMCID: PMC3892208.

85. Ata-Ali J, Flichy-Fernández AJ, Alegre-Domingo T, Ata-Ali F, Palacio J, Peñarrocha-Diago M. Clinical, microbiological, and immunological aspects of healthy versus peri-implantitis tissue in full arch reconstruction patients: a prospective cross-sectional study. BMC Oral Health. 2015 Apr 1;15:43. doi: 10.1186/s12903-015-0031-9. PMID: 25888355; PMCID: PMC4391105.

86. Ciabattoni G, Acocella A, Sacco R. Immediately restored full arch-fixed prosthesis on implants placed in both healed and fresh extraction sockets after computer-planned flapless guided surgery. A 3-year follow-up study. Clin Implant Dent Relat Res. 2017 Dec;19(6):997-1008. doi: 10.1111/cid.12550. Epub 2017 Oct 29. PMID: 29082655.

87. Polizzi G, Cantoni T. Five-year follow-up of immediate fixed restorations of maxillary implants inserted in both fresh extraction and healed sites using the NobelGuide™ system. Clin Implant Dent Relat Res. 2015 Apr;17(2):221-33. doi: 10.1111/cid.12102. Epub 2013 Jun 23. PMID: 23789721.

88. Moraschini V, Velloso G, Luz D, Barboza EP. Implant survival rates, marginal bone level changes, and complications in full-mouth rehabilitation with flapless computer-guided surgery: a systematic review and meta-analysis. Int J Oral Maxillofac Surg. 2015 Jul;44(7):892-901. doi: 10.1016/j.ijom.2015.02.013. Epub 2015 Mar 17. PMID: 25790741.

89. Meloni SM, De Riu G, Pisano M, Lolli FM, Deledda A, Campus G, Tullio A. Implant Restoration of Edentulous Jaws with 3D Software Planning, Guided Surgery, Immediate Loading, and CAD-CAM Full Arch Frameworks. Int J Dent. 2013;2013:683423. doi: 10.1155/2013/683423. Epub 2013 Jul 29. PMID: 23983690; PMCID: PMC3745845.

90. Schmidt A, Billig JW, Schlenz MA, Rehmann P, Wöstmann B. Influence of the Accuracy of Intraoral Scanbodies on Implant Position: Differences in Manufacturing Tolerances. Int J Prosthodont. 2019 Sep/Oct;32(5):430-432. doi: 10.11607/ijp.6371. PMID: 31486814.

91. Mangano F, Veronesi G. Digital versus Analog Procedures for the Prosthetic Restoration of Single Implants: A Randomized Controlled Trial with 1 Year of Follow-Up. Biomed Res Int. 2018 Jul 18;2018:5325032. doi: 10.1155/2018/5325032. PMID: 30112398; PMCID: PMC6077568.

92. Arcuri L, Pozzi A, Lio F, Rompen E, Zechner W, Nardi A. Influence of implant scan body material, position and operator on the accuracy of digital impression for complete-arch: A randomized in vitro trial. J Prosthodont Res. 2020 Apr;64(2):128-136. doi: 10.1016/j.jpor.2019.06.001. Epub 2019 Jun 27. PMID: 31255546.

93. Mizumoto RM, Yilmaz B. Intraoral scan bodies in implant Dentistry: A systematic review. J Prosthet Dent. 2018 Sep;120(3):343-352. doi: 10.1016/j.prosdent.2017.10.029. Epub 2018 Apr 5. PMID: 29627211.

94. Moslemion M, Payaminia L, Jalali H, Alikhasi M. Do Type and Shape of Scan Bodies Affect Accuracy and Time of Digital Implant Impressions? Eur J Prosthodont Restor Dent. 2020 Feb 27;28(1):18-27. doi: 10.1922/EJPRD_1962Moslemion10. PMID: 32036633.

95. Latham J, Ludlow M, Mennito A, Kelly A, Evans Z, Renne W. Effect of scan pattern on complete-arch scans with 4 digital scanners. J Prosthet Dent. 2020 Jan;123(1):85-95. doi: 10.1016/j.prosdent.2019.02.008. Epub 2019 Apr 12. PMID: 30982616.

96. Tan MY, Yee SHX, Wong KM, Tan YH, Tan KBC. Comparison of Three-Dimensional Accuracy of Digital and Conventional Implant Impressions: Effect of Interimplant Distance in an Edentulous Arch. Int J Oral Maxillofac Implants. 2019 March/April;34(2):366–380. doi: 10.11607/jomi.6855. Epub 2018 Dec 5. PMID: 30521661.

97. Flügge T, van der Meer WJ, Gonzalez BG, Vach K, Wismeijer D, Wang P. The accuracy of different dental impression techniques for implant-supported dental prostheses: A systematic review and meta-analysis. Clin Oral Implants Res. 2018 Oct;29 Suppl 16:374-392. doi: 10.1111/clr.13273. PMID: 30328182.

98. Huang R, Liu Y, Huang B, Zhang C, Chen Z, Li Z. Improved scanning accuracy with newly designed scan bodies: An in vitro study comparing digital versus conventional impression techniques for complete-arch implant rehabilitation. Clin Oral Implants Res. 2020 Jul;31(7):625-633. doi:

99. Nagy Z, Simon B, Mennito A, Evans Z, Renne W, Vág J. Comparing the trueness of seven intraoral scanners and a physical impression on dentate human maxilla by a novel method. BMC Oral Health. 2020 Apr 7;20(1):97. doi: 10.1186/s12903-020-01090-x. PMID: 32264943; PMCID: PMC7137345.

100. Schwendicke F, Golla T, Dreher M, Krois J. Convolutional neural networks for dental image diagnostics: A scoping review. J Dent. 2019 Dec;91:103226. doi: 10.1016/j.jdent.2019.103226. Epub 2019 Nov 5. PMID: 31704386.

101. Hwang JJ, Jung YH, Cho BH, Heo MS. An overview of deep learning in the field of Dentistry. Imaging Sci Dent. 2019 Mar;49(1):1-7. doi: 10.5624/isd.2019.49.1.1. Epub 2019 Mar 25. PMID: 30941282; PMCID: PMC6444007.

102. Ferro AS, Nicholson K, Koka S. Innovative Trends in Implant Dentistry Training and Education: A Narrative Review. J Clin Med. 2019 Oct 4;8(10):1618. doi: 10.3390/jcm8101618. PMID: 31590228; PMCID: PMC6832343.

103. Hung K, Montalvao C, Tanaka R, Kawai T, Bornstein MM. The use and performance of artificial intelligence applications in dental and maxillofacial radiology: A systematic review. Dentomaxillofac Radiol. 2020 Jan;49(1):20190107. doi: 10.1259/dmfr.20190107. Epub 2019 Aug 14. PMID: 31386555; PMCID: PMC6957072.

104. Kraus RD, Epprecht A, Hämmerle CHF, Sailer I, Thoma DS. Cemented vs screw-retained zirconia-based single implant reconstructions: A 3-year prospective randomized controlled clinical trial. Clin Implant Dent Relat Res. 2019 Aug;21(4):578-585. doi: 10.1111/cid.12735. Epub 2019 Mar 12. PMID: 30861635.

105. Marra R, Acocella A, Alessandra R, Ganz SD, Blasi A. Rehabilitation of Full-Mouth Edentulism: Immediate Loading of Implants Inserted With Computer-Guided Flapless Surgery Versus Conventional Dentures: A 5-Year Multicenter Retrospective Analysis and OHIP Questionnaire. Implant Dent. 2017 Feb;26(1):54-58. doi: 10.1097/ID.0000000000000492. PMID: 27749520.

106. Arisan V, Karabuda CZ, Ozdemir T. Implant surgery using bone- and mucosa-supported stereolithographic guides in totally edentulous jaws: surgical and post-operative outcomes of computer-aided vs. standard techniques. Clin Oral Implants Res. 2010 Sep;21(9):980-8. doi: 10.1111/j.1600-0501.2010.01957.x. Epub 2010 May 24. PMID: 20497439.

107. Arısan V, Bölükbaşı N, Öksüz L. Computer-assisted flapless implant placement reduces the incidence of surgery-related bacteremia. Clin Oral Investig. 2013 Dec;17(9):1985-93. doi: 10.1007/s00784-012-0886-y. Epub 2012 Dec 6. PMID: 23224042.

108. Vercruyssen M, Cox C, Naert I, Jacobs R, Teughels W, Quirynen M. Accuracy and patient-centered outcome variables in guided implant surgery: a RCT comparing immediate with delayed loading. Clin Oral Implants Res. 2016 Apr;27(4):427-32. doi: 10.1111/clr.12583. Epub 2015 Mar 28. PMID: 25817883.

109. Jacobs R, Quirynen M. A randomized clinical trial comparing guided implant surgery (bone- or mucosa-supported) with mental navigation or the use of a pilot-drill template. J Clin Periodontol. 2014 Jul;41(7):717-23. doi: 10.1111/jcpe.12231. Epub 2014 Apr 10. PMID: 24460748.

110. Vercruyssen M, Cox C, Coucke W, Naert I, Jacobs R, Quirynen M. A randomized clinical trial comparing guided implant surgery (bone- or mucosa-supported) with mental navigation or the use of a pilot-drill template. J Clin Periodontol. 2014 Jul;41(7):717-23. doi: 10.1111/jcpe.12231. Epub 2014 Apr 10. PMID: 24460748.

111. Van Assche N, Vercruyssen M, Coucke W, Teughels W, Jacobs R, Quirynen M. Accuracy of computer-aided implant placement. Clin Oral Implants Res. 2012 Oct;23 Suppl 6:112-23. doi: 10.1111/j.1600-0501.2012.02552.x. PMID: 23062136.

112. Mangano FG, Hauschild U, Admakin O. Full in-Office Guided Surgery with Open Selective Tooth-Supported Templates: A Prospective Clinical Study on 20 Patients. Int J Environ Res Public Health. 2018 Oct 25;15(11):2361. doi: 10.3390/ijerph15112361. PMID: 30366435; PMCID: PMC6266226.

113. Spielau T, Hauschild U, Katsoulis J. Computer-assisted, template-guided immediate implant placement and loading in the mandible: a case report. BMC Oral Health. 2019 Apr 11;19(1):55. doi: 10.1186/s12903-019-0746-0. PMID: 30975113; PMCID: PMC6460533.

APPENDIX

RESEARCH ARTICLE   **Open Access**

Trueness of 12 intraoral scanners in the full-arch implant impression: a comparative in vitro study

Francesco Guido Mangano[1]* , Oleg Admakin[1], Matteo Bonacina[2], Henriette Lerner[3], Vygandas Rutkunas[4] and Carlo Mangano[5]

Abstract

Background: The literature has not yet validated the use of intraoral scanners (IOSs) for full-arch (FA) implant impression. Hence, the aim of this in vitro study was to assess and compare the trueness of 12 different IOSs in FA implant impression.

Methods: A stone-cast model of a totally edentulous maxilla with 6 implant analogues and scanbodies (SBs) was scanned with a desktop scanner (Freedom UHD®) to capture a reference model (RM), and with 12 IOSs (ITERO ELEM ENTS 5D®; PRIMESCAN® and OMNICAM®; CS 3700® and CS 3600®; TRIOS3®; i-500®; EMERALD S® and EMERALD®; VIRTUO VIVO® and DWIO®; RUNEYES QUICKSCAN®). Ten scans were taken using each IOS, and each was compared to the RM, to evaluate trueness. A mesh/mesh method and a nurbs/nurbs method were used to evaluate the overall trueness of the scans; linear and cross distances between the SBs were used to evaluate the local trueness of the scans. The analysis was performed using reverse engineering software (Studio®, Geomagics; Magics®, Materialise). A statistical evaluation was performed.

Results: With the mesh/mesh method, the best results were obtained by CS 3700® (mean error 30.4 μm) followed by ITERO ELEMENTS 5D® (31.4 μm), i-500® (32.2 μm), TRIOS 3® (36.4 μm), CS 3600® (36.5 μm), PRIMESCAN® (38.4 μm), VIRTUO VIVO® (43.8 μm), RUNEYES® (44.4 μm), EMERALD S® (52.9 μm), EMERALD® (76.1 μm), OMNICAM® (79.6 μm) and DWIO® (98.4 μm). With the nurbs/nurbs method, the best results were obtained by ITERO ELEMENTS 5D® (mean error 16.1 μm), followed by PRIMESCAN® (19.3 μm), TRIOS 3® (20.2 μm), i-500® (20.8 μm), CS 3700® (21.9 μm), CS 3600® (24.4 μm), VIRTUO VIVO® (32.0 μm), RUNEYES® (33.9 μm), EMERALD S® (36.8 μm), OMNICAM® (47.0 μm), EMER ALD® (51.9 μm) and DWIO® (69.9 μm). Statistically significant differences were found between the IOSs. Linear and cross distances between the SBs (local trueness analysis) confirmed the data that emerged from the overall trueness evaluation.

Conclusions: Different levels of trueness were found among the IOSs evaluated in this study. Further studies are needed to confirm these results.

Keywords: Intraoral scanner, Full-arch implant impression, Scanbody, Trueness, Comparative study

* Correspondence: francescomangano1@mclink.net
[1]Department of Prevention and Communal Dentistry, Sechenov First State
Medical University, 119992 Moscow, Russia
Full list of author information is available at the end of the article

Mangano *et al. BMC Oral Health* (2020) 20:263

Page 2 of 21

Background

Intraoral scanners (IOSs) are changing the world of implant prosthodontics [1, 2]. IOSs use structured light and/or laser to capture sequential images of the patient's dental arches, allowing three-dimensional (3D) reconstruction of their surface using powerful reconstruction software. These software applications generate point clouds that are triangulated to give surface reconstructions (meshes), i.e. virtual models of the patient's dental arches [2, 3].

IOS optical impressions allow the dentist to capture virtual models of the patient's dental arches, with no conventional impression using trays and materials (which have always been unwelcome to patients) and without having to pour any plaster cast, saving time and space [2, 4, 5]. The clinical procedure is technically simplified, and the virtual models can be immediately sent to the laboratory as standard tessellation language (STL) files, without disinfection or shipping costs [2, 5, 6]. The optical impressions improve the communication with the dental laboratory, which becomes more efficient, and represents the gateway to the world of computer-aided design and manufacturing (CAD/CAM) [5, 6].

To date, in fixed implant prosthodontics, the scientific literature has validated the use of IOSs for capturing optical impressions for the design and manufacture of short-span restorations such as single crowns (SCs) [7–10] and partial prostheses (PPs) [11–13]. However, in the case of long-span restorations, and in particular for full arches (FAs), IOSs do not yet seem to be sufficiently accurate, as reported by several studies [14, 15] and reviews of the literature [16, 17].

In metrics, accuracy is "the closeness of agreement between a measured quantity value and a true quantity value of a measurand" (JCGM 200:2012; ISO 5725–1, 1994) [2, 4, 13], and when it comes to IOSs, it is the combination of trueness and precision. Trueness is the most important factor, defined as "the closeness of agreement between the arithmetic mean of a large number of test results and the true or accepted reference value". Trueness expresses how much the average of a series of measurements approaches reality; a measurement is truer the closer it is to the actual value of the object. To evaluate the trueness of a measurement requires a reference: in the case of dental models, this is an acquisition made with a machine with certified accuracy (possibly ≤5 μm), such as a coordinate measuring machine (CMM), or an industrial optical or desktop scanner [2, 4, 13]. Specifically, the acquisitions obtained with IOSs must be compared with those obtained with one of these reference machines to be mathematically validated. Precision is "the closeness of agreement between measured quantity values obtained by replicate measurements on the same objects under specified conditions": it refers to the closeness of agreement and deviations between test results. To evaluate precision does not require a reference: it is sufficient to compare the measurements made with the same IOS and evaluate the deviations between them [2, 4, 14].

Because it is not possible to use machines with certified accuracy such as CMMs, articulated arms or industrial scanners in the patient's mouth, and having a certified reference file is not possible, measuring the trueness of optical impressions with IOS in vivo is difficult [2, 4, 18]. Some authors have recently tried to introduce indexes [19, 20] or geometric shapes with known dimensions (custom measuring aids) [21, 22] in the mouth to evaluate the distortions affecting the optical impression in vivo, but the vast majority of studies of the trueness of IOSs have been made in vitro on plaster models [14, 15, 23–26].

Among these in vitro studies, many have used a mesh/mesh method, directly superimposing the meshes (virtual models) derived from intraoral scanning with different IOSs onto a reference mesh obtained with a certified industrial or desktop scanner [14, 15, 23, 24]. Although this approach is intuitive and immediate, and provides reliable information about the overall trueness of a scan, it has limitations. First, it uses meshes that are surface reconstructions and therefore geometric approximations of the scanned model, on which it is impossible to perform reliable distance calculations between the different scanbodies (SBs), i.e. the digital transfers of the implant position. In addition, this approach does not really replicate what happens in the early stages of prosthetic CAD modelling. In implant prosthodontics, the first CAD step involves replacing the mesh (which is a surface reconstruction and therefore a geometric approximation) of the SB with the corresponding SB library file, available in the manufacturer's implant library [1, 25–27]. This library file, although saved in the same STL format, is not the result of a 3D acquisition (and therefore a surface reconstruction with geometric approximation, such as a mesh): it is a geometrically perfect file or a non-uniform rational b-spline (nurbs) file, originally designed in CAD, and linked to all the other components of the implant library (bonding bases of different height and diameter) on which the dental technician models the individual abutment or the restoration directly [25–27]. For this reason, investigating the accuracy of an intraoral scan after replacing each of the SBs in the mesh with the corresponding library file, and then superimposing two nurbs files (the position of the SBs in the space obtained with the reference scanner and with the IOSs, respectively), may be important to obtain more reliable information on the overall trueness and to be able to calculate the exact distances between the SBs with 3D calculation software, after having automatically identified

their centroids. This approach requires substantial work and hundreds of superimpositions but is probably the most suitable to be able to identify the overall and local trueness (distances between the SBs) of an IOS, considering that the distances between the SBs cannot be properly calculated on a mesh [26–28].

The purpose of this in vitro study was therefore to assess and compare the overall trueness of 12 different IOSs, using two different investigation methods (mesh/mesh and nurbs/nurbs superimposition), and to calculate the exact distances between the different SBs (linear distances between the SBs during the progression of the scan and cross distances, i.e., distances between SBs with different positions in the arch).

Methods

Study design

The present in vitro study was designed to assess and compare the trueness of 12 different IOSs (ITERO ELEMENTS 5D®, Align Technologies, San José, CA, USA; PRIMESCAN® and OMNICAM®, Dentsply Sirona, York, PA, USA; CS 3700® and CS 3600®, Carestream Dental, Atlanta, GA, USA; TRIOS3®, 3-Shape, Copenhagen, Denmark; i-500®, Medit, Seoul, South Korea; EMERALD S® and EMERALD®, Planmeca, Helsinki, Finland; VIRTUO VIVO® and DWIO®, Dentalwings, Montreal, Canada; RUNEYES QUICKSCAN®, Runeyes Medical Instruments, Ningbo, Zhejiang, China) in FA implant impression.

This study used a type IV gypsum model representing a totally edentulous maxilla with 6 implant analogues in positions #11, #14, #16, #21, #24 and #26 (right and left central incisors, first premolars and first molars) and high-precision non-reflective polyether-ether-ketone

(PEEK) SBs (Megagen®, Daegu, South Korea) screwed on (Fig. 1). The SBs were named by convention S1 (#26), S2 (#24), S3 (#21), S4 (#11), S5 (#14) and S6 (#16). The model, which had been also used in a previous study [14], presented pink gum in the areas of the implant analogues and simulated the situation of an implant-supported fixed FA prosthesis.

The gypsum model was first scanned with a powerful desktop scanner (Freedom UHD®, Dof Inc., Seoul, Korea), to acquire reference virtual models. This desktop scanner uses a white light-emitting diode and has two 5.0 mega-pixel cameras. It works under patented stable scan stage technology, which allows the cameras and lights to move and rotate above and around the model, which remains stationary. This allows rapid and effective capture of all details of the model in a few steps and in less than 1 min, generating virtual models in STL immediately usable by any CAD. The scanner has dimensions of $330 \times 495 \times 430$ mm and a weight of 15 kg, is powered at 110–240 V and 50–60 Hz, and works with Windows operating systems 7, 8, and 10 (64-bit). Three virtual models were captured with this desktop scanner and saved in a dedicated folder, labelled with the scanner name. Then, the quality of these meshes was investigated with reverse engineering software (Studio®, Geomagics, Morrisville, NC, USA), and always within the same software, the models were cut and trimmed in order to isolate the SBs and to eliminate the pink gingiva area. Once cut and made uniform, these meshes were superimposed for the validation of the superimposition method and for the choice of the reference model (RM) to be used in the study, as previously described [29]. The RM was saved in a specific folder, ready for use.

Fig. 1 In this in vitro study, a type IV gypsum model was used. This model represented a totally edentulous maxilla with 6 implant analogues in positions #11, #14, #16, #21, #24 and #26 (right and left central incisors, first premolars and first molars) and high-precision non-reflective polyether-ether-ketone (PEEK) SBs (Megagen®, Daegu, South Korea) screwed on

After the preparation of the desktop RM was completed, a single operator with over 10 years of experience with intraoral scanning (FGM) began to capture the scans with each of the IOSs in the study. All scans were taken in a 2-month period (January–February 2020) with the latest acquisition software available for each IOS at that time. The main characteristics of the IOSs used in this study are summarised in Table 1. In all, the operator captured 10 scans for each IOS. The scans had to include the entire area of the pink gum and the 6 different SBs in full. To minimise the potential effects of fatigue, the sequence of scan capture with the different IOSs was randomised. The scans were spaced from each other by a rest period of 5 min for the operator. In all cases, the operator started from the posterior sectors (right or left) and proceeded along the arch with a zig-zag technique. As reported in previous studies [14, 27], this technique provided for a slow and constant advancement of the scan along the arch, starting from the buccal area and then moving occlusally and palatally, and returning to the buccal area: an arch was described above the pink gum and implant SBs. All scans were captured in the same environmental conditions, in a room moderately lit by sunlight with a temperature of 21 °C, humidity of 45% and air pressure of 750 ± 5 mm. Ten virtual models were captured for each IOS, for a total of 120 STL files. These

files were saved in dedicated folders, labelled with the IOS name and progressively numbered from 1 to 10.

Outcome variables

Three different evaluations were performed using the RM acquired with the desktop scanner and the models derived from the different IOSs: a mesh/mesh evaluation and a nurbs/nurbs evaluation, to compute the overall general trueness of the intraoral scanning models, and the evaluation of the linear and cross distances between the different SBs, for analysis of the local trueness of the intraoral scanning models. The latter evaluation used the STL files generated during the nurbs/nurbs evaluation. The evaluation of the overall trueness with the mesh/mesh and nurbs/nurbs methods (overall general trueness) was performed using reverse engineering software (Studio®, Geomagics, Morrisville, NC, USA) by the same experienced operator (FGM) who captured all the scans. The evaluation of the distances between the SBs was performed by another operator (MB) with many years of experience with 3D calculation software, using different software (Magics®, Materialise, Leuven, Belgium).

Mesh/mesh evaluation

This evaluation was based exclusively on the meshes (STL files) generated by scanning with the desktop

Table 1 Features of the IOSs investigated in this study

Name	Manufacturer	Acquisition technology	Output files
ITERO ELEMENTS 5D®	Align Technologies, San Josè, CA, USA	Parallel Confocal Microscopy	3ds (proprietary format); ply and stl (open formats)
PRIMESCAN®	Dentsply Sirona, York, PN, USA	High-resolution Sensors and Shortwave Light with Optical High Frequency Contrast Analysis for Dynamic Deep Scan (20 mm)	dxd (proprietary format) with possibility to export .stl files (open format) with Cerec Connect®
OMNICAM®		Optical Triangulation and Confocal Microscopy	cs3, sdt, cdt, idt (proprietary format) with possibility to export .stl files (open format) with Cerec Connect®
CS 3700®	Carestream Dental, Atlanta, GA, USA	Active Triangulation with Smart-shade Matching via Bidirectional Reflectance Distribution Function	dcm (proprietary format); ply and stl (open formats)
CS 3600®		LED light scanner -Active Speed 3D Video	csz (proprietary format), ply and stl (open formats)
TRIOS3®	3-Shape, Copenhagen, Denmark	Confocal Microscopy and Ultrafast Optical Scanning	dcm (proprietary format), with possibility to export stl files (open formats) with Trios on Dental Desktop®
i-500®	Medit, Seoul, South Korea	3D in Motion Video Technology	obj, ply and stl (open formats)
EMERALD S®	Planmeca, Helsinki, Finland	Red, green and blue lasers- Projected Pattern Triangulation	3oxz (proprietary format), ply and stl (open formats)
EMERALD®		Red, green and blue lasers- Projected Pattern Triangulation	3oxz (proprietary format), ply and stl (open formats)
VIRTUOVIVO®	Dentalwings, Montreal, Canada	Blue laser-Multiscan Imaging Technology	xorder (proprietary format); ply, stl (open format)
DWIO®		Blue laser-Multiscan Imaging Technology	xorder (proprietary format); ply, stl (open format)
RUNEYES®	Runeyes MI, Ningbo, Zhejiang, China	Synchronous 3D Video Quick Technology	obj, ply and stl (open formats)

scanner (RM) and the different IOSs, and took place as described in previous studies [14, 23, 24]. Each of the 10 meshes generated by each of the 12 IOSs was imported into reverse engineering software (Studio®, Geomagics, Morrisville, NC, USA), cut and trimmed with a single pre-formed template that included the pink gingiva area to be uniform in size, and then superimposed onto the RM captured with the desktop scanner, to evaluate the mean distance (± standard deviation, SD) between the models. The superimposition consisted of two steps. First, the software performed a rough alignment of the IOS model over the RM, determined by three or more points that were identified on the surface of the same SBs present in the two models. This first rough alignment was subsequently perfected by the software through the application of a best-fit algorithm that allowed the surfaces to fully overlap. The parameters for this last superimposition were set with a minimum of 100 iterations per case, and the surface registration was completed by a robust-iterative-closest-point (RICP) algorithm. With this RICP algorithm, the distances between the RM and the IOS models were minimised using a point-to-plane method and the congruence between corresponding structures was calculated. Finally, the signed mean ± SD of the distances in µm between the two superimposed models was calculated by the software, and a colorimetric map was generated to immediately visualise the distances between the models. The "3D deviation" function was used to generate the colorimetric map and quantify the distances between specific points, overall and in all space planes. The same setting for this map was used for all models, with the colour scale ranging from a maximum deviation of + 100 µm to − 100 µm, and the best result given by the deviations between + 30 µm and − 30 µm. The generated colour map indicated an outward (red) or inward (blue) deviation between the overlaid structures, while a minimal displacement (< 30 µm) was indicated by green. The data retrieved from these superimpositions for each IOS were saved in specific electronic datasheets (Excel®, Microsoft, Redmond, WA, USA) ready for statistical analysis, whereas the visual screenshots derived from each single superimposition were saved in another format (PowerPoint®, Microsoft, Redmond, WA, USA).

Nurbs/nurbs evaluation

This evaluation took place after replacing, within each mesh (the RM from the desktop scanner and all virtual models from the IOSs), the 6 SB meshes with the corresponding SB library file, downloaded from the official library of the implant manufacturer (Megagen®, Daegu, South Korea). A new STL file was saved for each virtual model, which included only 6 SBs (nurbs files) free in the space, representing the implant positions. These nurbs files were used for superimpositions.

In detail, each of the meshes, already cut and trimmed as previously described, was opened with reverse engineering software (Studio®, Geomagics, Morrisville, NC, USA). Then, 6 identical STL files were uploaded, those of the reference (nurbs) SB library file, provided directly from the implant library of the manufacturing company. At this point, these library files were superimposed onto each of the SBs present in the mesh, through the same superimposition procedure described above. First, a rough alignment of the library file was performed over the SB mesh; then, the surface superimposition was performed by the software, using the aforementioned RICP algorithm. This procedure was repeated for each single SB in the mesh, to obtain an STL file with the 6 SB library files in the correct position in the space. Then, the mesh was cancelled and a new file (nurbs file) with only the 6 SB library files in the proper position was saved. At the end of this procedure, which simulated what happens in the early stages of work in prosthetic CAD software (where the dental technician replaces the SB library file on the 3D reconstruction of the SB in the mesh, thus obtaining a hybrid model), it was possible to save files consisting of 6 SBs from the implant library free in the space, in a position derived from that of SBs in the mesh. These nurbs files were saved in special folders, labelled with the different IOS names and progressively numbered from 1 to 10, and were ready for analysis.

The analysis consisted of the superimposition of each of these nurbs STL files, derived from the different IOSs, over the RM nurbs. The procedure was the same as used in the mesh/mesh evaluation. Within the reverse engineering software (Studio®, Geomagics, Morrisville, NC, USA), the operator proceeded with an initial alignment of the nurbs file from the IOS onto the RM nurbs from the desktop scanner. This initial rough alignment took place by points, which were identified on the body of the scan abutments. Subsequently, the operator launched the best-fit algorithm, which perfected a surface alignment, generating the signed mean (± SD) of the distance in µm between the two nurbs files. Also in this case, the distances were represented graphically with a colorimetric map. The same settings used in the mesh/mesh evaluation were used, except for the green area, which was defined for an error < 25 µm. Once again, the data retrieved from these superimpositions for each IOS were saved in specific electronic datasheets (Excel®, Microsoft, Redmond, WA, USA) ready for statistical analysis, whereas the visual screenshots derived from each single superimposition were saved in another format (PowerPoint®, Microsoft, Redmond, WA, USA).

Linear and cross distances

A 3D calculation software (Magics®, Materialise, Leuven, Belgium) was used to compute the distances in µm between the different SBs. The calculation of the linear
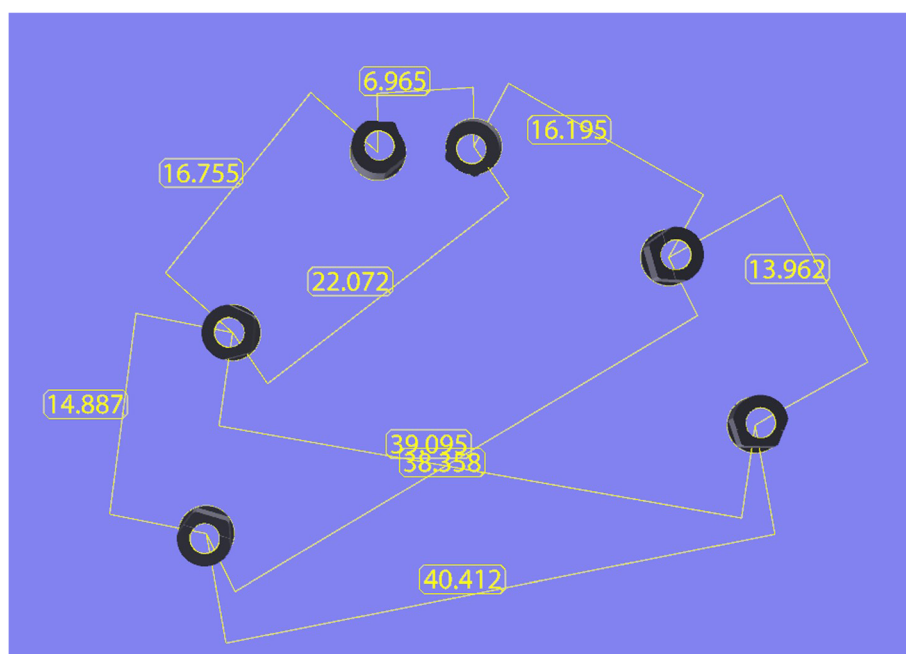
Fig. 2 Automatic evaluation of the linear and cross distances with the reference file, in mm (Magics Magics®, Materialise, Leuven, Belgium)

and cross distances was first performed on the RM nurbs file, to define the reference values for each distance. The following linear distances (i.e. distances of the SBs during the progression of the scan) were computed: S1–S2, S2–S3, S3–S4, S4–S5 and S5–S6. The cross distances (i.e. distances between SBs with different positions in the arch) were computed as follows: S1–S6, S1–S5, S2–S6 and S3–S5. The distances were automatically computed by the software as distances between the centroids at the bases of the SBs (Fig. 2). Once the reference values for each single distance were computed and

saved in a specific datasheet (Excel®, Microsoft, Redmond, WA, USA), the same computation was repeated for each nurbs file from each single IOS scan. Tables were generated with all values for each scan taken from each IOS, and these values were used for statistical analysis.

Statistical analysis

Data analysis and visualisation were performed using R (version 3.6.3) environment for statistical computing (R Foundation for Statistical Computing, Vienna, Austria).

Table 2 Descriptive statistics (error in µm, medians and quartiles, means and 95% CIs) for mesh/mesh and nurbs/nurbs evaluations
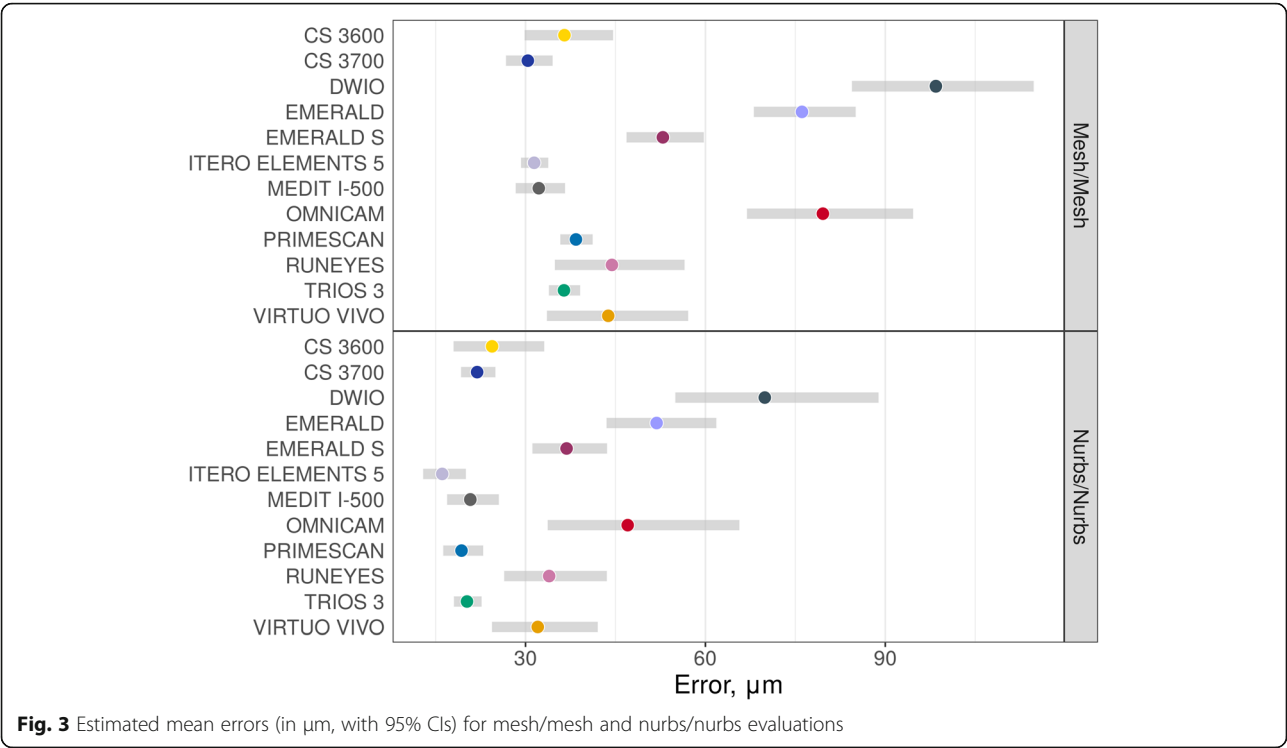
Scanner	Mesh/Mesh		Nurbs/Nurbs	
	Median (Q_1–Q_3)	**Mean (95% CI)**	**Median (Q_1–Q_3)**	**Mean (95% CI)**
CS 3600®	35.5 (31.5–46.0)	36.5 [29.8; 44.6]	23.5 (21.5–34.0)	24.4 [18.0; 33.1]
CS 3700®	29.5 (27.2–34.5)	30.4 [26.7; 34.5]	22.0 (19.8–24.8)	21.9 [19.3; 25.0]
DWIO®	90.5 (84.2–110.8)	98.4 [84.4; 114.8]	65.0 (51.0–82.2)	69.9 [55.0; 88.9]
EMERALD®	76.0 (67.5–81.0)	76.1 [68.1; 85.1]	54.5 (40.8–60.5)	51.9 [43.5; 61.8]
EMERALD S®	51.0 (46.5–54.8)	52.9 [46.8; 59.7]	37.0 (31.2–40.8)	36.8 [31.1; 43.6]
ITERO ELEMENTS 5D®	32.0 (30.2–33.8)	31.4 [29.2; 33.8]	15.0 (14.2–16.8)	16.1 [12.9; 20.1]
MEDIT I-500®	31.5 (29.0–33.8)	32.2 [28.4; 36.6]	20.5 (17.5–25.8)	20.8 [16.9; 25.5]
OMNICAM®	80.5 (72.2–90.8)	79.6 [66.9; 94.6]	56.0 (33.2–62.5)	47.0 [33.7; 65.7]
PRIMESCAN®	39.5 (35.5–41.8)	38.4 [35.8; 41.2]	19.0 (17.0–23.8)	19.3 [16.3; 22.9]
RUNEYES®	41.5 (33.5–56.0)	44.4 [34.9; 56.5]	32.5 (26.0–43.0)	33.9 [26.4; 43.6]
TRIOS 3®	36.0 (35.2–38.5)	36.4 [33.9; 39.1]	20.5 (19.0–23.0)	20.2 [18.1; 22.7]
VIRTUO VIVO®	38.0 (35.2–42.2)	43.8 [33.6; 57.1]	28.0 (26.2–33.2)	32.0 [24.4; 42.0]

Table 3 Mesh/mesh evaluation. Differences (with standard errors) are presented at the top and right of the table, and correspond to row scanner names minus column scanner names. p-values for comparison are placed at the bottom and left of the table

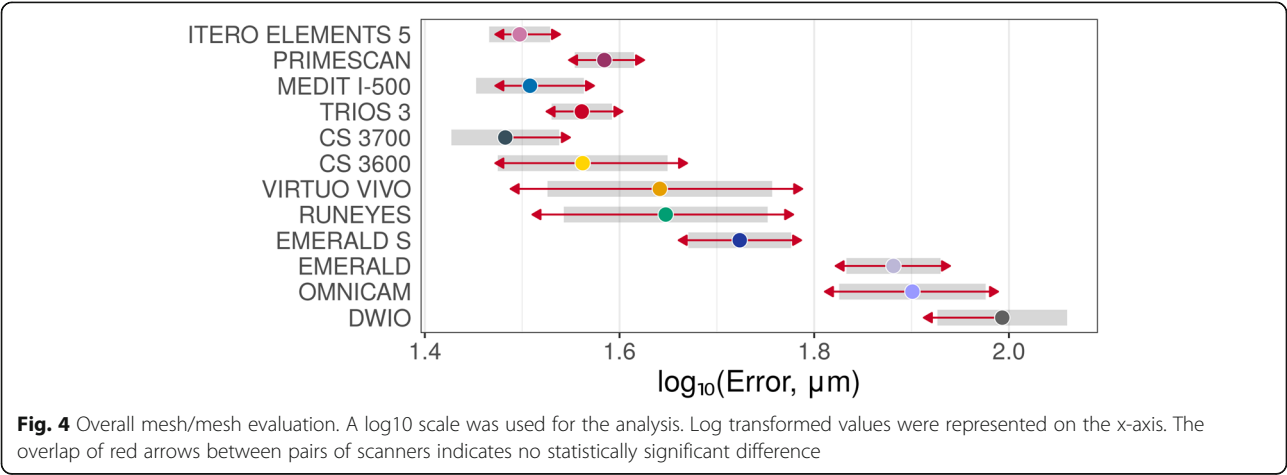|	CS 3600®	CS 3700®	DWIO®	EMERALD®	EMERALD S®	ITERO ELEMENTS 5D®	MEDIT I-500®	OMNICAM®	PRIMESCAN®	RUNEYES®	TRIOS 3®	VIRTUO VIVO®
CS 3600®		0.08 (0.05)	−0.43 (0.06)	−0.32 (0.05)	−0.16 (0.05)	0.06 (0.05)	0.05 (0.05)	−0.34 (0.06)	−0.02 (0.05)	−0.09 (0.07)	0.00 (0.05)	−0.08 (0.07)
CS 3700®	0.9		−0.51 (0.04)	−0.40 (0.04)	−0.24 (0.04)	−0.01 (0.03)	−0.03 (0.04)	−0.42 (0.05)	−0.10 (0.03)	−0.16 (0.06)	−0.08 (0.03)	−0.16 (0.06)
DWIO®	< 0.0001	< 0.0001		0.11 (0.04)	0.27 (0.04)	0.50 (0.04)	0.49 (0.04)	0.09 (0.05)	0.41 (0.04)	0.35 (0.06)	0.43 (0.04)	0.35 (0.07)
EMERALD®	< 0.0001	< 0.0001	0.2		0.16 (0.04)	0.38 (0.03)	0.37 (0.04)	−0.02 (0.05)	0.30 (0.03)	0.23 (0.06)	0.32 (0.03)	0.24 (0.06)
EMERALD S®	0.09	< 0.0001	< 0.0001	0.002		0.23 (0.03)	0.22 (0.04)	−0.18 (0.05)	0.14 (0.03)	0.08 (0.06)	0.16 (0.03)	0.08 (0.06)
ITERO ELEMENTS 5D®	1.0	1.0	< 0.0001	< 0.0001	< 0.0001		−0.01 (0.03)	−0.40 (0.04)	−0.09 (0.02)	−0.15 (0.06)	−0.06 (0.02)	−0.14 (0.06)
MEDIT I-500®	1.0	1.0	< 0.0001	< 0.0001	< 0.0001	1.0		−0.39 (0.05)	−0.08 (0.03)	−0.14 (0.06)	−0.05 (0.03)	−0.13 (0.06)
OMNICAM®	< 0.0001	< 0.0001	0.8	1.0	< 0.0001	< 0.0001	< 0.0001		0.32 (0.04)	0.25 (0.07)	0.34 (0.04)	0.26 (0.07)
PRIMESCAN®	1.0	0.08	< 0.0001	< 0.0001	0.0009	0.007	0.4	< 0.0001		−0.06 (0.06)	0.02 (0.02)	−0.06 (0.06)
RUNEYES®	1.0	0.2	< 0.0001	0.006	1.0	0.2	0.5	0.009	1.0		0.09 (0.06)	0.01 (0.08)
TRIOS 3®	1.0	0.4	< 0.0001	< 0.0001	< 0.0001	0.2	0.9	< 0.0001	1.0	0.9		−0.08 (0.06)
VIRTUO VIVO®	1.0	0.4	< 0.0001	0.01	1.0	0.4	0.6	0.02	1.0	1.0	1.0	

Table 4 Nurbs/nurbs evaluation. Differences (with standard errors) are presented at the top and right of the table, and correspond to row scanner names minus column scanner names. *p*-values for comparison are placed at the bottom and left of the table

	CS 3600®	CS 3700®	DWIO®	EMERALD®	EMERALD S®	ITERO ELEMENTS 5D®	MEDIT I-500®	OMNICAM®	PRIMESCAN®	RUNEYES®	TRIOS 3®	VIRTUO VIVO®
CS 3600®		0.05 (0.07)	−0.46 (0.09)	−0.33 (0.08)	−0.18 (0.08)	0.18 (0.08)	0.07 (0.08)	−0.28 (0.10)	0.10 (0.08)	−0.14 (0.09)	0.08 (0.07)	−0.12 (0.09)
CS 3700®	1.0		−0.50 (0.06)	−0.37 (0.05)	−0.23 (0.05)	0.13 (0.06)	0.02 (0.05)	−0.33 (0.08)	0.05 (0.05)	−0.19 (0.06)	0.03 (0.04)	−0.16 (0.07)
DWIO®	< 0.0001	< 0.0001		0.13 (0.07)	0.28 (0.06)	0.64 (0.07)	0.53 (0.07)	0.17 (0.09)	0.56 (0.06)	0.31 (0.08)	0.54 (0.06)	0.34 (0.08)
EMERALD®	0.003	< 0.0001	0.7		0.15 (0.05)	0.51 (0.06)	0.40 (0.06)	0.04 (0.08)	0.43 (0.05)	0.18 (0.07)	0.41 (0.05)	0.21 (0.07)
EMERALD S®	0.5	0.0003	0.002	0.2		0.36 (0.06)	0.25 (0.06)	−0.11 (0.08)	0.28 (0.05)	0.04 (0.07)	0.26 (0.04)	0.06 (0.07)
ITERO ELEMENTS 5D®	0.6	0.4	< 0.0001	< 0.0001	< 0.0001		−0.11 (0.07)	−0.47 (0.09)	−0.08 (0.06)	−0.32 (0.07)	−0.10 (0.05)	−0.30 (0.08)
MEDIT I-500®	1.0	1.0	< 0.0001	< 0.0001	0.002	0.9		−0.35 (0.09)	0.03 (0.06)	−0.21 (0.07)	0.01 (0.05)	−0.19 (0.07)
OMNICAM®	0.2	0.003	0.8	1.0	1.0	< 0.0001	0.004		0.39 (0.08)	0.14 (0.09)	0.37 (0.08)	0.17 (0.09)
PRIMESCAN®	1.0	1.0	< 0.0001	< 0.0001	< 0.0001	1.0	1.0	0.0005		−0.24 (0.07)	−0.02 (0.05)	−0.22 (0.07)
RUNEYES®	0.9	0.1	0.004	0.2	1.0	0.001	0.1	0.9	0.02		0.22 (0.06)	0.03 (0.08)
TRIOS 3®	1.0	1.0	< 0.0001	< 0.0001	< 0.0001	0.8	1.0	0.0004	1.0	0.01		−0.20 (0.06)
VIRTUO VIVO®	1.0	0.4	0.002	0.1	1.0	0.009	0.3	0.8	0.09	1.0	0.10	

Fig. 3 Estimated mean errors (in μm, with 95% CIs) for mesh/mesh and nurbs/nurbs evaluations

Descriptive statistics for quantitative variables were presented as medians (1st and 3rd quartiles; Tables 2 and 3) and medians (median absolute deviations; Table 4). Before regression modelling, mesh/mesh and nurbs/nurbs distance were log_{10}-transformed (due to substantial right skewness on the raw scale); means and corresponding 95% confidence intervals (CI) were estimated using models then re-transformed to the raw scale (Tables 2 and 3). Linear and cross distances were used in raw scale. Linear models were used to estimate and compare mean mesh/mesh and nurbs/nurbs errors (on the log_{10}-scale) between scanners. The Sandwich standard error estimator was used to address heteroskedasticity, and the Satterthwaite method was used to approximate degrees of freedom. The Tukey method (implemented in emmeans 1.4.5) was used to adjust *p*-values. A linear mixed effects model (implemented in lme4 1.1–21) was used to estimate and compare mean linear and cross distances (on raw scale) between scanners (to account hierarchy: scanner → pairs of SBs). The Sandwich cluster-robust variance-covariance matrix estimator was used to address heteroskedasticity, and the Satterthwaite method was again used to approximate degrees of freedom. The Tukey method was used to adjust p-values.
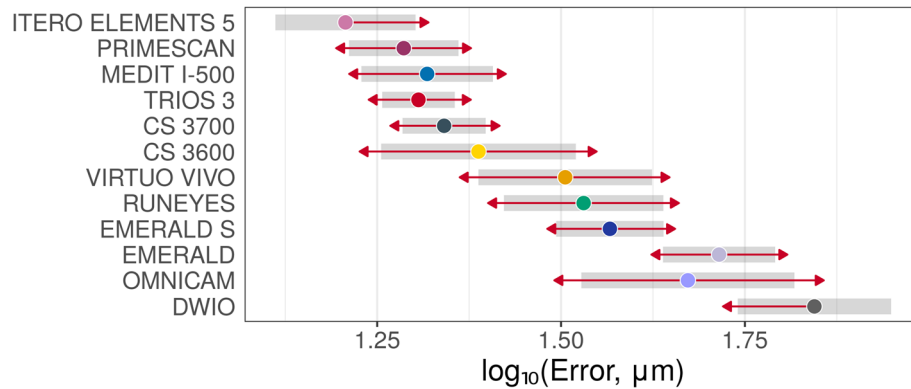

Fig. 4 Overall mesh/mesh evaluation. A log10 scale was used for the analysis. Log transformed values were represented on the x-axis. The overlap of red arrows between pairs of scanners indicates no statistically significant difference

Fig. 5 Overall nurbs/nurbs evaluation. A log10 scale was used for the analysis. Log transformed values were represented on the x-axis. The overlap of red arrows between pairs of scanners indicates no statistically significant difference

Results

Descriptive statistics (medians and quartiles; means and 95% CIs) for mesh/mesh and nurbs/nurbs errors are presented in Table 2. Estimated mean errors (with 95% CIs – symmetrical on the log scale) on raw scales are presented in Figs. 3, 4 and 5. In thes latter two figures, the overlap of the red arrows between pairs of scanners indicates no statistically significant difference. A statistically significant difference was found among different scanner pairs.

Nurbs/nurbs errors were systematically lower than mesh/mesh errors, as evidenced in the scatter plot in Fig. 6, as the test result for H0: $\beta_1 = 1$ (corresponds to model: nurbs/nurbs = β_0 [different for each scanner –

random intercept] + 1 × mesh/mesh): t = 10.7, non-centrality parameter = 1, df = 87.6, $p < 0.0001$. $\beta_1 = 1.21$ (95% CI 1.10; 1.33). Pairwise differences in errors (on log_{10}-scale/orders of differences with corresponding standard errors and *p*-values) with the different methods are presented in Tables 3 and 4.

With the mesh/mesh method, the best results were obtained by CS 3700® (mean error 30.4 μm; 95% CI 26.7–34.5 μm) followed by ITERO ELEMENTS 5D® (mean error 31.4 μm; 95% CI 29.2–33.8 μm), i-500® (mean error 32.2 μm; 95% CI 28.4–36.6 μm); TRIOS 3® (mean error 36.4 μm; 95% CI 33.9–39.1 μm), CS 3600® (mean error 36.5 μm; 95% CI 29.8–44.6 μm), PRIMESCA N® (mean error 38.4 μm; 95% CI 35.8–41.2 μm),
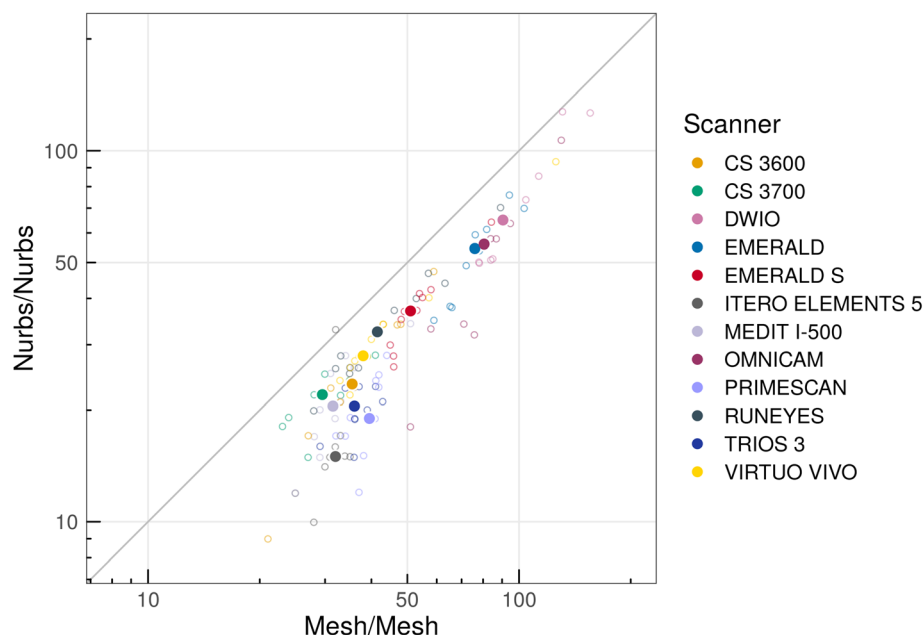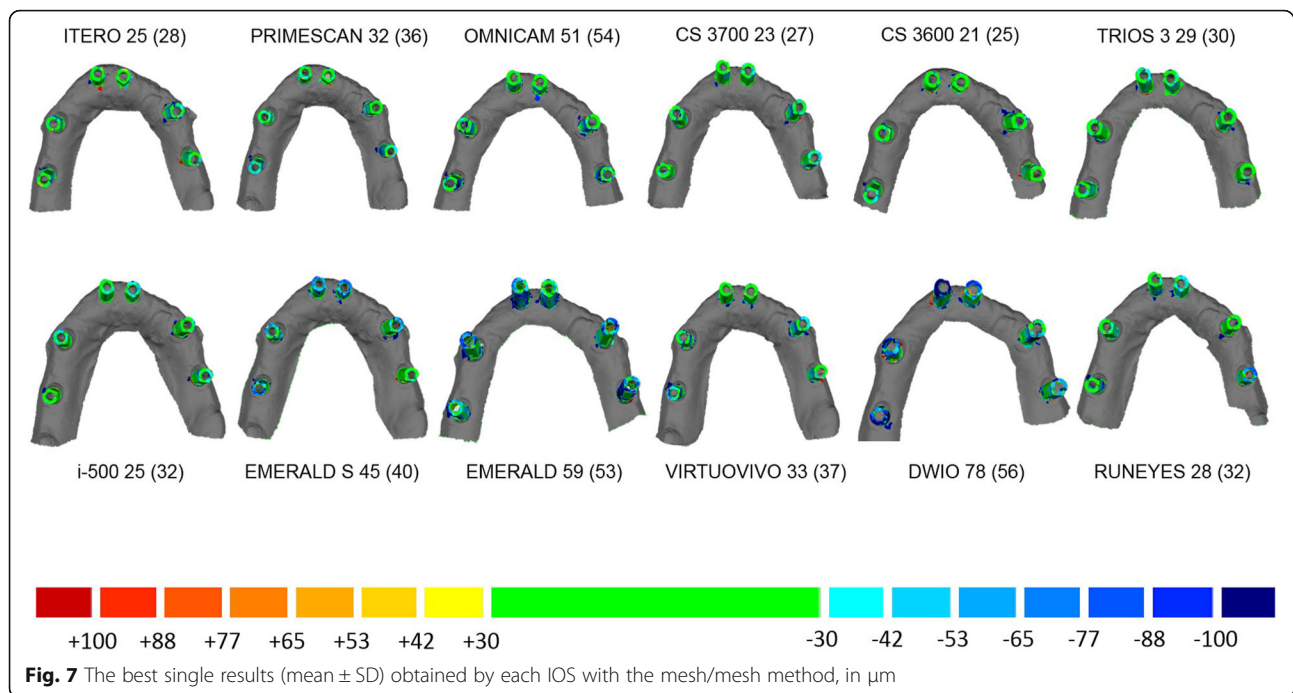

Fig. 6 Circles correspond to individual observations, filled dots – medians for each scanner. The scatter plot highlighted that nurbs/nurbs errors were systematically lower than mesh/mesh errors

Fig. 7 The best single results (mean ± SD) obtained by each IOS with the mesh/mesh method, in μm

VIRTUO VIVO® (mean error 43.8 μm; 95% CI 33.6–57.1 μm), RUNEYES® (mean error 44.4 μm; 95% CI 34.9–56.5 μm), EMERALD S® (mean error 52.9 μm; 95% CI 46.8–59.7 μm), EMERALD® (mean error 76.1 μm; 95% CI 68.1–85.1 μm), OMNICAM® (mean error 79.6 μm; 95% CI 66.9–94.6 μm) and DWIO® (mean error 98.4 μm; 95% CI 84.4–114.8 μm). The best single results obtained by each IOS with the mesh/mesh method were summarized in Fig. 7. Statistically significant differences

were found between the IOSs, as reported at the bottom and left of Table 3.

With the nurbs/nurbs method, the best results were obtained by ITERO ELEMENTS 5D® (mean error 16.1 μm; 95% CI 12.9–20.1 μm), followed by PRIMESCAN® (19.3 μm; 95% CI 16.3–22.9 μm), TRIOS 3® (mean error 20.2 μm; 95% CI 18.1–22.7 μm), i-500® (mean error 20.8 μm; 95% CI 16.9–25.5 μm), CS 3700® (mean error 21.9 μm; 95% CI 19.3–25.0 μm), CS 3600® (mean error
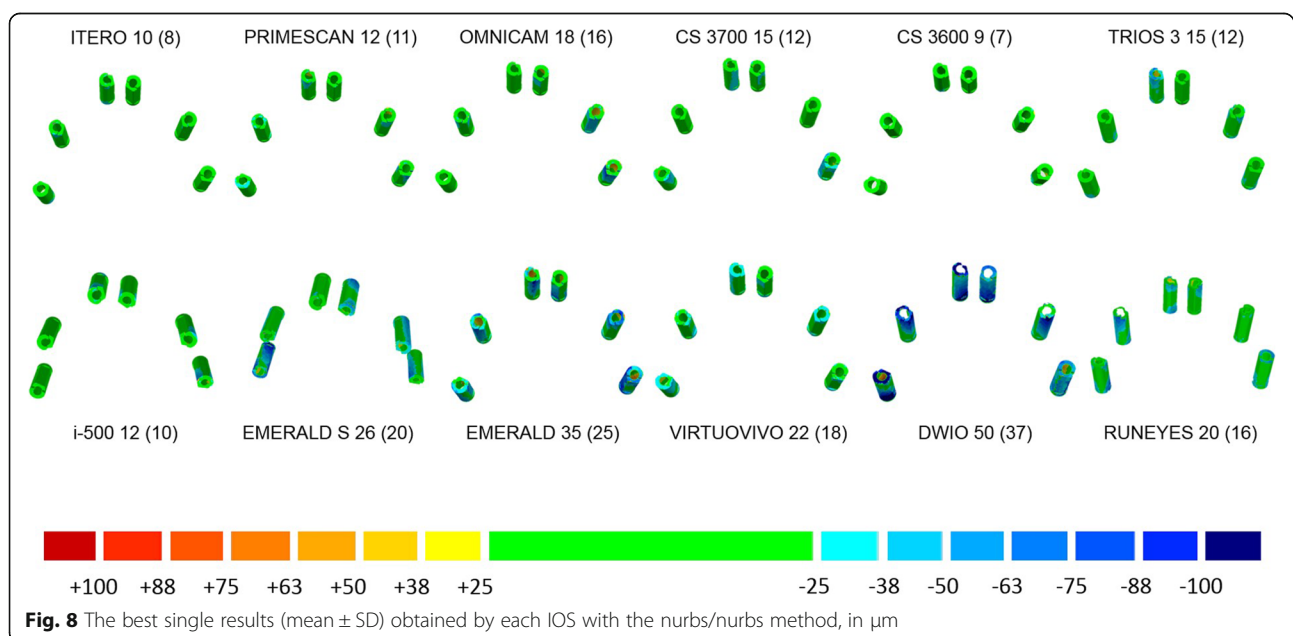

Fig. 8 The best single results (mean ± SD) obtained by each IOS with the nurbs/nurbs method, in μm

Table 5 Descriptive statistics (error in µm, medians and quartiles, means and 95% CIs) for linear and cross distances

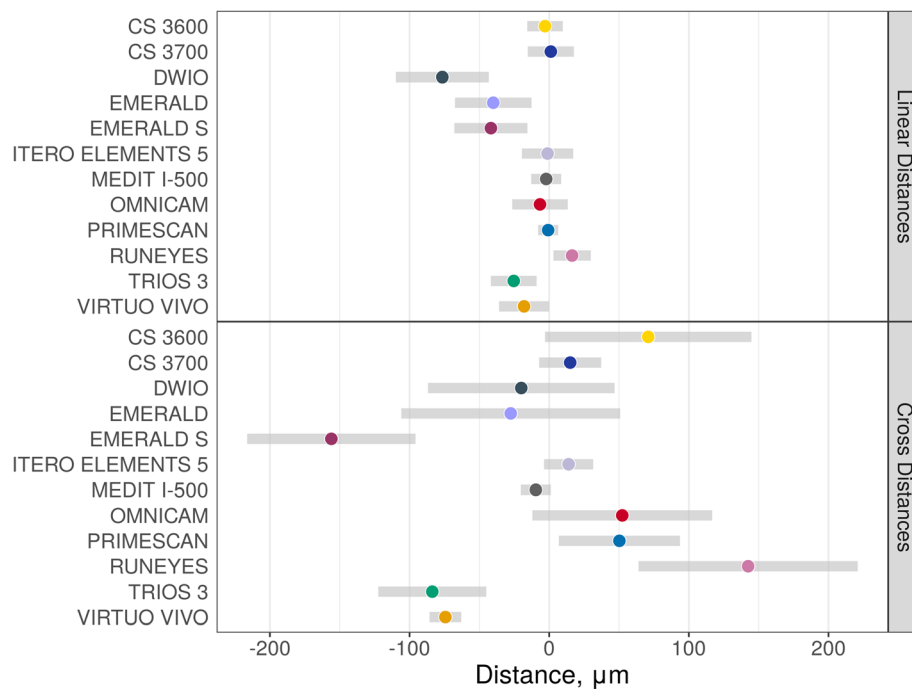| Scanner	Linear distances			Cross distances		
	Median (Q₁–Q₃)[a]	Median (Q₁–Q₃)[b]	Mean (95% CI)[c]	Median (Q₁–Q₃)[a]	Median (Q₁–Q₃)[b]	Mean (95% CI)[c]
CS 3600®	0.0 (−9.2–8.0)	8.0 (4.0–19.0)	−3.0 [−15.7; 9.7]	60.5 (−2.5–109.2)	62.5 (19.2–109.2)	70.9 [−3.0; 144.8]
CS 3700®	5.5 (−15.8–19.5)	19.0 (10.0–26.8)	1.2 [−15.3; 17.7]	5.5 (−25.0–39.2)	35.0 (20.5–50.0)	15.0 [−7.2; 37.2]
DWIO®	−58.5 (−104.5–−36.2)	58.5 (36.2–104.5)	−76.5 [−109.8; −43.3]	−12.5 (−119.0–55.5)	111.0 (46.5–230.2)	−20.0 [−86.8; 46.8]
EMERALD®	−35.0 (−69.8–−11.8)	41.0 (16.0–69.8)	−40.1 [−67.4; −12.7]	−24.0 (−112.8–40.8)	103.0 (34.5–122.0)	−27.6 [−105.9; 50.8]
EMERALD S®	−38.0 (−51.8–19.2)	38.0 (19.2–51.8)	−41.7 [−67.9; −15.6]	−131.0 (−220.8–−97.2)	131.0 (97.2–220.8)	−156.0 [−216.3; −95.7]
ITERO ELEMENTS 5D®	0.0 (−6.0–13.0)	11.0 (4.0–17.8)	−1.2 [−19.5; 17.2]	8.5 (−18.2–46.8)	36.0 (14.5–57.2)	13.9 [−3.7; 31.5]
MEDIT I-500®	−0.5 (−11.5–5.8)	8.0 (3.0–16.8)	−2.2 [−12.9; 8.6]	−6.0 (−27.5–23.5)	27.0 (15.5–54.0)	−9.6 [−20.3; 1.2]
OMNICAM®	−8.5 (−30.5–10.5)	23.0 (9.8–52.0)	−6.6 [−26.5; 13.3]	15.0 (−48.5–138.2)	88.5 (27.5–150.2)	52.3 [−12.0; 116.7]
PRIMESCAN®	3.5 (−2.0–9.0)	6.5 (3.0–11.0)	−0.8 [−8.0; 6.4]	41.5 (7.0–86.8)	41.5 (14.8–86.8)	50.2 [6.9; 93.6]
RUNEYES®	18.5 (−1.0–33.2)	23.0 (15.0–34.8)	16.4 [3.0; 29.8]	114.0 (49.2–216.8)	114.0 (49.2–216.8)	142.4 [64.0; 220.9]
TRIOS 3®	−30.0 (−37.0–−19.2)	30.0 (22.0–37.0)	−25.4 [−41.8; −9.0]	−78.5 (−124.2–−50.0)	78.5 (56.0–124.2)	−83.7 [−122.4; −45.1]
VIRTUO VIVO®	−14.0 (−25.5–0.5)	15.5 (6.2–25.5)	−18.0 [−35.9; −0.1]	−51.0 (−85.5–−11.0)	55.5 (30.2–87.8)	−74.4 [−85.7; −63.0]

[a]Median (interquartile range) error calculated on raw data
[b]Median (interquartile range) absolute error
[c]Mean error (95% CI) estimated using linear mixed effects models

Fig. 9 Estimated mean errors (in µm, with 95% CIs) for linear and cross distances

Mangano *et al. BMC Oral Health* (2020) 20:263

Page 13 of 21

Table 6 Linear distances. Differences (with standard errors) are presented at the top and right of the table, and correspond to row scanner names minus column scanner names. *p*-values for comparison are placed at the bottom and left of the table
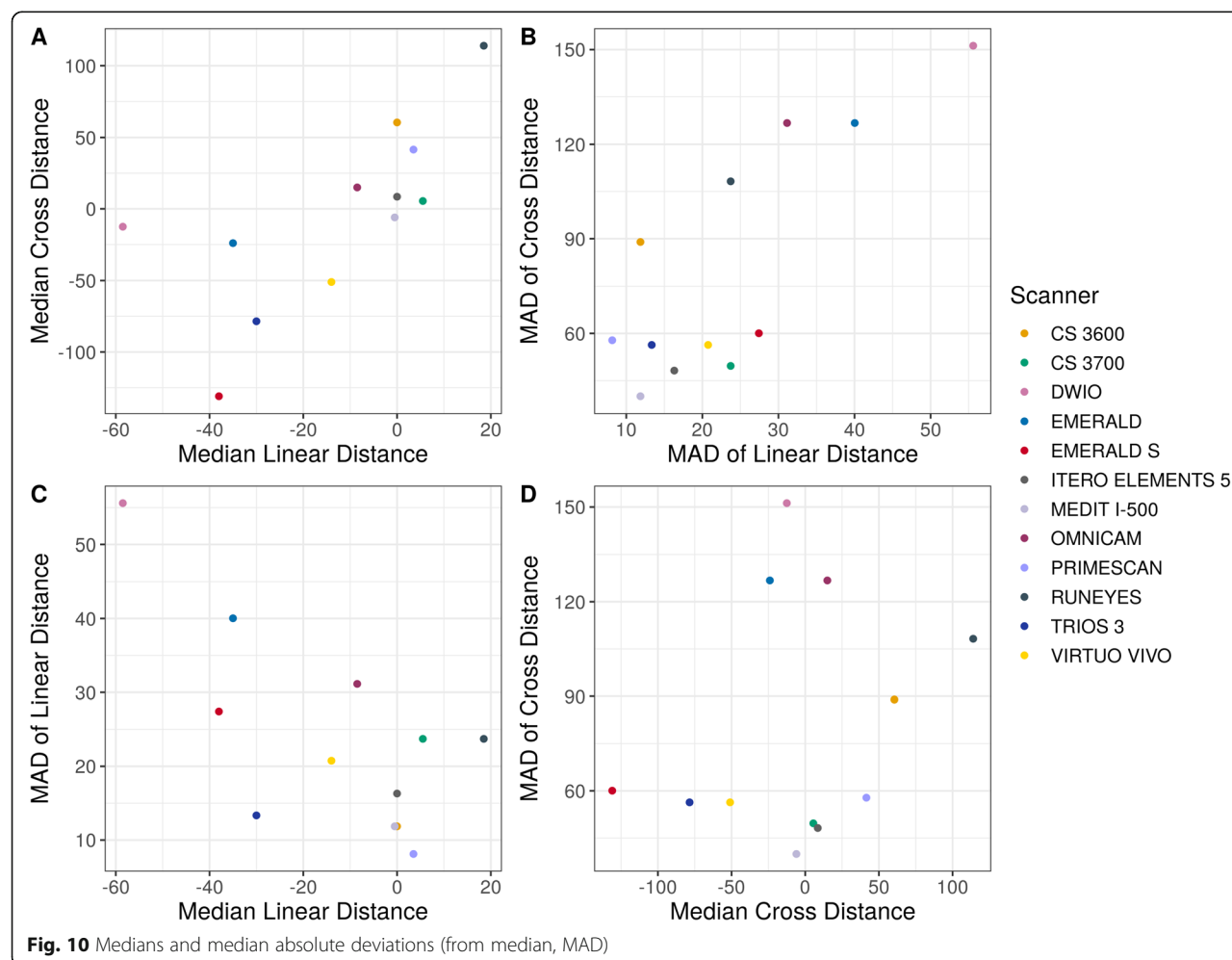
	CS 3600®	CS 3700®	DWIO®	EMERALD®	EMERALD S®	ITERO ELEMENTS 5D®	MEDIT I-500®	OMNICAM®	PRIMESCAN®	RUNEYES®	TRIOS 3®	VIRTUO VIVO®
CS 3600®		−4.1 (8.9)	73.5 (18.7)	37.1 (11.6)	38.8 (7.2)	−1.8 (4.5)	−0.8 (5.5)	3.6 (10.3)	−2.2 (4.2)	−19.4 (6.0)	22.4 (8.2)	15.0 (9.1)
CS 3700®	1.0		77.7 (20.5)	41.2 (17.2)	42.9 (11.4)	2.3 (12.6)	3.3 (11.3)	7.8 (7.7)	1.9 (7.5)	−15.2 (10.9)	26.6 (14.2)	19.2 (6.8)
DWIO®	0.005	0.009		−36.5 (26.3)	−34.8 (24.8)	−75.4 (17.8)	−74.4 (14.4)	−69.9 (23.7)	−75.8 (15.4)	−92.9 (15.0)	−51.1 (13.0)	−58.5 (24.3)
EMERALD®	0.06	0.4	1.0		1.7 (14.3)	−38.9 (11.4)	−37.9 (12.5)	−33.5 (12.5)	−39.3 (14.2)	−56.5 (16.1)	−14.7 (13.6)	−22.1 (14.2)
EMERALD S®	< 0.0001	0.010	1.0	1.0		−40.6 (9.4)	−39.6 (12.6)	−35.1 (13.1)	−41.0 (10.8)	−58.1 (11.2)	−16.3 (14.9)	−23.7 (10.4)
ITERO ELEMENTS 5D®	1.0	1.0	0.002	0.03	0.001		1.0 (5.1)	5.4 (12.8)	−0.4 (6.8)	−17.6 (7.9)	24.2 (6.1)	16.8 (13.4)
MEDIT I-500®	1.0	1.0	< 0.0001	0.1	0.08	1.0		4.4 (12.0)	−1.4 (4.2)	−18.6 (6.4)	23.2 (3.1)	15.8 (12.7)
OMNICAM®	1.0	1.0	0.1	0.2	0.2	1.0	1.0		−5.8 (10.4)	−23.0 (14.7)	18.8 (14.5)	11.4 (8.4)
PRIMESCAN®	1.0	1.0	< 0.0001	0.2	0.008	1.0	1.0	1.0		−17.2 (4.8)	24.6 (7.1)	17.2 (9.7)
RUNEYES®	0.06	1.0	< 0.0001	0.02	< 0.0001	0.5	0.1	0.9	0.02		41.8 (8.2)	34.4 (11.7)
TRIOS 3®	0.2	0.8	0.005	1.0	1.0	0.005	< 0.0001	1.0	0.03	< 0.0001		−7.4 (15.7)
VIRTUO VIVO®	0.9	0.2	0.4	0.9	0.5	1.0	1.0	1.0	0.8	0.1	1.0	

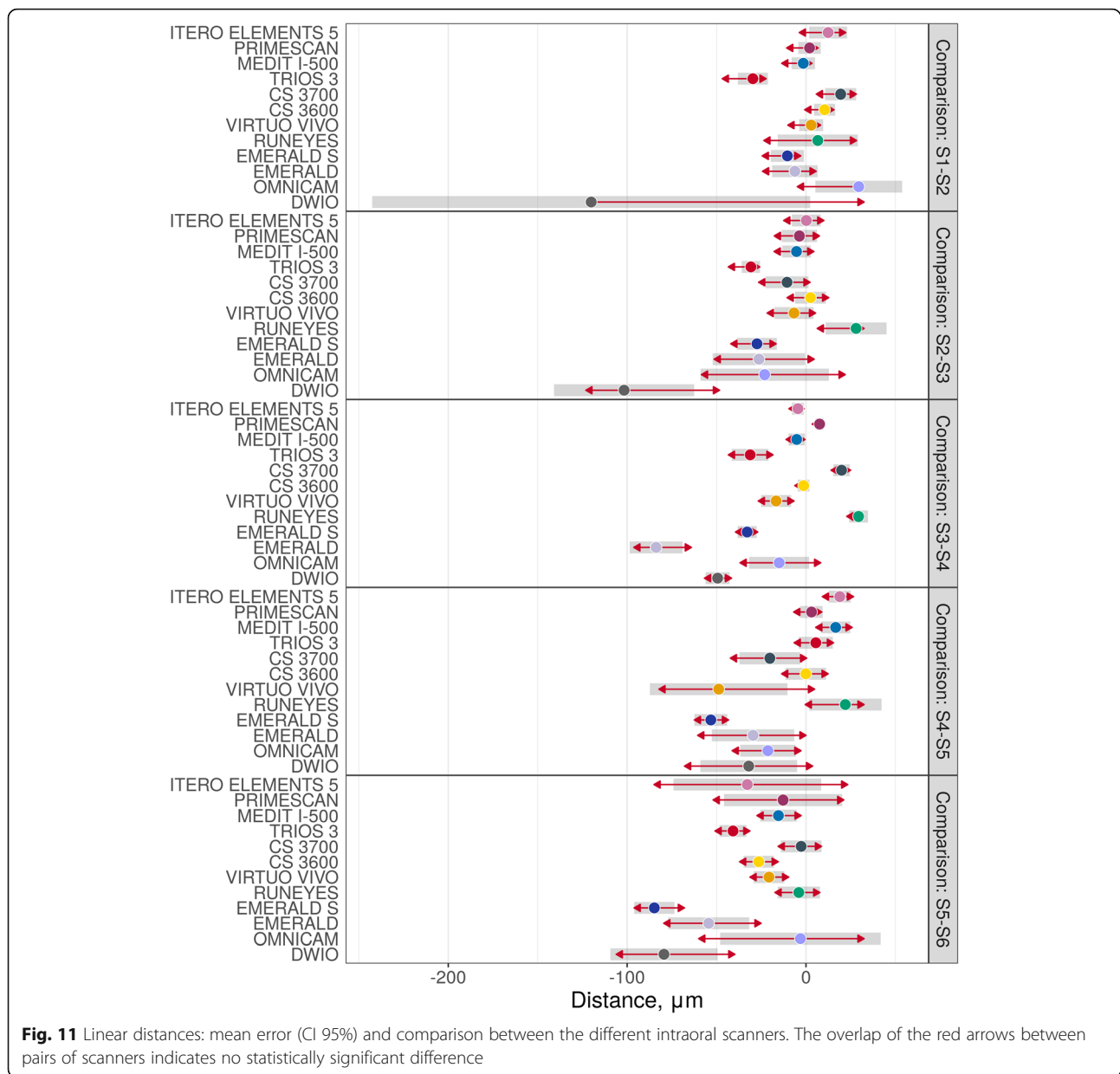Mangano *et al. BMC Oral Health*   (2020) 20:263

Page 14 of 21

Table 7 Cross distances. Differences (with standard errors) are presented at the top and right of the table, and correspond to row scanner names minus column scanner names. *p*-values for comparison are placed at the bottom and left of the table

	CS 3600®	CS 3700®	DWIO®	EMERALD®	EMERALD S®	ITERO ELEMENTS 5D®	MEDIT I-500®	OMNICAM®	PRIMESCAN®	RUNEYES®	TRIOS 3®	VIRTUO VIVO®
CS 3600®		55.9 (27.9)	90.9 (35.7)	98.4 (4.2)	226.9 (47.3)	57.0 (27.2)	80.5 (36.4)	18.6 (13.0)	20.6 (23.2)	−71.6 (18.5)	154.6 (52.6)	145.2 (32.6)
CS 3700®	0.7		35.0 (23.4)	42.6 (29.5)	171.0 (36.8)	1.1 (4.6)	24.6 (9.4)	−37.3 (21.6)	−35.2 (10.2)	−127.4 (26.9)	98.8 (25.4)	89.4 (12.1)
DWIO®	0.3	0.9		7.5 (36.8)	136.0 (58.1)	−33.9 (26.3)	−10.4 (28.0)	−72.3 (30.2)	−70.3 (16.6)	−162.5 (23.8)	63.7 (39.2)	54.3 (34.8)
EMERALD®	< 0.0001	1.0	1.0		128.5 (49.9)	−41.4 (29.3)	−18.0 (38.3)	−79.9 (11.5)	−77.8 (24.4)	−170.0 (17.3)	56.2 (54.4)	46.8 (34.6)
EMERALD S®	0.0001	0.0003	0.5	0.3		−169.9 (32.8)	−146.4 (33.2)	−208.3 (48.4)	−206.3 (45.4)	−298.5 (58.3)	−72.3 (36.1)	−81.7 (25.0)
ITERO ELEMENTS 5D®	0.6	1.0	1.0	1.0	< 0.0001		23.5 (9.3)	−38.4 (22.8)	−36.4 (13.0)	−128.5 (29.0)	97.6 (25.4)	88.3 (9.1)
MEDIT I-500®	0.5	0.3	1.0	1.0	0.0008	0.3		−61.9 (30.8)	−59.8 (18.8)	−152.0 (36.0)	74.2 (16.3)	64.8 (10.1)
OMNICAM®	1.0	0.9	0.4	< 0.0001	0.001	0.9	0.7		2.1 (16.4)	−90.1 (12.9)	136.1 (46.5)	126.7 (28.7)
PRIMESCAN®	1.0	0.03	0.002	0.07	0.0004	0.2	0.07	1.0		−92.2 (17.4)	134.0 (34.2)	124.6 (21.8)
RUNEYES®	0.007	0.0002	< 0.0001	< 0.0001	< 0.0001	0.0007	0.002	< 0.0001	< 0.0001		226.2 (51.5)	216.8 (37.0)
TRIOS 3®	0.1	0.007	0.9	1.0	0.7	0.008	0.0004	0.1	0.006	0.0008		−9.4 (22.1)
VIRTUO VIVO®	0.0006	< 0.0001	0.9	1.0	0.05	< 0.0001	< 0.0001	0.0008	< 0.0001	< 0.0001	1.0	

Table 8 Medians and median absolute deviations (from median, MAD)

Scanner	Linear distances median (MAD)	Cross distances median (MAD)
CS 3600®	0.0 (11.9)	60.5 (89.0)
CS 3700®	5.5 (23.7)	5.5 (49.7)
DWIO®	−58.5 (55.6)	−12.5 (151.2)
EMERALD®	−35.0 (40.0)	−24.0 (126.8)
EMERALD S®	−38.0 (27.4)	−131.0 (60.0)
ITERO ELEMENTS 5®	0.0 (16.3)	8.5 (48.2)
MEDIT I-500®	−0.5 (11.9)	−6.0 (40.0)
OMNICAM®	−8.5 (31.1)	15.0 (126.8)
PRIMESCAN®	3.5 (8.2)	41.5 (57.8)
RUNEYES®	18.5 (23.7)	114.0 (108.2)
TRIOS 3®	−30.0 (13.3)	−78.5 (56.3)
VIRTUO VIVO®	−14.0 (20.8)	−51.0 (56.3)

Fig. 10 Medians and median absolute deviations (from median, MAD)

Fig. 11 Linear distances: mean error (CI 95%) and comparison between the different intraoral scanners. The overlap of the red arrows between pairs of scanners indicates no statistically significant difference

24.4 μm; 95% CI 18.0–33.1 μm), VIRTUO VIVO® (mean error 32.0 μm; 95% CI 24.4–42.0 μm), RUNEYES® (mean error 33.9 μm; 95% CI 26.4–43.6 μm), EMERALD S® (mean error 36.8 μm; 95% CI 31.1–43.6 μm), OMNI-CAM® (mean error 47.0 μm; 95% CI 33.7–65.7 μm), EMERALD® (mean error 51.9 μm; 95% CI 43.5–61.8 μm) and DWIO® (mean error 69.9 μm; 95% CI 55.0–88.9 μm). The best single results obtained by each IOS with the nurbs/nurbs method were summarized in Fig. 8. Statistically significant differences were found between the IOSs, as reported at the bottom and left of Table 4.

Descriptive statistics (medians and quartiles, means and 95% CIs) for linear and cross distances are presented in Table 5. Estimated mean distances (with 95%

CIs) on raw scales are presented in Fig. 9. Pairwise differences in distances (on raw scales with corresponding standard errors and *p*-values) are presented in Tables 6 and 7; significant differences were found between the IOSs, as reported at the bottom and left of the tables. Medians and median absolute deviations (from median, MAD) are presented in Table 8 and Fig. 10. Correlations were found between these values: medians of linear and cross distances (0.80, 95% CI 0.41–0.94, *p* = 0.0019), MADs of linear and cross distances (0.66, 95% CI 0.14–0.90, *p* = 0.019), medians and MADs of linear distances (− 0.52, 95% CI -0.84–0.07, *p* = 0.082), and medians and MADs of cross distances (0.13, 95% CI -0.48–0.65, *p* = 0.696). Finally, linear and cross distances were evaluated
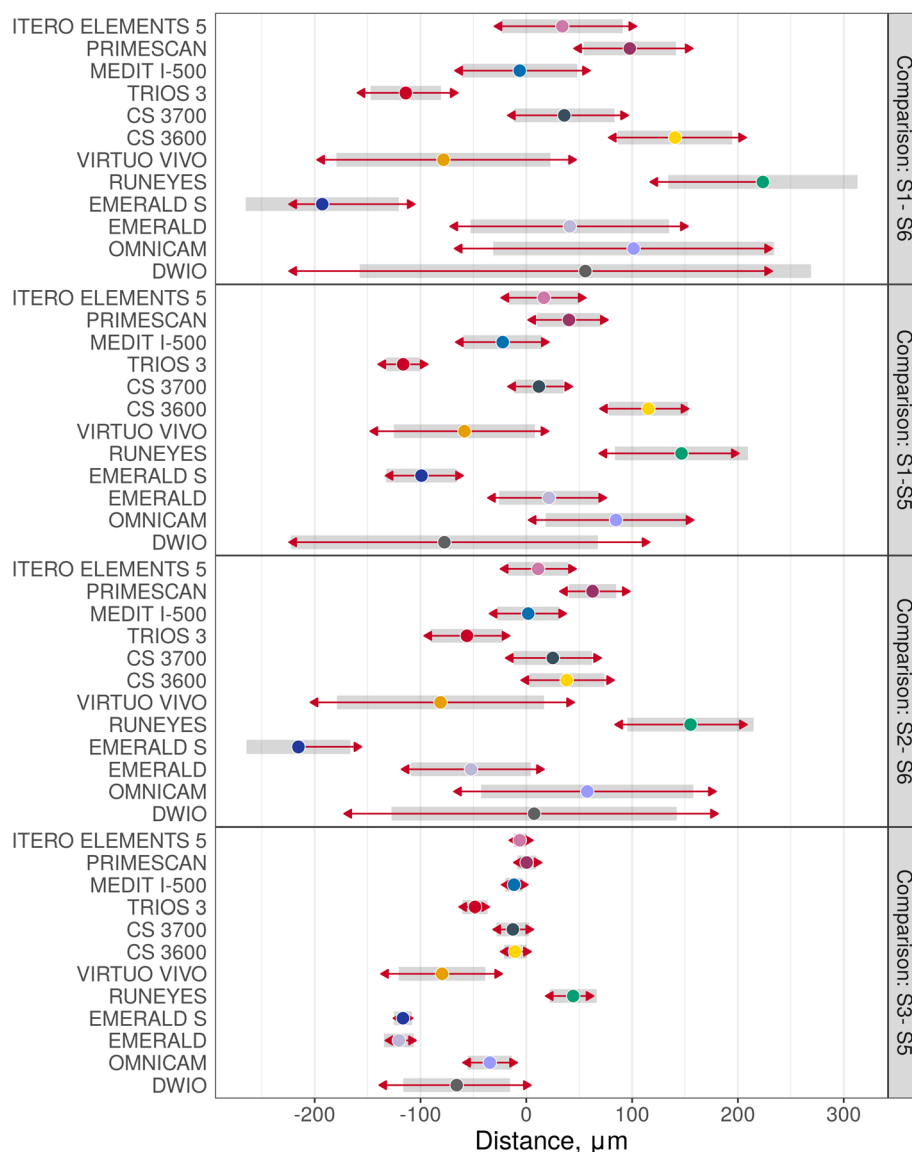
Fig. 12 Cross distances: mean error (CI 95%) and comparison between the different intraoral scanners. The overlap of the red arrows between pairs of scanners indicates no statistically significant difference

for each of the SB pairs, as reported in Figs. 11 and 12, respectively. In these figures, the overlap of the red arrows between pairs of scanners indicates no statistically significant difference. Once again, a statistically significant difference was found among different scanner pairs.

Discussion

To date, few clinical studies have supported the use of optical impression for manufacturing FA restorations in the completely edentulous patient; these studies are limited to the restorations of patients with 4 implants [30–32]. In more complex clinical situations, with FA supported by between 6 and 8 implants, the scientific literature has not yet validated the use of optical impression

[16, 17, 33]. For this reason, and since the technological development of IOSs is constant through the improvement and implementation of new software and hardware, constant updates are needed on the accuracy of the scanners on the market.

In recent years, the scientific literature has attempted to investigate the accuracy of IOSs to extend the use of the optical impression to complex clinical applications, such as capturing impressions for modelling and manufacturing FA restorations via a full digital workflow [14, 15, 19–26, 29].

Most studies investigating the trueness of optical impressions that are currently available in the scientific literature have used a mesh/mesh approach,

Mangano *et al. BMC Oral Health*   (2020) 20:263

Page 18 of 21

superimposing IOS models onto an RM using best-fit algorithms, and these functions align the meshes to assess the minimum error [14, 15, 23, 24, 29]. As a consequence, the error is distributed homogeneously throughout the whole mesh [14, 15, 29]. This method is valid to assess the overall trueness because it is immediate and not affected by other variables (tolerances in the fabrication of the SBs, for example) [15, 29]. However, in implant-supported restorations, it is also important to assess the error between fixation points; even a single error localised in one point can determine a clinical misfit of the prosthetic structure. Some studies have therefore attempted to assess distance or angulation errors between fixation points [25, 26]. To make linear measurements that are reliable, however, it is necessary to work on library files (or nurbs files), on which specific landmarks (such as the centroids) can be precisely and automatically identified by the software. Working with nurbs files also allows more faithfully replicating what happens clinically in the early stages of prosthetic CAD [27].

Our present in vitro study therefore used three different methods to investigate the trueness of 12 IOSs in the FA implant impression: a mesh/mesh method and a nurbs/nurbs method to evaluate overall trueness, and the computation of linear and cross distances between the SBs to evaluate local trueness. In our study, statistically significant differences were found between the different IOSs, as previously reported [14, 15, 19–26, 29]. In particular, the mesh/mesh and nurbs/nurbs analysis have allowed identifying three groups of scanners, characterised by different levels of trueness. The first group, comprising the IOSs with the highest accuracy, consisted of ITERO ELEMENTS 5D°, PRIMESCAN°, CS 3700°, CS 3600°, TRIOS3° and i-500°. These scanners have an average intrinsic error < 40 μm with the mesh/mesh method and < 25 μm with the nurbs/nurbs method and represent a theoretically compatible solution for taking impressions for FA restorations. The second group of scanners presented positive results, although probably still not compatible with the capture of a FA impression. These were EMERALD S°, EMERALD°, OMNICAM°, VIRTUO VIVO° and RUNEYES°, which presented an average intrinsic error between 40 and 80 μm with the mesh/mesh method and between 25 and 50 μm with the nurbs/nurbs method. DWIO° remained distanced from all the others, with an intrinsic error > 80 μm in the mesh/mesh analysis and > 50 μm in the nurbs/nurbs analysis, certainly incompatible with the FA impression. The data of the overall trueness were confirmed by the analysis of the local distances between the SBs, i.e. the linear and cross distances, which again highlighted the existence of three groups of IOSs in this study, characterised by different performances. In fact, linear error analysis along

the scan revealed higher reliability for ITERO ELEMENTS 5D°, PRIMESCAN°, CS 3700°, CS 3600°, TRIOS3° and i-500°, which showed lower errors than other IOSs. For the particular scanning strategy used in this study, it was not possible to evaluate in detail, for each scanner, the percentage growth of the error as the scan proceeded; however, it was evident that greater variability was present in the paths S2-S3 and S4-S5, corresponding to the area of greatest curvature of the physical model. This finding must be confirmed by further studies, but it would seem to indicate difficulty for IOSs in accurately detecting stretches of curvature. The evaluation of cross measurements naturally resulted in larger errors, in direct proportion to the actual distance between the SBs. Here, too, the evaluation showed significant differences between the different IOSs.

The main advantage of this study is in having compared 12 IOSs, and done so using different techniques, to understand the intrinsic trueness of the scanners at a global and local level by measuring the distances between the different SBs. On one hand, the evaluation with the mesh/mesh method has the advantage of directly highlighting the quality of the scan. In this study, with the mesh/mesh analysis, the best absolute performance was obtained by CS 3700° (mean error 30.4 μm; 95% CI 26.7–34.5 μm) followed by ITERO ELEMENTS 5D° (mean error 31.4 μm; 95% CI 29.2–33.8 μm) and i – 500° (mean error 32.2 μm; 95% CI 28.4–36.6 μm). These IOSs were the best in the representation of the SBs and the tissues around them, although in an in vitro study, the soft tissues are a resin copy of the real human gums. On the other hand, the nurbs/nurbs evaluation allows replicating what happens clinically, when within the CAD software the meshes of the SBs are replaced with the corresponding library file, generating a hybrid virtual model on which the modelling takes place. This approach specifically assesses the sole trueness of the position of the implants after the mesh/nurbs replacement in CAD, without any interference from the soft tissues; it is also prerequisite for the correct implementation of the analysis of the distances between the SBs, carried out as an evaluation of the distances between the centroids at their bases. In the analysis of the overall trueness with the nurbs/nurbs method, the best results were obtained by ITERO ELEMENTS 5D° (mean error 16.1 μm; 95% CI 12.9–20.1 μm), followed by PRIMESCAN° (19.3 μm; 95% CI 16.3–22.9 μm) and TRIOS 3° (mean error 20.2 μm; 95% CI 18.1–22.7 μm). These results reflect a very low error in the position of the SBs with these IOSs, which could certainly be considered compatible, in all cases, with the realisation of a FA restoration via a full digital workflow. The evaluation of the distances between the single SBs confirmed these positive results, particularly with regard to the linear distances

(distances along the arch). Obviously, as expected, the local errors tended to grow in the cross distances, particularly between the most distal SBs, but this error is certainly contained compared to what was described only a few years ago in similar studies [25, 33].

However, the data presented in this study, which refer to the intrinsic trueness of the different IOSs analysed, must be taken with caution. The IOS is not the only factor involved in determining the final accuracy of an optical impression: the operator [34], patient [35], light conditions [36] and SB [37–40] are also key. The operator is essential because different scanning strategies and different levels of experience can determine different results, as reported in the literature [34]. In the present study, all models were captured by the same operator with many years of experience in intraoral scanning; however, the choice of scan strategy may have favoured some IOSs over others. To date, unfortunately, little is known about the effects of different scanning strategies, since the scientific literature on this topic is scarce [2, 34], and even the manufacturers have not clarified this aspect in full. The patient is equally important. Implants can be inserted in different positions, inclinations and depths, and these factors can positively (or negatively) influence the final trueness of the scan [35]. With regard to this aspect, the literature is scarce too [16, 33], and investigating more deeply the effects of these variables is advisable. In the present study, the SBs were rather parallel to each other, simulating an ideal condition with implants placed after a guided surgery procedure; this condition can be considered ideal but is not always found in clinical practice. Light conditions are another factor of great importance in intraoral scanning [36]. In the present in vitro study, all scans were captured in the same environment, under controlled light conditions; however, these conditions are very different from those of the oral cavity, and the literature must certainly investigate in more detail how much this can affect the quality of the scans [36]. Finally, the SB plays a fundamental role, being the device for transferring the implant position [37–41]. Manufacturing tolerances [37] can cause errors in the transfer of the implant position in the space. This is particularly true for implants with a conical connection, where a minimal tolerance can have important effects on the vertical position of the fixture in the space (i.e. z-axis) with respect to the library. Assembly errors (in the case of SBs composed of two assembled portions), as well as an incongruous screwing [38], can represent other sources of error. Finally, the shape and material of the SBs are important because they respectively influence the behaviour of the CAD superposition algorithm [27, 39] and the absorption or reflection of light [39, 40].

Finally, the present study has some limitations. First, it is an in vitro study. Although scrupulously conducted, and although it is not possible to determine the trueness of an IOS in vivo, an in vitro study cannot exactly reproduce the characteristics present in the patient's mouth (conditions of light, humidity, saliva). The scanning of plaster models is certainly easier than an intraoral scan, which has limits of space. Furthermore, the patient's tissues are radically different from a plaster model and have different optical behaviour when hit by light. This must always be kept in mind, although in the edentulous patient to be rehabilitated with FA, no teeth are present. A further limitation of the present work, as already described, lies in the choice of the scanning technique [14], which could have favoured some scanners over others. The use of a desktop scanner for the capture of the reference model could also be considered a limitation. Although this machine is certified for an accuracy of 5 μm, and although this approach has been used in many previous studies [14], a CMM or articulated arm can be considered more reliable tools in capturing reference measurements. Only the centroids at the base (and not the centroids at the top of the SBs) were used for the evaluation of linear and cross distances. Finally, the present study could have collected further and interesting data relating to the linear error increase during scan progression, if only the scan strategy had foreseen the departure from a specific sector of the physical model (x example, right posterior sector only). In fact, as previously reported [5, 16, 17, 25] and recently confirmed by Walter Renne and colleagues in an in vitro study on a dentate model [42], the progression of the scan tends to bring with it an increase in percentage linear error. Unfortunately, this evaluation was not possible in the present study, since the operator was free to start from the right or left posterior area of the model indifferently; the data thus collected do not allow an evaluation of the exact percentage growth of the error along the progression of the scan. In this study, all scans were captured in a specific period (January–February 2020) and therefore with the latest version of the acquisition software available for each of the machines at that time. However, the release of new acquisition software is known to be able to significantly improve the accuracy of an IOS; therefore, the results presented in this study are valid for that period and specific acquisition software. Further studies on the same IOSs with the latest acquisition software are thus needed, to better understand the trueness of the different scanners that are now available.

Conclusions

The present in vitro study investigated the trueness of 12 IOSs in FA implant impression using three different methods: a mesh/mesh method and a nurbs/nurbs

Mangano *et al. BMC Oral Health*   (2020) 20:263

Page 20 of 21

method for the evaluation of the overall trueness, and measurement of linear and cross distances between SBs for the evaluation of local trueness. Statistically significant differences emerged in accuracy between different IOSs, and some may be more suitable for optical impression for the manufacture of implant-supported long-span restorations such as FAs. The results of the overall trueness assessment were confirmed by the local analysis of the distances between the different SBs. Despite some limitations, this study can provide important information relating to the intrinsic error with different IOSs, and therefore useful indications for choosing the ideal machine for FA impression. However, it is important to remember that other factors are important in determining the reliability of an optical impression, including the operator, patient, environmental conditions and SB. Further studies are therefore necessary to understand the weight of each factor in determining the final error in the optical impression.

Abbreviations
IOS: Intraoral scanner; 3D: Three-dimensional; STL: Standard tessellation language; CAD/CAM: Computer-aided-design/ computer-assisted manufacturing; SC: Single crown; PP: Partial prosthesis; FA: Full-arch; CMM: Coordinate measuring machine; SB: Scanbodies; CAD: Computer-aided-design; NURBS: Non-uniform rational b-spline; PEEK: Polyether-ether-ketone; LED: Light-emitting-diode; SS: Stable scan stage; RM: Reference model; RICP: Robust-iterative-closest-point; PTP: Point-to-plane; SD: Standard deviation; CI: Confidence interval

Author details
[1]Department of Prevention and Communal Dentistry, Sechenov First State Medical University, 119992 Moscow, Russia. [2]Ars and Technology, Sotto il Monte Giovanni XXIII, 24039 Bergamo, Italy. [3]Academic Teaching and Research Institution of Johann Wolfgang Goethe University, 60323 Frankfurt am Main, Germany. [4]Department of Prosthodontics, Institute of Odontology, Faculty of Medicine, Vilnius University, LT-01513 Vilnius, Lithuania. [5]Department of Dental Sciences, Vita and Salute University San Raffaele, 20132 Milan, Italy.

References
1. Joda T, Ferrari M, Gallucci GO, Wittneben JG, Brägger U. Digital technology in fixed implant prosthodontics. Periodontol 2000. 2017;73(1):178–92.
2. Mangano F, Gandolfi A, Luongo G, Logozzo S. Intraoral scanners in dentistry: a review of the current literature. BMC Oral Health. 2017;17(1):149.
3. Joda T, Zarone F, Ferrari M. The complete digital workflow in fixed prosthodontics: a systematic review. BMC Oral Health. 2017;17(1):124.
4. Joda T, Ferrari M, Bragger U, Zitzmann NU. Patient reported outcome measures (PROMs) of posterior single-implant crowns using digital workflows: a randomized controlled trial with a three-year follow-up. Clin Oral Implants Res. 2018;29(9):954–61.
5. Papaspyridakos P, Vazouras K, Chen YW, Kotina E, Natto Z, Kang K, Chochlidakis K. Digital vs conventional implant impressions: a systematic review and meta-analysis. J Prosthodont. 2020. https://doi.org/10.1111/jopr.13211 Online ahead of print.
6. Gallardo YR, Bohner L, Tortamano P, Pigozzo MN, Laganá DC, Sesma N. Patient outcomes and procedure working time for digital versus conventional impressions: a systematic review. J Prosthet Dent. 2018;119(2):214–9.
7. Mangano F, Veronesi G. Digital versus analog procedures for the prosthetic restoration of single implants: a randomized controlled trial with 1 year of follow-up. Biomed Res Int. 2018;2018:5325032.
8. Joda T, Bragger U, Zitzmann NU. CAD/CAM implant crowns in a digital workflow: five-year follow-up of a prospective clinical trial. Clin Implant Dent Relat Res. 2019;21(1):169–74.
9. Lerner H, Mouhyi J, Admakin O, Mangano F. Artificial intelligence in fixed implant prosthodontics: a retrospective study of 106 implant-supported monolithic zirconia crowns inserted in the posterior jaws of 90 patients. BMC Oral Health. 2020;20(1):80.
10. de Oliveira NRC, Pigozzo MN, Sesma N, Laganá DC. Clinical efficiency and patient preference of digital and conventional workflow for single implant crowns using immediate and regular digital impression: a meta-analysis. Clin Oral Implants Res. 2020;31(8):669–86.
11. Sailer I, Mühlemann S, Fehmer V, Hämmerle CHF, Benic GI. Randomized controlled clinical trial of digital and conventional workflows for the fabrication of zirconia-ceramic fixed partial dentures. Part I: time efficiency of complete-arch digital scans versus conventional impressions. J Prosthet Dent. 2019;121(1):69–75.
12. Mühlemann S, Benic GI, Fehmer V, Hämmerle CHF, Sailer I. Randomized controlled clinical trial of digital and conventional workflows for the fabrication of zirconia-ceramic posterior fixed partial dentures. Part II: time efficiency of CAD-CAM versus conventional laboratory procedures. J Prosthet Dent. 2019;121(2):252–7.
13. Benic GI, Sailer I, Zeltner M, Gütermann JN, Özcan M, Mühlemann S. Randomized controlled clinical trial of digital and conventional workflows for the fabrication of zirconia-ceramic fixed partial dentures. Part III: marginal and internal fit. J Prosthet Dent. 2019;121(3):426–31.
14. Mangano FG, Hauschild U, Veronesi G, Imburgia M, Mangano C, Admakin O. Trueness and precision of 5 intraoral scanners in the impressions of single and multiple implants: a comparative in vitro study. BMC Oral Health. 2019;19(1):101.
15. Di Fiore A, Meneghello R, Graiff L, Savio G, Vigolo P, Monaco C, Stellini E. Full arch digital scanning systems performances for implant-supported fixed

Mangano *et al. BMC Oral Health*   (2020) 20:263

Page 21 of 21

dental prostheses: a comparative study of 8 intraoral scanners. J Prosthodont Res. 2019;63(4):396–403.

16. Wulfman C, Naveau A, Rignon-Bret C. Digital scanning for complete-arch implant-supported restorations: a systematic review. J Prosthet Dent. 2020; 124(2):161–7.

17. Ahlholm P, Sipilä K, Vallittu P, Jakonen M, Kotiranta U. Digital versus conventional impressions in fixed prosthodontics: a review. J Prosthodont. 2018;27(1):35–41.

18. Albdour EA, Shaheen E, Vranckx M, Mangano FG, Politis C, Jacobs R. A novel in vivo method to evaluate trueness of digital impressions. BMC Oral Health. 2018;18(1):117.

19. Schmidt A, Billig JW, Schlenz MA, Wöstmann B. A new 3D-method to assess the inter implant dimensions in patients - a pilot study. J Clin Exp Dent. 2020;12(2):e187–92.

20. Mandelli F, Zaetta A, Cucchi A, Mangano FG. Solid index impression protocol: a hybrid workflow for high accuracy and passive fit of full-arch implant-supported restorations. Int J Comput Dent. 2020;23(2):161–81.

21. Iturrate M, Lizundia E, Amezua X, Solaberrieta E. A new method to measure the accuracy of intraoral scanners along the complete dental arch: a pilot study. J Adv Prosthodont. 2019;11(6):331–40.

22. Gómez-Polo M, Ballesteros J, Perales-Padilla P, Perales-Pulido P, Gómez-Polo C, Ortega R. Guided implant scanning: a procedure for improving the accuracy of implant-supported complete-arch fixed dental prostheses. J Prosthet Dent. 2020;124(2):135–9.

23. Mangano FG, Veronesi G, Hauschild U, Mijiritsky E, Mangano C. Trueness and precision of four intraoral scanners in Oral Implantology: a comparative in vitro study. PLoS One. 2016;11(9):e0163107.

24. Bilmenoglu C, Cilingir A, Geckili O, Bilhan H, Bilgin T. In vitro comparison of trueness of 10 intraoral scanners for implant-supported complete-arch fixed dental prostheses. J Prosthet Dent. 2020;S0022-3913(19)30754-1. https://doi.org/10.1016/j.prosdent.2019.11.017 Online ahead of print.

25. van der Meer WJ, Andriessen FS, Wismeijer D, Ren Y. Application of intra-oral dental scanners in the digital workflow of implantology. PLoS One. 2012;7(8):e43312.

26. Roig E, Garza LC, Álvarez-Maldonado N, Maia P, Costa S, Roig M, Espona J. In vitro comparison of the accuracy of four intraoral scanners and three conventional impression methods for two neighboring implants. PLoS One. 2020;15(2):e0228266.

27. Mangano F, Lerner H, Margiani B, Solop I, Latuta N, Admakin O. Congruence between meshes and library files of implant scanbodies: an in vitro study comparing five intraoral scanners. J Clin Med. 2020;9(7):E2174.

28. Jablonski R, Elneklawy M, Osnes C, Ferrari M, Wu J, Keeling A. Guided scanning improves full arch precision of an intra-Oral scanner. Vancouver: IADR/AADR/CADR General Poster Session; 2019. p. 1574.

29. Imburgia M, Logozzo S, Hauschild U, Veronesi G, Mangano C, Mangano FG. Accuracy of four intraoral scanners in oral implantology: a comparative in vitro study. BMC Oral Health. 2017;17(1):92.

30. Ender A, Attin T, Mehl A. In vivo precision of conventional and digital methods of obtaining complete-arch dental impressions. J Prosthet Dent. 2016;15:313–20.

31. Chochlidakis K, Papaspyridakos P, Tsigarida A, Romeo D, Chen YW, Natto Z, Ercoli C. Digital versus conventional full-arch implant impressions: a prospective study on 16 edentulous maxillae. J Prosthodont. 2020;29:281–6.

32. Mangano F, Mangano C, Margiani B, Admakin O. Combining intraoral and face scans for the design and fabrication of computer-assisted design/computer-assisted manufacturing (CAD/CAM) polyether-ether-ketone (PEEK) implant-supported bars for maxillary overdentures. Scanning. 2019;2019:4274715.

33. Flügge T, van der Meer WJ, Gonzalez BG, Vach K, Wismeijer D, Wang P. The accuracy of different dental impression techniques for implant-supported dental prostheses: a systematic review and meta-analysis. Clin Oral Implants Res. 2018;29(Suppl. 16):374–92.

34. Latham J, Ludlow M, Mennito A, Kelly A, Evans Z, Renne W. Effect of scan pattern on complete-arch scans with 4 digital scanners. J Prosthet Dent. 2020;123:85–95.

35. Tan MY, Yee SHX, Wong KM, Tan YH, Tan KBC. Comparison of three-dimensional accuracy of digital and conventional implant impressions: effect of Interimplant distance in an edentulous arch. Int J Oral Maxillofac Implants. 2019;34:366–80.

36. Revilla-León M, Jiang P, Sadeghpour M, Piedra-Cascón W, Zandinejad A, Özcan M, Krishnamurthy VR. Intraoral digital scans-part 1: influence of

37. ambient scanning light conditions on the accuracy (trueness and precision) of different intraoral scanners. J Prosthet Dent. 2019:S0022-3913(18)30992-2. https://doi.org/10.1016/j.prosdent.2019.06.003 Online ahead of print.

37. Schmidt A, Billig JW, Schlenz MA, Rehmann P, Wöstmann B. Influence of the accuracy of intraoral Scanbodies on implant position: differences in manufacturing tolerances. Int J Prosthodont. 2019;32:430–2.

38. Arcuri L, Pozzi A, Lio F, Rompen E, Zechner W, Nardi A. Influence of implant scanbody material, position and operator on the accuracy of digital impression for complete-arch: a randomized in vitro trial. J Prosthodont Res. 2020;64(2):128–36.

39. Mizumoto RM, Yilmaz B. Intraoral scan bodies in implant dentistry: a systematic review. J Prosthet Dent. 2018;120:343–52.

40. Moslemion M, Payaminia L, Jalali H, Alikhasi M. Do type and shape of scan bodies affect accuracy and time of digital implant impressions? Eur J Prosthodont Restor Dent. 2020;28:18–27.

41. Huang R, Liu Y, Huang B, Zhang C, Chen Z, Li Z. Improved scanning accuracy with newly designed scan bodies: an in vitro study comparing digital versus conventional impression techniques for complete-arch implant rehabilitation. Clin Oral Implants Res. 2020;31:625–33.

42. Nagy Z, Simon B, Mennito A, Evans Z, Renne W, Vág J. Comparing the trueness of seven intraoral scanners and a physical impression on dentate human maxilla by a novel method. BMC Oral Health. 2020;20(1):97.

Publisher's Note

Continuous Scan Strategy (CSS): A Novel Technique to Improve the Accuracy of Intraoral Digital Impressions

Authors

Mario Imburgia *
(DDS, PhD)

John Kois §
(DMD, MSD)

Elio Marino ^
(MD, DDS)

Henriette Lerner †
(DDS)

Francesco G. Mangano ∆
(DDS, PhD)

Address for Correspondence

Francesco G. Mangano ∆

Email: francescomangano1@mclink.net

* *Private Practice, Palermo, Italy*

§ *Kois Center, Private Practice, Seattle (WA) USA;*
Assistant Professor, University of Washington,
Seattle (WA), USA

^ *Private Practice, Milan, Italy*

† *Private Practice, Baden-Baden, Germany*

∆ *Private Practice, Gravedona (CO) Italy;*
Lecturer, Sechenov First State Medical
University, Moscow, Russia

ABSTRACT

Purpose: To present the results obtained with the "Continuous Scan Strategy" (CSS), a direct intraoral scanning technique based on the connection of the implant scan bodies (SBs) with thermoplastic resin. Methods: 40 patients were restored with 45 long-span monolithic implant-supported zirconia restorations (10 partial prostheses [PP] and 35 full arches [FA]) fabricated via a full-digital workflow after the capture of an intraoral impression (Trios3®) using the CSS technique. The primary outcomes were the marginal adaptation and passive fit of the superstructures, checked at T0 (intraoral try-in of polyurethane or metal replica of the final prosthesis) and T1 (delivery of the final zirconia restoration). The secondary outcomes, registered at T2 (2 years after the delivery of the final prosthesis), were implant survival, prosthetic success, and complications. A throughout statistical analysis was performed. Results: At T0, 40/45 replicas demonstrated a perfect passive fit and adaptation. At T1, one prosthesis had fractured, and at T2, an additional prosthesis had fractured and one had chipped. The implant survival rate was 100%. The prosthetic success was 93.3%. Conclusions: CSS seems to represent a viable option for capturing accurate intraoral digital impressions for the fabrication of precise long-span implant-supported restorations.

INTRODUCTION

The digital revolution is transforming the world of dentistry. Intraoral,[1,2] desktop[3] and face scanners,[4] condylographs and digital occlusometers,[5] and cone-beam computed tomography (CBCT)[6] allow practitioners to acquire three-dimensional (3D) patient information. This information, when loaded into computer-assisted-design (CAD) software, can be combined, allowing patient virtualization,[7] and is used for the diagnosis and planning of treatment.[8] Finally, powerful machines such as milling units[9] and 3D printers[10] allow for the physical production of a whole series of devices, usable in various clinical disciplines (restorative dentistry,[11] prosthetics,[12] surgery[13] and orthodontics[14]).

Intraoral scanners (IOSs) are digital devices that capture optical impressions.[2] The operating mechanism of the IOS is relatively simple: they emit a structured light grid (or less commonly, a laser beam) with known characteristics that impacts the surface of the model.[2] Upon impact, the grid undergoes deformation that is captured by powerful cameras, which send the signal to the reconstruction software.[2] This software produces a point cloud, combining all the images captured from different angles, taking

into account the relative movements of the machine, and the distances from the scanned object;[2,15] this point cloud is tri-angulated to generate a mesh, or surface reconstruction, of the object.[15]

In implant prosthodontics, IOSs allow for direct capture (without the need to take an impression and pour a plaster cast of positive models of the dental arches and therefore of the position of the implants) through the use of the scan bodies (SBs), which are the digital version of the old impression transfer copings.[2,15] The SBs are mathematically coupled to an implant library; in the CAD software, therefore, the dental technician replaces the mesh of the SB with a bonding base and can model a screwed superstructure or a customized abutment above it, to support the future prosthetic restoration.[2,15]

The advantages of IOSs are manifold. They eliminate the discomfort caused by conventional tray impressions, which is extremely helpful in patients with a strong gag reflex.[16] Furthermore, they simplify the capture of the impression for the clinician (particularly in the case of multiple implants or in the presence of undercuts), reduce the number of clinical procedures (no need to pour plaster models), and make communication with the dental laboratory easier, saving time and money.[2,16,17] Finally, IOSs represent a powerful marketing tool with the patient.[17]

Several *in vitro*[1,18-20] and *in vivo*[12,15,21] studies have demonstrated that IOSs represent an accurate and reliable solution for the capture of impressions in partially edentulous patients for the fabrication of short-span restorations (single crowns [SCs] and partial prostheses [PPs]).

However, other studies[22,23] and reviews[24-26] have reported a persistent accuracy problem with intraoral scanning when long-span prosthetic restorations (fixed partial prostheses supported by multiple implants, and full arches [FAs]) must be fabricated. Screw-retained superstructures, (i.e. fixed prostheses screwed directly onto multiple implants) require the highest accuracy, because the acceptable tolerances are minimal, and there is a need for absolute passive fitting.[27] Although recent technological improvements have been impressive, IOSs still have challenges when scanning multiple fixtures.[27] These difficulties are mainly due to the mechanism by which the IOS acquires the images, which requires "attaching" frames to each other during the process of acquisition. Regardless of the acquisition technology, this intrinsic error is expected to grow with the extension of the scan.[2,24-26,28] In fully edentulous patients, due to lack of reference points, accuracy is more difficult to achieve when the IOS reads the distance between different SBs, which are also at a different height than the soft tissues.[28] Nevertheless, other factors that could be potential sources of inaccuracy include the light conditions,[29] the level of operator experience,[30] the implant position, depth and angulation,[28] and the SBs themselves.[31] Reducing the distances and the "jump" between the implant SBs could improve the accuracy of the scan, reducing the intrinsic scan error. In totally edentulous patients, Tallarico *et al.*[32] introduced a method based on the

3D-printing duplication of the pre-existing removable complete prosthesis. This replica, ground out in the SB area and inserted into the mouth, allows for the capture of a sufficiently accurate impression for the manufacture of a FA fixed restoration (Toronto bridge), as well as simplifying the registration of the vertical dimension of occlusion. Mangano *et al.*[33] developed this strategy, and applied it to the manufacture of bar-retained overdentures, with the bar milled in polyether-ether-ketone (PEEK). More recently, hybrid digital-analog approaches have been proposed, which use custom measuring aids (CMAs)[34,35] and solid indexes[36] to connect the SBs to improve the accuracy of FA digital impressions. The rationale of these approaches is to reduce the distances between the different SBs and to provide artificial landmarks to reduce inaccuracies, thereby allowing for the fabrication of long-span screw-retained superstructures to fit onto implants passively.[35,36]

Our present retrospective study focuses on this latter strategy, intending to present the clinical results obtained using a novel scanning technique named "Continuous Scan Strategy" (CSS), based on the connection of the scan abutments through thermoplastic resin, thereby eliminating the "jump" between the different SBs and reducing the intrinsic scan error.

MATERIALS AND METHODS

PATIENT DATA, INCLUSION AND EXCLUSION CRITERIA

Patients enrolled in this retrospective clinical study were selected from the customized dental records of two private dental centres (M.I. and E.M. private dental clinics, Palermo and Milan, Italy, respectively).

Inclusion criteria for enrollment in this study were patients who had been treated with multiple (≥4) implants (Nobel Active Internal Connection®) via a full digital workflow with the "Continuous Scan Strategy" (CSS) for the restoration with fixed implant-supported prostheses (fixed partial prostheses [PPs] and full arches, [FAs]), over a 4-year period (2014–2017). Further inclusion criteria were the presence of complete documentation within the customized records and a follow-up of at least 2 years from the delivery of the final prosthetic restoration.

Exclusion criteria for this study included any of the following: the presence of systemic diseases or immunocompromised status, uncontrolled diabetes, bisphosphonate therapy (administered parenterally or orally, in the past and/or at the time of enrollment in the study), anti-cancer treatments, alcohol and drug abuse, incomplete documentation, or absence of a follow-up for at least 2 years. Pre- and peri-implant regenerative bone therapies were not considered as criteria of exclusion for the present study (pre-implant regenerative therapies were considered bone regenerative therapies to which the patient underwent 4 to 6 months before implant surgery; conversely, peri-implant regenerative therapies were regenerative procedures made at the time of implant placement).

For the enrolled patients, the chart review included the collection of patient-related (gender, age at the delivery of final implant-supported restoration, presence/absence of parafunctions such as bruxism and clenching, smoking habit), implant-related (site/position of the fixtures, type, length and diameter of the fixtures, presence/absence of bone regeneration procedures), and restoration-related (the type of restoration and delivery date) information. In addition, the customized patient records noted all the biologic or prosthetic complications (mechanical or technical) that had occurred during the entire follow-up period, as well as any implant failure that had occurred. Complications or failures were noted both if patients returned to the dental clinic for treatment and were also intercepted during annual scheduled check-ups (at least 2 control visits per year for all patients, with professional oral hygiene sessions). All this information, along with the clinical photographs taken during the different phases of the prosthetic treatment and the related radiographs, were the basis for this retrospective study and were used for the statistical analysis.

The present retrospective clinical study was conducted in full compliance with the principles of the Declaration of Helsinki on Clinical Research and Experimentation in Humans (revision 2008).

PROSTHETIC TECHNIQUE

The proposed intraoral scanning technique presented in the study, named the "Continuous Scan Strategy" (CSS), is based on the direct connection between the implant SBs through thermoplastic resin. This technique aims to reduce the level of inaccuracy of intraoral digital impressions by eliminating the problem of the distance between the SBs, which are connected by thermoplastic resin; this connection also reduces the vertical "jump" that the IOS must make from one SB to another and during the registration of soft tissues between the different SBs.

The scanning technique proceeded as described. One-piece titanium SBs (Scan Abutment AQ®) were screwed onto the implants, with the notch surface or the oblique section in the head oriented towards the buccal side. After confirming the SBs were screwed correctly, the thermoplastic resin was heated and molded intraorally to connect the different SBs to each other on the palatal/lingual side. To increase the stability of the thermoplastic resin and avoid detachments, small quantities of flowable composite resin were added laterally to the SBs to connect them with the thermoplastic resin. They were then polymerized to ensure the assembly. Neither the thermoplastic material nor the composite interfered with the notch surface (marker surface) of the SB, whose head must be completely free and visible. Once the stability and rigidity of the elements thus assembled were verified (SB, thermoplastic resin and flowable composite resin), it was possible to proceed with the scanning using the IOS (Trios3®), conducted through a "zig-zag" technique. The technique started from the more distal SB (palatal/lingual side) and passed above it to end in the buccal area, with progressive advancement guided by the thermoplastic resin until the next SB. Particular attention was paid to the capture of all the details of the SB. Once the scan was captured and the mesh quality checked, the standard tessellation files (.STL) were sent to the dental technician for modelling the final structure in CAD software. Care was taken during the CAD modelling to perform the best possible superimposition (best-fit) of the library files of the SB onto the corresponding meshes. If the superimposition was perfect, with an overall mean deviation of ≤ 20 µm, the technician could proceed.

In the CAD software, appropriate titanium bases were selected, and the final prosthetic superstructure was designed. Then a replica of the same superstructure was milled with a 5-axis milling machine (DWX-52®) into a rigid and radiopaque material (polyurethane for the PPs, metal for the FAs). This replica was used to test the passive intraoral adaptation (verification of the "passive fitting" or Sheffield test) of the final prosthesis. This grey and radiopaque replica was screwed into the mouth on the corresponding titanium bases and its marginal adaptation was verified, both clinically and radiographically. A series of intraoral x-rays were captured to verify the quality of the fitting. If the quality of the passive adaptation was optimal, the technician could proceed with the manufacture of the final zirconia prosthesis, starting from the CAD project itself. If it was not, or the values detected through the best fit in the early stages of the CAD were considered unreliable (≥ 30 µm), the clinician proceeded to separate the polyurethane replica into several parts until a passive adaptation was obtained; these portions were connected intraorally with low-contraction resin, and the assembly was transferred to the technician who re-scanned it with a desktop scanner and modified the CAD project accordingly. After the passive fitting and the optimal adaptation of the structures were confirmed, the prosthetic CAD project was ready to be used for the manufacture of the final prosthesis. The final monolithic zirconia prosthesis (Katana ML®) was milled with the same 5-axis milling machine (DWX-52®), sintered and, if necessary, coloured on the buccal surfaces. Particular attention was paid to the milling of the engagements for the titanium luting bases, to provide close correspondence between the parts, and a unique position. The position of the luting base was determined only and exclusively by the housing milled inside the zirconia structure. The milling parameters of the aforementioned interface were kept "tight", thus avoiding any play that could have inserted inaccuracies and, consequently, a misfit of the structure. At this point, the dental technician could cement the luting bases chosen during the CAD modelling inside the monolithic structure. This cementation took place extraorally, using anaerobic cement (Variolink Hybrid Abutment®); no luting was performed within the patient's oral cavity. The luting of the titanium bases to the monolithic structure was carried out in all cases without the aid of any 3D printed model. After this, the final monolithic zirconia prosthesis was ready to be delivered to the clinician for application.

OUTCOME VARIABLES

The primary outcome of this study was the marginal quality of closure of the superstructures and their passive fit. This outcome was recorded in two stages: at the time of testing the final structure, by means of a milled replica in polyurethane or metal (time 0 = T0), and at the time of delivery of the final monolithic zirconia restoration (time 1 = T1). The marginal closure and adaptation were determined through careful clinical and manual inspection by the prosthodontist, who worked with magnifying glasses (Zeiss 4.5%®), and were confirmed by intraoral radiographs of all implant platforms.

The secondary outcomes of the present study were the survival of the implants and the success of the prostheses. These outcomes were collected 2 years after delivery of the final prostheses (time 2 = T2) and were recorded during the scheduled recall visits for professional hygiene. Implant survival indicated that all the implants were regularly in function, under masticatory load; implants that were lost for any reason (fracture of the fixture, loss of osseointegration, or removal of the implant due to mechanical overload or infection) were classified as failures. Finally, prosthetic success indicated that the final monolithic zirconia prosthesis was regularly in function during the entire period 2-year follow-up (from delivery to final inspection) without the occurrence of any major mechanical (such as macroscopic fractures of the framework), minor mechanical (related to the pre-established components sold by the implant manufacturer, e.g., screw loosening) or minor technical (related to superstructure problems, such as chipping) complications.

STATISTICAL ANALYSIS

The data collected from the records of the patients enrolled in the study were entered into a spreadsheet (Excel 2003®) and included in statistical analysis. First, a descriptive analysis of the patient population and the implant-supported restorations were performed. This analysis was based on patient demographics (gender, age at the delivery of the final restoration, smoking habit, and history of parafunctions), distribution of the implants (site and position, length and diameter, association with bone regeneration procedures), and type of implant-supported prosthesis (PP or FA). For this descriptive analysis, mean ± standard deviation (SD), range, median, and 95% confidence interval (CI) were calculated for quantitative variables (e.g., patient age). For the qualitative variables (i.e., patient gender, smoking habit, history of parafunction; site and position, length and diameter of the implants, association with bone regenerative procedures and type of prosthetic restoration), absolute (n°) and relative (%) distributions were calculated. Using this information, the Chi-square test was utilized to assess homogeneity or non-homogeneity within the groups, with a level of significance set at $p<0.05$.

The primary outcomes of the study (i.e., the clinical and radiographic quality of the adaptation and the passive fitting of the prosthetic superstructures) were investigated both at the time of testing the final structure through a polyurethane or metal (T0) replica, and at the time of delivery of the final monolithic zirconia prosthesis (T1), and were assessed by the prosthodontist. A binary code of satisfactory or unsatisfactory was used. If the adaptation and passive fitting were satisfactory at T0, the laboratory could fabricate the final zirconia prosthesis, using the same CAD project; if they were not, the dentist had to separate the polyurethane or metal replica into several parts until a passive adaptation was obtained. These portions were then luted intraorally with low-contraction resin, and the assembly was transferred to the technician who re-scanned it with a desktop scanner and modified the CAD project accordingly. If the adaptation or passive fitting were adequate at T0, but not adequate at T1, the work was sent back to the laboratory for refurbishment.

Finally, with regards to the secondary outcomes of the study, i.e., the variables investigated during the scheduled follow-up control 2 years after the delivery of the final prosthesis, the incidence (%) of failures and complications was calculated. The survival of implants and of the prostheses were calculated at the implant- and at the restoration-level, respectively. The occurrence of a single event or complication during the 2-year follow-up period was sufficient to allocate the prosthesis into the failure category.

RESULTS

The analysis of the personalized medical records of the two different dental offices involved in this retrospective clinical study revealed that over a period of 4 years (2014–2017), a total of 40 patients (15 males, 25 females; age 45–74 years, average age 62.1 ± 8.1 years; median 65 years; CI 95% 59.6–64.6 years) met the conditions set out in the inclusion criteria, and also did not have any of the conditions established in the exclusion criteria. Of these patients, 6 had a clinical history of parafunction or bruxism, and 9 were smokers. The characteristics of the enrolled patients are summarized in Table 1. Most of the enrolled patients were non-smokers (p = .010) and had no parafunctions (p = .0008).

In all, over the period indicated above, 45 prosthetic rehabilitations were constructed, of which 10 fixed PP (8 maxillary, 2 mandibular) were supported by ≥4 implants, and 35 FA (20 maxillary, 15 mandibular) were supported by 6–8 implants. In all cases, the implants used were Nobel Active Internal Connection®. The characteristics of the implants, their distribution based on position, length and diameter, the association (or not) with bone regeneration techniques and the type of restoration supported by them are summarized in Table 2. The majority of the implants were located in the maxilla (p<.00001), and most of the implants were in native bone (p<.00001), and placed to support FAs (p<.00001).

In all cases, the rehabilitations were performed following the CSS protocol, starting from a direct optical impression with IOS and consisting of monolithic full zirconia prostheses, screwed

Table 1. Distribution (number, %) of the patients by gender, age at surgery, smoking habit and history of parafunctions (clenching and bruxism).

	Patients number	%	p*
Gender			
Males	15	37.5%	.259
Females	25	62.5%	
Age at surgery			
45- 54 years	8	20%	
55- 64 years	10	25%	.186
65- 74 years	22	55%	
Smoke			
Yes	9	22.5%	.010
No	31	77.5%	
History of parafunction			
Yes	6	15%	.0008
No	34	85%	
Total	40	100%	–
p* = Chi-square test.			

Table 2. Distribution (number, %) of the implants by position, length, diameter, bone regeneration and type of prosthesis.

	Implants number	%	p*
Position			
Maxilla	215	83.3%	<.00001
Mandible	43	16.7%	
Length			
10 mm	114	44.2%	
11.5 mm	87	33.7%	.007
13 mm	57	22.1%	
Diameter			
3.0 mm	59	22.8%	
3.5 mm	91	35.3%	.021
4.3 mm	108	41.9%	
Bone regeneration			
Yes	28	10.9%	<.00001
No	230	89.1%	
Type of prosthesis			
PP	48	18.6%	<.00001
FA	210	81.4%	
Total	258	100%	
p* = Chi-square test.			

directly onto the implants *(Figures 1-12)*. Implant disparallelisms were limited due to computer-guided implant planning and positioning; however, if, for anatomical limits, the implant axis did not coincide with the prosthetic axis, a digital correction of the angled screw hole was made, using connection screws with Cardan engagement.

In 40 out of 45 cases, the marginal adaptation of the prostheses at T0 (proof of the replica in polyurethane or metal) was optimal and the case could proceed directly to the production phase of the final prosthesis. In five cases, however, passive adaptation was not optimal; therefore, the clinician proceeded to separate the polyurethane or metal replica into several parts, until a passive adaptation was obtained. These portions were then luted intraorally with low-contraction resin, and the assembly was transferred to the technician who re- scanned it with a desktop scanner and modified the CAD project accordingly. In all these cases, > 30 μm distances between meshes and libraries of multiple SBs had emerged during the early stages of CAD (best-fit).

At the time of delivery of the final monolithic zirconia prostheses (T1), there were no complications, since the passive fit and the marginal adaptation of 44 of the 45 prosthetic structures was optimal. However, in a case of mandibular FA in a 56-year-old woman, a minimal friction problem emerged at the time of screwing, which did not seem to prevent the correct positioning of the prosthesis. The prosthesis was screwed on, but a few minutes later, following a patient yawn, the prosthesis fractured in the middle portion (area of the incisors). This fracture was therefore attributed to an imperfect passive fit and mandibular flexure in maximum opening. In addition, the design of the structure had reduced thicknesses in the area surrounding the Ti Base of the more anterior implant. This complication was solved by redesigning a new prosthesis.
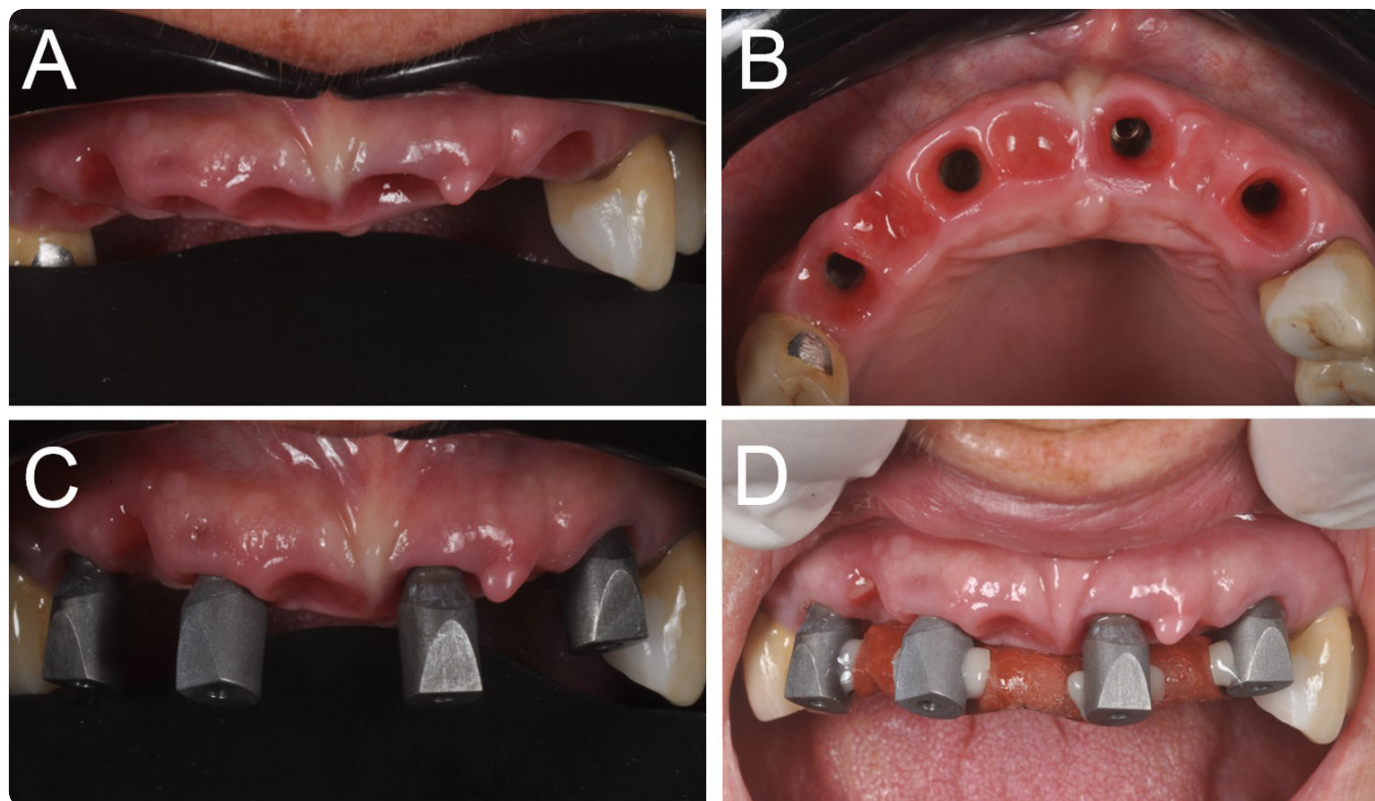
Figure 1: Partially edentulous patient with four implants in the anterior maxilla: clinical pictures of the scanning procedure. (A) Frontal view: the mucosal collars after the removal of the healing abutments. (B) Occlusal view: the mucosal collars are visible. (C) The SBs are screwed on the four implants. (D) Thermoplastic material and composite resin are used to connect the SBs, avoiding any interference with their marker surfaces and heads.
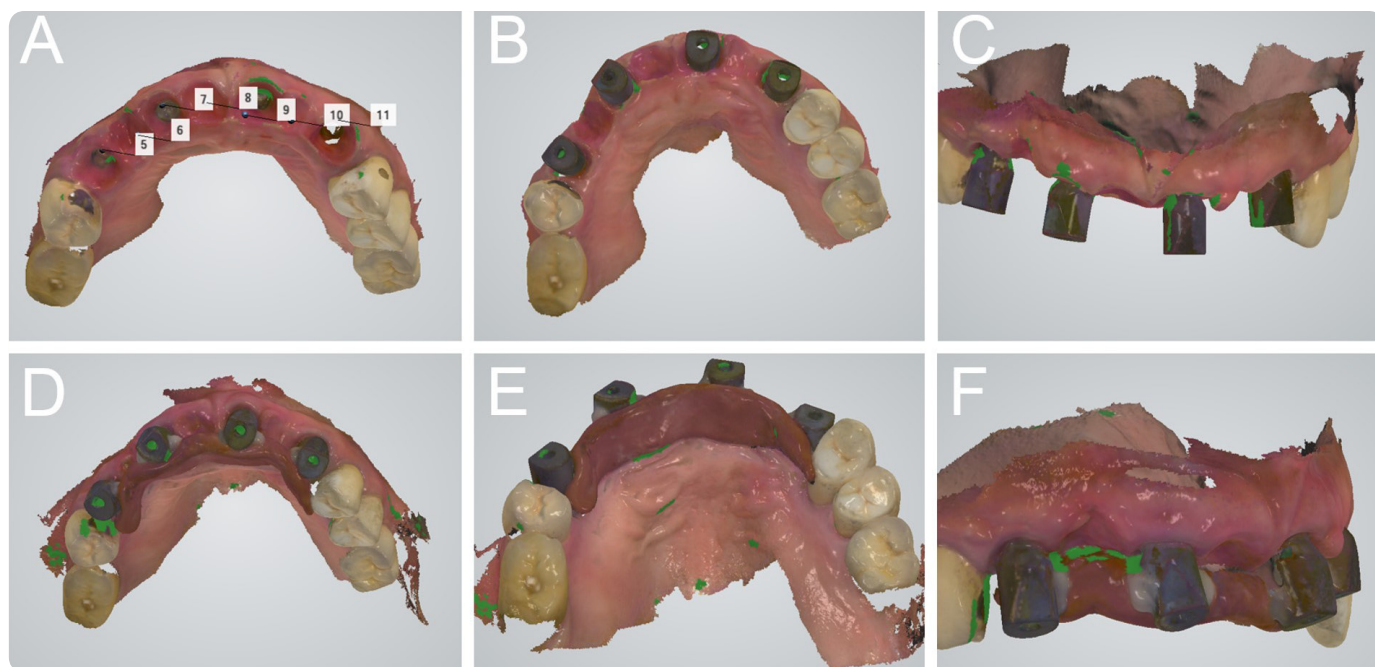

Figure 2: Partially edentulous patient with four implants in the anterior maxilla: screenshots of the intraoral scan. (A) Occlusal view: the mucosal collars after the removal of the healing abutments. (B) Occlusal view: the SBs are screwed on the four implants. (C) Frontal view of the SBs. (D) Occlusal view: thermoplastic material and composite resin connect the SBs, avoiding interference with the SB marker surfaces and heads. (E) Palatal view of the SBs linked with thermoplastic material and resin. (F) Lateral view of the assembly.

Figure 3: A replica of the final CAD project is milled in polyurethane hard resin and screwed intraorally to verify the passive fitting and the marginal adaptation. Intraoral radiographs are taken to verify the adaptation. (A) Radiographic image of the replica, implants in the right side. (B) The milled replica screwed intraorally. (C) Radiographic image of the replica, implants in the left side.

Figure 4: The final screw-retained fixed PP is ready to be delivered to patient. (A) Right view. (B) Frontal view. (C) Left view.
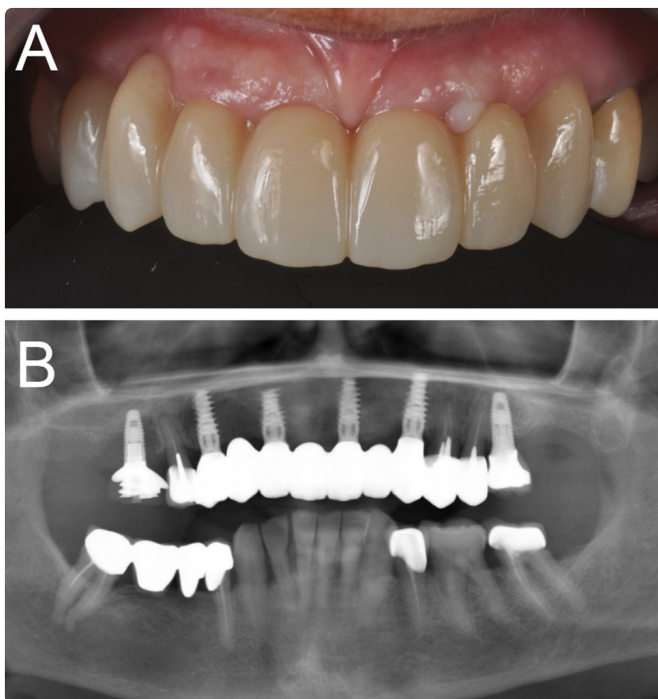

Figure 5: Delivery of the final screw-retained fixed PP. The same CAD project of the milled prototype is duplicated in zirconia. (A) Clinical view. (B) Panoramic radiograph.

Two years after the delivery of the final restorations (T2), the implant success was high (100%) with all implants in function, but another prosthesis fracture occurred in a mandibular FA of a 66-year-old man. The prosthesis had to be replaced with a new one, and again the fracture occurred in an area where

the thickness of zirconia was non-optimal. Another complication occurred in a maxillary FA of a 68-year-old female, due to chipping of a distal extension on the right upper first molar; however, this complication was solved simply by polishing the surface of the fractured connector. At the end of the study, 42/45 final zirconia prosthesis (93.3%) were considered successful because they functioned without any complications registered during the subsequent two years. Conversely, the incidence of prosthetic complications was 6.7%. Among these complications, two (fractures of the zirconia framework) were major, and one (chipping) was minor. Regardless, all these complications were technical.

DISCUSSION

To date, multiple published reports have proposed that the insufficient accuracy of IOS in capturing impressions for the manufacture of long-span restorations (such as FA) is the significant limit to the use of these machines in implant prosthodontics.[22-26]

Although there are statistically significant differences in the accuracy of the various IOS on the market, numerous scientific studies[22,23] and reviews of the literature[24-26] have confirmed the intrinsic difficulty of scanners in capturing multiple implant impressions, particularly in completely edentulous patients. It is now clear that the inaccuracy of the models generated by direct intraoral scanning does not depend solely on the machine and therefore on the technology used for the acquisition,[2] but also on other factors (lighting conditions,[29]
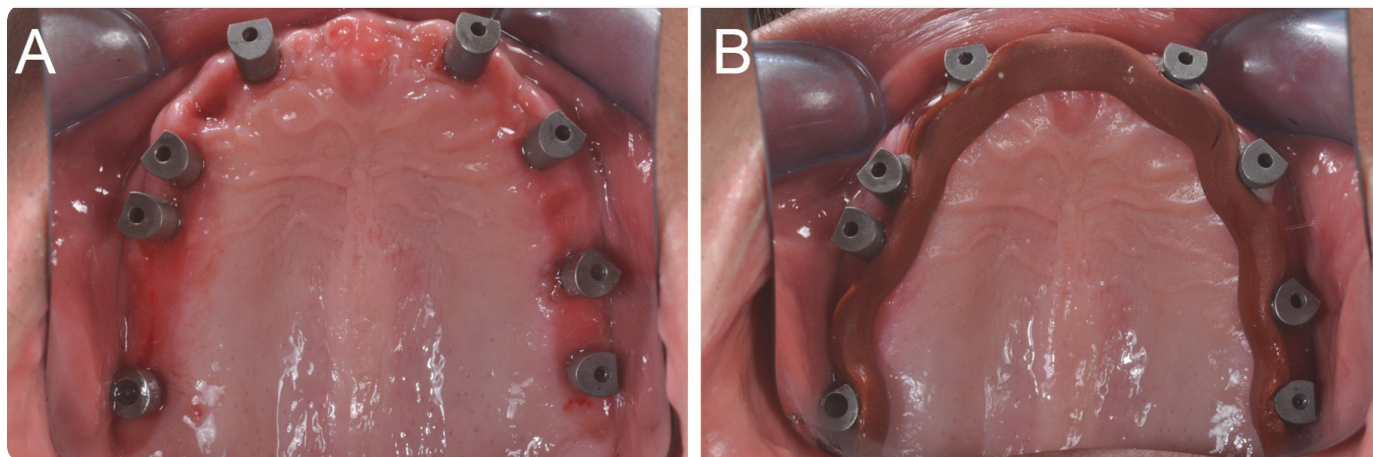
Figure 6: Fully edentulous patient with eight implants in the maxilla: intraoral scan. (A) Occlusal view of the SBs screwed on the eight implants. (B) Before taking the intraoral scan, thermoplastic resin is used to connect the SBs, avoiding any interference with their marker surfaces and heads.
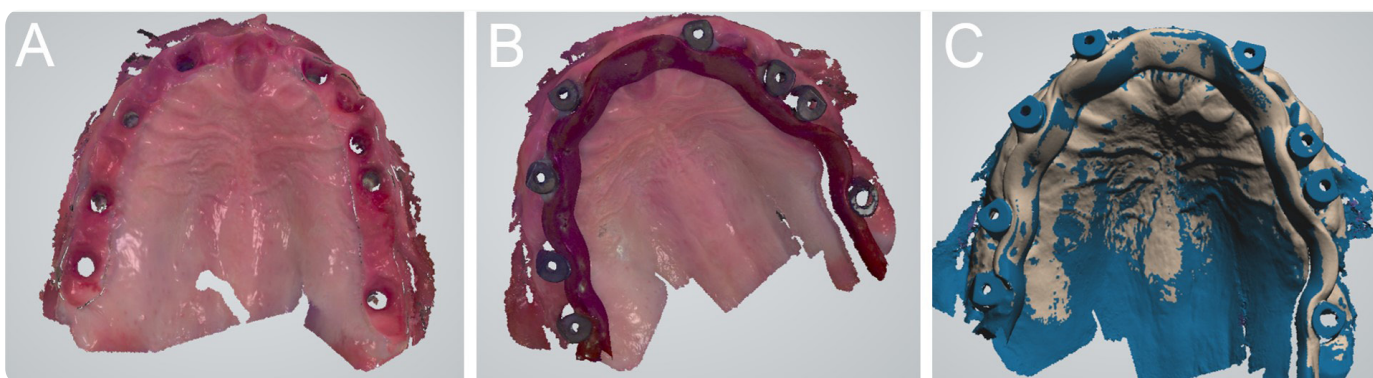

Figure 7: An intraoral scan of a fully edentulous patient with eight implants in the maxilla. (A) Occlusal view of the mucosal collars. (B) Occlusal view of the implant SBs screwed on the eight implants and linked with thermoplastic resin. (C) Occlusal view of the assembly. Thermoplastic resin is used to connect the SBs, avoiding any interference with their marker surfaces and heads.
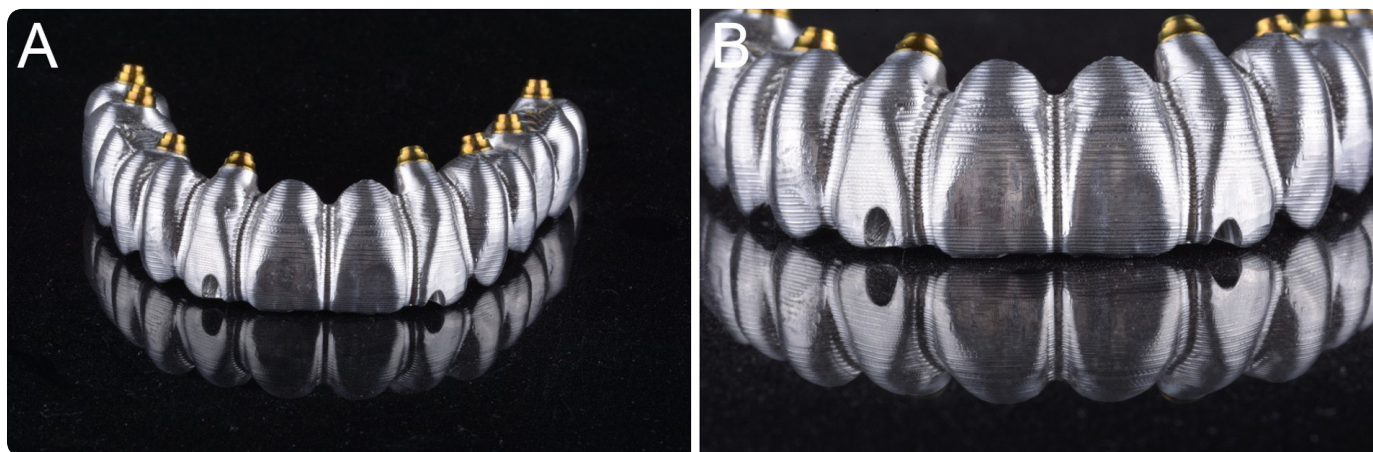

Figure 8: A replica of the final CAD project milled in metal. This replica is useful to verify the passive fit and the marginal adaptation intraorally. (A) The milled replica, frontal view. (B) Details of the milled replica.

operator experience and scanning strategy,[30] position, inclination and depth of the implants, design and material of the SB[31]).

At the level of intrinsic error, however, it is now established that one of the most significant difficulties for IOS lies in the correct reading and reproduction of the spaces between the different SBs.[23,28] These spaces are, in fact, devoid of physical references, with a "vertical" spatial "jump" between two SBs. It is precisely this distance and the absence of spatial reference points that cause difficulties for the IOS reconstruction software.[28] For this reason, some authors have tried to reduce these spaces and distances, introducing replicas or custom devices to facilitate reading by scanners.[32-36]

Figure 9: The final fixed FA is screwed onto the implants with excellent adaptation and passive fit. (A) Occlusal view of the prosthesis in position. (B-C-D-E) Intraoral radiographs confirm the absence of gaps and misfts at the level of the connection.

Figure 10: The final fixed FA is delivered to the patient.

In an *in vivo* study, Tallarico *et al.*[32] introduced a replica of the patient's total prosthesis, open in the SB area, to facilitate the scanning and reading of the spaces between one scan abutment and the other. This replica allows for accurate capture, through intraoral scanning, of the initial vertical dimension of patient occlusion, very useful data for the dental technician.[32] A similar approach has been followed by Mangano *et al.*[33], who resolved 15 cases of completely edentulous patients rehabilitated with an overdenture supported by a polyether-ether-ketone (PEEK) bar and four implants. This approach is notable because it also allows for the capture of the vertical dimension of occlusion and, potentially, the development of a completely digital prosthesis project. This improvement is due to the physical capture of the pre-existing prosthesis extraorally, which is then virtually superimposed to that which is captured intraorally.[33] This capture allows, due to the inversion of the normals, for

functionalized mucosal bases to be obtained, useful for the digital modelling of the prosthesis.[33] The limit of this approach is, however, that an additional appointment is required to capture the impression for the fabrication of the replica of the pre- existing prosthesis. In addition, a 3D printer is needed to fabricate this replica, which must be "opened" virtually or manually, to allow the SB to be housed without impeding their complete acquisition during the optical impression.[32,33]

A different approach has been proposed by other authors: the introduction of custom devices of different shapes, also useful for assessing and checking the accuracy of intraoral scanning.[34-36] In an *in vitro* study, Iturrate *et al.*[34] introduced a custom device of known dimensions, manufactured and connected onto a model of an edentulous maxilla with 4 SBs. This model was scanned with different IOSs, with and without the auxiliary device.[34] At the end of the study, the presence of the
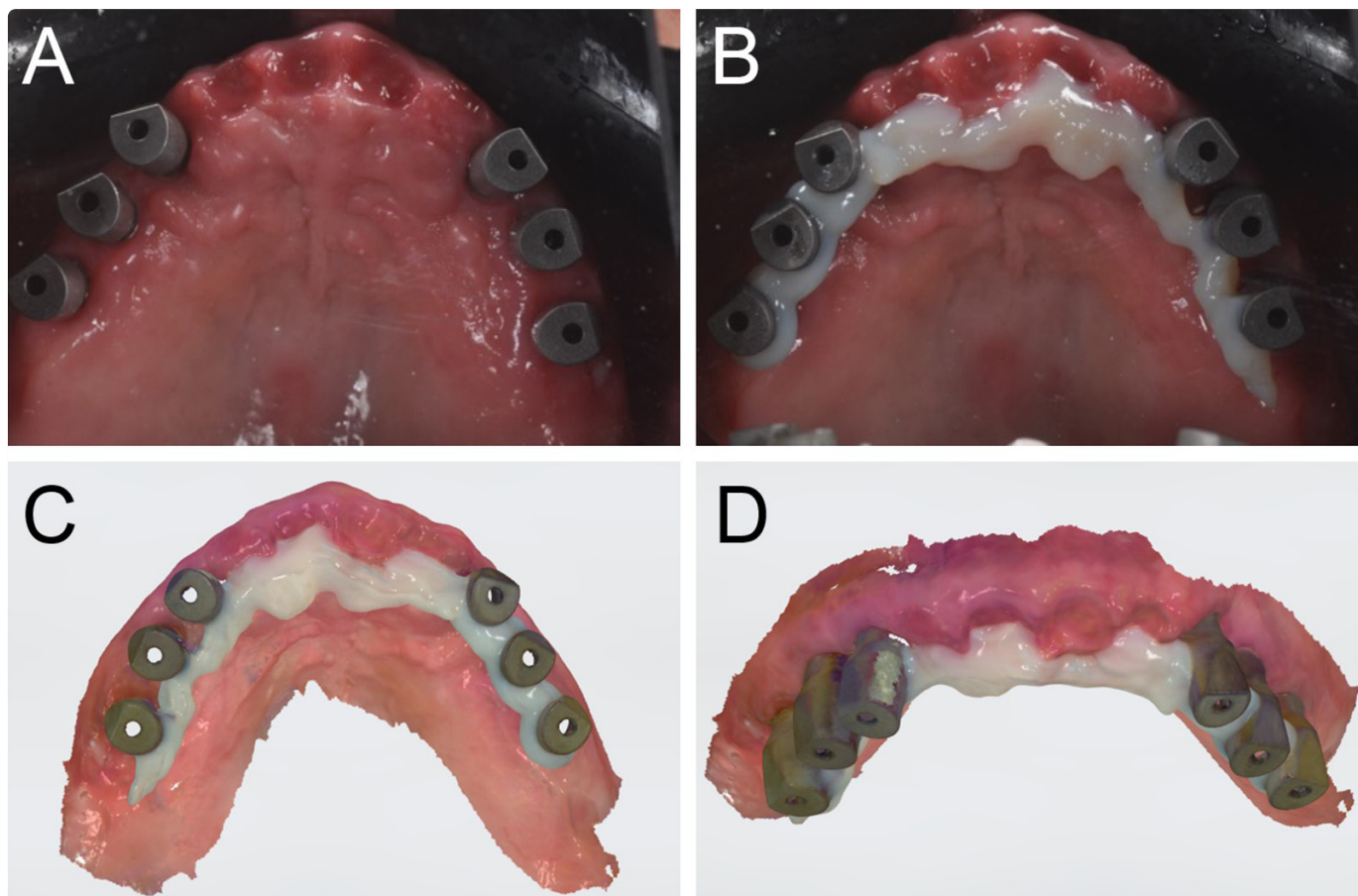
Figure 11: Fully edentulous patient with six implants in the maxilla. (A) The SBs are screwed on the six implants. (B) Prior to taking the intraoral scan, composite resin (that can be used, as a variant of the technique, instead of thermoplastic resin) is used to connect the SBs, avoiding any interference with their marker surfaces and heads. (C) Occlusal view of the scan captured with the SBs linked with composite resin. (D) Frontal view of the SBs linked with composite resin.

auxiliary device proved useful as it served as a spatial reference rich in anatomical landmarks for scanning, and was, therefore, able to improve the accuracy of the optical impression, regardless of the type of IOS used.[34] A similar strategy was employed by Gomez-Polo et al.,[35] who presented a technique for increasing the accuracy of intraoral scanning for FA prostheses and for correcting deviations and distortions that occur during direct intraoral scanning processes. The strategy employed a reference-marked rigid splint with known geometric features capable of providing the scanner with reference points and therefore reducing the deviation and errors given by the "jump" between the different SBs.[35] This method was based on sectioning and best-aligning the scanned files to generate a more accurate definitive cast and consequently a better-fitting restoration.[35]

Finally, the approach proposed by Schmidt et al.[36] and Mandelli et al.[37] is different but notable. Schmidt et al.[36] used a solid index to better assess inter-implant distances in vitro and in vivo. The authors prepared an in vitro model of a partially edentulous maxilla with four implant analogues in the posterior regions; they screwed on the SBs and scanned the model with a reference industrial machine.[36] Then, the same model was scanned with an IOS 10 times. The authors then connected the SBs to a custom solid index or CMA, consisting of four hollow

connected cylinders with a parallelepiped of known dimensions positioned on the palate. A minimum quantity of polyether impression material was used for connecting the SBs to the solid index. After the material had hardened, the assembly was unscrewed and sent to the dental laboratory to undergo investigation with a coordinate measuring machine (CMM). The inter-implant distances were assessed. Finally, 10 conventional impressions of the maxilla were taken, plaster models were poured and the same CMM was used to assess the implant distances.[36] The authors compared the accuracy of the different methods and found that significantly higher trueness was achieved with the solid index.[36] These results were confirmed in vivo, in a series of three cases made under the same protocol. The authors concluded that the CMA was proven to reproduce the 3-D inter-implant distances better than conventional or digital impression, with significantly higher accuracy.[36]

Mandelli et al.[37] presented the clinical results obtained with a similar hybrid digital–analogue technique, solid index impression protocol (SIIP), which used a solid custom-made index to capture accurate impressions of multiple implants for the fabrication of implant-supported fixed full arches (FAs). Five patients were treated with a FA supported by four implants. Three months after implant placement, impressions were taken for
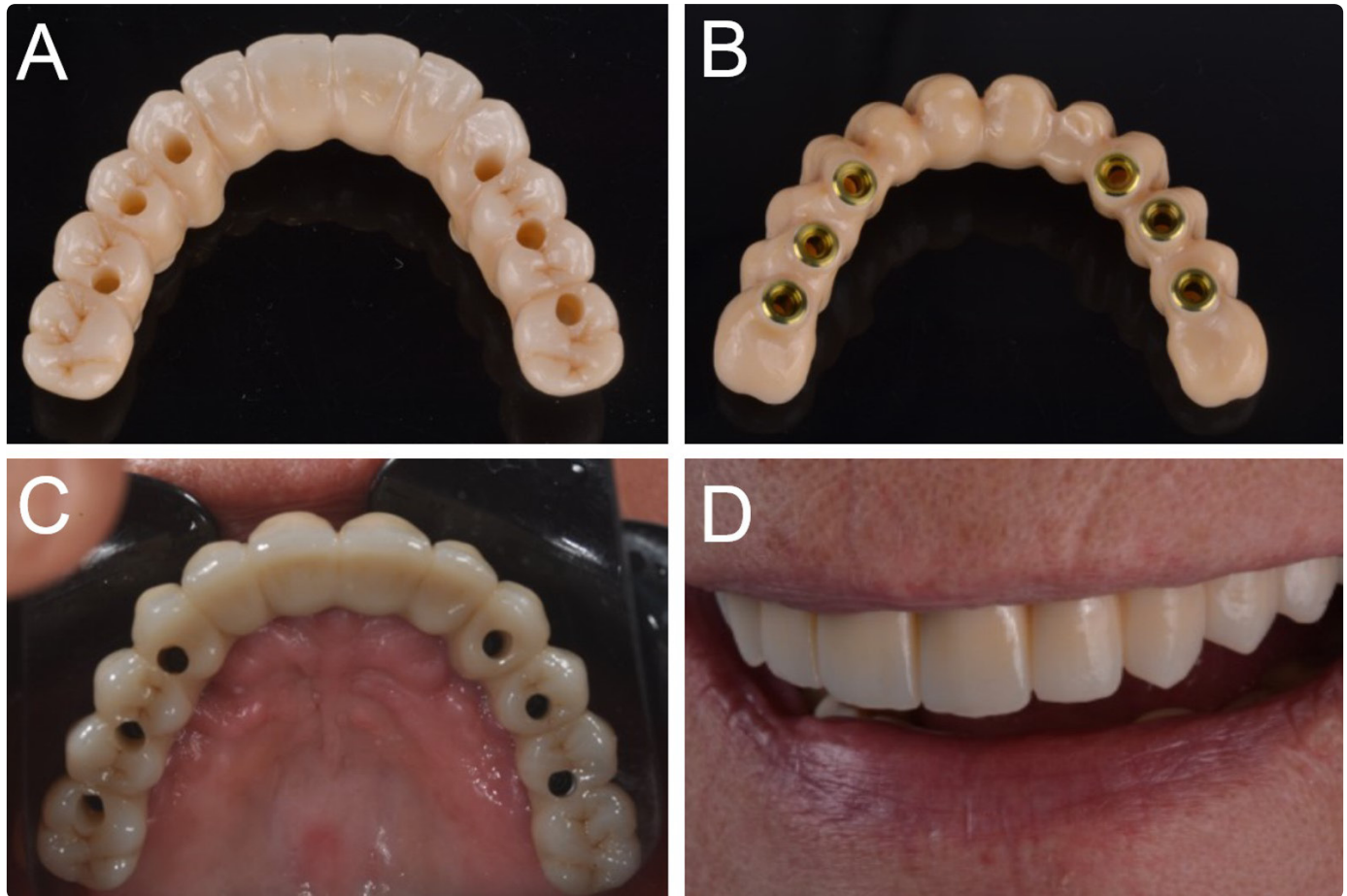
Figure 12: Fully edentulous patient with six implants in the maxilla. (A) The final restoration as fabricated by the laboratory. (B) View of the implant connections. (C) Delivery of the final restoration. (B) Aesthetic integration of the final restoration.

all patients with an IOS (direct digital impression) and with SIIP, using a custom tray consisting of four hollow cylinders connected with a bar.[37] This index, linked to the implant transfers, was transferred to the laboratory and used as the basis for fabricating the definitive FAs.[37] Excellent clinical precision and passive fit were obtained in all five implant-supported fixed FAs fabricated with SIIP.[37] One year after delivery, all fixed FAs were functional without any complications.[37] Finally, differences in accuracy were found between SIIP and direct intraoral scanning.[37] The authors concluded that SIIP seems to represent a viable option for capturing accurate impressions for the fabrication of clinically precise implant-supported fixed FAs with a hybrid digital–analogue workflow.[37] The advantage of the approach presented by Schmidt *et al.*[36] and Mandelli *et al.*[37] is the ability to register a highly accurate impression, using a solid custom index, and also the possibility of controlling the quality of the direct intraoral scan, also with the aid of CMM. The limit of this approach, however, is given by the need for an extra intraoral scan, preliminary to the preparation of the solid index, which must be modelled and printed in 3D: this requires time and specific skills. Furthermore, the workflow, in this case, is not entirely digital.[36,37]

Our present retrospective clinical study presents an easier and more direct, entirely digital approach, which consists of the intraoral connection of the implant SBs using thermoplastic

resin. Once modelled and cured, this resin is further fixed to the SBs through flowable composite, and the entire assembly is scanned through direct intraoral scanning with Trios3®, an IOS that several studies have reported being highly accurate.[19,21,27,38] This approach allowed us to obtain excellent passive fit and marginal adaptation of the implant superstructures at T0 (intraoral try-in of the polyurethane or metal replicas) with only 5/45 prostheses revealing unsatisfactory clinical precision. In these 5 FA cases, however, the clinician proceeded to separate the polyurethane or metal replica into several parts until a passive adaptation was obtained. These portions were then luted intraorally with low- contraction resin, and the assembly was transferred to the technician who re-scanned it with a desktop scanner and modified the CAD project accordingly. It is important to underline the fact that one-piece titanium SBs have been used in this study. This may represent an advantage because one-piece metal SBs are easier to fabricate for the manufacturer (as manufacturing tolerances with PEEK are more difficult to control) and help to minimize the positional errors that may potentially affect two-pieces (titanium-PEEK) SBs, due to tolerances in the assembly.[39] It is also important to note how in all these cases, a distance > 30 μm between meshes and libraries of multiple SBs had emerged during the early stages of CAD (best-fit): this may be considered an indicator of error and may highlight the importance of the

congruence between the mesh and the library file of the SBs. In fact, in the absence of perfect congruence between these two files in the early CAD stages, a positional error may arise. This topic needs to be adequately addressed by the scientific literature. At T1, however, all final monolithic zirconia revealed excellent passive fit and adaptation, except one that revealed a minimal friction, and fractured several minutes after being screwed. The authors believe this minimal misfit had caused fracture due to mandibular flexion since it occurred following a patient yawn. At T2, the implant success was high (100%), and no mechanical complications (i.e., complications affecting pre-established components sold by the implant manufacturer) occurred. However, another prosthesis fracture occurred. Finally, a chipping occurred in a distal extension on the right upper first molar; however, this complication was solved simply by polishing the surface of the fractured connector. Therefore, the incidence of prosthetic complications was 6.7%, and the overall 2-year prosthetic success was 93.3%.

The limitations of this study include a relatively brief (up to 2 years) follow-up period after the delivery of the final zirconia restorations; in addition, the retrospective study design is not the most suitable to draw definitive conclusions on the reliability of the present direct intraoral scanning technique. Furthermore, most of the prosthetic restorations were delivered in the maxilla, that offers more stable landmarks for the IOS (such us the palate) to reduce scan inaccuracies, when compared with the mandible (that lacks of references and has the tongue that may disturb the operator during scanning). The design of this study is essentially clinical, the protocol does not allow for proper mathematical quantification of the scanning error. In other words, it is not possible to quantitatively verify the mathematical accuracy of the scans, since the only controls are clinical, with a clinical and radiographic assessment of the marginal closure of the superstructures and their passive fit: this can be considered another limit of this study. Finally, in this clinical study, a highly accurate IOS (Trios3®) has been used by an experienced operator, and the results obtained here cannot be generalized and automatically considered valid also for other scanners. Hence, further long-term prospective clinical studies are essential to confirm the positive outcomes observed.

CONCLUSIONS

At present, the scientific literature does not consider direct intraoral scanning a sufficiently reliable method to capture impressions for the fabrication of long-span implant-supported prosthetic restorations, particularly in the case of FAs. Our present retrospective clinical study presents the clinical results obtained with a novel intraoral scanning technique, named "Continuous Scan Strategy" (CSS), based on the connection of the scan abutments through thermoplastic resin, to eliminate the "jump" between the different SBs and therefore reduce the intrinsic scan error. Over a four-year period, 40 patients were enrolled in our study and restored with 45 long-span implant-supported restorations (10 fixed PPs supported by ≥4 implants

and 35 FAs supported by 6–8 implants) fabricated via a full-digital workflow after the capture of an intraoral impression following the CSS technique. At the time of the intraoral try-in of the polyurethane or metal replica of the final prosthesis, 40/45 replicas had a perfect passive fit and adaptation. At the delivery of the final restorations, one prosthesis fractured, and another fracture and a chipping occurred at T2. The implant survival rate amounted to 100%. The prosthetic success was 93.3%, with a low incidence (6.7%) of complications. Therefore, CSS appears to represent a viable option for capturing accurate intraoral digital impressions for the fabrication of precise long-span implant-supported restorations. However, this study is retrospective and has a short follow-up. Most of the prosthetic restorations were delivered in the maxilla, that offers more stable landmarks for the IOS (such us the palate) to reduce scan inaccuracies, when compared with the mandible. Moreover, the design of this study is essentially clinical, since the protocol does not allow for proper mathematical quantification of the scanning error. Finally, only one IOS (Trios3®) has been used in this study, by an experienced operator, and the results obtained here cannot be generalized also to other scanners. Further long-term follow-up studies are needed to confirm these positive results.

MANUFACTURERS' DETAILS

- Nobel Active Internal Connection®, Nobel Biocare, Zurich, Switzerland
- Scan Abutment AQ®, New Ancorvis Srl, Calderara di Reno, BO, Italy
- Trios3®, 3-SHAPE, Copenhagen, Denmark
- DWX-52®, DGSHAPE a Roland Company, Hamamatsu, Japan
- Zeiss 4.5%®, Zeiss, Oberkochen, Germany
- Katana ML®, Kuraray Noritake, Japan, Tokyo
- Variolink Hybrid Abutment®, Ivoclar Vivadent, Schaan, Liechtenstein
- Excel 2003®, Microsoft, Redmond, WA, USA

ABBREVIATIONS

Cone beam computed tomography (CBCT); three-dimensional (3D); computer-assisted- design (CAD); intraoral scanner (IOS); scanbody (SB); single crown (SC); partial prosthesis (PP); full arch (FA); polyether-ether-ketone (PEEK); custom measuring aid (CMA); Continuous Scan Strategy (CSS); standard tesselletion language (.STL); standard deviations (SD); confidence intervals (CI); coordinate measuring machine (CMM); solid index impression protocol (SIIP).

REFERENCES

1. Medina-Sotomayor, P., Pascual-Moscardó, A., Camps, I. Accuracy of four digital scanners according to scanning strategy in complete-arch impressions. *Plos One*. 2018; **13**: e0202916.

2. Mangano, F., Gandolfi, A., Luongo, G., Logozzo, S. Intraoral scanners in dentistry: a review of the current literature. *BMC Oral Health*, 2017; **17**: 149.

3. Joós-Kovács, G., Vecsei, B., Körmendi, S., Gyarmathy, V.A., Borbély, J., Hermann, P. Trueness of CAD/CAM digitization with a desktop scanner – an *in vitro* study. *BMC Oral Health*, 2019; **19**: 280.

4. Menéndez López-Mateos, M.L., Carreño-Carreño, J., Palma, J.C., Alarcón, J.A., Menéndez López-Mateos, C., Menéndez-Núñez, M. Three-dimensional photographic analysis of the face in European adults from southern Spain with normal occlusion: reference anthropometric measurements. *BMC Oral Health*, 2019; **19**: 196.

5. Ayuso-Montero, R., Mariano-Hernandez, Y., Khoury-Ribas, L., Rovira-Lastra, B., Willaert, E., Martinez-Gomis, J. Reliability and Validity of T-scan and 3D Intraoral Scanning for Measuring the Occlusal Contact Area. *J Prosthodont.*, 2020; **29**: 19-25.

6. Dong, T., Xia, L., Cai, C., Yuan, L., Ye, N., Fang, B. Accuracy of *in vitro* mandibular volumetric measurements from CBCT of different voxel sizes with different segmentation threshold settings. *BMC Oral Health*, 2019; **19**: 206.

7. Mangano, C., Luongo, F., Migliario, M., Mortellaro, C., Mangano, F.G. Combining Intraoral Scans, Cone Beam Computed Tomography and Face Scans: The Virtual Patient. *J Craniofac Surg.* 2018; **29**: 2241-2246.

8. Hämmerle, C.H., Cordaro, L., van Assche, N., Benic, G.I., Bornstein, M., Gamper, F., Gotfredsen, K., Harris, D., Hürzeler, M., Jacobs, R., Kapos, T., Kohal, R.J., Patzelt, S.B., Sailer, I., Tahmaseb, A., Vercruyssen, M., Wismeijer, D. Digital technologies to support planning, treatment, and fabrication processes and outcome assessments in implant dentistry. Summary and consensus statements. The 4th EAO consensus conference 2015. *Clin Oral Implants Res.*, 2015; **26**: 97-101.

9. Lerner, H., Mouhyi, J., Admakin, O., Mangano, F. Artificial intelligence in fixed implant prosthodontics: a retrospective study of 106 implant-supported monolithic zirconia crowns inserted in the posterior jaws of 90 patients. *BMC Oral Health* 2020; **20**: 80

10. Javaid, M. and Haleem, A. Current status and applications of additive manufacturing in dentistry: A literature-based review. *J Oral Biol Craniofac Res.*, 2019; **9**: 179-185.

11. Aslan, Y.U., Coskun, E., Ozkan, Y., Dard, M. Clinical Evaluation of Three Types of CAD/CAM Inlay/ Onlay Materials After 1-Year Clinical Follow Up. E*ur J Prosthodont Restor Dent.*, 2019; **27**: 131-140.

12. Zarone, F., Di Mauro, M.I., Ausiello, P., Ruggiero, G., Sorrentino, R. Current status on lithium disilicate and zirconia: a narrative review. *BMC Oral Health*, 2019; **19**: 134.

13. D'haese, J., Ackhurst, J., Wismeijer, D., De Bruyn, H., Tahmaseb, A. Current state of the art of computer-guided implant surgery. *Periodontol 2000.*, 2017; **73**: 121-133.

14. Baan, F., de Waard, O., Bruggink, R., Xi, T., Ongkosuwito, E.M., Maal, T.J.J. Virtual setup in orthodontics: planning and evaluation. *Clin Oral Investig.*, 2020; **24**: 2385-2393.

15. Joda, T., Bragger, U., Zitzmann, N.U. CAD/CAM implant crowns in a digital workflow: Five-year follow-up of a prospective clinical trial. *Clin Implant Dent Relat Res.*, 2019; **21**: 169-174.

16. Grünheid, T., McCarthy, S.D., Larson, B.E. Clinical use of a direct chairside oral scanner: an assessment of accuracy, time, and patient acceptance. *Am J Orthod Dentofacial Orthop.*, 2014; **146**: 673-682.

17. Gallardo, Y.R., Bohner, L., Tortamano, P., Pigozzo, M.N., Laganá, D.C., Sesma, N. Patient outcomes and procedure working time for digital versus conventional impressions: A systematic review. *J Prosthet Dent.*, 2018; **119**: 214-219.

18. Kim, R.J., Benic, G.I., Park, J.M. Trueness of digital intraoral impression in reproducing multiple implant position. *Plos One.*, 2019; **14**: e0222070.

19. Mangano, F.G., Hauschild, U., Veronesi, G., Imburgia, M., Mangano, C., Admakin, O. Trueness and precision of 5 intraoral scanners in the impressions of single and multiple implants: a comparative *in vitro* study. *BMC Oral Health*, 2019; **19**: 101.

20. Sami, T., Goldstein, G., Vafiadis, D., Absher, T. An *in vitro* 3D evaluation of the accuracy of 4 intraoral optical scanners on a 6-implant model. *J Prosthet Dent.*, 2020 Feb 6. Pii: S0022-3913(19)30693-6.

21. Giachetti, L., Sarti, C., Cinelli, F., Russo, D.S. Accuracy of Digital Impressions in Fixed Prosthodontics: A Systematic Review of Clinical Studies. *Int J Prosthodont.*, 2020; **33**: 192-201.

22. Hack, G., Liberman, L., Vach, K., Tchorz, J.P., Kohal, R.J., Patzelt, S.B.M. Computerized optical impression making of edentulous jaws – An in vivo feasibility study. *J Prosthodont Res.* 2020 Feb 13. Pii: S1883-1958(19)30709-1. Doi: 10.1016/j.jpor.2019.12.003. [Epub ahead of print]

23. Keul, C. and Güth, J.F. Accuracy of full-arch digital impressions: an i*n vitro* and *in vivo* comparison. *Clin Oral Investig.* 2020; **24**: 735-745.

24. Wulfman, C., Naveau, A., Rignon-Bret, C. Digital scanning for complete-arch implant- supported restorations: A systematic review. *J Prosthet Dent.*, 2019 Nov 19. Pii: S0022- 3913(19)30426-3. Doi: 10.1016/j.prosdent.2019.06.014. [Epub ahead of print]

25. Goracci, C., Franchi, L., Vichi, A., Ferrari, M. Accuracy, reliability, and efficiency of intraoral scanners for full-arch impressions: a systematic review of the clinical evidence. *Eur J Orthod.*, 2016; **38**: 422-428.

26. Ahlholm, P., Sipilä, K., Vallittu, P., Jakonen, M., Kotiranta, U. Digital Versus Conventional Impressions in Fixed Prosthodontics: A Review. *J Prosthodont.*, 2018; **27**: 35-41.

27. Rutkunas, V., Larsson, C., Vult von Steyern, P., Mangano, F., Gedrimiene, A. Clinical and laboratory passive fit assessment of implant-supported zirconia restorations fabricated using conventional and digital workflow. *Clin Implant Dent Relat Res.* 2020; **22**: 237-245.

28. Abduo, J. and Elseyoufi, M. Accuracy of Intraoral Scanners: A Systematic Review of Influencing Factors. *Eur J Prosthodont Restor Dent.*, 2018; **26**: 101-121.

29. Revilla-León, M., Jiang, P., Sadeghpour, M., Piedra-Cascón, W., Zandinejad, A., Özcan, M., Krishnamurthy, V.R. Intraoral digital scans-Part 1: Influence of ambient scanning light conditions on the accuracy (trueness and precision) of different intraoral scanners. *J Prosthet Dent.* 2019 Dec 18. Pii: S0022-3913(18)30992-2.

30. Motel, C., Kirchner, E., Adler, W., Wichmann, M., Matta, R.E. Impact of Different Scan Bodies and Scan Strategies on the Accuracy of Digital Implant Impressions Assessed with an Intraoral Scanner: An *In Vitro* Study. *J Prosthodont.* 2020; **29**: 309-314

31. Moslemion, M., Payaminia, L., Jalali, H., Alikhasi, M. Do Type and Shape of Scan Bodies Affect Accuracy and Time of Digital Implant Impressions? *Eur J Prosthodont Restor Dent.* 2020; **28**: 18-27

32. Tallarico, M., Schiappa, D., Schipani, F., Cocchi, F., Annucci, M., Xhanari, E. Improved fully digital workflow to rehabilitate edentulous patient with an implant overdenture in 4 appointments: A case report. *J Oral Science Rehabilitation.* 2017; **3**: 38-46.

33. Mangano, F., Mangano, C., Margiani, B., Admakin, O. Combining Intraoral and Face Scans for the Design and Fabrication of Computer-Assisted Design/Computer-Assisted Manufacturing (CAD/CAM) Polyether-Ether-Ketone (PEEK) Implant-Supported Bars for Maxillary Overdentures. *Scanning.* 2019; **2019**: 4274715.

34. Iturrate, M., Eguiraun, H., Solaberrieta, E. Accuracy of digital impressions for implant- supported complete-arch prosthesis, using an auxiliary geometry part- An *in vitro* study. *Clin Oral Implants Res.* 2019; **30**: 1250-1258.

35. Gómez-Polo, M., Ballesteros, J., Perales-Padilla, P., Perales-Pulido, P., Gómez-Polo, C., Ortega, R. Guided implant scanning: A procedure for improving the accuracy of implant- supported complete-arch fixed dental prostheses. *J Prosthet Dent.* 2019 Nov 21. Pii: S0022-3913(19)30614-6.

36. Schmidt, A., Billig, J.W., Schlenz, M.A., Wöstmann, B. A new 3D-method to assess the inter implant dimensions in patients – A pilot study. *J Clin Exp Dent.* 2020; **12**: e187- e192.

37. Mandelli, F., Zaetta, A., Cucchi, A., Mangano, F. Solid index impression protocol: a hybrid workflow for high accuracy and passive fit of full-arch implant-supported restorations. *Int J Comput Dent* 2020; **23**: 161-181.

38. Roig, E., Garza, L.C., Álvarez-Maldonado, N., Maia, P., Costa, S., Roig, M., Espona, J. *In vitro* comparison of the accuracy of four intraoral scanners and three conventional impression methods for two neighboring implants. *PLoS One.* 2020; **15**: e0228266.

39. Mizumoto, R.M., Yilmaz, B. Intraoral scan bodies in implant dentistry: A systematic review. *J Prosthet Dent.* 2018; **120**: 343-352.

BMC Oral Health

RESEARCH ARTICLE   **Open Access**

Artificial intelligence in fixed implant prosthodontics: a retrospective study of 106 implant-supported monolithic zirconia crowns inserted in the posterior jaws of 90 patients

Henriette Lerner[1,2*], Jaafar Mouhyi[3,4], Oleg Admakin[5] and Francesco Mangano[6]

Abstract

Background: Artificial intelligence (AI) is a branch of computer science concerned with building smart software or machines capable of performing tasks that typically require human intelligence. We present a protocol for the use of AI to fabricate implant-supported monolithic zirconia crowns (MZCs) cemented on customized hybrid abutments.

Methods: The study protocol consisted of: (1) intraoral scan of the implant position; (2) design of the individual abutment and temporary crown using computer-aided design (CAD) software; (3) milling of the zirconia abutment and the temporary polymethyl-methacrylate (PMMA) crown, with extraoral cementation of the zirconia abutment on the relative titanium bonding base, to generate an individual hybrid abutment; (4) clinical application of the hybrid abutment and the temporary PMMA crown; (5) intraoral scan of the hybrid abutment; (6) CAD of the final crown with automated margin line design using AI; (7) milling, sintering and characterisation of the final MZC; and (8) clinical application of the MZC. The outcome variables were mathematical (quality of the fabrication of the individual zirconia abutment) and clinical, such as (1) quality of the marginal adaptation, (2) of interproximal contact points and (3) of occlusal contacts, (4) chromatic integration, (5) survival and (6) success of MZCs. A careful statistical analysis was performed.

Results: 90 patients (35 males, 55 females; mean age 53.3 ± 13.7 years) restored with 106 implant-supported MZCs were included in the study. The follow-up varied from 6 months to 3 years. The quality of the fabrication of individual hybrid abutments revealed a mean deviation of 44 µm (± 6.3) between the original CAD design of the zirconia abutment, and the mesh of the zirconia abutment captured intraorally at the end of the provisionalization. At the delivery of the MZCs, the marginal adaptation, quality of interproximal and occlusal contacts, and aesthetic integration were excellent. The three-year cumulative survival and success of the MZCs were 99.0% and 91.3%, respectively.

(Continued on next page)

---

* Correspondence: h.lerner@web.de
[1]Private Practice, Ludwing-Wilhelm Strasse, 17 Baden-Baden, Germany
[2]Lecturer, Academic Teaching and Research Institution of Johann Wolfgang
Goethe-University, Frankfurt am Main, Germany
Full list of author information is available at the end of the article

(Continued from previous page)

Conclusions: AI seems to represent a reliable tool for the restoration of single implants with MZCs cemented on customised hybrid abutments via a full digital workflow. Further studies are needed to confirm these positive results.

Keywords: Artificial intelligence, Monolithic zirconia crowns, Individual hybrid abutments, Full digital workflow, Marginal adaptation, Survival, Success

Background

In implant-supported digital fixed prosthesis, one ideal option today is the use of customised abutments [1–3]. These custom abutments, designed with computer-aided design (CAD) software and subsequently milled and sintered in zirconia, are cemented extraorally on titanium bonding bases. Once applied, they allow obtaining an ideal emergence profile, high compatibility with soft tissues and high aesthetics [4]. Above these customised abutments, it is possible to cement monolithic restorations [4, 5]. However, while several clinical studies show that the use of these abutments can represent an ideal solution for the fixed rehabilitation of the implant patient, not only in the anterior [4] but also in the posterior areas [6], some practical problems are related to this approach.

In modern digital protocols, the dentist must capture an intraoral scan of the implant scanbody as accurately as possible [6, 7], and the technician must carefully perform the replacement of the mesh captured by scanning with the implant library files on which to model [8]; furthermore, implant libraries within the CAD software must not present errors. However, working well in these phases may not be sufficient: in fact, during the extraoral cementation of the customised zirconia abutment on the bonding base, tolerances between the components may cause cementing errors [8, 9]. These errors, even if only a few degrees, can generate positional problems during the delivery of the customised abutment and the temporary restoration to the patient: these components will not be in the exact CAD-planned position in the mouth [9]. During the delivery of the temporary restoration, small adjustments in resin or polymethylmethacrylate (PMMA) can be tolerated at the level of interproximal contacts or occlusion, but these adjustments are not acceptable for monolithic ceramic restorations, such as zirconia [9, 10]. The definitive monolithic zirconia restorations cannot be retouched in the mouth [10, 11], so they must not show positional errors at delivery.

To overcome this problem, experienced dental technicians generally position the individual abutments already assembled on a three-dimensional (3D) printed model, with the implant analogues inserted, and scan them with a desktop scanner. This allows obtaining the relative position and anatomy of the abutments, including the margin line [12]. Although this is possible, it is an extra step that forces the technician to print a model, with

related costs and problems [13], but above all to model the definitive zirconia restorations on meshes that are, by definition, surface reconstructions and geometric approximations of the scanned objects [9, 14].

These additional steps can now be avoided by using artificial intelligence (AI). AI is a wide-ranging branch of computer science concerned with building smart software or machines capable of performing tasks that typically require human intelligence [15, 16]. It is commonly defined as "the ability of a system to interpret external data, learn from them, and use those learnings to achieve objectives and goals through flexible adaptation" [15, 16]. Machine learning, as a subset and foundation of AI, is the ability of computer systems to perform specific tasks to approximate human cognition, without using explicit instructions, solely relying on patterns and mathematical models [17]. AI can represent a valuable addition to fixed implant prosthodontics. CAD software can be 'instructed' to save the stereolithographic (.STL) file of the individual abutment, modelled by the technician, in a specific folder, and then to retrieve it automatically when needed [9]. At the end of the provisional period, the dentist can capture a new intraoral impression of the hybrid abutment in the correct position, after removal of the temporary restoration, without worrying about the visibility of the abutment margins, which are generally subgingival. The mesh captured with this intraoral impression is then imported into the CAD software. The portion relative to the individual abutment, captured in the mouth, is automatically recognised and eliminated because it is replaced with the original. STL file of the zirconia abutment, previously modelled by the dental technician [9].

The advantage of this approach is two-fold. The technician can model on a library file much more accurately than on a mesh, which is always a geometric approximation [9, 14]. Additionally, the software can automatically detect the margin line, even if subgingival, and draw it without error, using AI [9, 15]. This allows the technician to model without regarding the margins, focusing only on tooth shape, volumes, and interproximal and occlusal contacts. This innovative approach, which exploits the AI of the software, allows the technician to save time, while reducing errors and costs of prosthetic therapy; it is not necessary to print the 3D model with the digital analogues, nor to scan it [13]. Moreover, this

approach could extend the use of individual hybrid abutments even in the posterior sites. An additional advantage of this method is that it allows quantitative verification and measurement of the overall mathematical quality of the digital workflow, for the fabrication of individual zirconia abutments [9].

The purpose of this retrospective clinical study is to present a protocol for the use of AI to fabricate implant-supported monolithic zirconia crowns (MZCs) cemented on customised hybrid abutments, via a full digital workflow.

Methods

Patient selection and inclusion/exclusion criteria

The present retrospective study was based exclusively on data collected on patients who had been treated through prosthetic restoration of single locking-taper connection implants (Exacone®, Leone, Florence, Italy) with MZCs in the posterior jaws (premolars and molars), between June 2016 and April 2019, in a single dental centre. The MZCs were made through a full digital workflow, without therefore producing any physical model, and were supported in all cases by individual hybrid abutments, composed of an upper portion in zirconia, cemented on a titanium bonding base. The data collected in the electronic medical records and necessary for the inclusion of the patients in the present study consisted of intraoral scans captured from the patient during the different work phases, the CAD scenes generated at the end of modelling the different components (individual abutments, temporary crowns in PMMA and definitive crowns in zirconia), and clinical, radiographic and photographic data normally collected during prosthetic implant treatment. All patients had previously signed a generic informed consent to prosthetic implant treatment, and a condition for inclusion in this study, on the nature of which all patients were properly informed, was signing a further specific consent. Exclusion criteria from this retrospective study were patients treated with implants produced by different manufacturers, or with multiple implants supporting fixed restorations such as bridges and full-arch prostheses; all patients treated with analog methods (i.e., through the capture of analog impressions with trays and conventional materials) or not full digital techniques; patients who were treated with full digital techniques, but through the printing of 3D models and modelling of zirconia copings to be layered with ceramic; all patients who had no opposing dentition; and patients who did not give consent for enrolment. The study was conducted in full accordance with the principles of the Helsinki Declaration on Human Experimentation of 1975 (and Revision of 2008) and was approved by the Ethics Committee of Sechenov University in Moscow, Russia.

Clinical and laboratory procedures

The procedures for prosthetic rehabilitation consisted of the following eight phases (four clinical and four laboratory), based on the proprietary protocol #ScanPlanMake-Done, as already described in a previous scientific work [9].

1. Capture of the first optical impression with the CS 3600® intraoral scanner (Carestream Dental, Atlanta, GA, USA) using the 'implant' module (Fig. 1). Once the healing abutment was removed, the dentist took an impression of the master model without a scanbody, to capture the mucosal collar and, where present, the adjacent teeth. The first phase of the capture of the impression was completed with acquisition of the antagonist model and the bite. Then, the dentist selected the area of the mucosal collar on the master model and, after positioning the implant scanbody of the same diameter of the implant, captured it. Care was taken to capture the whole scanbody. The scanner perfected the image, and after a careful verification that confirmed the quality of the impression, the clinician removed the implant scanbody, repositioning the healing abutment. The. STL files derived from the optical impression were sent to the dental laboratory.

2. Modelling of the individual abutment and temporary crown in CAD software (Valletta®, Exocad, Darmstadt, Germany) (Fig. 2). The technician imported the. STL files into the CAD software and, after placing the order, replaced the mesh of the scanbody captured by the dentist with the corresponding library file, through superimposition by points and surfaces, using the software's powerful algorithm. Having carried out this replacement, the technician selected the bonding base from a range of possible options (4-mm height straight base, or 6-mm height straight or angled base) according to the specific clinical indications of the case. Next, the technician modelled the individual abutment in its lower and upper portions, and the temporary crown to be cemented over it. The individual abutment was integral and did not show any screw holes, as the implants used in this study had a screwless, Morse-taper implant–abutment connection. However, the technician modelled a small hole at the top of the abutment to facilitate the outflow of cement during the cementation. The abutment and crown files were saved in. STL format and were ready for production. The. STL file of the individual abutment was saved in a specific folder created within the CAD software, containing all the modelling of individual abutments of all treated patients. Each model carried the patient's name in addition to the number
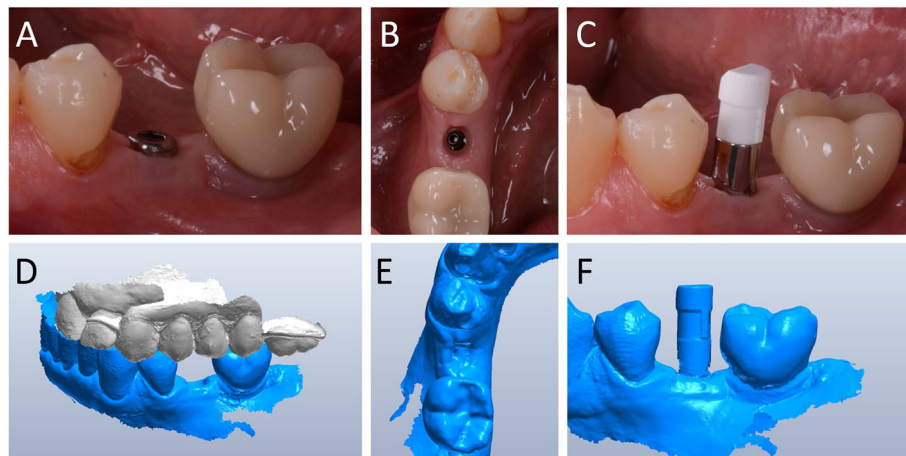
Fig. 1 First intraoral scan of a second mandibular premolar. (**A**) The healing abutment in position. (**B**) The healing abutment is removed for the scan. (**C**) The scanbody is placed in position. (**D**) Intraoral scan of the master model without the scanbody and the antagonist arch. (**E**) The mucosal collar. (**F**) The implant scanbody in position

corresponding to the dental element that was prosthetically rehabilitated.

3. Production of the individual abutment and temporary crown. The individual abutment was milled in zirconia with a powerful five-axis milling machine (DWX-51®, DGShape a Roland Company, Hamamatsu, Japan) and then sintered in an oven (Tabeo®, Mimh-Vogt, Stutensee, Germany). At this point, the abutment was cemented by the dental technician on the titanium bonding base chosen during CAD modelling, which was purchased by the implant manufacturer. The cementation of the two components of the future individual hybrid zirconia–titanium abutment (upper portion individualised in zirconia on a standard titanium bonding base) occurred in the laboratory, under 4.5x magnification (Zeiss 4.5x®, Zeiss, Oberkochen, Germany), using a resin cement (Bifix SE®, Voco, Cuxhaven, Germany), taking care not to make macroscopic errors, due to the inevitable presence of minimal tolerances between the parts. The temporary crown

was milled in PMMA from the modelling. STL file, using the same milling machine. It was then characterised, polished and fitted onto the individual abutment for control of marginal closure. At the end of these procedures, the dental technician sent the individual hybrid abutment and temporary crown to the dentist for clinical application.

4. Clinical application of the individual hybrid abutment and the temporary PMMA crown (Fig. 3). After removing the healing abutment, the dentist placed the hybrid abutment in the correct position, using the temporary crown as a guide. The abutment was engaged in the positional hexagon and activated with a percussion hammer, as previously described for locking-taper implants [9]. The margins were generally positioned 1 mm subgingival or juxtagingival, and the lower portion of the abutment generated minimal compression on the soft tissues, with ischaemisation of the peri-implant mucosa. After the abutment activation, the dentist verified the quality of the modelling, with particular regard to interproximal and
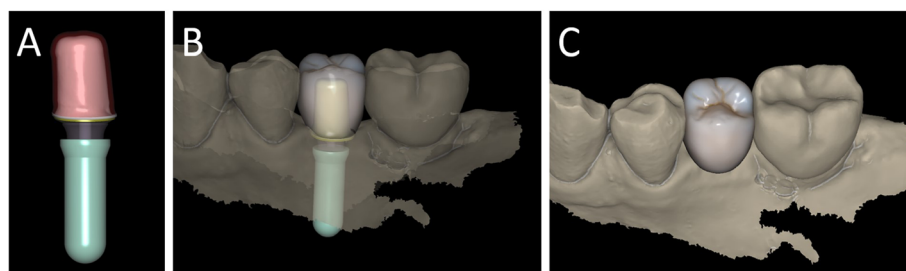

Fig. 2 Computer-assisted-design (CAD) of the individual abutment and the provisional crown. (**A**) The individual abutment is modelled in CAD and saved in a dedicated folder of the software. (**B**) The individual abutment and the provisional crown. (**C**) Photorealistic rendering of the provisional crown
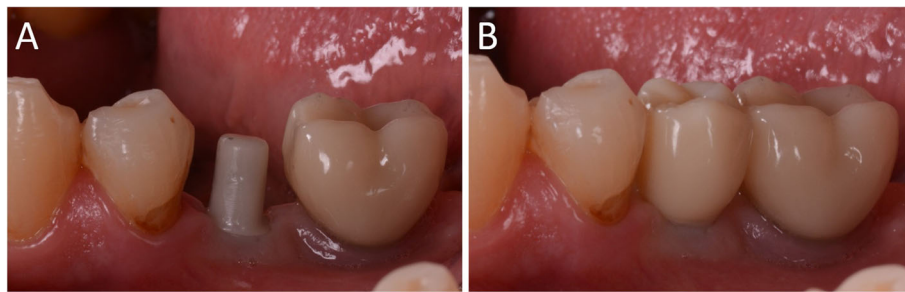
Fig. 3 Delivery of the individual hybrid abutment and the provisional crown. (**A**) The individual hybrid abutment is placed. (**B**) The provisional polymethyl-methacrylate (PMMA) crown is cemented over it

occlusal contacts. In all cases in which small adaptations were necessary, they were performed directly in the mouth, until the final polishing of the provisional crown and its cementation on the individual abutment with a temporary cement (Tempbond®, Kerr, Orange, CA, USA). The provisional crown lasted from one to 2 months, to verify the adaptation of the implant under load and the maturation of the mucosal tissues. At the end of this period, the patient was recalled for the final scan.

5. Scanning the position of the hybrid abutment in the mouth (Fig. 4). The patient was recalled and subjected to a new intraoral scan of the dental arches with the CS 3600® scanner. Scanning was performed in 'restoration' mode. The first scan of the master model was captured with the temporary

restoration in situ, to provide the dental technician with additional information on the anatomical limits of the modelling. The scan was completed with the capture of the opposing arch and the bite. Then, the dentist removed the temporary crown, and captured a fourth scan of the zirconia abutment in position, with the tissues conditioned by the temporary restoration. In this scan, the dentist focused on capturing the entire zirconia prosthetic abutment, and on capturing the contact points with adjacent teeth, where present. The. STL files or meshes derived from this scan were sent to the laboratory, and the temporary crown was cemented again on the abutment.

6. In the laboratory, the scan files were opened by the dental technician in the CAD software. First, the
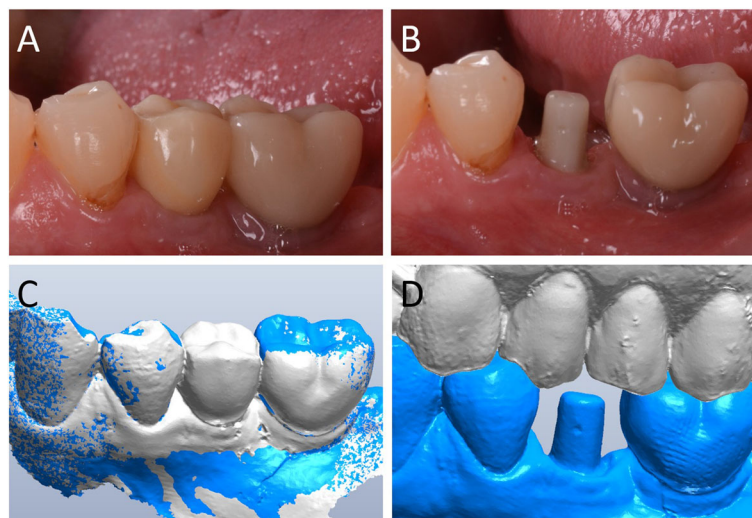
Fig. 4 When the provisionalization period ends, a second digital impression is taken with and without the provisional crown, in order to capture the bite, the intraoral position of the zirconia individual abutment, and the status of the soft tissues. (**A**) The PMMA crown in position after a period of 2 months. (**B**) The individual hybrid abutment 2 months after placement. The abutment is carefully cleaned by any residual cement particles, the soft tissues are mature and everything is ready for the intraoral digital impression. (**C**) The first impression of the master model is captured with the functionalized provisional in position, in order to provide the dental technician information on the anatomy of the provisional and its occlusal limits. (**D**) after the removal of the provisional, the intraoral digital impression of the master model with the abutment in position is captured

technician highlighted the area of the individual abutment on the mesh captured with the intraoral scan. Then the software was able to recall, within the specific folder containing all the modelling of the individual abutments of all the patients treated, the modelling corresponding to the patient in question, and to the implant in question. The original CAD file of the upper portion of the customized abutment was "extruded" like a model die, and "cut" or sectioned on the basis, in order to look like an "open" file, mimicking a mesh: in fact, Exocad® does not allow the dental technician to model on "closed" files (i.e., ready to be milled or printed). All the following procedures were performed using the intrinsic AI and the algorithms of the software. The software then replaced only the highlighted portion of mesh captured intraorally, with the corresponding. STL file of the original abutment modelling. The dental technician could test the quality of the overlap in micrometres by generating a colorimetric map. The original modelling file of the individual abutment was now integrated with the mesh of the master model, in the correct spatial position. Using intrinsic AI, the software was able to automatically trace the margin line of the implant abutment, though subgingival (Fig. 5). The technician could intervene on the design of the margin line, being able to modify it at will, but this was never necessary since the margin line drawn by AI was perfect in all cases. It was drawn on a file modelled in CAD, and therefore extremely clear. The software was able to detect it automatically and to design it without any problems. At this point, the dental technician could

shape the final crown (Fig. 6). By opting for a monolithic zirconia restoration, it was not necessary to draw any model to print in 3D. The technician had to focus solely on modelling the shapes and volumes of the tooth, interproximal contact points and occlusion. The final 3D modelling was saved in. STL format and ready for production.

7. Production of the definitive monolithic crown in translucent zirconia. The final modelling file was processed by the aforementioned five-axis milling machine (DWX-51®, DGShape a Roland Company, Hamamatsu, Japan) to obtain the MZC, which was infiltrated when still green for better characterisation, and subsequently sintered. The crown was polished and ready for clinical application.

8. Clinical application of the MZC (Fig. 7). The patient was called back to the dental clinic, and the temporary PMMA crown was removed and replaced with the definitive MZC. At the time of application, the dentist carefully checked the congruity of the shape and volumes of the tooth, the quality of the interproximal contact points and the occlusal contacts, and the quality of the marginal fit and closure. Control of the marginal fit and closure of the restoration took place both clinically and radiographically. Before cementation with temporary cement (Tempbond®, Kerr, Orange, CA, USA), the MZC was positioned and an endoral x-ray was taken. Clinical control of the marginal closure occurred under 4.5x magnification (Zeiss 4.5x®, Zeiss, Oberkochen, Germany), with physical probing of the circumference of the crown with a periodontal probe to intercept any misfits, gaps or
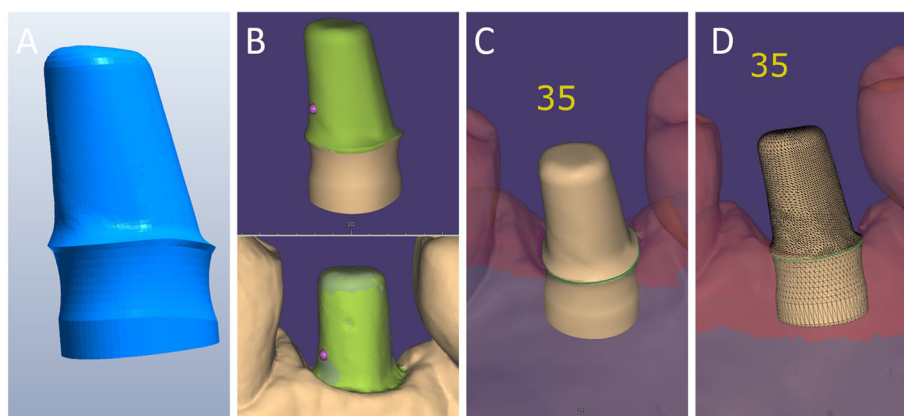
Fig. 5 Artificial Intelligence (AI) application in fixed implant prosthodontics. (**A**) The original .STL file of the CAD design of the individual abutment, which was previously saved in a dedicated folder, is recalled by the system. (**B**) The original CAD design of the abutment is superimposed on the mesh captured intraorally. (**C**) Automatic margin line detection. (**D**) Details of the original CAD model, in which the abutment margins, although subgingival, are clearly represented and visible

Lerner *et al. BMC Oral Health*   (2020) 20:80

Page 7 of 16
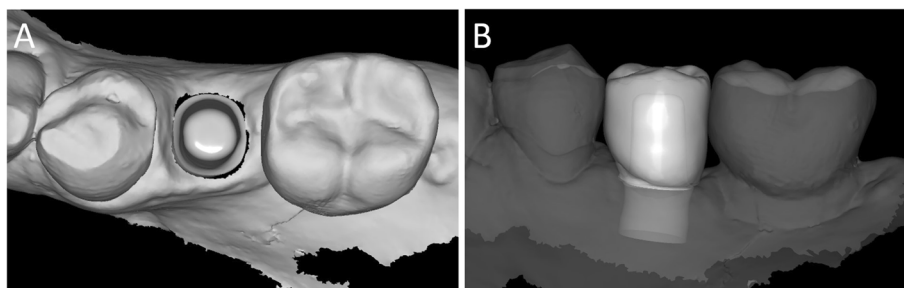
Fig. 6 The final CAD scene. (**A**) details of the individual abutment in position: the technician will model the final zirconia crown over it; the dental technician can model the final crown on a library file. (**B**) CAD design of the final crown. The software is capable to automatically detect the margin line, because the final crown is modelled on the original CAD design of the individual hybrid abutment in the correct position, and not over a mesh. The technician can, anyway, modify the margin line, but this is not recommended because the software is able to detect it perfectly, better than the human eye

undercuts. Occlusal control was very careful and performed with occlusion papers so that any light precontacts were polished. At the end of these checks, and once the aesthetic adaptation of the restoration and the colour had been verified, the crown was cemented and the patient was included in a program of annual checks (two professional hygiene sessions a year, with one planned every 6 months).

Study outcome variables

The variables investigated in this study were of two types: mathematical and clinical. First, the mathematical quality of the protocol for the fabrication of the individual hybrid abutments was inspected, by means of the superimposition of the original CAD design of the upper portion of the abutment over the mesh of the actual zirconia abutment captured intraorally with digital impressions. This type of mathematical evaluation made it possible to calculate the mean spatial error in the production (milling/ sintering) of the individual zirconia abutment, and to highlight the areas were any dimensional errors were concentrated. Then, the clinical variables (divided into primary and secondary clinical variables) were investigated. The clinical outcome

variables were divided into primary and secondary not by importance, but because they were evaluated at different times.

Mathematical quality

The mathematical quality of the protocol for the fabrication of the individual hybrid abutments was controlled when the superimposition of the original CAD design of the upper portion of the abutment over the mesh of the actual zirconia abutment captured intraorally was performed. In fact, the CAD files of the drawing of the individual hybrid abutment, and the mesh of the actual position of the zirconia abutment captured intraorally were saved as individual STL files after the superimposition in Exocad®, and were imported in a powerful reverse-engineering (Studio2012®, Geomagics, Morrisville, NC, USA). This software was employed to calculate the distance (mean ± SD in μm) between the visible, supramucosal surfaces of these two different STL files. In order to avoid any error given by the presence of the soft tissues, the calculation was limited to the area above the soft tissues. This type of mathematical evaluation made it possible to calculate the spatial error in the production (milling/ sintering) of the individual zirconia abutment. Finally, a digital colorimetric map was
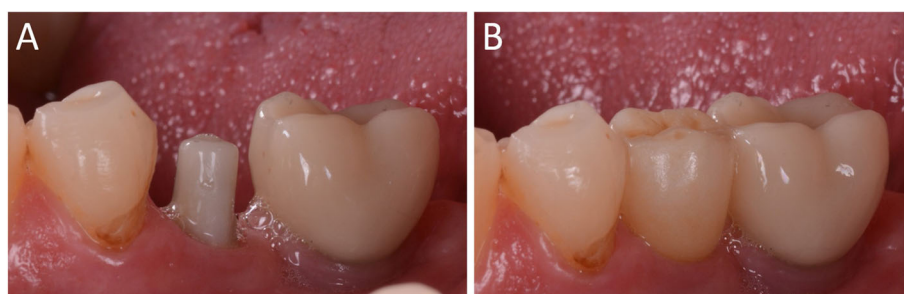

Fig. 7 Delivery of the final zirconia crown. (**A**) Details of the individual hybrid abutment at the delivery of the final crown. (**B**) The final zirconia crown and its aesthetic integration

generated by the software, in order to better highlight the spatial deviations between the different files, at different levels. The threshold was set at 30 μm, so that any deviation < 30 μm was represented in green colour; deviations > 30 μm were represented in blue colour (dark blue for major deviations).

Clinical quality

1. Primary clinical variables (evaluated immediately on delivery of the MZC and related to the quality of the prosthetic implant restoration).

2. Secondary clinical variables (evaluated from 6 months to 3 years later and related to the survival and success of the MZC over time).

These variables were investigated by a prosthodontist and a periodontist, both experts.

The primary clinical variables were

1A. Quality of the marginal adaptation and closure

The quality of the marginal closure was clinically investigated through visual inspection with magnifying glasses (Zeiss 4.5x®, Zeiss, Oberkochen, Germany) and tactile analysis through a circumferential probing at the crown positioned on the individual abutment, with a periodontal probe, and finally, through radiographic analysis with evaluation of endoral RX. The purpose of this analysis was to assess the presence of any defects, misfits, gaps or undercuts.

1B. Quality of interproximal contact points

Quality control of interproximal contact points with adjacent teeth, where present, was performed visually and using dental floss.

1C. Quality of occlusal contacts

Occlusion control was performed clinically, using articulating papers (Bausch Articulating Paper®, Bausch Inc., Nashua, NH, USA).

1D. Chromatic and aesthetic integration

The quality of the colour integration of the restoration was assessed visually.

At the end of the evaluation, the two operators who evaluated the quality of the MZCs assigned each restoration a score from 1 to 5 (with 5 as the highest value, expressing fully satisfactory quality; 4 for satisfactory quality; 3 for acceptable quality; and 2 and 1 as the lowest values, expressing a restoration of unsatisfactory quality) for each of the aforementioned parameters. If even one of the four parameters investigated by the two operators was of unsatisfactory quality, and had therefore received a grade < 3, the definitive restoration was not cemented and was sent back to the dental technician for remaking. This happened if the marginal adaptation

of the restoration was unsatisfactory, in the presence of gaps or over-boundaries; if the interproximal contact points were missing or unsatisfactory, to avoid stagnation of food and hygiene problems; where there were excessive occlusal contacts that could not be eliminated by simple polishing, or a lack of appropriate occlusal contacts (infra-occlusion restoration); and where the colour of the MZC did not fit the context of the patient's oral cavity, and the aesthetic integration was then unsatisfactory.

The secondary clinical variables were

2A. Survival of the restoration

An implant-supported restoration was called a 'survivor' when functioning properly until the final check-up [18]. It was defined as 'failed' if it went into failure (for example, failure of the implant, or fracture of the monolithic crown in translucent zirconia) during the whole post-delivery period [18].

2B. Success of the restoration

An implant-supported restoration was defined as 'successful' if it did not present any complication during the whole period after delivery [9, 19]. The restoration was considered 'unsuccessful' if, although not failed and still physically present in the mouth, it presented or had presented during the period of follow-up any biological complications (peri-implant mucositis with gingival swelling, discomfort, and/or bleeding [20]; and/or peri-implantitis with pain, suppuration, bleeding, and/or marginal bone resorption [21]); prosthetic (mechanical) complications [22, 23] (problems affecting pre-formed components sold by the manufacturer, such as the loss of connection between abutment and implant, or fracture of the fixture or bonding base); or technical complications [23, 24], (problems affecting the components designed by the dental technician, such as debonding of the upper portion of the zirconia abutment from the titanium base, fracture of the upper portion of the zirconia abutment, or decementation or chipping of the MZC [2, 10, 11]).

These variables were investigated during the twice-annual scheduled check-ups, during which the patients underwent professional oral hygiene sessions, by the two aforementioned clinicians (prosthodontist and periodontist).

Statistical analysis

The data related to the present study were collected in the patients' electronic medical records and used for statistical analysis. The statistical analysis was first descriptive, based on the demographic characteristics of the patients (age, gender, smoking habit and presence of bruxism) and the features of the restorations (location and position of the crowns, as well as type of bonding base used and implant diameter). Mean, standard

deviation (SD), median, range and 95% confidence interval (CI) were calculated for quantitative variables, such as patient age and mathematical quality of the protocol for the fabrication of the individual hybrid abutments; absolute and relative (%) distributions were calculated for qualitative variables such as gender, smoking habit and parafunction, as well as location and position of crowns, type of bonding base and implant diameter. The Chi-square test was used to assess homogeneity or inhomogeneity within the groups, with a level of significance set at 0.05. With regard to the primary clinical outcomes of the study, i.e. the variables investigated at the delivery of the final crowns (marginal adaptation and closure, quality of the interproximal contacts, quality of the occlusal contacts, aesthetic outcome), the mean scores ($\pm$SD) given by the different independent observers (prosthodontist and periodontist) were calculated, as well as the incidence of complications or issues found within the different groups, with absolute and relative distributions. For the secondary clinical outcomes, i.e. the variables investigated during the scheduled twice-annual check-ups, the incidence of failures and complications were respectively calculated, and the cumulative survival and success of the implant-supported restorations were calculated using the life-table analysis of Cutler and Ederer [25]. Survival and success of the crowns were calculated at the restoration level; in the context of the calculation of success, even a single complication was sufficient to allocate the restoration into the group of failures.

Results

Patient population and implant-supported crowns

Ninety patients (35 males and 55 females; aged between 22 and 79 years, with a mean age of 53.3 ± 13.7 years, median 54 years, CI 95% 50.5–56.1 years) who had been restored with 106 implant-supported MZCs were included in the study. Among the 90 patients included, 15 were smokers and 22 were bruxists. The restorations were positioned in both arches (66 maxilla, 40 mandible), in the posterior sectors of the mouth (35 premolars, 71 molars). All implants featured a locking-taper implant–abutment connection, presenting a screwless self-locking connection between the abutment and fixture, with angle 1.5°. The restored implants were of different diameters (3.3 mm: five fixtures; 4.1 mm: 45 fixtures; 4.8 mm: 56 fixtures). All 106 restorations were supported by individual hybrid abutments; the chosen bonding bases in titanium were 4-mm straight (23 Tibase®, Leone, Florence, Italy), 6-mm straight (43 Multitech® straight, Leone, Florence, Italy) and 6-mm angled 15° (40 Multitech® angled, Leone, Florence, Italy). The distributions of the patients and restorations are summarised in Table 1 and Table 2. The distribution of the

Table 1 Distribution of the patients by gender, age at enrollment, presence of smoking habit and bruxism

	N°	p*
Gender		
Males	35 (38.9%)	0.133
Females	55 (61.1%)	
Age		
< 35 years	8 (8.9%)	0.0003
35–55 years	42 (46.7%)	
> 55 years	40 (44.4%)	
Smoke		
Yes	15 (16.7%)	< 0.0001
No	75 (83.3%)	
Bruxism		
Yes	22 (24.4%)	0.0003
No	68 (75.6%)	
Overall	90	–

*Chi-square test

patients was homogeneous by gender ($p = 0.133$), but not homogeneous in terms of age ($p = 0.0003$), smoking habit ($p < 0.0001$) or bruxism (p = 0.0003): most were aged > 35 years, non-smokers and without parafunction. The distribution of the crowns was homogeneous by location ($p = 0.071$) and bonding base ($p = 0.162$), but not homogeneous in terms of position ($p = 0.012$) or supporting implant diameter ($p < 0.00001$): most were molars, and only a few 3.3-mm diameter implants were used.

Table 2 Distribution of the restorations by location, position, titanium bonding base, implant diameter and length

	N°	p*
Location		
Maxilla	66 (62.3%)	0.071
Mandible	40 (37.7%)	
Position		
Premolar	35 (33%)	0.012
Molar	71 (77%)	
Bonding base		
Tibase®	23 (21.7%)	0.162
Multitech® straight	43 (40.6%)	
Multitech® angled 15°	40 (37.7%)	
Diameter		
3.3 mm	5 (4.7%)	< 0.00001
4.1 mm	45 (42.5%)	
4.8 mm	56 (52.8%)	
Overall	106	–

*Chi-square test

Mathematical quality of the protocol

The evaluation of the quality of the protocol for the fabrication of individual hybrid abutments revealed a mean deviation of 44 μm (± 6.3; median 45; range 28–64; confidence interval 95% 42.9–45.1) between the original CAD design of the zirconia abutment, and the mesh of the zirconia abutment captured intraorally at the end of the provisionalization (Fig. 8).

Primary clinical outcomes

The mean (±SD) scores given by the two independent operators, related to the four primary outcomes (quality of the marginal closure and adaptation, quality of the interproximal contacts, quality of the occlusal contacts and aesthetic integration) are summarised in Table 3. The issues encountered at the delivery of the final crowns are summarised in Table 4.

Quality of the marginal closure

The marginal closure and adaptation of the final MZCs were checked clinically with visual inspection (under 4.5x magnification) and probing, as well as radiographically. The mean score (±SD) was the same for both the prosthodontist and the periodontologist, amounting to 4.41 (0.7). In almost all cases (102/106 crowns, 96.2%), the marginal adaptation was excellent, and the operators detected insufficient quality (score < 3) in only four cases. In these cases, the crowns were sent back to the technician for remodelling and milling. The incidence of complications therefore amounted to 1.8%.

Quality of interproximal contacts

The quality of the interproximal contacts was excellent in almost all cases, with a mean score (±SD) of 4.49 (0.7) and 4.43 (0.6) for the prosthodontist and the periodontologist, respectively. However, in two crowns (1.8%), the contact points were rather weak and loose, with a score < 3. To avoid food impaction, these crowns were sent back to the technician for remodelling and milling.

Quality of occlusal contacts

The quality of the occlusal contact points was rather good, with a mean score (±SD) of 3.84 (0.8) and 3.94 (0.9) for the prosthodontist and the periodontologist, respectively. However, in six cases of the 106 (5.6%), the occlusal adaptation of the final crowns was not acceptable because of the presence of precontacts (five cases) or the absence of occlusal contacts (infraocclusion, one case). In the cases of precontacts, two crowns were retouched by polishing the cusps before cementation, and were applied without issues; in three crowns, however, the occlusal precontacts were marked such that it was not possible to polish and apply them. These crowns were therefore sent back to the technician for remodelling and milling, exactly as in the case of the crown characterised by the absence of occlusal contact, where remaking was needed.

Aesthetic integration

From the chromatic perspective, the results were excellent, with a score of 4.25 (0.7) and 4.04 (0.6) for the prosthodontist and the periodontist, respectively. Overall, the chromatic and aesthetic integration of the
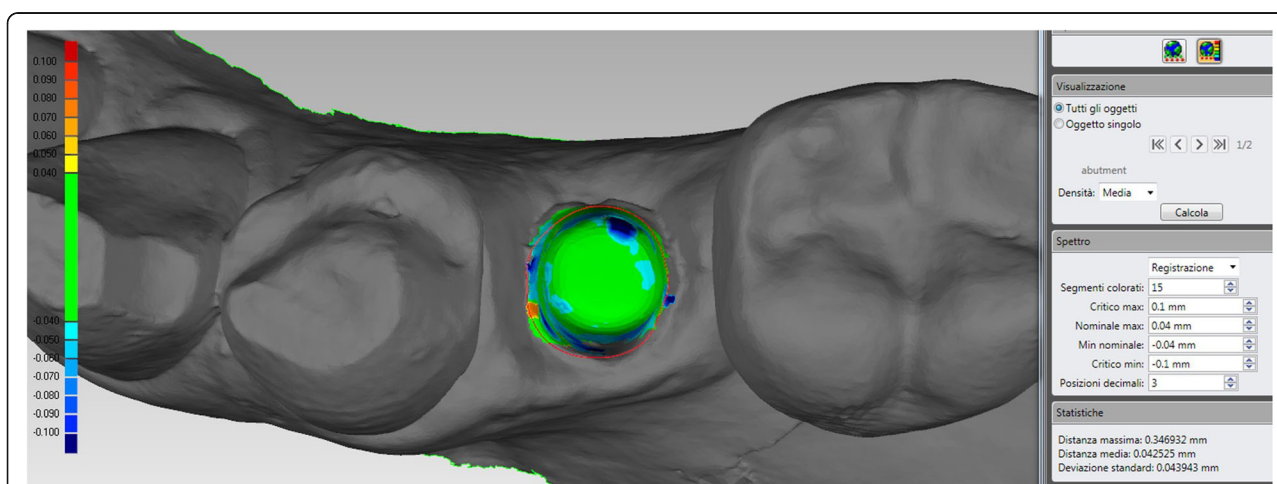

Fig. 8 For the present case, the quality in the fabrication of the individual hybrid abutment was good, with a mean deviation of 42 μm (±43) between the original CAD design and the mesh of the zirconia abutment captured intraorally. It must be noted that the presence of a little hole on the top of the actual abutment (very useful to facilitate the outflow of the cement in excess, during the extraoral cementation in the laboratory of the upper zirconia portion on the titanium base), depicted here in dark blue, may increase the mathematical error; however, this is clinically not relevant. The software used for this calculations was a powerful reverse engineering (Studio 2012, Geomagics, Morrisville, NC, USA) able to detect deviations up to 1 μm

Lerner *et al. BMC Oral Health*   (2020) 20:80

Page 11 of 16

Table 3 Means (±SD) for the primary outcomes (quality of the marginal adaptation/ closure, interproximal contact points, occlusal contacts and aesthetic integration) of the study, as assigned by two experienced operators, using a score from 1 to 5 (with 5 as the highest value, expression of a fully satisfactory quality; 4 for a satisfactory quality; 3 for a quality acceptable; 2 and 1 as the lowest values, expression of a restoration of unsatisfactory quality)

	Prosthodontist Mean score (±SD)	Periodontist Mean score (±SD)	Overall Mean score (±SD)
Quality of the marginal adaptation/ closure	4.41 (0.7)	4.41 (0.7)	4.41 (0.7)
Quality of interproximal contact points	4.49 (0.7)	4.43 (0.6)	4.46 (0.6)
Quality of occlusal contacts	3.84 (0.8)	3.94 (0.9)	3.89 (0.8)
Chromatic and aesthetic integration	4.25 (0.7)	4.04 (0.6)	4.15 (0.7)
Overall mean score (±SD)	4.25 (0.8)	4.20 (0.7)	4.23 (0.7)

monolithic translucent zirconia crowns was good, with only three restorations (2.8%) scoring < 3. In these cases, the crowns were not remade, but sent back to the technician for better characterisation.

Secondary clinical outcomes

The secondary outcomes of the study, i.e. the survival and success of the restoration, were evaluated during the scheduled twice-yearly follow-up sessions, by the same operators involved in the evaluation of the primary outcomes.

Survival of the restorations

During the first year after the delivery of the final restorations, only one implant-supported MZC (a maxillary molar) was lost. This failure occurred 2 months after the delivery of the final crown, and was caused by the loss of the supporting implant, which was extra short (6.5 mm) and inserted in a smoker and bruxist. The supporting implant showed marked and progressive bone loss, in the absence of any clinical signs of infection. No further implant failures were observed, and no fractures of the MZCs occurred. The cumulative survival rate of the implant-supported restorations 3 years after the delivery of the final MZCs was 99.0% (Fig. 9), as reported in the life-table analysis of Cutler and Ederer (Table 5).

Success of the restorations

After the delivery of the final MZCs, among the 105 surviving restorations, only a few biologic and prosthetic complications were reported. Two biologic complications

Table 4 Problems encountered at the delivery of the final monolithic translucent zirconia crowns, and rate of complications

Type of issue	Incidence	Complication rate
Marginal adaptation	2/106	1.8%
Interproximal adaptation	2/106	1.8%
Occlusal adaptation	6/106	5.6%
Chromatic integration	3/106	2.8%
Overall	10/106	9.4%

were reported, both peri-implant mucositis, for an overall incidence of 1.9%. Prosthetic complications were slightly more frequent, with six adverse events registered, for an incidence of 5.7%. Two prosthetic complications were mechanical in nature, with a loss of connection between the hybrid abutment and the fixture occurring in two crowns. These abutments were repositioned and reactivated, and no further issues were reported for these restorations; the complication was defined as minor in nature because it did not require any intervention from the technician. In two additional patients, unfortunately, the upper portions of the hybrid abutment (part in zirconia) decemented from the bonding bases. These complications were technical in nature and required a new extraoral cementation of the individual abutments on the titanium bases. These procedures were performed after careful cleaning and sandblasting of the bonding bases (with the aim to increase the adhesion) and required the intervention of the technician, so they were defined major in nature, also because the removal of the bonding bases from the fixtures was not easy for the dentist. Finally, two MZCs decemented from the hybrid abutments. In these cases, recementing them was sufficient. These last two complications were technical and minor in nature, as they did not require any intervention from the technician. The cumulative success rate of the implant-supported MZCs restorations 3 years after the delivery was 91.3%, as reported in the life-table analysis of Cutler and Ederer (Table 6).

Discussion

Less than a decade after breaking the Nazi encryption machine Enigma and helping the Allied Forces win World War II, mathematician Alan Turing changed history a second time, posing himself a simple question: 'Can machines think?' In 1950, with the paper titled 'Computing Machinery and Intelligence', Turing established the fundamental goal and vision of AI: to replicate or simulate human intelligence in machines [15, 26, 27]. Several years later, the first famous success of AI was that of Deep Blue, an IBM machine, that defeated the
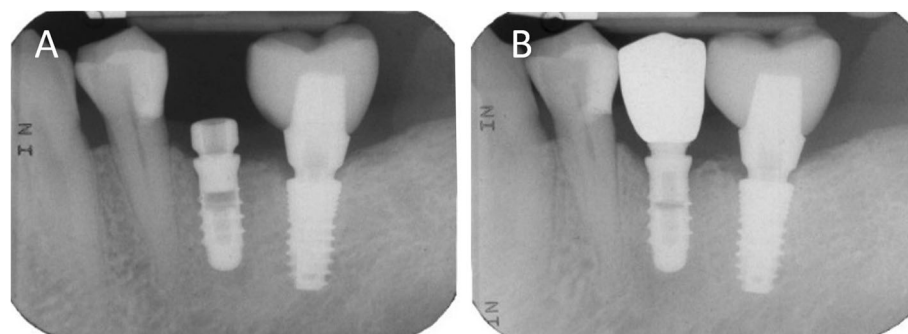
Fig. 9 Radiographic controls before and after the prosthetic restoration. (**A**) Endoral periapical radiograph taken at the beginning of the restorative process, before the first intraoral scan, with the healing abutment in position. (**B**) Three years later, the crown is in function and seated with high precision over the abutment, with little or no gap

reigning chess champion Garry Kasparov. Although the first meetings were won by Kasparov, the continuous improvements brought to the learning system of Deep Blue allowed the machine to achieve victory in successive games. The victory, as declared by Kasparov, was possible because "the machine has reached such a high level of creativity, that goes beyond the knowledge of the player". The foundation of AI is machine learning, a branch of computer science that builds algorithms to solve problems, guided by statistics and data [16, 17, 26, 27].

The concept of AI has evolved over time. From the fascinating but rather cinematographic idea of a "strong" AI in which super-intelligent robots (like the ones from *Westworld* or *Star Trek: The Next Generation*) overrun humanity, able to solve any problem, it has become something more "narrow" but concrete: basically, a way to construct algorithms that can learn from data and make predictions [26–28]. AI can today be defined as a branch of computer science that allows the programming and design of both hardware and software systems with certain characteristics that are typically considered human, such as visual, spatio-temporal and decision-making perceptions [26, 27]. "Narrow" or as it is sometimes called "weak" AI, therefore, is focused on performing single tasks extremely well, with several examples in daily life (from Google Search to Siri, Alexa and other personal assistants; and from IBM's Watson to self-driving cars) [17, 27].

In the medical field, AI uses algorithms and software applications to approximate human cognition in the analysis of complex data, approaching levels of human expertise, changing the role of computer-assisted diagnosis from a 'second-opinion' tool to a more collaborative one [28]. The development of AI applications is already remarkable, particularly in radiology and 3D imaging, as an aid to human clinicians in diagnostic and treatment planning, and recently AI has been integrated into image processing software and CAD, with promising results [29].

AI systems can also be extremely useful in dentistry, as their common feature is that they need data to be processed to build algorithms useful for determining actions [17, 18, 28, 29], and the dentist produces a large amount of digital data that can be extremely useful to take advantage of AI benefits [17].

In the dental world, in fact, a real revolution is in progress, determined by the advent of digital technologies [30]. Intraoral [6, 7, 14], desktop [31] and face scanners [8], cone beam computed tomography [32] and digital condylographs allow acquiring a huge amount of 3D data useful for patient virtualisation [8]. This easily accessible data [17] can be used by computers for many purposes, not only to perform different CAD modelling

Table 5 Cumulative survival rate of the implant-supported MZCs by means of the life-table analysis of Cutler and Ederer. An implant-supported MZC was defined "survivor" if still in function, at the end of the different time intervals

Time interval (months)	Implant-supported crowns at the start of the interval	Drop-outs during the interval	Implant-supported crowns at risk	Failures during the interval	Survival rate within the period (%)	Cumulative survival rate (%)
0–6	106	2	104	1	99.03%	99.03%
6–12	94	1	93	0	100%	99.03%
12–18	84	0	84	0	100%	99.03%
18–24	75	1	74	0	100%	99.03%
24–30	69	0	69	0	100%	99.03%
30–36	40	0	40	0	100%	99.03%

Table 6 Cumulative success rate of the implant-supported MZCs by means of the life-table analysis of Cutler and Ederer. An implant-supported MZC was defined as "successful" in the absence of any biologic and/or prosthetic complication, at the end of the different time intervals

Time interval (months)	Implant-supported crowns at the start of the interval	Drop-outs during the interval	Implant-supported crowns at risk	Failures during the interval	Survival rate within the period (%)	Cumulative survival rate (%)
0–6	106	2	104	5	95.2%	95.2%
6–12	94	1	93	1	98.9%	94.1%
12–18	84	0	84	0	100%	94.1%
18–24	75	1	74	1	98.6%	92.7%
24–30	69	0	69	1	98.5%	91.3%
30–36	40	0	40	0	100%	91.3%

(surgical [8, 33], prosthetic [2–5, 10, 30] and orthodontic [34]) that will then be produced physically for clinical use but also to instruct the same software so that it 'learns' certain mechanisms, and can therefore respond or act automatically, with an overall benefit for the workflow in terms of reducing processing times and costs [9].

In the field of implant prosthodontics, for example, the new digital workflows involve the use of intraoral scanners to capture the position of the implants through the scanbody, the digital version of the old implant transfer [6–9]. The accuracy of intraoral scanners is high today [6, 14], and these tools allow replacing the classic impression with trays and materials, with benefits for the patient and the entire prosthetic workflow [30]. Taking the impression is easier for the operator, involves less discomfort for the patient, and takes place in greater comfort and in a shorter time, with reproducible results [9, 14]. Communication with the laboratory is facilitated, and costs and time can be reduced. However, the introduction of digital technologies implies the need to adopt new protocols, and this is not always easy for the dentist and dental technician, especially when they are 'native analog'.

The optical impression is transferred, generally in. STL format (sometimes in proprietary format) to the laboratory, which replaces the scanbody mesh with the corresponding library file, coupled to the whole set of files of the different bonding bases available [9, 30]. The dental technician can therefore choose to model an individual zirconia abutment, which will be milled, sintered and extraorally cemented onto the chosen titanium bonding base. This approach is probably the best from a clinical viewpoint, because the individual zirconia abutment makes it possible to model the emergence profile in an ideal way, is highly aesthetic and pleases the mucosal tissues, with excellent biological integration [2–6, 9–11, 30, 35].

However, the full digital workflow that involves the use of individual abutments, even in the presence of mathematically perfect libraries, presents pitfalls. In particular, a very delicate moment is the cementation of the upper zirconia portion of the hybrid abutment on the titanium bonding base [9]. This cementing takes place outside the mouth, in the laboratory, and although the technician pays the utmost attention to it, it is possible and even probable that the tolerances between the components determine position errors, i.e. a minimum degree of rotation between the components, at least compared to the original CAD project. This situation leads to incomplete correspondence between the CAD project and the intraoral situation at the time of the clinical application of the hybrid abutment [9]. This may not be a problem at the time of insertion of the temporary restoration in PMMA, which can be adapted through small adjustments and polishing, but certainly is a greater problem when working with definitive zirconia restorations, which by definition cannot be retouched in the mouth once applied [2–6, 9–11, 30].

In the present retrospective clinical study, which represents the development of a previously published work [9], we have presented a clinical protocol that is able to solve these problems in a simple and very predictable way, and with lower costs. This protocol is based on a second intraoral scan, at the end of the provisional period, with the mucosal tissues suitably conditioned by the temporary restoration. The patient is recalled, the provisional is removed and an optical impression of the individual hybrid abutment in situ is captured, regardless of the margins of the preparation, which are generally subgingival. This mesh, loaded into the CAD software, is automatically recognised by the software AI and replaced by the original modelling file, stored in a special folder. The technician can therefore model the final crown directly on the original modelling file of the abutment (and not on a mesh, which by definition is a geometrical approximation of the object), which is transported to the correct spatial position, the actual position of the hybrid abutment in the mouth. Furthermore, the software can automatically trace the margin line, which is recognised by the AI. The technician can thus model the final restoration on an abutment with clear margins, with the margin line already traced by the computer, although subgingival, and perform modelling

on a library file (not on a mesh). This guarantees maximum clinical precision and the elimination of several risk factors (scanbody scanning errors, intrinsic library errors and cementation errors) in a context of simplification of procedures. In our present study, with 90 patients included, AI was a reliable tool for the restoration of 106 single locking-taper implants with MZCs cemented on customised hybrid abutments via a full digital workflow. In fact, the protocol for the fabrication of individual hybrid abutments revealed a high mathematical quality and reliability, with a mean deviation of 44 μm (± 6.3) between the original CAD design of the zirconia abutment, and the mesh of the zirconia abutment captured intraorally at the end of the provisionalization project. At the delivery of the final MZCs, the marginal adaptation, quality of the interproximal and occlusal contacts, and aesthetic integration were excellent, with satisfactory high scores. Moreover, the incidence of failures and complications was low, with three-year cumulative survival and success of 99.0 and 91.3%, respectively.

An alternative to our present AI protocol, run by the most experienced dental technicians, is today the 3D printing of physical models in which laboratory analogues are inserted, on which the individual abutments are screwed. The whole model plus the abutments are then scanned with a desktop scanner, and the technician models the final restorations on a mesh. Following this protocol, the technician transforms implant abutments into natural abutments, solving the issues related to the extraoral assembly or cementation of the individual zirconia portion on the titanium base. To do so, however, more steps are introduced, such as the need to print a model, with relative uncertainties [13, 36] and an increase in time and cost of the therapy. In fact, it is well known that 3D-printed models may present issues, if not printed with high-quality and accurate machines, and it is clear that the manual positioning of analogues inside them can cause positional errors (not only rotational but also in height) [36]. Furthermore, modelling on mesh is not ideal: it is certainly preferable to model on library files.

Our clinical protocol and AI may simplify the procedures, eliminating a series of steps, and it may therefore help to extend the use of individual hybrid abutments even in the posterior sites, for the replacement of premolars and molars. This can be important from a mechanical point of view, as it could help reduce prosthetic complications. In fact, the direct cementation of fixed superstructures (crowns, bridges) on titanium gluing bases is still not adequately documented in literature, and may lead to the onset of mechanical complications [2, 37]. The titanium gluing bases, in fact, are prefabricated and have standard height/ thickness, therefore may not withstand in the medium- and long term, the occlusal forces transmitted by monolithic structures

characterized by larger dimensions [2, 37]. In addition, with the present AI protocol, as previously reported [9] it is possible to mathematically evaluate and therefore to exactly quantify the degree of error, in the fabrication (milling/ sintering) of the individual zirconia abutment. In fact, using a reverse engineering software, it is possible to calculate the distance between the surface of the original CAD design of the zirconia abutment, and the mesh of the zirconia abutment captured intraorally at the end of the provisionalization project. This can give relevant information on the quality of the production process, and it may allow to identify issues; however, it must be noted that digital impressions themselves entail a certain degree of error [6], which could, in part, jeopardize this quality control.

It should be stressed that the present AI protocol seems to work particularly well with the Morse taper connection implants used in this study. These implants do not have a connecting screw between the bonding base and fixture, but the engagement is a locking taper, with an angle of approximately 1.5 ° between the parts [23, 24]. This 'cold fusion' allows, in addition to the mechanical and stability advantages of the connection that are well described in the scientific literature [23, 24], modelling integral abutments without any hole for a passing screw, which does not exist. This strengthens the abutment, but also facilitates the task of the AI system. Most implant systems on the market today have instead a screw for the assembly of the bonding base and therefore of the individual abutment on the implant; the presence of the screw hole can weaken the implant abutment [38], causing difficulties in modelling where the screw hole is angled. Moreover, it makes the correct extraoral cementation of the zirconia portion on the titanium bonding base more difficult, and could potentially make the task of the AI system of the CAD software more challenging. Having 'full' integral abutments, as for locking-taper connection implants, facilitates the task of the software and paves the way for the AI system [9, 30]: these abutments are drawn with a very small hole in the head, designed only to facilitate the correct outflow of the cement during cementation. This hole is much smaller than a screw hole. However, the removal of hybrid conometric abutments can be difficult once activated, and this may represent a limitation. Another limitation is the absence of long-term clinical data on the reliability of customised zirconia abutments, particularly in the posterior areas of the jaws [39]. Moreover, the present protocol assumes that the hybrid abutments, once milled, sintered and assembled, are not modified in the laboratory: otherwise, the AI of the software may encounter difficulties in coupling the modelling file with the mesh captured in the mouth. In addition, the AI application presented here has to be

Lerner *et al. BMC Oral Health*   (2020) 20:80

Page 15 of 16

considered "narrow" as the product of the application of specific algorithms and therefore "weak" in nature; this can be considered a further limitation of the present study. In fact, the only tasks performed automatically by the software are the recovery of the CAD file originally modeled by the dental technician, and the replacement of the mesh captured in the mouth with it. The automatic identification of the margins is itself to be considered a "narrow" application. It would be totally different if the software were able to automatically model the individual abutments, based on specific skills or knowledge acquired through deep learning: that would be an example of a "strong" AI application, but this is not yet possible. Finally, further studies with an adequate design (randomised clinical trials and/or prospective studies) are certainly necessary to confirm the results of our present work, and to validate this clinical protocol and the use of AI also with other implant systems, software and components. In fact, with different implant systems or connections, results may vary, and this should be adequately investigated.

Conclusions

In this retrospective clinical study, a full digital protocol employing AI allowed the successful restoration of single locking-taper implants with MZCs cemented on customised hybrid abutments. In fact, 90 patients restored with 106 implant-supported MZCs were included in the study. The quality of the fabrication of individual hybrid abutments was high, as it revealed a mean deviation of 44 μm (± 6.3) between the original CAD design of the zirconia abutment, and the mesh of the zirconia abutment captured intraorally at the end of the provisionalization. At the delivery of the MZCs, the marginal adaptation, quality of interproximal and occlusal contacts, and aesthetic integration were excellent. During the period of observation and the follow-up, few biologic (1.9%) and prosthetic (5.7%) complications affected the implant-supported MZCs, for a three-year cumulative survival and success of 99.0 and 91.3%, respectively. Further studies with a longer follow-up and with different prosthetic restorations (such as implant-supported fixed partial prostheses) are needed to confirm the validity of this protocol.

Abbreviations
3D: three-dimensional; AI: Artificial intelligence; CAD: Computer assisted design; CBCT: Cone beam computed tomography; CI: Confidence interval; ML: Machine learning; MZCs: Monolithic zirconia crowns; PMMA: Polymethylmethacrylate; SD: Standard deviation; STL: Stereolitographic

Authors' contributions
Conceptualization: HL, FM; Data curation: FM; Formal analysis: FM; Investigation: FM; Methodology: HL, FM; Project administration: HL; Resources: HL; Supervision: OA; Validation: OA; Visualization: JM, FM; Writing original draft: FM; Writing review & editing: FM, OA. All authors read and approved the final manuscript.

Availability of data and materials
The complete documentation of all patients enrolled in this study belong to the authors, and are available only upon reasonable request.

Ethics approval and consent to participate
The present study was approved by the Ethics Committee of the Sechenov First Moscow State Medical University. All patients had previously signed a generic informed consent to prosthetic implant treatment, and a condition for inclusion in this study, on the nature of which all patients were properly informed, was signing a further specific consent.

Consent for publication
Not applicable.

Competing interests
The authors declare that they have no competing interests in relation to the present study. Francesco Mangano is the editor of the Digital Dentistry section of BMC Oral Health.

Author details
[1]Private Practice, Ludwing-Wilhelm Strasse, 17 Baden-Baden, Germany. [2]Lecturer, Academic Teaching and Research Institution of Johann Wolfgang Goethe-University, Frankfurt am Main, Germany. [3]Casablanca Oral Rehabilitation Training & Education Center (CORTEC), Casablanca, Morocco. [4]Biomaterials Research Department, International University of Agadir (Universiapolis), Agadir, Morocco. [5]Department of Prevention and Communal Dentistry, Sechenov First Moscow State Medical University, 119992 Moscow, Russia. [6]Lecturer, Department of Prevention and Communal Dentistry, Sechenov First Moscow State Medical University, Moscow, Russia.

References
1. Schepke U, Meijer HJ, Kerdijk W, Raghoebar GM, Cune M. Stock Versus CAD/CAM Customized Zirconia Implant Abutments - Clinical and Patient-Based Outcomes in a Randomized Controlled Clinical Trial. Clin Implant Dent Relat Res. 2017;19(1):74–84.
2. Pitta J, Hicklin SP, Fehmer V, Boldt J, Gierthmuehlen PC, Sailer I. Mechanical stability of zirconia meso-abutments bonded to titanium bases restored with different monolithic all-ceramic crowns. Int J Oral Maxillofac Implants. 2019;34(5):1091–7.
3. Gehrke P, Bleuel K, Fischer C, Sader R. Influence of margin location and luting material on the amount of undetected cement excess on CAD/CAM implant abutments and cement-retained zirconia crowns: an in-vitro study. BMC Oral Health. 2019;19(1):111.
4. Amorfini L, Storelli S, Mosca D, Scanferla M, Romeo E. Comparison of Cemented vs Screw-Retained, Customized Computer-Aided Design/Computer-Assisted Manufacture Zirconia Abutments for Esthetically Located Single-Tooth Implants: A 10-Year Randomized Prospective Study. Int J Prosthodont. 2018;31(4):359–66.
5. Laass A, Sailer I, Hüsler J, Hämmerle CH, Thoma DS. Randomized Controlled Clinical Trial of All-Ceramic Single-Tooth Implant Reconstructions Using Modified Zirconia Abutments: Results at 5 Years After Loading. Int J Periodontics Restorative Dent. 2019;39(1):17–27.
6. Mangano FG, Hauschild U, Veronesi G, Imburgia M, Mangano C, Admakin O. Trueness and precision of 5 intraoral scanners in the impressions of single and multiple implants: a comparative in vitro study. BMC Oral Health. 2019; 19(1):101.

7. Albdour EA, Shaheen E, Vranckx M, Mangano FG, Politis C, Jacobs R. A novel in vivo method to evaluate trueness of digital impressions. BMC Oral Health. 2018;18(1):117.

8. Mangano F, Mangano C, Margiani B, Admakin O. Combining Intraoral and Face Scans for the Design and Fabrication of Computer-Assisted Design/ Computer-Assisted Manufacturing (CAD/CAM) Polyether-Ether-Ketone (PEEK) Implant-Supported Bars for Maxillary Overdentures. Scanning. 2019; 2019:4274715.

9. Mangano F, Margiani B, Admakin O. A Novel Full-Digital Protocol (SCAN-PLAN-MAKE-DONE®) for the Design and Fabrication of Implant-Supported Monolithic Translucent Zirconia Crowns Cemented on Customized Hybrid Abutments: A Retrospective Clinical Study on 25 Patients. Int J Environ Res Public Health, 2019. 16(3).

10. Schepke U, Gresnigt MMM, Browne WR, Abdolahzadeh S, Nijkamp J, Cune MS. Phase transformation and fracture load of stock and CAD/CAM-customized zirconia abutments after 1 year of clinical function. Clin Oral Implants Res. 2019;30(6):559–69.

11. Moris ICM, Chen YC, Faria ACL, Ribeiro RF, Fok AS, Rodrigues RCS. Fracture loads and failure modes of customized and non-customized zirconia abutments. Dent Mater. 2018;34(8):e197–204.

12. Oberoi G, Nitsch S, Edelmayer M, Janjić K, Müller AS, Agis H. 3D Printing-Encompassing the Facets of Dentistry. Front Bioeng Biotechnol. 2018;6:172.

13. Park ME, Shin SY. Three-dimensional comparative study on the accuracy and reproducibility of dental casts fabricated by 3D printers. J Prosthet Dent. 2018; 119 (5): 861.e1–861.e7.

14. Mangano F, Gandolfi A, Luongo G, Logozzo S. Intraoral scanners in dentistry: a review of the current literature. BMC Oral Health. 2017;17(1):149.

15. Kulkarni S, Seneviratne N, Baig MS, Khan AHA. Artificial Intelligence in Medicine: Where Are We Now? Acad Radiol. 2019. pii: S1076–6332(19)30458–30451. doi: https://doi.org/10.1016/j.acra.2019.10.001. [Epub ahead of print].

16. Park WJ, Park JB. History and application of artificial neural networks in dentistry. Eur J Dent. 2018;12(4):594–601.

17. Joda T, Waltimo T, Probst-Hensch N, Pauli-Magnus C, Zitzmann NU. Health Data in Dentistry: An Attempt to Master the Digital Challenge. Public Health Genomics. 2019;22(1–2):1–7.

18. Sailer I, Makarov NA, Thoma DS, Zwahlen M, Pjetursson BE. All-ceramic or metal-ceramic tooth-supported fixed dental prostheses (FDPs)? A systematic review of the survival and complication rates. Part I: Single crowns (SCs). Dent Mater. 2015;31(6):603–23.

19. Zembic A, Bösch A, Jung RE, Hämmerle CH, Sailer I. Five-year results of a randomized controlled clinical trial comparing zirconia and titanium abutments supporting single-implant crowns in canine and posterior regions. Clin Oral Implants Res. 2013;24(4):384–90.

20. Lee CT, Huang YW, Zhu L, Weltman R. Prevalences of peri-implantitis and peri-implant mucositis: systematic review and meta-analysis. J Dent. 2017;62:1–12.

21. Tallarico M, Canullo L, Wang HL, Cochran DL, Meloni SM. Classification Systems for Peri-implantitis: A Narrative Review with a Proposal of a New Evidence-Based Etiology Codification. Int J Oral Maxillofac Implants. 2018; 33(4):871–9.

22. Salvi GE, Brägger U. Mechanical and technical risks in implant therapy. Int J Oral Maxillofac Implants. 2009;24(Suppl):69–85.

23. Mangano F, Macchi A, Caprioglio A, Sammons RL, Piattelli A, Mangano C. Survival and complication rates of fixed restorations supported by locking-taper implants: a prospective study with 1 to 10 years of follow-up. J Prosthodont. 2014;23(6):434–44.

24. Mangano F, Lucchina AG, Brucoli M, Migliario M, Mortellaro C, Mangano C. Prosthetic Complications Affecting Single-Tooth Morse-Taper Connection Implants. J Craniofac Surg. 2018;29(8):2255–62.

25. Cutler SJ, Ederer F. Maximum utilization of the life table method in analyzing survival. J Chronic Dis. 1958;6:699–712.

26. Schwendicke F, Golla T, Dreher M, Krois J. Convolutional neural networks for dental image diagnostics: A scoping review. J Dent. 2019;5:103226. https://doi.org/10.1016/j.jdent.2019.103226 [Epub ahead of print].

27. Hwang JJ, Jung YH, Cho BH, Heo MS. An overview of deep learning in the field of dentistry. Imaging Sci Dent. 2019;49(1):1–7.

28. Ferro AS, Nicholson K, Koka S. Innovative Trends in Implant Dentistry Training and Education: A Narrative Review. J Clin Med. 2019;8(10).

29. Hung K, Montalvao C, Tanaka R, Kawai T, Bornstein MM. The use and performance of artificial intelligence applications in dental and maxillofacial radiology: A systematic review. Dentomaxillofac Radiol. 2019:20190107.

30. Mangano F, Veronesi G. Digital versus Analog Procedures for the Prosthetic Restoration of Single Implants: A Randomized Controlled Trial with 1 Year of Follow-Up. Biomed Res Int. 2018;2018:5325032.

31. Joós-Kovács G, Vecsei B, Körmendi S, Gyarmathy VA, Borbély J, Hermann P. Trueness of CAD/CAM digitization with a desktop scanner - an in vitro study. BMC Oral Health. 2019;19(1):280.

32. Dong T, Xia L, Cai C, Yuan L, Ye N, Fang B. Accuracy of in vitro mandibular volumetric measurements from CBCT of different voxel sizes with different segmentation threshold settings. BMC Oral Health. 2019;19(1):206.

33. Mouhyi J, Salama MA, Mangano FG, Mangano C, Margiani B, Admakin O. A novel guided surgery system with a sleeveless open frame structure: a retrospective clinical study on 38 partially edentulous patients with 1 year of follow-up. BMC Oral Health. 2019;19(1):253.

34. Elnagar MH, Aronovich S, Kusnoto B. Digital Workflow for Combined Orthodontics and Orthognathic Surgery. Oral Maxillofac Surg Clin North Am. 2020;32(1):1–14.

35. Chen YW, Moussi J, Drury JL, Wataha JC. Zirconia in biomedical applications. Expert Rev Med Devices. 2016;13(10):945–63.

36. Revilla-León M, Fogarty R, Barrington JJ, Zandinejad A, Özcan M. Influence of scan body design and digital implant analogs on implant replica position in additively manufactured casts. J Prosthet Dent. 2019. pii: S0022–3913(19)30487–30481. doi: https://doi.org/10.1016/j.prosdent.2019.07.011. [Epub ahead of print].

37. Kraus RD, Epprecht A, Hämmerle CHF, Sailer I, Thoma DS. Cemented vs screw-retained zirconia-based single implant reconstructions: A 3-year prospective randomized controlled clinical trial. Clin Implant Dent Relat Res. 2019;21(4):578–85.

38. Thulasidas S, Givan DA, Lemons JE, O'Neal SJ, Ramp LC, Liu PR. Influence of implant angulation on the fracture resistance of zirconia abutments. J Prosthodont. 2015;24(2):127–35.

39. Vechiato-Filho AJ, Pesqueira AA, De Souza GM, dos Santos DM, Pellizzer EP, Goiato MC. Are Zirconia Implant Abutments Safe and Predictable in Posterior Regions? A Systematic Review and Meta-Analysis. Int J Prosthodont. 2016;29(3):233–44.

Publisher's Note

BMC Oral Health

Complete-arch fixed reconstruction by means of guided surgery and immediate loading: a retrospective clinical study on 12 patients with 1 year of follow-up

Henriette Lerner[1,2*†], Uli Hauschild[3,4†], Robert Sader[2] and Shahram Ghanaati[5,6]

Abstract

Background: Guided implant surgery is considered as a safe and minimally invasive flapless procedure. However, flapless guided surgery, implant placement in post-extraction sockets and immediate loading of complete-arch fixed reconstructions without artificial gum are still not throughly evaluated. The aim of the present retrospective clinical study was to document the survival and success of complete-arch fixed reconstructions without artificial gum, obtained by means of guided surgery and immediate loading of implants placed also in fresh extraction sockets.

Methods: A total of 12 patients (5 males and 7 females, with a mean age of 50.0 ± 13.8) were enrolled in this study. Implant planning was performed with a guided surgery system (RealGuide®, 3Diemme, Como, Italy), from which 3D-printed surgical templates were fabricated. All implants (Esthetic Line-EL®, C-Tech, Bologna, Italy) were placed through the guides and immediately loaded by means of a temporary fixed full-arch restoration without any artificial gum; the outcome measures were implant stability at placement, implant survival, complications, prosthetic success, soft-tissue stability, and patient satisfaction.

Results: One hundred ten implants (65 of them post-extractive) were placed flapless through a guided surgery procedure and then immediately loaded by means of provisional fixed full arches. Successful implant stability at placement was achieved in all cases. After a provisionalization period of 6 months, 72 fixed prosthetic restorations were delivered. Only 2 implants failed to osseointegrate and had to be removed, in one patient, giving a 1-year implant survival rate of 98.2% (108/110 surviving implants); 8/12 prostheses did not undergo any failure or complication during the entire follow-up period. At the 1-year follow-up control, soft-tissue was stable in all patients and showed satesfactory aesthetic results.

Conclusions: Within the limits of this study, complete-arch fixed reconstruction by means of guided surgery and immediate loading of implants placed in fresh extraction sockets appears to be a reliable and successful procedure. Further long-term prospective studies on a larger sample of patients are needed to confirm these positive outcomes.

Keywords: Guided implant surgery, Flapless, Immediate implant placement, Immediate loading, Complete-arch reconstructions, Survival, Success

* Correspondence: h.lerner@web.de
†Henriette Lerner and Uli Hauschild contributed equally to this work.
[1]Baden-Baden, Germany
[2]Department of Oral, Cranio-Maxillofacial and Facial Plastic Surgery, Johann Wolfgang Goethe-University, Frankfurt am Main, Germany
Full list of author information is available at the end of the article

Background

The immediate functional loading of implant-supported, fixed full-arch prostheses can today represent a predictable solution for the rehabilitation of edentulous patients [1–3], even in the case of implant placement in fresh post-extraction sockets [4].

Such procedures as immediate prosthetic loading and immediate placement of implants in fresh extraction sockets are highly appreciated by patients, because they reduce the invasiveness and the number of surgical and prosthetic sessions, as well as the length of time needed for treatment [5, 6].

However, the immediate placement of implants in post-extraction sockets and their immediate functionalization in a complete-arch reconstruction represent a serious challenge for clinicians [2, 4, 6]. Surgically, in fact, clinicians must be able to mentally visualize the future prosthetic rehabilitation and, consequently, the ideal position and axis of implant insertion; in a rather large field such as that of the edentulous maxilla or mandible, this can be particularly complex [2, 4, 6]. Furthermore, it may be difficult to obtain adequate primary stability when placing implants in post-extraction sockets [2, 4, 6, 7]. These mental and clinical difficulties may result in a non-optimal placement of the implants [4, 6].

This non-optimal positioning, even if it does not lead to the violation of anatomical risk structures (such as the inferior alveolar nerve and the maxillary sinus), can have serious aesthetic consequences, and may force the prosthodontist to seek compromise rehabilitative solutions that might not be appreciated by the patient [3–8]. In fact, it is known from the literature how the aesthetics, survival, and long-term success of implant-supported restorations depend not solely on the volume of bone and mucosal tissues available, but also on other parameters, including the implant insertion axis [9–12].

Modern digital technologies [13], in particular guided implant surgery [14–16], now offer a solution to these problems.

Conceived in the mid-nineties, guided implant surgery has rapidly grown in popularity, and is now widely used all over the world [14–16]. The introduction of cone-beam computed tomography (CBCT) allowed the acquisition of the three-dimensional (3D) bone volumes of the jaws in a simple way and with a considerable reduction in the dose of radiation absorbed by the patient, compared to that of conventional computerized tomography [17, 18].

The information on the patient's bone anatomy, captured by CBCT, may be imported as digital imaging and communication in medicine (DICOM) files into specific software for implant surgery planning and combined with the wax-up of the ideal prosthetic restoration [14–18]. In this software, the surgeon can plan the implant insertion, based on the anatomy of the residual bone and the ideal prosthetic

project. According to the planning, a surgical guide is drawn, produced with additive techniques, and used during the implantation for the guided placement of the fixtures [14–19].

In 2002, the concept of guided implant planning linked to immediate functional loading was first introduced in Leuven, Belgium. The first treatments were limited to the edentulous jaws and required full-thickness flaps, as the surgical templates were bone-supported [14–19]. Subsequently, planning procedures have been optimized, opening the way for new types of increasingly precise surgical templates, with mucosal and dental support, to be used in both arches, in partially and completely edentulous subjects [14–19]. The possibility of a flapless approach has further increased the benefits of guided surgery, as this approach reduces the invasiveness and timing of surgical treatment, simplifying the procedure for the clinician and reducing discomfort and morbidity for the patient [20, 21].

However, in most clinical studies in the literature, full-arch restorations are represented by Toronto Bridges, also known as "all-on-four" and "all-on-six" dentures, i.e., hybrid fixed prostheses characterized by the presence of a bar connecting the implants and, more importantly, artificial gum (either in porcelain or in resin, depending by the restorative treatment chosen) [22–25]. There is no doubt that even in this context, guided implant surgery offers advantages, such as more precise implant placement, especially with respect to the screw holes, and the availability to pre-fabricate a milled provisional for same- (or next-) day delivery [14–16, 20, 22–25]. However, these types of implant-supported dentures, although easier to manage for clinicians, cannot represent the maximum of aesthetics, precisely because of the presence of the artificial gum [26, 27]. Moreover, the correct maintenance of daily oral hygiene can be much more difficult for the patient with such types of prosthetic rehabilitation [26, 27].

Today there are few scientific works on complete-arch fixed reconstruction without artificial gum, by means of guided surgery with flapless placement of implants also in post-extraction sockets, and immediate functional loading [28–31].

The aim of the present study is therefore to present the outcome of guided surgery, flapless implant placement, and immediate functional loading of complete-arch fixed prostheses without artificial gum. In particular, we aim to demonstrate how a correct planning of the 3D positioning of the implants allows to obtain complete-arch fixed rehabilitations with highly predictable aesthetics.

Methods

Patient selection

A retrospective evaluation was conducted on the customized records of patients that were treated with guided implant surgery during the period from January 2014 to December 2017, in a private dental clinic in Baden-Baden, Germany (Henriette Lerner Dental Clinic).

Patients were included according to the following criteria.

Inclusion criteria:

– Adult and able to provide informed consent;
– Patients in need to tooth extraction and immediate implantation;
– Patients that recieved flapless guided surgery and complete-arch fixed prostheses without artificial gum;
– Patients, that were followed up for at least 1 year.

Exclusion criteria:

– Patients with any other prosthetic rehabilitation than complete-arch fixed prostheses without artificial gum.

The analyzed records included patient-related information (gender, age at surgery, systemic health, smoking habit) details about the inserted implants (type, position, length, and diameter) and the prosthetic rehabilitation (single crown, fixed partial prosthesis, fixed full arch) including the dates of delivery. In addition, the analyzed data included all information about any implant failure or complication that occurred during the intervention, after the surgery, and at each follow-up visit. According to the inclusion and exclusion criteria, only patients treated with guided implant surgery and immediate loading by means of complete-arch fixed reconstruction without artificial gum were considered eligible and thus enrolled in the study. A necessary condition for enrollment in the present study was also the patient's willingness to present him/herself at a final control visit. All other patients (i.e., patients treated with dental implants to restore partially or totally edentulous jaws, without the aid of guided surgery; or patients treated with guided implant surgery but restored with fixed full-arch maxillary prostheses with artificial gum) were excluded from this study. The principles highlighted in the Helsinki Declaration on experimentation on human subjects were strictly followed. This retrospective study received ethical approval from the Institutional Review Board of the Goethe University of Frankfurt, Germany (number: 182/19). All patients were fully informed on the nature of this retrospective study, read and signed a written consent form for inclusion, and for the analysis of their records, that was approved by the University. In addition, the authors obtained written consent for publication from the patients enrolled in this retrospective study.

Data acquisition

A complete clinical, photographic, and radiographic dataset was acquired for each patient. In particular, photographs of the initial situation were taken (Fig. 1a, b, c, d, e) accompanied by two-dimensional (panoramic) radiographs (Fig. 1f),

periodontal probing and three-dimensional radiographs (CBCT of both arches). General impressions were taken, and stone casts were obtained for the study of the case (Fig. 1g, h). Starting from the photographic data, a digital smile-design software was used for a first evaluation of the length and width of the teeth. The information taken from this analysis was used for the preparation of a diagnostic wax-up on the stone cast models (Fig. 2a, b, c). Finally, the initial situation, the diagnostic wax-up (and therefore the ideal morphology of the teeth) and the situation after virtual extractions were then scanned with a desktop scanner (Deluxe®, Open Technologies srl, Brescia, Italy), in order to have all the. STL files available for upload in the guided surgery software (Fig. 2d).

Digital implant planning and laboratory workflow

In a guided surgery software, the. STL files with the ideal teeth morphology, derived from the scan of the diagnostic wax-up, were imported and superimposed on the bone anatomy, obtained from the CBCT. Then, the surgeon (H.L.) and the dental technician (U.H.) were able to plan the placement of the implants in the correct position, depth, and inclination, guided by the prosthetic wax-up, in a prosthetically-driven manner (Fig. 3a, b, c, d). Care was taken to try to engage the fixtures as much as possible in the residual bone, exceeding the apex of fresh extraction sockets at least 3–4 mm, by choosing appropriate implant length. At the same time, care was taken to position the implants in the palatal portion of the sockets, ideally at a distance of 2–3 mm from the residual buccal bone walls, and at a proper inclination. Ideally the axis of the implants had to be in the center of the teeth, to achive a perfect prosthetic plan. The same procedure was repeated in both maxilla and mandible. After the planning was successfully completed and carefully controlled, the models of the situation were 3D printed in the laboratory with a desktop printer and the implant analogues were inserted in these models (Fig. 4a, b). These models not only included the correct position of the planned implants, but also the mucosa and the residual teeth, which had not been removed in the planning, in order to facilitate the superimposition in the guided surgery software and to stabilize the surgical guide during the intervention (these hopeless teeth had to be removed at the end of the intervention). Based on the virtual planning, surgical guides were then printed, and the sleeves were manually inserted in (Fig. 4c, d). In the lower jaw, since the sleeves of the central incisors touched each other, two different guides were 3D printed. Finally, before surgery, provisional full-arch restorations were prepared for immediate loading and aesthetics. A burn-out framework based on the prosthetic project and virtual implant position was milled (Fig. 5a, b). This led to a metal structure on which resin composite (Nexco®, Ivoclar Vivadent, Schaan, Liechtestein) was manually stratified, in order to obtain a
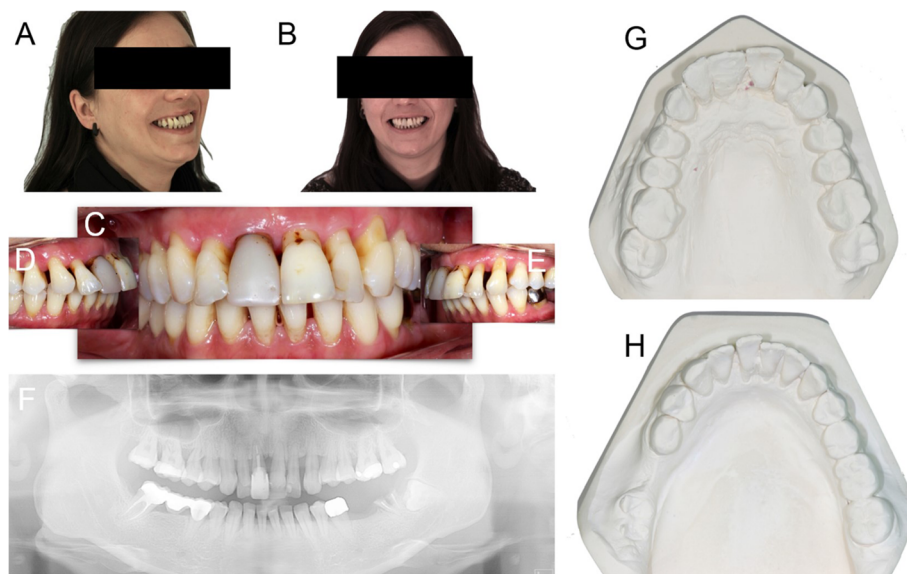
Fig. 1 Pre-operative initial situation. Lateral (**a**) and frontal (**b**) view of a 32-year-old female patient, in good systemic health, presented with an advanced chronic periodontitis, teeth mobility and recurrent infections, persisting over years. In the upper jaw, in particular, all teeth were sensitive and elongated and this seriously compromised the function and the aesthetic of the smile. The patient suffered from this situation and she was strongly motivated to solve this biological, functional and aesthetic problem. **c** Frontal and (**d**, **e**) lateral intraoral pictures. **f** Panoramic radiograph. In the maxilla, the severe chronic periodontitis determined an advanced bone loss, that compromised the stability of all teeth. **g** Upper and (**h**) lower jaw precision models
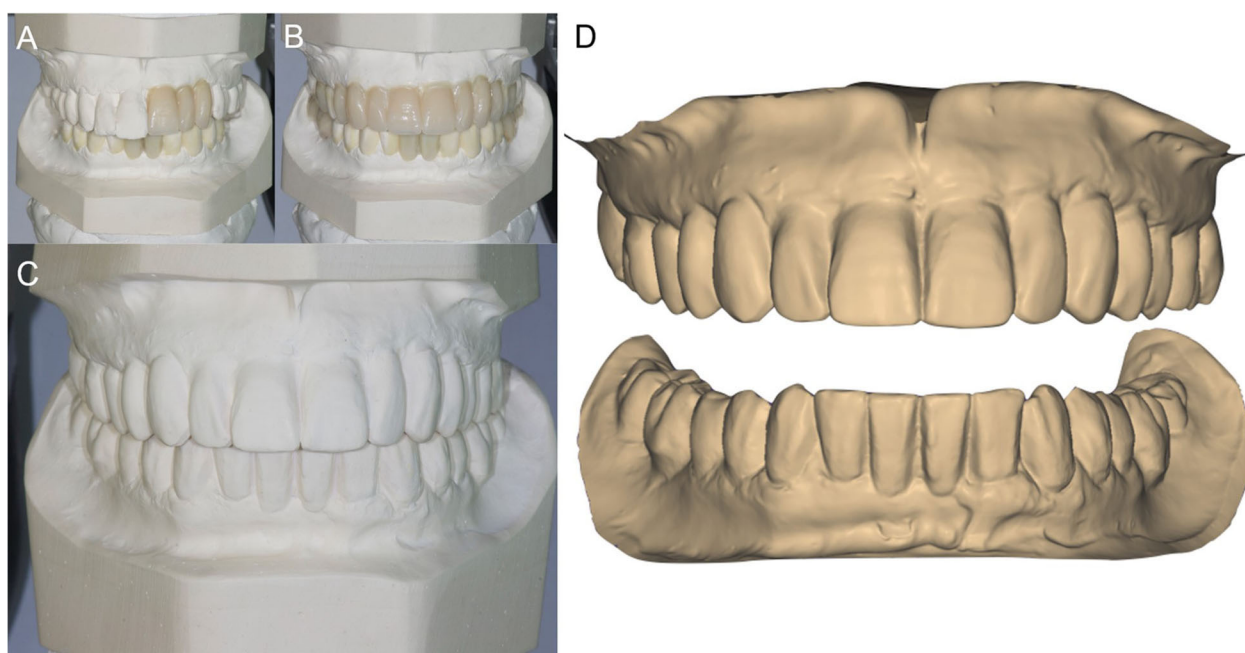

Fig. 2 Digital smile design and diagnostic wax-up. **a** Starting from the photographic data, a digital smile design software was used for a first evaluation of the length and width of the teeth. The smile design indicated the need to increase the length and the width of the patient's teeth, particularly in the anterior maxilla. There was a need to modify the teeth shape as well. **b** The information taken from the smile design was then used for the preparation of a diagnostic wax-up. **c** The models were mounted in articulator and the indications of the smile design were manually replicated in the wax-up. **d** The initial situation, the wax-up and the situation after extractions were then scanned with a desktop scanner (Deluxe®, Open Technologies srl, Brescia, Italy), in order to have all the. STL files available for upload in the guided surgery software
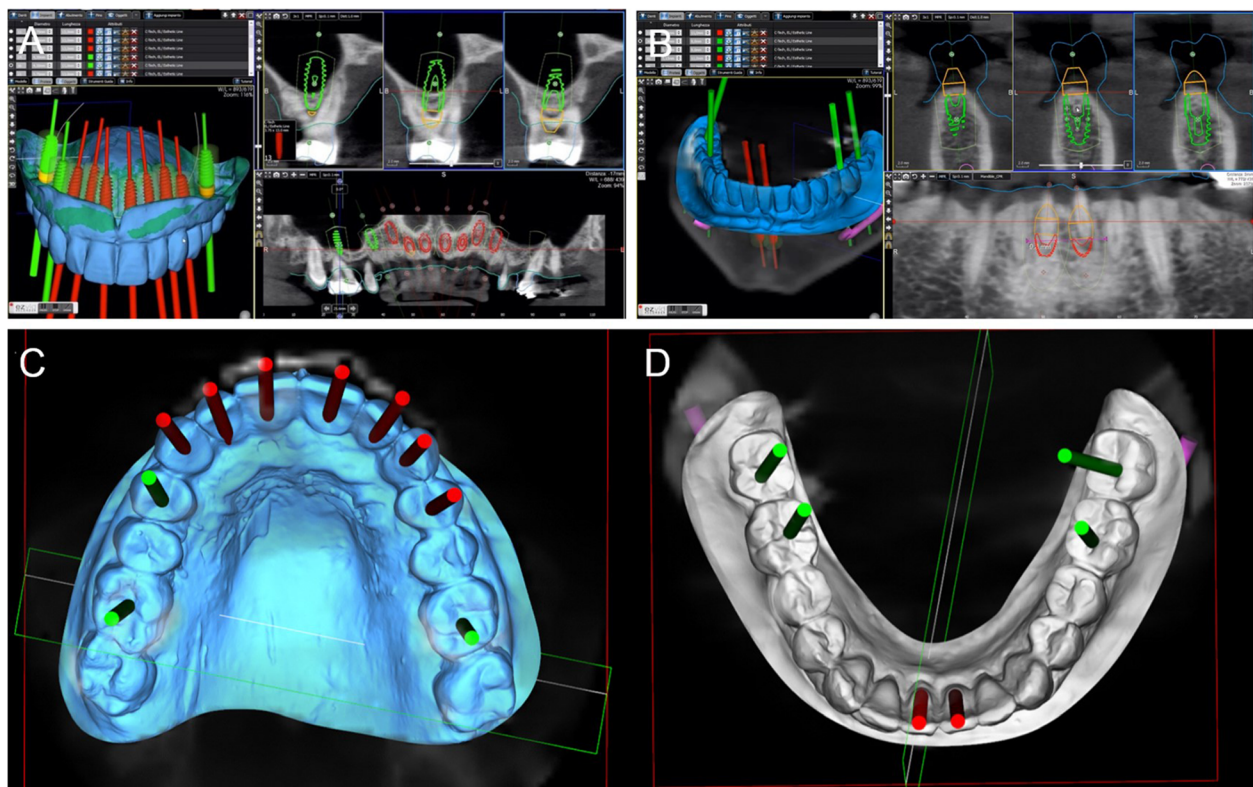
Fig. 3 Prosthetically driven 3D implant planning. **a** In a guided surgery software (RealGuide®, 3Diemme, Como, Italy) the. STL file with the ideal teeth morphology (model of the maxilla with included wax-up) was imported and superimposed on the bone anatomy, obtained from the CBCT. Ten immediate post-extraction implants (#16, #14, #13, #12, #11, #21, #22, #23, #24, #26) were planned in the cross sections of the CBCT (placement of #16 and #26 required maxillary sinus augmentation). The implant position, inclination and depth were carefully planned, trying to engage the fixtures as much as possible into the bone, to increase primary implant stability in the fresh extraction sockets, and taking into account the emergence profile and the overlying future prosthesis, so that implants were placed in a prosthetically driven matter. The final prosthetic plan foresaw rehabilitation with single crowns in the frontal area (from #14 to #24) and rehabilitation with partial fixed prosthesis for the posterior sectors (from #15 to #17, and from #25 to #27, respectively). **b** A similar procedure was performed in the mandible, with the superimposition of the. STL file with the ideal teeth morphology on the bone, and therefore the implant planning. Six implants were originally planned (#47, #46, #41, #31, #35, #37) in the cross sections of the CBCT. Once again, the implant position, inclination and depth were carefully planned, trying to engage the fixtures as much as possible into the bone, to increase primary implant stability, and taking into account the emergence profile and the overlying future prosthesis, so that implants were placed in a prosthetically driven position. **c**, **d** Visualization of the implant emergence profiles in relation to the ideal position of the teeth and the prosthetic plan, in the maxilla and mandible. The prosthetic axes of the posterior implants emerged in the masticatory center of each tooth, in the anterior individual zirconia abutments cemented on titanium bases were chosen. On the upper jaw ten implants were planned, on the lower jaw six

highly aesthetic temporary full-arch prosthesis for immediate loading (Fig. 5c). This prosthesis had to be seated on temporary abutments immediately after implant placement.

Implant type

The implants used in this study (Esthetic Line-EL®, C-Tech, Bologna, Italy) were conical, with a Morse-taper hexed connection and an acid-etched surface. In details, these implants incorporate three different threading profiles, designed to adapt to the different bone structures that occurr along the depth of the fixture. In the coronal portion, in fact, microgrooving is present, whereas in the intermediate portion, the fixtures present a double lead thread, to facilitate insertion and to increase primary

stability, particularly in soft bone. In the apical portion, these implants are endowed with aggressive apical threading which is particularly indicated to stabilize the fixture in post-extraction sockets, in the case of immediate placement after extraction; however, a rounded apex protects such anatomical structures as the maxillary sinus membrane and inferior alveolar nerve. Further characteristics of these implants are a beveled shoulder, to facilitate bone growth in the case of subcrestal placement in post-extraction sockets; a Morse-taper hexed connection, to reduce screw loosening and micromovements of the abutment; and a concave aesthetic concept with platform switching, for better soft-tissue healing. The presence of one connection for all implant diameters
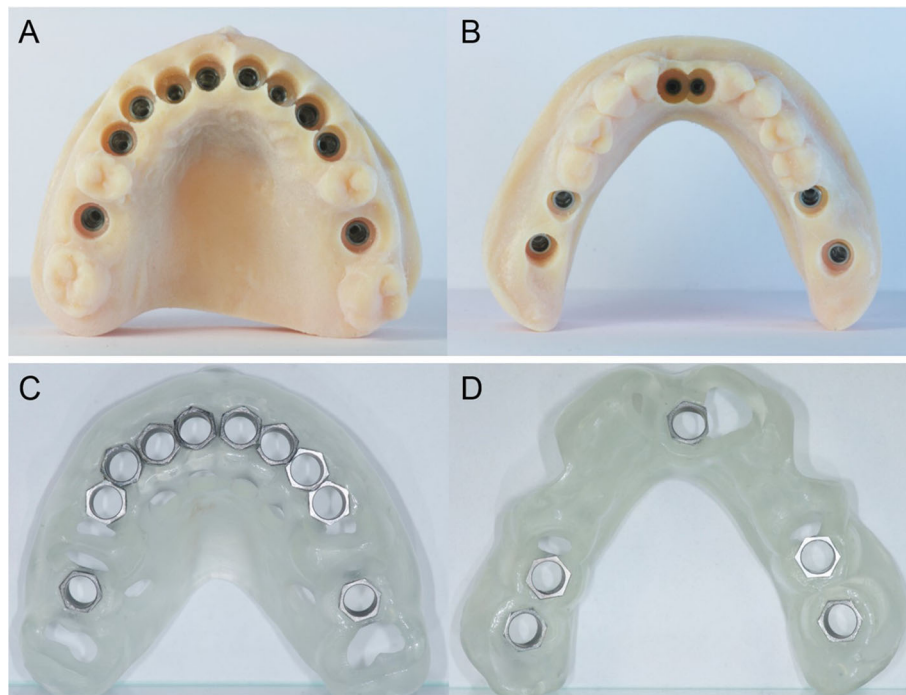
Fig. 4 3D printing of the models and the surgical guides. **a**, **b** The models were printed in the laboratory with a 3D printer (Form2®, Formlabs Inc., Somerville, MA, USA) and the implant analogues were positioned. These models not only included the correct position of the planned implants, but also the mucosa and the residual teeth, that have not been removed in the planning, in order to facilitate the superimposition in the guided surgery software, and to stabilize the surgical guide during the intervention. The compromised teeth had to be subsequently removed during surgery. **c**, **d** 3D printing of the models and the surgical guides. Based on the virtual planning, surgical guides were printed too. The sleeves were then inserted in the guides. In the lower jaw, since the sleeves of the incisors touched each other, two different guides were 3D printed

facilitates the prosthetic treatment, by offering a large range of tissue-shaping possibilities. The fixtures used in this study were available in different lengths (8,9,10,11,12, 13, and 14 mm) and diameters (3.8, 4.3, 5.1, 6, and 7 mm).

Surgical and prosthetic treatment

After this, flapless surgery could start with the atraumatic extraction of all hopeless teeth (with the exception of the ones used to stabilize the guide; those teeth had to be removed after the removal of the guide). During extraction, care was taken not to damage the alveoli and particularly the delicate maxillary buccal bone wall (Fig. 6a, b). After the digital planning, the surgical template was positioned, the fit was carefully checked (Fig. 6c), and the guided surgery started with the preparation of all implant sites, using drills of incremental diameter, and ended with the placement of all planned implants, through the guide (Fig. 6d, e). After implant placement, the surgeon could verify the positioning as well as the soft-tissue status and proceed with simultaneos minor/major grafting procedures, where needed. The need for grafting procedures obviously forced the clinician to raise a full-thickness flap, but this procedure was limited exclusively to the area or areas that required bone augmentation; in all other cases and in all other areas, a flapless

surgery was carried out. After the surgery was completed, the temporary fixed full-arch provisional in resin with metal framework was carefully adapted and relined on temporary abutments, removed, accurately polished, and then delivered to the patient (Fig. 7a). This fixed full-arch temporary was cemented and a panoramic radiograph was taken (Fig. 7b). Six months after surgery, when the period of provisionalization ended, the clinician recalled the patient and took two different impressions: (i) generic alginate impressions with the provisional prostheses in position; and (ii) precision impression with polyether open tray over multi-unit intermediary abutments, to avoid damaging the peri-implant structures (Fig. 8a, b). These two impressions were sent to the dental laboratory, where plaster casts were poured and scanned with the same aforementioned desktop scanner. These models were then overlapped in a computer-assisted-design (CAD) software, in order to have a guide for modeling the final restorations and performing aesthetic modifications (Fig. 9a). All these modifications, however, were done manually, on 3D-printed models (Fig. 9b, c). Then the final shapes were scanned again. At this point, the dental technician could proceed to design, in a CAD software (Exocad®, Darmstadt, Germany), the final individual, customized abutments (which had to be cemented extraorally on
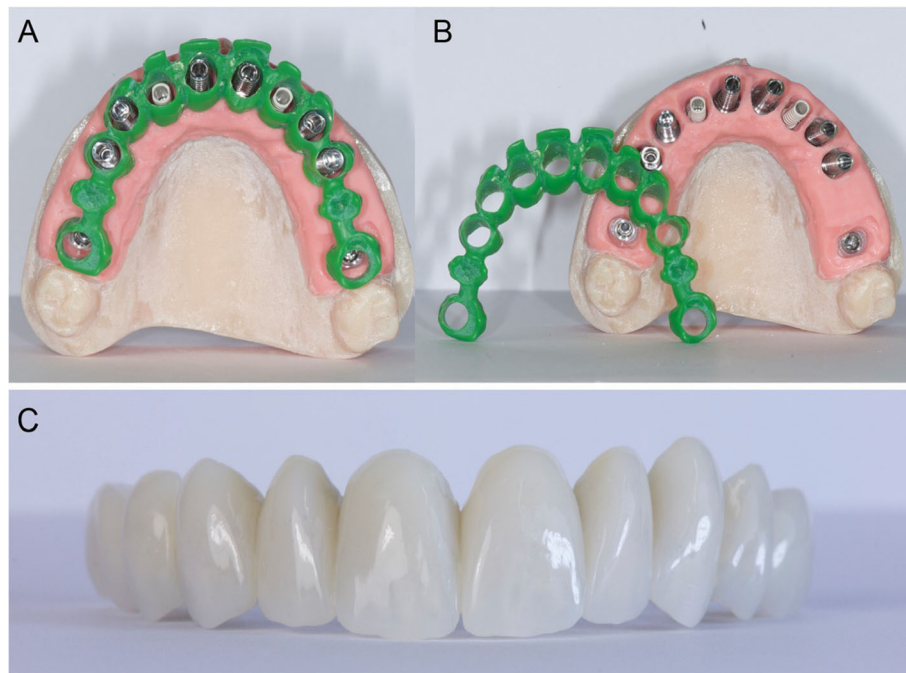
Fig. 5 Preparation of the temporary fixed full arch for immediate loading. **a**, **b** After CAD design, a burn-out framework based on the prosthetic project and virtual implant position was milled. **c** This led to a metal structure on which resin composite was manually stratified, in order to obtain a highly aesthetic temporary full-arch prosthesis for immediate loading

selected titanium bases) and the final restorations (Fig. 10a, b, c). Both the individual, customized abutments and the final restorations were full-ceramic and milled in zirconia with a powerful milling machine (M1 WET Heavy Metal®, Zirkonzhan, Bolzano, Italy), in order to improve the aesthetic outcome. The restorations had to be single crowns (in the frontal area, for a better biological response, with physiological auto-detersion, and to allow for excellent oral hygiene maneuvers, such as the passage of dental floss) and fixed partial prostheses (in the posterior areas, to improve the functional response). At the delivery of the final restorations, the customized abutments were screwed in the correct position: the margins were positioned subgingivally, in accordance with the original surgical and prosthetic plan (Fig. 10d) and all restorations were placed. The marginal adaptation was checked clinically using magnifying glasses (Zeiss 4.5x®, Zeiss, Oberkochen, Germany) and the occlusion was carefully evaluated using articulating papers (Bausch Articulating Paper®, Bausch Inc., Nashua, NH, USA) as well as digital devices (Tekscan®, Boston, MA, USA) prior to cementation. Clinical pictures (Fig. 11a, b) and a panoramic radiograph (Fig. 11c) were taken, along with a digital analysis of the occlusion (Fig. 11d).

Outcome measures
The outcome measures for the present study were implant stability at placement, implant survival, complications, prosthetic success, marginal bone remodeling, soft-tissue stability, and patient satisfaction.

Implant stability at placement
Implant stability was measured at placement. Insertion torque (IT) and resonance frequence analysis (RFA) were used as methods for measuring implant stability, as previously described [32, 33]. IT was measured before the removal of the surgical guide. Since all implants were placed using the implant motor, a standard IT of 50 Ncm was set at placement. If the machine-driven insertion was discontinued because of high IT (> 50 Ncm), the implant insertion was completed manually, through the guide, with a dedicated wrench. Conversely, if the final IT was < 45 Ncm, the full procedure was guided by the implant motor. The IT was considered poor when < 35 Ncm. Finally, RFA was used to confirm the stability of each implant, immediately after implant placement, after the removal of the guide. For each implant, the average value from 4 different measurements (buccal, palatal, mesial, and distal) was obtained. The stability of the fixture was considered acceptable with an implant stability quotient (iSQ) ranging from 55 to 85, low with an iSQ < 55. Regardless of the stability value that emerged, all implants were subjected to immediate functional loading, splinted through a temporary full-arch restoration.
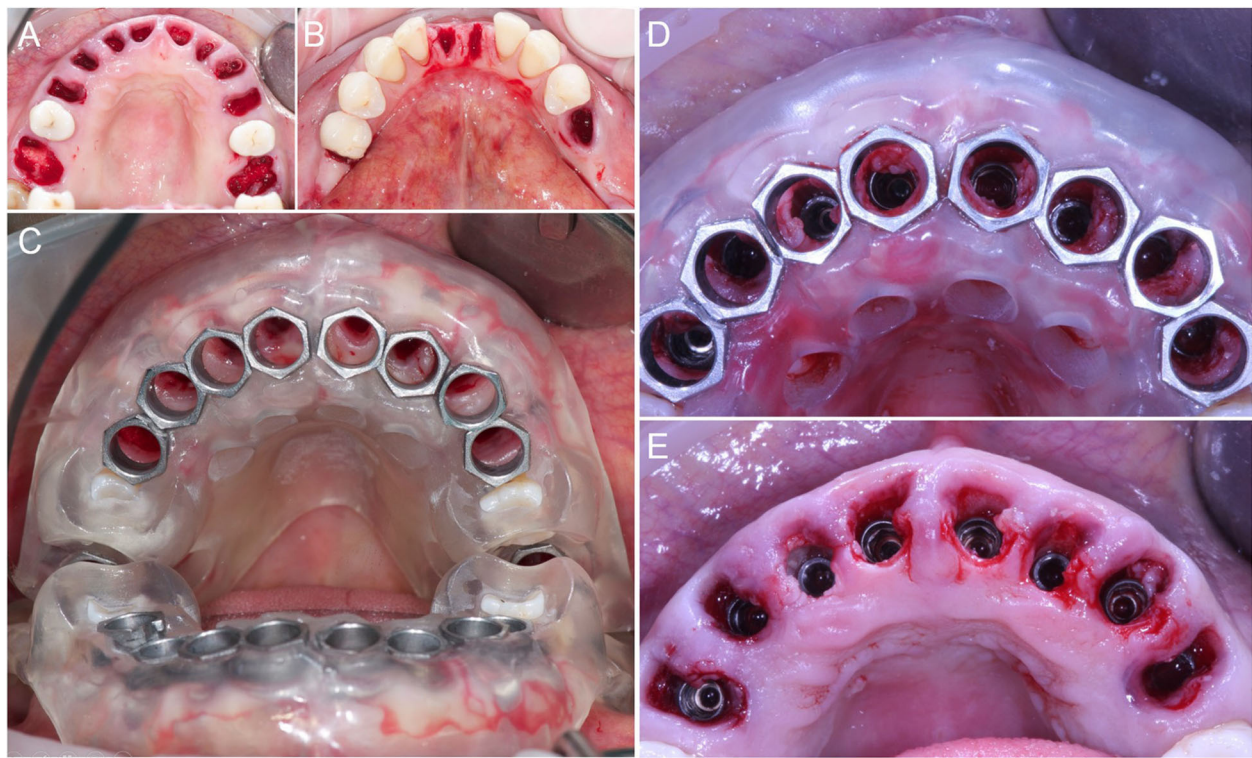
Fig. 6 Extraction of the compromised teeth and guided implant surgery. **a** Ten compromised teeth were extracted in the maxilla and (**b**) five teeth in the mandible. **c** Superior guide in position. The guide was stabilized and supported by the teeth #15, #25, the hard tissues of the maxillary ridge and palate. **d** The surgeon performed the implantation through the guide, for a fully guided procedure, so that an aesthetically driven positioning of the implants was achieved. **e** After removal of the guide, it is evident how buccal tissues have been preserved, in order to achieve a highly predictable aesthetic outcome

Implant survival

An implant was classified as "surviving" if still functioning regularly at the 1-year follow-up control. Conversely, in all cases in which the implant failed and had to be removed, it was classified as "failed." The reasons for implant failure were:

(1) mobility due to lack of osseointegration, in the absence of clinical symptoms/signs of infection (pain, suppuration, exudation), during the healing period (i.e., the period of provisionalization) or after the delivery of the final restoration;
(2) infection with pain, suppuration, exudation, related bone loss (peri-implantitis), and implant loosening;
(3) progressive marginal bone loss due to occlusal overloading, in the absence of clinical symptoms/ signs of infection (pain, suppuration, exudation);
(4) fracture of the fixture.

Complications

The assessment of immediate operative/ post-operative, biologic, and prosthetic complications included identification of any problem or complication that had affected the guided implant procedures and the implant-supported restorations, from the initial surgery until the end of the 1-year follow-up period. Complications were divided into immediate operative / post-operative (related to the guided surgery procedure), biologic, and prosthetic. Biologic and prosthetic complications could be early or late, according to when they occurred: a complication was defined as early if it occurred no later than the third month after implant placement; conversely, a complication was late if it occurred more than 3 months from implant placement.

Immediate operative/ post-operative complications were

(1) bad adaptation of the surgical guide, i.e., a non-perfect adaptation of the surgical guide when positioning and fixing it;
(2) fracture of the surgical guide during surgery, including partial and incomplete fractures of the template structure, which occurred during the preparation of the surgical sites and the positioning of the implants;
(3) insufficient implant stability at the removal of the surgical guide;
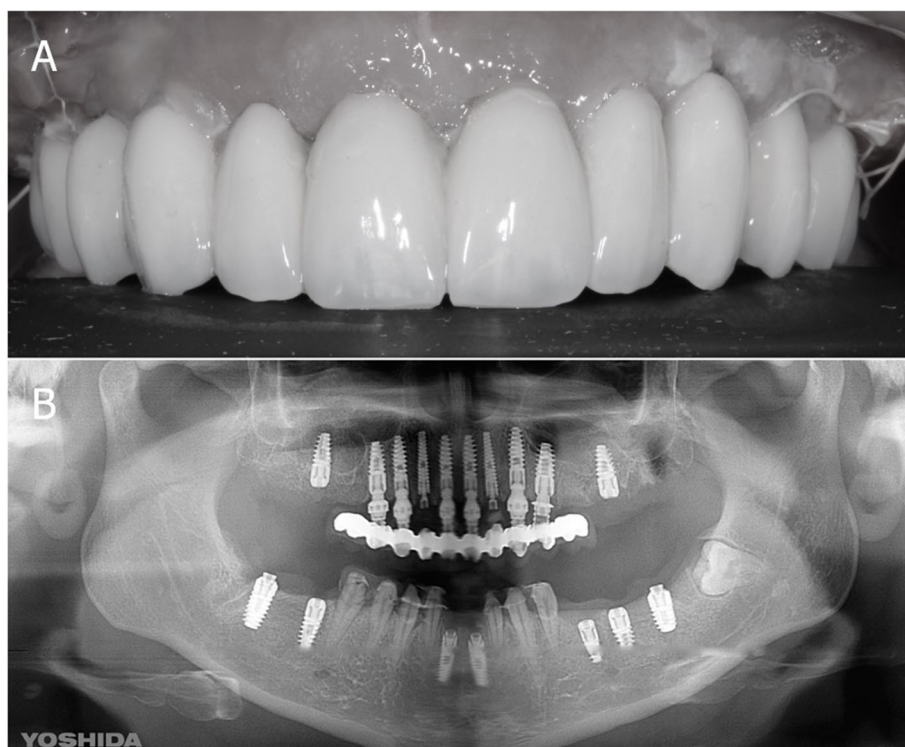
Fig. 7 Immediate loading and panoramic control radiograph. **a** Temporary Prosthesis in position 3 days after surgery. **b** Post-operative situation: panoramic radiograph. During surgery, one more mandibular tooth had to be extracted and replaced by an implant
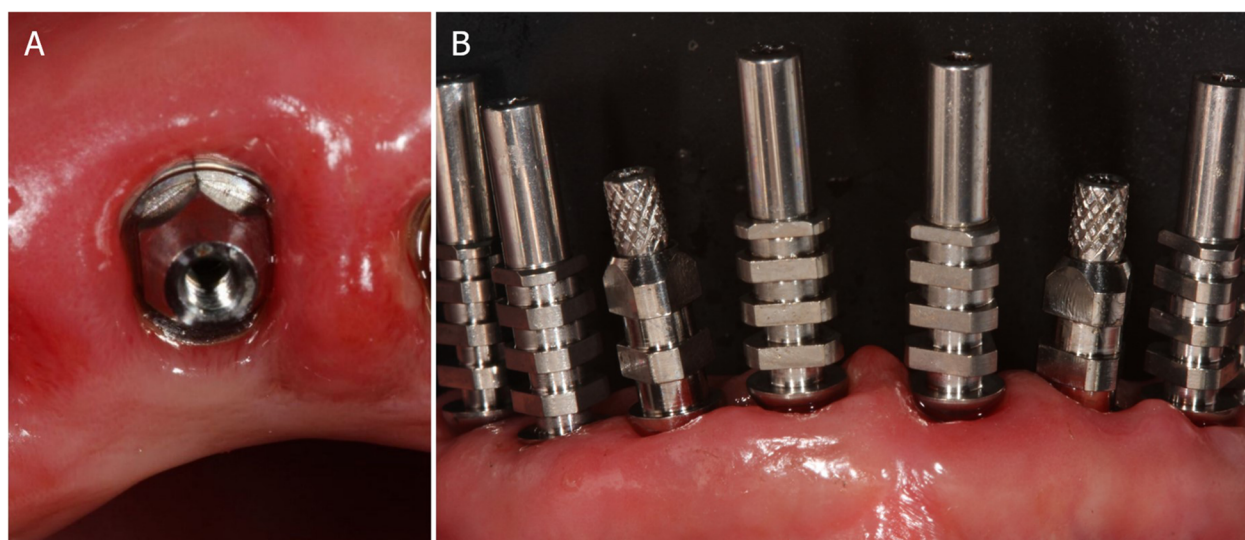
Fig. 8 Final intraoral impressions. **a** Impression taking with open tray over multi-unit intermediary abutments, to avoid the damaging of the peri-implant structures. **b** This analogic procedure was considered at the time the most precise for full arch

Fig. 9 Aesthetic refinement. **a** the clinician took an alginate impression of the provisionals in place, and a precision impression in polyether with open tray, to capture the position of the implants. These impressions were sent to the dental technician who poured plaster models and scanned them. These models were then overlapped in a CAD software, in order to have a guide for modeling the final restorations and to perform aesthetic modifications. All these modifications, however, were done manually, on 3D printed models. Then, the final shapes were scanned again
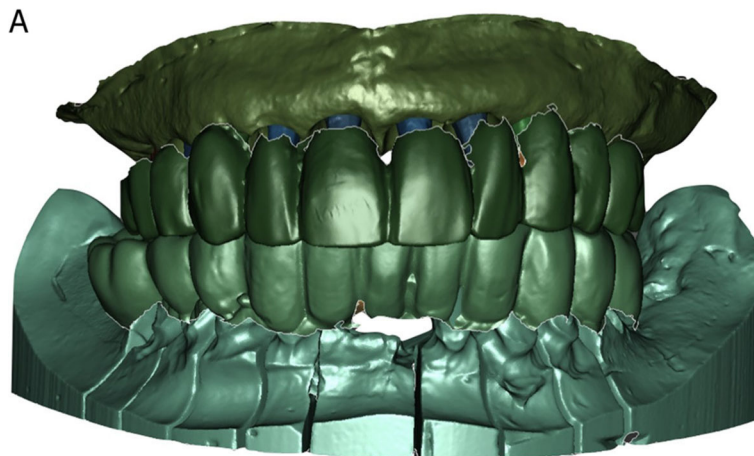
(4) aberrant implant position with buccal bone dehiscence;
(5) intra-operative bleeding;
(6) lack of passive fitting of the immediate resin prosthesis.

Biologic complications were

(1) post-operative pain and/or swelling;
(2) peri-implant mucositis, i.e., superficial inflammation of the peri-implant tissues with involvement of the soft tissues only, characterised by mild discomfort, swelling, and gingival reddening, in the absence of any radiographic evidence of marginal bone loss;
(3) peri-implantitis, i.e., deep infection of the peri-implant tissues with involvement of the bone tissue, characterised by pain or discomfort on occlusion, suppuration/exudation, abscess, fistula formation, and/or advanced marginal bone loss (≥ 2.5 mm);
(4) progressive marginal bone resorption in the absence of any kind of infection, i.e., a radiographic peri-implant bone loss > 1.5 mm after the first year of function, and/or exceeding 0.2 mm each following year.

Finally, prosthetic complications were

(1) mechanical complications, i.e., complications that occurred on pre-formed components and part of the implant system, such as unscrewing of the connecting screw and loss of connection between the implant and the abutment (abutment screw loosening), fracture of the connecting screw (abutment screw fracture), or fracture of the prosthetic abutment;

(2) technical complications, i.e., complications on prosthetic parts designed and built by the dental technician, such as customized zirconia individual abutments

and prosthetic restorations (whether temporary or definitive). Among these complications were fracture of the individual abutments as well as fracture or chipping of the prosthetic restorations.

Prosthetic success

An implant-supported prosthetic restoration was considered successful if it did not present any failure or complication, either of a biological or a prosthetic nature, throughout the entire course of the study, i.e., from the moment of placement with the immediate functional load of the temporary restoration, until replacement with the definitive restoration, and for the whole period in which the definitive restoration remained in situ, from delivery up to the 1-year follow-up control. The possible complications that could occur were the aforementioned procedural, biological, and prosthetic complications, which could affect the implants and/or the prosthetic structure.

Soft-tissue stability

The soft-tissue stability was verified from clinical photographs, taken at the placement of the definitive restoration and at the 1-year follow-up, with the same digital camera (d7100®, Nikon, Tokyo, Japan) under the same settings (distance 0.6 m, f 22). Only the area of the smile, from the first right premolar to the first left premolar was investigated. The authors compared the stability of the tissues on these frontal pictures, focusing their attention on the stability of the papillae and the soft-tissue contours, using a novel index modified from Furhauser [34].
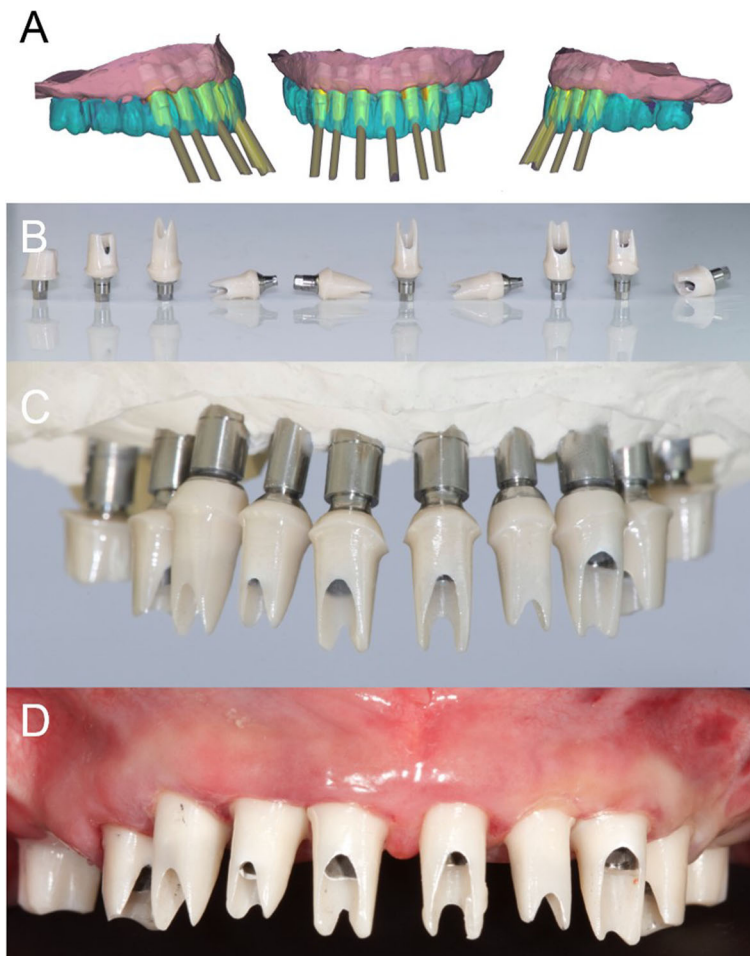
Fig. 10 Final CAD/CAM procedures and clinical application. **a** CAD design of individual zirconia abutments. These abutments were designed for extraoral cementation on titanium bases. **b** The milled zirconia abutments glued on titanium bases. **c** The milled zirconia abutments placed on the model. **d** The milled zirconia abutments placed in the patient's mouth. The abutment margins were planned 0.5 mm below the gingival margin
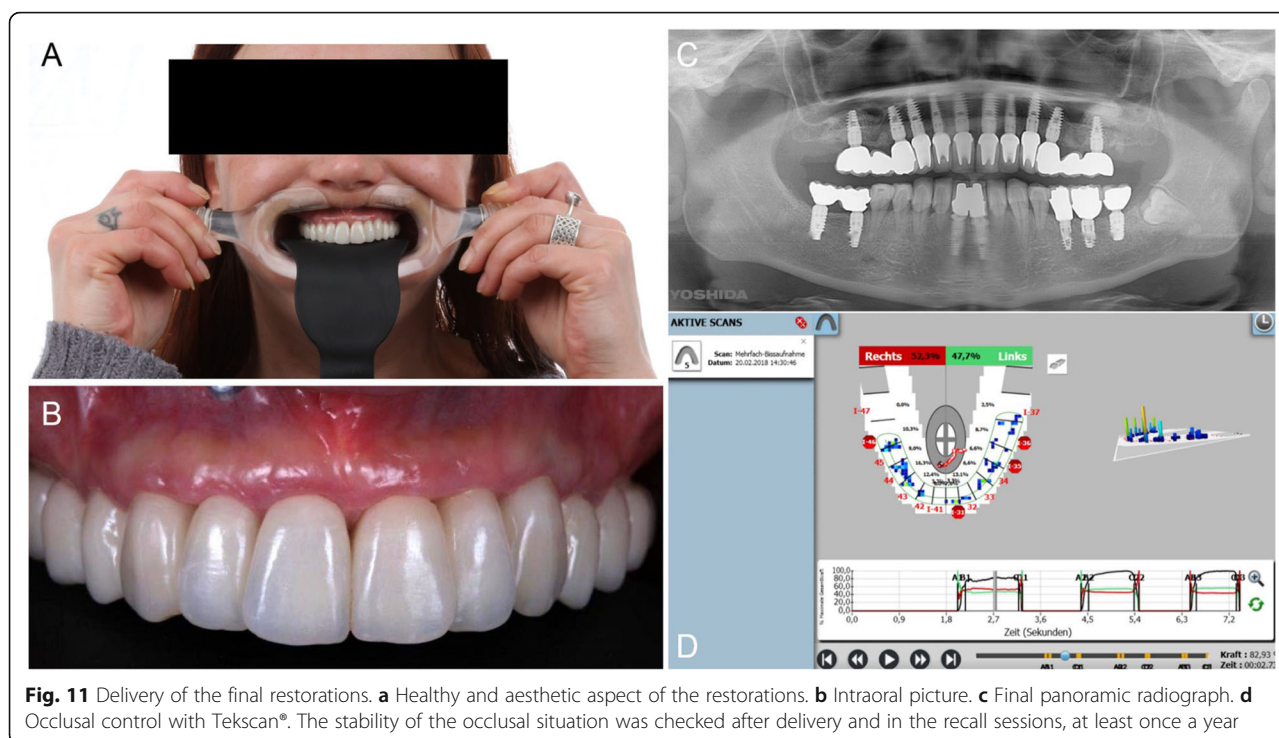
Patient satisfaction

At the 1-year follow-up control, each patient was asked to fill out a patient satisfaction questionnaire consisting of 4 different questions. The questions read as follows:

1. Overall, how satisfied are you with the treatment received?
2. Are you satisfied with the function of your implant-supported restorations?
3. Are you satisfied with the aesthetics of your implant-supported restorations?
4. Are you satisfied with the cleanability of your implant-supported restorations?

For each question, the patient could give 5 possible replies: a) very satisfied; b) satisfied; c) neither satisfied nor dissatisfied; d) dissatisfied; e) very dissatisfied.

Statistical evaluation

All patients' data were rigorously collected during the study and entered on a spreadsheet for statistical analysis (Excel 2003; Microsoft, Redmond, WA, USA). Descriptive statistics were used to describe the distribution of patients, implants, and restorations. For all qualitative variables (gender, systemic health, smoking habit, distribution of implants per site, position, length, diameter, distribution of restorations), values were expressed in absolute terms and in percentages (%); then, homogeneity or non-homogeneity in the distribution of patients (per gender, age classes, systemic health conditions, and smoking habit), implants (per site and position, length, and diameter), and restorations (per site and type) was calculated using the chi-square test (a statistically significant difference was reported with $p < 0.05$). For quantitative variables (age at surgery), the means, standard

Fig. 11 Delivery of the final restorations. **a** Healthy and aesthetic aspect of the restorations. **b** Intraoral picture. **c** Final panoramic radiograph. **d** Occlusal control with Tekscan®. The stability of the occlusal situation was checked after delivery and in the recall sessions, at least once a year

deviations (SD), medians, ranges, and 95% confidence intervals (CI) were calculated. The incidence of implant failures and complications was calculted and expressed in absolute values and in percentages (%). Implant survival was calculated at both the implant level and the patient level; with the patient as the statistical unit, he/she was classified as failure even if only one implant failure occurred. Similarly, the prosthetic success was calculated at both the restoration level and the patient level; with the patient as statistical unit, the presence of even a single complication (biologic or prosthetic) determined the allocation of the patient into the category of failure.

Results
Patient population, implant distribution, and prostheses
A total of 12 patients (5 males and 7 females, mean age 50.0 ± 13.8 years, median age 54.5 years, CI 95% 42.2–57.9 years) were enrolled in the present retrospective clinical study; 110 implants (65 of them post-extractive) were installed, immediately loaded by means of a provisional fixed full arch. After 6 months of provisionalization, then, 72 fixed prosthetic restorations (53 single crowns, 17 bridges, and 2 fixed full arches) were delivered, in order to prosthetically reconstruct the complete arch. The distribution of patients is summarized in Table 1. The patients' groups were homogeneous in distribution according to gender ($p = 0.563$) and age class ($p = 0.738$), whereas most of the patients were systemically healthy ($p = 0.049$, with only 2 patients with diabetes mellitus and 2 others with autoimmune diseases) and non-smokers ($p = 0.008$, with only

3 smoking patients). The distribution of the implants is summarized in Table 2. Most of the implants were placed in the maxilla ($p < 0.001$), but the distribution of the fixtures was homogeneous per position ($p = 0.735$). However, the distribution of the fixtures was non-homogeneous per length (p < 0.001, with most of the placed fixtures being

Table 1 Patient distribution

	N°	Percentage (%)	p*
Overall	12	100%	-
Gender			
Males	5	41.7%	0.563
Females	7	58.3%	
Age at surgery			
20-39	4	33.3%	0.778
40-59	5	41.7%	
60-79	3	25.0%	
Systemic health			
No systemic diseases	8	66.6%	0.049
Diabetes mellitus	2	16.7%	
Immunological disorders	2	16.7%	
Smoking habit			
Non-smokers	9	75.0%	0.008
Light smokers (<10 cigarettes/day)	2	16.7%	
Heavy smokers (≥ 10 cigarettes/day)	1	8.3%	

* $p = \chi^2$ test. A statistically significant difference in the distribution of patients was set with $p < 0.05$

Table 2 Implant distribution

	N°	Percentage (%)	p*
Overall	110	100%	-
Site			
Maxilla	75	68.2%	<0.001
Mandible	35	31.8%	
Position			
Incisors	24	21.8%	0.735
Cuspids	26	23.6%	
Premolars	28	25.5%	
Molars	32	29.1%	
Length			
8 mm	10	9.1%	<0.001
9 mm	13	11.8%	
10 mm	12	10.9%	
11 mm	32	29.1%	
12 mm	9	8.2%	
13 mm	23	20.9%	
14 mm	4	3.6%	
15 mm	7	6.4%	
Diameter			
3.8 mm	16	14.5%	0.001
4.3 mm	31	28.2%	
5.1 mm	28	25.5%	
6 mm	27	24.5%	
7 mm	8	7.3%	

* $p = \chi^2$ test. A statistically significant difference in the distribution of patients was set with $p < 0.05$

11 or 13 mm in lenght) and per diameter ($p = 0.001$, most of the installed fixtures being 4.3, 5.1, and 6 mm in diameter). Finally, the distribution of the prosthetic restorations is summarized in Table 3. Most of the 72 fixed restorations (45) were delivered in the maxilla, versus only 27 delivered in the mandible, and there was a statistically

Table 3 Prosthetic restoration distribution

	N°	Percentage (%)	p*
Overall		100%	-
Site			
Maxilla	45	62.5%	0.033
Mandible	27	37.5%	
Type			
Single crowns	53	73.6%	<0.001
Two-units fixed partial prostheses	10	13.9%	
Three-units fixed partial prostheses	7	9.7%	
Full-arch prostheses	2	2.8%	

* $p = \chi^2$ test. A statistically significant difference in the distribution of patients was set with $p < 0.05$

significant difference in the number of restorations between maxilla and mandible ($p = 0.033$), with the groups that were considered non-homogeneous. Similarly, most of the restorations delivered in this retrospective clinical study were single-crown (53) or short-span restorations (17); thus there was a statistically significant difference in the distribution of the restorations, per type ($p < 0.001$).

Implant stability
The mean implant stability at placement, as measured by IT and RFA (iSQ), is summarized in Table 4.

Implant survival
Two implants failed and had to be removed, in the same 57-year-old diabetic female patient. The patient was a light smoker. These implants were lost in the posterior maxilla because they failed to osseointegrate 1 month after surgery and before the final restorations were delivered. Thus, the 1-year implant-based survival rate was 98.2% (108/110 surviving implants). Considering the patient as a statistical unit, with one patient experiencing implant failure and therefore categorized as failure, the 1-year patient-based survival rate was 91.6% (11/12 patients not having any implant failure).

Complications
During guided surgery procedures, no complications were reported. All surgical guides showed an excellent fit and were sufficiently resistant not to break during the insertion of the fixtures. All implants were sufficiently stable at the removal of the guides and they appeared to be in the planned position, without any evident mistake or aberrant positioning. The immediate provisional fixed full arch was easily adapted on the fixture after implant placement. In addition, over the 1-year follow-up period, no major biological complications affected the surviving (108/110) implants. Two patients had peri-implant mucosal inflammation with bleeding on probing around two post-extraction implants after 3 months, but the improved oral hygiene reduced the inflammation. No peri-implantitis occurred, nor progressive marginal bone resorption. The incidence of biologic complications amounted to 1.8% (2/108 implants). No issues were registered with the provisional restorations. With regard to the final implant-supported fixed restorations, only two single crowns underwent abutment screw loosening; these abutments were re-screwed and no further loosening was reported. The incidence of mechanical complications was therefore 1.8% (2/108) implants. No technical complications were reported.

Prosthetic success
Considering the implant failures that occurred and the different biologic and prosthetic complications that were encountered, the 1-year prosthetic success of this study

Table 4 Distribution of the insertion torque (IT) and implant stability quotient (ISQ) measured at placement

	IT at placement < 35 Ncm (%)	IT at placement ≥ 35 Ncm (%)	ISQ at placement < 55 (%)	ISQ at placement 55<×<85 (%)
Overall	25/110	85/110	28/110	82/110
Maxilla	20/75	55/75	21/75	54/75
Mandible	5/35	30/35	7/35	28/35

amounted to 66.6% (8/12 prostheses did not undergo any failure or complication).

Soft-tissue stability

The photographic analysis revealed little or no differences between the pictures taken at the delivery of the final restorations and those at the 1-year controls. A certain degree of maturation of soft tissues was also evidenced, with growth of inter-implant papillae and adequate stability of soft-tissue contours.

Patient satisfaction

The results of the patient satisfaction questionnarie are summarized in Table 5. The great majority of patients were satisfied with the treatment received (Fig. 12a, b, c, d, e) and no patients reported being dissatisfied when answering the 4 questions asked in the questionnaire.

Discussion

Although guided surgery has become increasingly popular and widespread, there are currently only a few studies in the literature that present the results obtained with the guided flapless placement of implants in post-extraction sockets and their immediate functional loading by means of complete fixed-arch reconstructions without artificial gum [28–31].

Most of the studies in the literature, in fact, refer to the immediate loading of *hybrid* prostheses (such as Toronto Bridges, "all-on-four," and "all-on-six" dentures), characterized by the presence of a bar connecting the implants and, more relevant, artificial gum [22–26]. It is obvious how such prosthetic rehabilitations differ so thoroughly from a full-arch fixed prosthesis, which is characterized by the absence of artificial gum and much

more delicately manageable for the clinician, from an aesthetic point of view [28–31].

In a recent clinical and radiographic study on implants placed in post-extractive and healed sites, inserted using flapless guided surgery, and immediately loaded, Ciabattoni et al. [28] have reported successful clinical results. In that study, 285 implants were installed in 32 patients with a double-guide template technique [28]; in detail, 197 implants were inserted in fresh extraction sockets (137 maxilla, 60 mandible) and 88 in healed sites (58 maxilla, 30 mandible). All implants were immediately loaded by means of fixed full-arch restorations and followed for a period of 3 years [28]. The outcome variables were implant survival, prosthesis survival, and marginal bone levels [28]. At the end of the study, a high implant survival rate (97.5%) was reported, with only 7 fixtures failed (3 in fresh extraction sockets of the maxilla, 2 in fresh extraction sockets in the mandible, and 2 in maxillary healed sites) [28]. All fixed full arches maintained stability and good functionality during the entire follow-up. Finally, the marginal bone loss accounted to 1.32 mm (± 0.41) at the 3-year follow-up control [28]. The authors concluded that flapless guided implant surgery with the double-guide template technique is a predictable treatment procedure, capable of guaranteeing predictable outcomes while decreasing length of treatment time and patient discomfort [28].

Polizzi et al. investigated the clinical and radiographic outcomes of immediate fixed restorations on maxillary implants, inserted in fresh extraction and healed sites by using the NobelGuide® system [29]. Twenty-seven patients were included in the study and were treated with flapless guided implant surgery and immediate full-arch or partial restorations. The patients were followed for a period of up to 5 years and the clinical outcomes were

Table 5 Patient satisfaction wth the treatment received

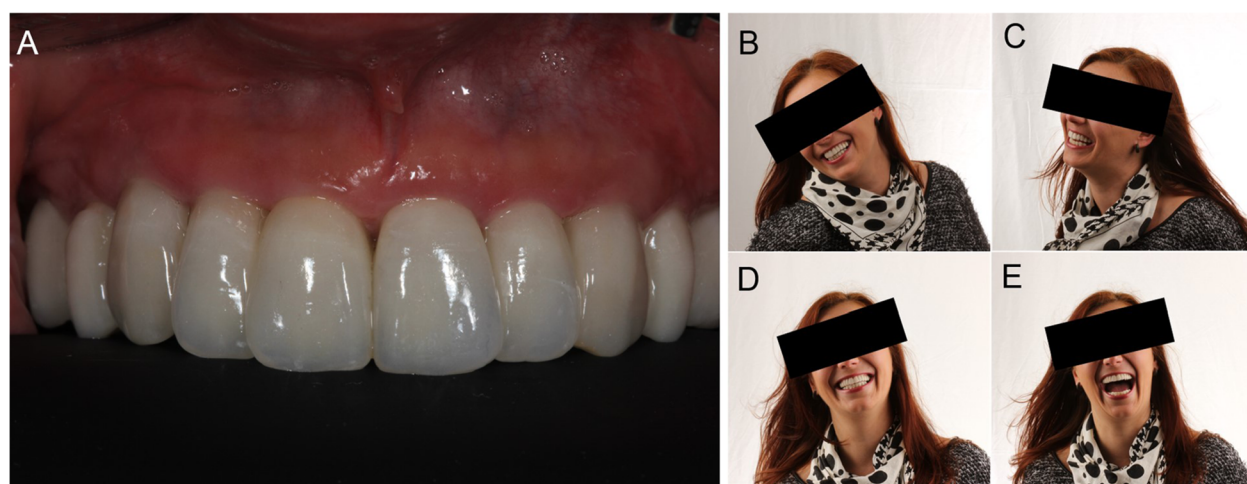| Question	Very satisfied	Satisfied	Neither satisfied nor dissatisfied	Dissatisfied	Very dissatisfied
Overall, how satisfied are you with the treatment received?	10/12 (83.3%)	2/12 (16.7%)	0/12 (0%)	0/12 (0%)	0/12 (0%)
Are you satisfied with the function of your implant-supported restorations?	12/12 (100%)	0/12 (0%)	0/12 0%	0/12 (0%)	0/12 (0%)
Are you satisfied with the esthetics of your implant-supported restorations?	11/12 (91.7%)	1/12 (8.3%)	0/12 (0%)	0/12 (0%)	0/12 (0%)
Are you satisfied with the cleanability of your implant-supported restorations?	9/12 (75%)	3/12 (25%)	0/12 (0%)	0/12 (0%)	0/12 (0%)

Fig. 12 One year follow-up control. **a** Detail of the aesthetic integration. **b**, **c**, **d**, **e** Life changing dentistry: the patient is happy with complete rehabilitation, satisfactory aesthetic and functional results

implant survival, marginal bone remodeling, soft-tissue parameters, and complications [29]. Among the 160 implants assessed, only four failures were reported, for a cumulative survival rate of 97.3%. At the end of the study, all prostheses were functioning. The marginal bone resorption from insertion to 2 years amounted to 0.85 mm (± 1.28); from insertion to the last radiographic control was 1.39 mm (± 1.88); and between 2 years and the last control was 0.64 mm (± 1.66) [29]. Finally, the soft-tissue response was excellent and only a few minor complications were reported [29].

In 2013, Meloni et al. [30] reported on a guided implant surgery protocol for the immediate delivery and functional loading of screw-retained provisional metal-acrylic full-arch prostheses. In total, 60 implants were placed in 10 patients: among these implants, 22 were inserted in fresh extraction sockets [30]. The final prostheses were delivered after 6 to 12 months. All patients were followed for a period of at least 1 year [30]. The outcome measures of this study were implant survival, patient satisfaction, and marginal bone loss [30]. At the end of the study, no implants were lost, for a survival rate of 100%; in addition, no complications (either biological or prosthetic) were reported [30]. All patients felt comfortable with the treatment procedures and were fully satisfied with the final functional and aesthetic result [30]. Finally, the mean marginal bone loss amounted to 1.4 mm (± 0.3) [30].

In a subsequent prospective clinical study, which represented the development of the previous one, the same researchers reported on the clinical and radiographic outcomes of 20 patients treated with guided implant surgery and immediate loading of computer-assisted-design/ computer-assisted-manufacturing (CAD/CAM) fixed full-arches [31]. In total, 120 fixtures were installed

in 23 jaws, supporting immediately loaded fixed full-arch prostheses [31]. After 30 months, the implant survival rate was 97.7%, with only minor prosthetic complications encountered, a marginal bone remodeling of 1.08 mm (± 0.34), a mean probing-pocket-depth value of 2.84 mm (± 0.55), and a mean bleeding-on-probing of 4% (± 2.8%) [31]. The authors concluded that guided implant surgery and immediate functional loading of fixed full arches represent a viable option for the treatment of completely edentulous jaws [31].

The results of our present study seem to confirm the evidence emerging from the aforementioned literature [28–31]. In our present study, 12 patients received 110 implants (65 of them post-extractive), placed flapless through a guided surgery procedure and then immediately loaded by means of a provisional fixed full arch. After a provisionalization period of 6 months, 72 fixed prosthetic restorations were delivered, in order to prosthetically reconstruct the complete arch. The implant stability at placement was successful. Only two implants failed and were removed, in one single patient, for a 1-year implant survival rate of 98.2% (108/110 surviving implants). A few biologic and prosthetic complications were reported, with 8/12 prostheses that did not undergo any failure or complication during the entire follow-up period. At the 1-year follow-up control, excellent soft-tissue stability was found, and patients were satisfied with the treatment.

The advantages of our present guided surgical and prosthetic protocol can be summarized as follows. First, the flapless implant placement can reduce intra- and post-operative patient discomfort and morbidity, as indicated by different systematic reviews [20, 35] and clinical studies [36–38]. In fact, this minimally invasive approach significantly reduces the time required for surgery [36, 37]. In a controlled study, Arisan et al. demonstrated that the

flapless guided surgery can significantly shorten surgical time, as compared to the conventional open-flap surgery [37]. Since the duration of the surgical intervention influences morbidity for the patient, computer-assisted flapless implant placement can reduce the incidence of surgery-related complications, such as bacteremia and infections [38]. Fortin at al. have demonstrated that the optimization of implant placement, through guided surgery, may be an option to successfully avoid having to use bone augmentation procedures [39]. But for the clinician, the main advantage in the use of guided surgery is the possibility of planning the implants (at the requisite position, inclination, and depth) in the best possible way, avoiding dangerous anatomical structures (inferior alveolar nerve and maxillary sinus) and taking into account the emergence profiles and the overlying prosthesis. It is the so-called "prosthetically guided" placement, where the implants are planned in the best possible way to support the prosthesis, which reduces the need of prosthetic compromises. In fact, during the planning of the fixtures in the software, the prosthetic suprastructure is imported and included; hence, the optimal position of the implants (depth, mesio-distal, bucco-lingual as well as inclination) in relation to the future prosthetic rehabilitation can be obtained. As such, the fixtures can be planned to support a prosthesis that provides the functional, biologic, and aesthetic requirements and at the same time the anatomy of the bone as well as prosthetic boundaries can be taken into account. In the present study, care was taken to plan the implants in the best position, depth, and inclination, in order to engage the fixtures as much as possible in the residual bone (exceeding the apex of fresh extraction sockets at least 3–4 mm) to maximize stability, and at a distance of 2–3 mm from the residual buccal bone walls, to avoid aesthetic problems. At the same time, however, the planning was prosthetically guided, with the axis of the implants that had to be, as much as possible, in the center of the teeth. The final planning was the result of a compromise between the residual amount of bone available, and the ideal prosthetic emergence profile. This is not a trivial matter, particularly when a fixed full arch without artificial gum is planned; in fact, with guided implant surgery, the improved accuracy in implant placement can provide a better platform for the final prosthetic restoration. Immediately after surgery, the pre-fabricated provisional full arch can be delivered to patients and loaded, improving patient satisfaction, comfort, and treatment acceptance, without the need to use any removable denture. The application of these pre-fabricated restorations results in acceptable success rates, as reported in the literature. In addition, the immediately loaded provisional restoration may guide the soft-tissue healing for an optimal aesthetic result with minimal recession, taking advantage also of the extraction socket healing potential.

In 2015, Furhauser et al. [40] published a clinical study in which stereolithographic surgical guides were used to insert single-tooth implants for the replacement of upper incisors. The authors evaluated the accuracy in implant placement and the aesthetic result by means of the pink aesthetic score (PES) after a mean follow-up of 2.3 years [40]. Even though guided, a mean deviation from the originally planned position of 0.84 mm (measured at the implant shoulder) was found [40]. However, the authors found that deviations ≥0.8 mm resulted in significantly worse aesthetic results (median PES: 9.5) than with more accurate implant positions (median PES: 13, $p = 0.039$) [40].

The issue of accuracy in transferring the implant position from the software to the surgery actually remains to be solved, as demonstrated by various studies [41, 42] and literature reviews [14–16, 20, 35]. Therefore, considering that these deviations may depend on several factors that cannot be completely controlled [14–16, 35, 41, 42], it is advisable for clinicians to carefully select patients as candidates for guided surgery, especially at the beginning of their own learning path of the technique.

In the coming years, the continuous technological advancements in the world of digital dentistry, together with improvements in devices such as scanners [43, 44] and software for planning and in the manufacturing of surgical guides [45], might actually reduce the inaccuracy of guided implant placement.

Moreover, in a recent systematic review of flapless guided surgery procedures, the authors have found excellent survival rates (97.2%) in the included studies and minimal mean marginal bone loss (1.45 mm) during 1–4 years of follow-up [20]; however, complications were also found, such as insufficient primary implant stability at placement in the fresh extraction sockets, as well as occasional surgical guide fractures or fractures of the immediate provisional restoration [20]. Once again, the authors concluded that there is a learning curve to achieve complete treatment success; certainly, the selection of the case is important and it would be advisable to start with simpler cases, then gradually learning how to deal with more complex cases [20].

Finally, the present study has certain limits, such as the limited number of patients enrolled and the short follow-up time. In addition, the retrospective is not the most suitable study design for obtaining indisputable scientific data [46, 47]. Moreover, this study was performed following a mixed, digital-analog workflow and this could be considered as another limitation of the present research, since the use of intraoral scanners is today well established [44] and could potentially reduce the number of steps and procedures described here. Therefore, new studies should be conducted with a prospective design and possibly randomized controlled trials, in order to draw more specific conclusions on the validity and effectiveness of this technique.

Conclusions

In our present study, 12 patients received 110 implants (65 of them post-extractive), placed flapless through a guided surgery procedure and then immediately loaded by means of a provisional fixed full arch. After a provisionalization period of 6 months, 72 fixed zirconia-ceramic prosthetic restorations (53 single crowns, 17 bridges, and 2 fixed full arches) were delivered. The results showed a 1-year implant survival rate of 98.2% (108/110 surviving implants) and good soft-tissue stability.

Our present surgical and prosthetic approach presents several advantages. First, only one surgical session is required for tooth extraction, implantation and application of provisional prosthesis. For the patients social life, this concept allows a reduction of discomfort and facilite their return to professional life. For the dental rehabilitation, provisional restoration guides the soft-tissue healing for an optimal aesthetic result. Within the limitations of this study, combining a CBCT-derived surgical guide to an immediate implant placement in post-extraction sockets together with immediate provisionalization and loading seems to be a safe and predictable therapy, with high survival rates and excellent aesthetic results, when applied in indicated cases. Further studies on larger samples of patients and with longer follow-up controls are needed to draw more specific conclusions about the long-term results with the present technique.

Abbreviations
3D: three-dimensional; BOP: Bleeding on probing; CBCT: Cone beam computed tomography; CT: computerized tomography; DICOM: digital imaging and communication in medicine; PES: pink aesthetic score; PPD: Probing pocket depth

Authors' contributions
Conceptualization: HL, UH; Data curation: HL, UH; Formal analysis: RS, SG; Investigation: HL, UH; Methodology: HL; Project administration: RS, SG; Resources: HL; Supervision: SG; Validation: RS; Visualization: HL; UH; Writing original draft: HL; Writing review & editing: UH, SG. All authors have read and approved the manuscript.

Availability of data and materials
The datasets used and/or analysed during the current study are available from the corresponding author on reasonable request.

Ethics approval and consent to participate
This study was approved by the local Ethics Committee at the University of Frankfurt, Germany (approval number: #182/19). All patients were fully informed about the nature of this study and signed an informed consent form for this treatment.

Consent for publication
The authors obtained written consent for publication from the patients enrolled in this study.

Competing interests
The authors declare that they have no competing interests.

Author details
[1]Baden-Baden, Germany. [2]Department of Oral, Cranio-Maxillofacial and Facial Plastic Surgery, Johann Wolfgang Goethe-University, Frankfurt am Main, Germany. [3]Department of Post-Graduate Medicine, Johann Wolfgang Goethe-University, Frankfurt am Main, Germany. [4]Sanremo, Italy. [5]Department of Oral, Cranio-Maxillofacial and Facial Plastic Surgery, Medical Center of the Goethe University Frankfurt, Frankfurt am Main, Germany. [6]Institute of Pathology, University Medical Center, Johannes Gutenberg University, Mainz, Germany.

References
1. Peñarrocha-Oltra D, Covani U, Peñarrocha-Diago M, Peñarrocha-Diago M. Immediate loading with fixed full-arch prostheses in the maxilla: review of the literature. Med Oral Patol Oral Cir Bucal. 2014;19(5):e512–7.
2. Peñarrocha-Oltra D, Covani U, Peñarrocha M, Peñarrocha-Diago M. Immediate versus conventional loading with fixed full-arch prostheses in mandibles with failing dentition: a prospective controlled study. Int J Oral Maxillofac Implants. 2015;30(2):427–34.
3. Papaspyridakos P, Mokti M, Chen CJ, Benic GI, Gallucci GO, Chronopoulos V. Implant and prosthodontic survival rates with implant fixed complete dental prostheses in the edentulous mandible after at least 5 years: a systematic review. Clin Implant Dent Relat Res. 2014;16(5):705–17.
4. Peñarrocha-Oltra D, Covani U, Aparicio A, Ata-Ali J, Peñarrocha-Diago M, Peñarrocha-Diago M. Immediate versus conventional loading for the maxilla with implants placed into fresh and healed extraction sites to support a full-arch fixed prosthesis: non-randomized controlled clinical study. Int J Oral Maxillofac Implants. 2013;28(4):1116–24.
5. Mello CC, Lemos CAA, Verri FR, Dos Santos DM, Goiato MC, Pellizzer EP. Immediate implant placement into fresh extraction sockets versus delayed implants into healed sockets: A systematic review and meta-analysis. Int J Oral Maxillofac Surg. 2017;46(9):1162–77.
6. Cercadillo-Ibarguren I, Sánchez-Torres A, Figueiredo R, Valmaseda-Castellón E. Bimaxillary simultaneous immediate loading of full-arch restorations: A case series. J Clin Exp Dent. 2017;9(9):e1147–52.
7. Hsu JT, Wu AY, Fuh LJ, Huang HL. Effects of implant length and 3D bone-to-implant contact on initial stabilities of dental implant: a microcomputed tomography study. BMC Oral Health. 2017;17(1):132.
8. Javaheri D. Achieving Anterior Aesthetics in a Full-Arch Implant Case. Dent Today. 2016;35(1):118 120–1.
9. Mangano FG, Mastrangelo P, Luongo F, Blay A, Tunchel S, Mangano C. Aesthetic outcome of immediately restored single implants placed in extraction sockets and healed sites of the anterior maxilla: a retrospective study on 103 patients with 3 years of follow-up. Clin Oral Implants Res. 2017;28(3):272–82.
10. Buser D, Martin W, Belser UC. Optimizing esthetics for implant restorations in the anterior maxilla: anatomic and surgical considerations. Int J Oral Maxillofac Implants. 2004;19(Suppl):43–61.
11. Link-Bindo EE, Soltys J, Donatelli D, Cavanaugh R. Common Prosthetic Implant Complications in Fixed Restorations. Compend Contin Educ Dent. 2016;37(7):431–6 quiz 439.
12. Khzam N, Arora H, Kim P, Fisher A, Mattheos N, Ivanovski S. Systematic Review of Soft Tissue Alterations and Esthetic Outcomes Following Immediate Implant Placement and Restoration of Single Implants in the Anterior Maxilla. J Periodontol. 2015;86(12):1321–30.
13. Mangano F, Shibli JA, Fortin T. Digital Dentistry: New Materials and Techniques. Int J Dent. 2016;2016:5261247.
14. Vercruyssen M, Laleman I, Jacobs R, Quirynen M. Computer-supported implant planning and guided surgery: a narrative review. Clin Oral Implants Res. 2015;26(Suppl. 11):69–76.
15. D'haese J, Ackhurst J, Wismeijer D, De Bruyn H, Tahmaseb A. Current state of the art of computer-guided implant surgery. Periodontol. 2017;73(1):121–33.
16. Colombo M, Mangano C, Mijiritsky E, Krebs M, Hauschild U, Fortin T. Clinical applications and effectiveness of guided implant surgery: a critical review based on randomized controlled trials. BMC Oral Health. 2017;17(1):150.

17. Bornstein MM, Scarfe WC, Vaughn VM, Jacobs R. Cone beam computed tomography in implant dentistry: a systematic review focusing on guidelines, indications, and radiation dose risks. Int J Oral Maxillofac Implants. 2014;29(Suppl):55–77.

18. Bornstein MM, Horner K, Jacobs R. Use of cone beam computed tomography in implant dentistry: current concepts, indications and limitations for clinical practice and research. Periodontol. 2017;73(1):51–72.

19. Bell CK, Sahl EF, Kim YJ, Rice DD. Accuracy of Implants Placed with Surgical Guides: Thermoplastic Versus 3D Printed. Int J Periodontics Restorative Dent. 2018;38(1):113–9.

20. Moraschini V, Velloso G, Luz D, Barboza EP. Implant survival rates, marginal bone level changes, and complications in full-mouth rehabilitation with flapless computer-guided surgery: a systematic review and meta-analysis. Int J Oral Maxillofac Surg. 2015;44(7):892–901.

21. Jesch P, Jesch W, Bruckmoser E, Krebs M, Kladek T, Seemann R. An up to 17-year follow-up retrospective analysis of a minimally invasive, flapless approach: 18 945 implants in 7783 patients. Clin Implant Dent Relat Res. 2018;20(3):393–402.

22. Daas M, Assaf A, Dada K, Makzoumé J. Computer-Guided Implant Surgery in Fresh Extraction Sockets and Immediate Loading of a Full-Arch Restoration: A 2-Year Follow-Up Study of 14 Consecutively Treated Patients. Int J Dent. 2015;2015:824127.

23. Browaeys H, Dierens M, Ruyffelaert C, Matthijs C, De Bruyn H, Vandeweghe S. Ongoing Crestal Bone Loss around Implants Subjected to Computer-Guided Flapless Surgery and Immediate Loading Using the All-on-4® Concept. Clin Implant Dent Relat Res. 2015;17(5):831–43.

24. Yamada K, Hoshina H, Arashiyama T, Arasawa M, Arai Y, Uoshima K, Tanaka M, Nomura S. Immediate implant loading following computer-guided surgery. J Prosthodont Res. 2011;55(4):262–5.

25. Allum SR. Immediately loaded full-arch provisional implant restorations using CAD/CAM and guided placement: maxillary and mandibular case reports. Br Dent J. 2008;204(7):377–81.

26. Montero J, Macedo de Paula C, Albaladejo A. The "Toronto prosthesis", an appealing method for restoring patients candidates for hybrid overdentures: A case report. J Clin Exp Dent. 2012;4(5):e309–12.

27. Ata-Ali J, Flichy-Fernández AJ, Alegre-Domingo T, Ata-Ali F, Palacio J, Peñarrocha-Diago M. Clinical, microbiological and immunological aspects of healthy versus periimplantitis tissue in full-arch reconstruction patients: a prospective cross-sectional study. BMC Oral Health. 2015;15:43.

28. Ciabattoni G, Acocella A, Sacco R. Immediately restored full arch-fixed prosthesis on implants placed in both healed and fresh extraction sockets after computer-planned flapless guided surgery. A 3-year follow-up study. Clin Implant Dent Relat Res. 2017;19(6):997–1008.

29. Polizzi G, Cantoni T. Five-year follow-up of immediate fixed restorations of maxillary implants inserted in both fresh extraction and healed sites using the NobelGuide™ system. Clin Implant Dent Relat Res. 2015;17(2):221–33.

30. Meloni SM, De Riu G, Pisano M, Tullio A. Full arch restoration with computer-assisted implant surgery and immediate loading in edentulous ridges with dental fresh extraction sockets. One year results of 10 consecutively treated patients: guided implant surgery and extraction sockets. J Maxillofac Oral Surg. 2013;12(3):321–5.

31. Meloni SM, De Riu G, Pisano M, Lolli FM, Deledda A, Campus G, Tullio A. Implant Restoration of Edentulous Jaws with 3D Software Planning, Guided Surgery, Immediate Loading, and CAD-CAM Full Arch Frameworks. Int J Dent. 2013;2013:683423.

32. Zita Gomes R, de Vasconcelos MR, Lopes Guerra IM, de Almeida RAB, de Campo Felino AC. Implant stability in the posterior maxilla: a controlled clinical trial. Biomed Res Int. 2017;2017:6825213.

33. Bechara S, Kubilius R, Veronesi G, Pires JT, Shibli JA, Mangano FG. Short (6-mm) dental implants versus sinus floor elevation and placement of longer (=10-mm) dental implants: a randomized controlled trial with a 3-year follow-up. Clin Oral Implants Res. 2017;28(9):1097–107.

34. Furhauser R, Florescu D, Benesch T, Haas R, Mailath G, Watzek G. Evaluation of soft tissue around single-tooth implant crowns: the pink esthetic score. Clin Oral Implants Res. 2005;16(6):639–44.

35. Hultin M, Svensson KG, Trulsson M. Clinical advantages of computer-guided implant placement: a systematic review. Clin Oral Implants Res. 2012;23:124–35.

36. Marra R, Acocella A, Alessandra R, Ganz SD, Blasi A. Rehabilitation of Full-Mouth Edentulism: Immediate Loading of Implants Inserted With Computer-Guided Flapless Surgery Versus Conventional Dentures: A 5-Year Multicenter Retrospective Analysis and OHIP Questionnaire. Implant Dent. 2017;26(1):54–8.

37. Arisan V, Karabuda CZ, Ozdemir T. Implant surgery using bone- and mucosa-supported stereolithographic guides in totally edentulous jaws: surgical and post-operative outcomes of computer-aided vs. standard techniques. Clin Oral Implants Res. 2010;21:980–8.

38. Arisan V, Bölükbasi N, Öksüz L. Computer- assisted flapless implant placement reduces the incidence of surgery-related bacteremia. Clin Oral Investig. 2013;17:1985–93.

39. Fortin T, Isidori M, Bouchet H. Placement of posterior maxillary implants in partially edentulous patients with severe bone deficiency using CAD/CAM guidance to avoid sinus grafting: a clinical report of procedure. Int J Oral Maxillofac Implants. 2009;24:96–102.

40. Fürhauser R, Mailath-Pokorny G, Haas R, Busenlechner D, Watzek G, Pommer B. Esthetics of Flapless Single-Tooth Implants in the Anterior Maxilla Using Guided Surgery: Association of Three-Dimensional Accuracy and Pink Esthetic Score. Clin Implant Dent Relat Res. 2015;17(Suppl 2):e427–33.

41. Vercruyssen M, Cox C, Naert I, Jacobs R, Teughels W, Quirynen M. Accuracy and patient-centered outcome variables in guided implant surgery: a RCT comparing immediate with delayed loading. Clin Oral Implants Res. 2016;27(4):427–32.

42. Vercruyssen M, Cox C, Coucke W, Naert I, Jacobs R, Quirynen M. A randomized clinical trial comparing guided implant surgery (bone- or mucosa-supported) with mental navigation or the use of a pilot-drill template. J Clin Periodontol. 2014;41(7):717–23.

43. Van Assche N, Vercruyssen M, Coucke W, Teughels W, Jacobs R, Quirynen M. Accuracy of computer-aided implant placement. Clin Oral Implants Res. 2012;23(Suppl 6):112–23.

44. Mangano F, Gandolfi A, Luongo G, Logozzo S. Intraoral scanners in dentistry: a review of the current literature. BMC Oral Health. 2017;17(1):149.

45. Joda T, Zarone F, Ferrari M. The complete digital workflow in fixed prosthodontics: a systematic review. BMC Oral Health. 2017;17(1):124.

46. Mangano FG, Hauschild U, Admakin O. Full in-Office Guided Surgery with Open Selective Tooth-Supported Templates: A Prospective Clinical Study on 20 Patients. Int J Environ Res Public Health. 2018;15(11).

47. Spielau T, Hauschild U, Katsoulis J. Computer-assisted, template-guided immediate implant placement and loading in the mandible: a case report. BMC Oral Health. 2019;19(1):55.

Publisher's Note

Springer Nature remains neutral with regard to jurisdictional claims in published maps and institutional affiliations.